# Preclinical Testing of an Upscaled Tissue Engineered Stem Cell Patch Towards Use in Translational Studies

*By Dr Richard John Jabbour*

*Thesis submitted for the degree of Doctor of Philosophy*

CID: 00396197

Department of Translational Medicine

National Heart and Lung Institute

Imperial College London

**Declaration of Originality and copyright declaration**

The work presented is my own unless otherwise stated. The original idea of the study was conceived and developed by Professors Sian Harding, Godfrey Smith, Fu Siong Ng and Cesare Terracciano who helped with me with developing my experiments and also provided me with practical advice and support throughout my PhD.

The copyright of this thesis rests with the author and is made available under a Creative Commons Attribution Non-Commercial No Derivatives licence.

Researchers are free to copy, distribute or transmit the thesis on the condition that they attribute it, that they do not use it for commercial purposes and that they do not alter, transform or build upon it. For any reuse or redistribution, researchers must make clear to others the licence terms of this work.

Dr R Jabbour

December 2019

***To my family***

**Acknowledgments**

I would like to sincerely thank my supervisor Prof Sian Harding, for her positive attitude and encouragement all throughout my PhD, which truly made my time in the lab an enjoyable experience. Additionally, I would like to thank Prof Cesare Terracciano and Dr Fu Siong Ng for their continued encouragement and support. A special thanks goes to Prof Godfrey Smith (University of Glasgow) and Prof Thomas Eschenhagen (Hamburg University), whose collaborative effort enabled me to carry out the work contained in this thesis. I would also like to thank all the members of Sian and Cesare's labs for helping in so many ways all throughout my PhD. Especially Dr Thomas Owen who helped and guided me all throughout my PhD, and helped me look after the EHTs (even at weekends over the Christmas period!). Also Mr Pragati Pandey, who really helped me during his 1st year of his PhD and is now taking over the rabbit work in his final 2 years. I would also like to thank Ms Daphne Pantou for her help during her MSc thesis. Particular thanks goes to Mr Oisin King and Mr Brian Wang for continuously supplying cells for us to make EHTs. Finally, I would like to thank Imperial College London for allowing me to take up this PhD while providing excellent infrastructure to carry out experiments and the British Heart foundation who awarded me my clinical research training fellowship, and therefore allowed me to carry out the work in the first instance. To my friends in the lab, thanking you in so many ways – you have made my PhD a most memorable experience. Lastly, I would like to thank my family and Federica for always being there for me and providing me with support and encouragement to keep me motivated all throughout the 3 years of my PhD.

**Abstract**

Heart failure is an epidemic which is increasing in prevalence and is associated with an enormous healthcare burden, accounting for 1-2% of the entire NHS healthcare budget. Existing treatment options are primarily focussed on preventing or retarding the progression of disease rather than reversing the disease process. The survival rate has been stubbornly slow to improve with a 5 year mortality rate of 50%. Therefore, at present there is an unmet need for novel treatment strategies.

Pluripotent stem cell derived cardiomyocytes (SC-CM) are an exciting and potentially revolutionary treatment option for repairing the damaged heart. Encouraging preclinical experiments have reported that it is possible SC-CMs to survive, electrically couple, and improve contractile function of the host heart, but an increase in arrhythmia has been observed. It has also been shown that the existing delivery methods (intracoronary and intramyocardial) used in human clinical trials of bone marrow mononuclear cells are inadequate to enable long term retention of cells in the heart and therefore newer strategies are needed. Biomaterials are promising, for example, engineered heart tissue has been shown in small animal studies to enable long term cell retention; however, to date the creation of engineered heart tissue suitable for the first in man clinical trials is lacking.

The aims of this PhD project were to explore the use of biomaterials including engineered heart tissue and conductive polymers in stem cell grafting experiments. Firstly, upscaled engineered heart tissue was characterised in-vitro and feasibility and efficacy tested in a preclinical intermediate model of myocardial infarction. A rabbit model was chosen and set up for these experiments due to the numerous

similarities with human myocardium and it being a suitable next step from small animal models. Cell retention was tested at various time points up to one month and efficacy was tested using changes in left ventricular function as determined by echocardiography. Potentially harmful side effects of arrhythmia burden were tested in-vivo and ex-vivo using telemetry and arrhythmia provocation protocols.

The experiments in this PhD described the successful in-vitro characterisation of upscaled engineered heart tissue and preclinical testing in a rabbit model of myocardial infarction. The patches were not associated with an increase in arrhythmia burden and improvements in ventricular function were observed when compared to infarcted hearts. We were also able to show that conductive polymers were able to alter the conductive properties of the epicardial surface of the heart and did not appear pro-arrhythmic in nature.

**Awards Related to Thesis**

1. 2019 - ISHR Young Investigator Travel Award – Beijing
    - Award to present my abstract at the International Society of Heart Research World Congress in Beijing, China

2. 2018 – Imperial College Provost's Excellence in Research Award
    - Award to recognise the successful implementation of the in-vivo rabbit model at Imperial College Hammersmith Campus and collaboration between a researcher and CBS staff

3. 2018 – Imperial College President's Excellence in Research Award
    - Team Award to recognise success set up of Human Langendorff at Imperial College London

4. 2018 – NHLI Postgraduate Research day – Highly Commended
    - Award for highly commended poster presentation at the annual postgraduate research day

5. 2018 – NIHR Research Academy – Highly commended
    - Highly commended team award at a national conference. I was accepted onto this conference due to the research carried out during my PhD and a recommendation from my supervisor.

**Publications obtained during / related to this thesis**

**Published manuscripts**

1. Watson SA, Duff J, Bardi I, Zabielska M, Atanur SS, **Jabbour RJ**, Simon A, Tomas A, Smolenski RT, Harding SE, Perbellini F, Terracciano CM. Biomimetic electromechanical stimulation to maintain adult myocardial slices in vitro. Nature Communications. 2019 May 15;10(1):2168. Original article.
2. Chow A, Stuckey DJ, Kidher E, Rocco M, **Jabbour RJ,** Mansfield CA, Darzi A, Harding SE, Stevens MM, Athanasiou T. Human Induced Pluripotent Stem Cell-Derived Cardiomyocyte Encapsulating Bioactive Hydrogels Improve Rat Heart Function Post Myocardial Infarction. Stem Cell Reports. 2017 Nov 14;9(5):1415-1422. Original article.
3. Dolatshad NF*, Hellen N*, **Jabbour RJ*,** Harding SE, Földes G. G-protein Coupled Receptor Signaling in Pluripotent Stem Cell-derived Cardiovascular Cells: Implications for Disease Modeling. Front Cell Dev Biol. 2015 Dec 9; 3:76. Review. *Joint first authors

**Manuscripts under review**

4. Hellen N, Owen T, Hasan A, Goulding J, Wright P, Kodagoda T, **Jabbour RJ**, Kloc M, Hill S, Gorelik J, Denning C, Harding SE. Constitutive beta-adrenoceptor-mediated cAMP production controls spontaneous automaticity of stem cell-derived cardiomyocytes. Original article. Under review in Cardiovascular Research.
5. Couch L, Fielder J, Chich G, Clayton R, Dries E, Wienecke L, Fourre J, Derda A, Wang B, **Jabbour RJ**, Shanmuganathan M, Lyon A, Wright P, Terracciano C, Thum T, Harding SE. Circulating microRNAs predispose to takotsubo

syndrome following high dose adrenaline exposure. Original article. Under review in JACC – basic to translational medicine.

6. Handa B, Li X, Baxan N, Roney C, Schendrygina A, Mansfield C, **Jabbour RJ,** Pitcher D, Chowdhury RA, Peters NS. The electrophenotype spectrum in myocardial fibrillation: a unifying hypothesis for mechanisms sustaining fibrillation. Original article. Under review in JACC.
7. **Jabbour RJ,** Owen TJ, Pandey P, Harding SE. Future potential of engineered heart tissue patches for repairing the damage caused by heart attacks. Editorial. Under review in Expert review of medical devices.
8. Majid QA, Davidenko N, Cruz OH, **Jabbour RJ,** Owen TJ, Basnett P, Lukasiewicz B, Stevens M, Best S, Cameron R, Sinha S, Harding SE, Roy I. Natural Biomaterials for Cardiovascular Tissue Engineering:
   A Highly Biocompatible Solution. Review. Under review in Frontiers in Cardiovascular Medicine.
9. **Jabbour RJ*,** Behradfar E*, Debney M, Nygren A, Hartley A, Efimov I, Hocini M, Harding SE, Peters NS, Vigmond EJ, Ng FS. Acute ischaemia and gap junction modulation modify propagation patterns across Purkinje-myocardial junctions. Original article. Under review in Heart Rhythm.

**Manuscripts in preparation**

10. **Jabbour RJ,** Kapnisi K, Mawad D, Handa B, Couch L, Mansfield C, Perbillini F, Terracciano C, Stevens M, Lyon A, Smith G, Peters N, Ng FS, Harding SE. Conductive polymers affect myocardial conduction velocity but are not pro-arrhythmic. Original article.
11. **Jabbour RJ**, Owen T, Weinberger F, Pandey P, Pantou D, Wang B, Couch L, King O, Perbellini F, Smith G, Stuckey D, Handa B, Pitcher D,

Shanmuganathan M, Lyon A, Siong Ng F, Terraciano C, Eschenhagen T, Harding SE. Preclinical Testing of an Upscaled Tissue Engineered Stem Cell Patch for Use in Translational Studies. Original Article.

12. Perbellini F, King O, Kit-Anan SW, **Jabbour RJ,** Watson SA, Saskia M, Wang B, Pitoulis F, Broyles C, Daniels M, Thum T, Harding SE, Terracciano CM. Human induced pluripotent stem cell-derived cardiomyocytes integration and maturation studied at a cellular/sub-cellular level using living myocardial slices. Original article.

**Selected Abstracts**

1. **Jabbour RJ,** Kapnisi K, Mawad D, Handa B, Couch L, Mansfield C, Perbillini F, Terracciano C, Stevens M, Lyon A, Smith G, Peters N, Ng FS, Harding SE. Conductive polymers affect myocardial conduction velocity but are not pro-arrhythmic. Poster Presentation. Munich, Germany, ESC Congress 2018.

2. **Jabbour RJ,** Owen T, Weinberger F, Pandey P, Pantou D, Wang B, Couch L, King O, Perbellini F, Smith G, Stuckey D, Handa B, Pitcher D, Shanmuganathan M, Lyon A, Siong Ng F, Terraciano C, Eschenhagen T, Harding SE. Development and Preclinical Testing of an Upscaled Tissue Engineered Stem Cell Patch for Use in Translational Studies. Oral Presentation, Beijing, China. ISHR 2019

**Selected Press Releases**

1. The Times

https://www.thetimes.co.uk/article/stem-cell-patch-beats-like-your-heart-tlsctw5zt

2. BBC news

https://www.bbc.co.uk/news/av/uk-england-london-47418245/stem-cell-heart-patches-could-savelives

3. BHF

https://www.bhf.org.uk/what-we-do/news-from-the-bhf/news-archive/2019/february/mending-broken-hearts-this-valentines-day

4. Imperial College London

https://www.imperial.ac.uk/news/190251/how-mend-brokenhearts/?ct=t(EMAIL_mainNL_2_27_2019_18_18)

5. Medscape

https://www.medscape.com/viewarticle/913862

**Grants Awarded**

2016 - British Heart Foundation PhD Clinical Research Training Fellowship - £215,481

- Mechanisms of arrhythmia generation from implanted stem cell-derived cardiomyocytes in infarcted hearts

2013 - BRC ACF pilot grant - £2000

- Award that enabled me to get pilot data towards my BHF PhD grant application

**Abbreviations**

ACEi: angiotensin converting enzyme inhibitor

ANP: atrial natriuretic peptide

ARNI: angiotensin II receptor–neprilysin inhibitor

APD: action potential duration

A.U.: arbitrary units

BB: beta-blocker

BDM: 2,3-Butanedione 2-monoxime

BHF: british heart foundation

BMNSCs: bone marrow mononuclear stem cells

BNP: B-type Natriuretic Peptide

BPM: beats per minute

Ca: calcium

CP: conductive polymer

CRT: cardiac resynchronisation therapy

CPCs: cardiospheres

CRISPR: clustered regularly interspaced short palindromic repeats

Cas: CRISPR associated protein 9

DAB: 3,3'-diaminobenzidine

ECG: electrocardiogram

ECs: endothelial cells

EHT: engineered heart tissue

FBS: fetal bovine serum

GMP: good manufacturing practice

GLP: good laboratory practice

H+E: hematoxylin-eosin

hESC-CM: human embryonic stem cell derived cardiomyocyte

HFmrEF: heart failure with mid-range ejection fraction

HFrEF: heart failure with reduced ejection fraction

HFpEF: heart failure with preserved ejection fraction

HLA:  human leukocyte antigen

ICD: Implantable cardiac defibrillator

LED: light emitting diode

LA: left atrium

LV: Left ventricle

LVAD: left ventricular assist device

MHRA: Medicines & Healthcare products Regulatory Agency

MSCs: Mesenchymal stem cells

NKM: non cardiomyocyte media

ipSC-CM: induced pluripotent stem cell derived cardiomyocyte

ICD: implantable cardioverter defibrillator

IM: intramuscular

MEA: microelectrode array

MHC: major histocompatibility complex

MM: millimetres

mRNA: Messenger RNA

MRI; magnetic resonance imaging

MS: milliseconds

NOS: Nitric oxide synthase

NCX: Sodium-Calcium transporter

NTproBNP: N-terminal –pro hormone B-type Natriuretic Peptide

PANI: polyaniline

PBS: phosphate buffered saline

PO: oral administration [per os]

PFA: paraformaldehyde

PMCA: plasma membrane Ca2+ ATPase

PSR: Picro Sirius Red

RA: right atrium

RAAS: renin-angiotensin-aldosterone system

Rh237: N-(4-Sulfobutyl)-4-(6-(4-(Dibutylamino)phenyl)hexatrienyl)Pyridinium

ROS: reactive oxygen species

RV: Right ventricle

RyR: ryanodine receptor

SSEA-1: stage-specific embryonic antigen-1

SMCs: smooth muscle cells

SNS: sympathetic nervous system

µm: micrometres

VF: ventricular fibrillation

VT: ventricular tachycardia

**Table of Contents**

**Declaration of Originality and copyright declaration** ..... **2**

**Acknowledgments** ..... **4**

**Abstract** ..... **5**

**Publications obtained during / related to this thesis** ..... **8**

**Manuscripts in preparation** ..... **9**

**Selected Abstracts** ..... **11**

**Selected Press Releases** ..... **12**

**Grants Awarded** ..... **13**

**Abbreviations** ..... **14**

**Table of Contents** ..... **17**

**List of Figures** ..... **24**

**List of Tables** ..... **28**

**1.1 Heart Failure** ..... **30**

1.1.1 Classification ..... 30

1.1.2 Epidemiology ..... 32

1.1.3 Aetiology of HFrEF ..... 33

1.1.4 Pathophysiology of HFrEF ..... 34

1.2 Medical Therapy ..... 40

1.3.1 Non-pharmacological therapies ..... 42

1.3.2 Implantable cardiac defibrillators ..... 43

1.3.3 Cardiac resynchronization therapy ..... 43

1.3.4 Mechanical circulatory support ..... 43

1.3.6 Transplantation ..... 45

1.3.7 Limitations of non-pharmacological therapy ..... 45

**1.4 Regenerative Medicine** ..... **46**

1.4.1 Exogenous stem cell therapy ..... 47

1.4.2 Clinical Data ..... 51

1.4.3 Skeletal myoblasts ..... 51

1.4.4 Bone marrow mononuclear cells ..... 52

1.4.5 Mesenchymal stem cells ..... 55
1.4.6 Resident cardiac progenitor stem cells ..... 58
1.4.7 c-kit Cardiac stem cells ..... 58
1.4.8 Cardiosphere-derived stem cells ..... 59
**1.5 Novel cell types and hurdles ..... 60**
1.5.1 Pluripotent stem cells ..... 61
1.5.2 The caveat of immaturity ..... 64
1.6 Preclinical and first in man data ..... 66
**1.7 Usefulness of biomaterials as an adjunct to cellular therapy ..... 68**
1.7.1 Engineered Heart Tissue ..... 68
1.7.2 Progression ..... 70
1.7.3 Improvements over monolayers ..... 72
1.7.4 Regenerative medicine application ..... 74
1.7.5 Upscaling ..... 75
1.7.6 Vascularisation ..... 76
1.7.7 Electromechanical integration ..... 76
1.7.8 Immunosuppression ..... 77
1.7.9 Ventricular arrhythmia ..... 78
1.7.10 Teratoma formation ..... 78
1.7.11 Clinical data ..... 78
1.7.12 Other uses: Drug Screening ..... 80
1.7.13 Disease modelling ..... 81
**1.8 Biomaterials - Conductive polymers ..... 81**
**1.9 Other regenerative medicine strategies ..... 84**
1.9.1 Gene therapy ..... 84
**1.10 Future regenerative strategies ..... 84**
1.10.1 Cell cycle re-entry ..... 84
1.10.2 Direct reprogramming ..... 86
**1.11 Conclusion ..... 86**
**Aims and hypothesis of current study ..... 87**
**Chapter 2: Materials and Methods ..... 89**
**2.1 Introduction ..... 90**
**2.2 In-vitro methods ..... 90**

2.2.1 Cell maintenance and differentiation of hiPSC ..... 90
2.2.2 Cardiomyocyte isolation ..... 91
**2.3 Engineered Heart Tissue ..... 92**
2.3.1 First generation ..... 92
2.3.2 Second generation ..... 93
2.3.3 EHT stock solutions ..... 95
**2.4 In-vitro engineered heart tissue characterisation ..... 97**
2.4.1 Contraction kinetics ..... 97
2.4.2 Calcium transients ..... 99
2.4.3 GECI ..... 99
2.4.4 Calcium Transient Analysis ..... 101
2.4.5 Cell Alignment ..... 102
2.4.6 Conduction velocities ..... 104
2.4.7 Calculation of Troponin T Retention in Graft ..... 106
2.4.8 Capillary density calculation ..... 108
**2.5 Immunohistochemistry ..... 110**
2.5.1 OCT embedding protocol ..... 110
2.5.2 Immunostaining protocol ..... 111
2.5.3 Paraffin staining protocol ..... 111
**2.5.4 Myocardial Histology ..... 112**
2.5.5 Haematoxylin and Eosin (H&E) ..... 113
2.5.6 Sirius Red ..... 113
**2.6 In-vivo methods ..... 114**
2.6.1 Animal husbandry ..... 114
2.6.2 Rabbits ..... 114
2.6.3 Terminal, non-recovery ..... 114
**2.6.4 Myocardial infarction ..... 116**
**2.6.5 Heart failure model ..... 120**
**2.7 EHT grafting protocol ..... 120**
**2.8 Telemetry ..... 122**
2.8.1 Reveal LINQ telemetry ..... 122
2.8.2 Indus Instruments Telemetry System ..... 123
2.8.3 Implantation ..... 125
2.8.4 Indus Recording Software ..... 126

**2.9 Echocardiography ..... 127**
**2.10 EHT explanation protocol ..... 128**
**2.11 Ex-vivo methods ..... 131**
2.11.1 Ex Vivo Isolated Rabbit Heart Perfusion ..... 131
2.11.2 Langendorff Perfusion Apparatus ..... 131
2.11.3 Heart isolation protocol ..... 132
**2.12 Optical Mapping ..... 134**
2.12.1 Principles ..... 134
2.12.2 Hardware configuration ..... 134
**2.13 Experimental protocols ..... 136**
2.13.1 Conductive polymer work ..... 136
2.13.2 Engineered heart tissue mapping ..... 136
2.13.3 Programmed electrical stimulation protocols ..... 138
**2.15 Statistical analysis ..... 140**

**Chapter 3: Characterisation of upscaled engineered heart tissue ..... 142**
**3.1 In-vitro characterisation of upscaled engineered tissue ..... 144**
**3.2 EHT calcium transient analyses ..... 147**
**3.3 Upscaled EHT immunohistochemistry ..... 149**
**3.4 Upscaled EHTs align over time ..... 151**
**3.5 Non-cardiomyocyte addition to EHT Mastermix ..... 155**
**3.6 EHT conduction velocity calculation ..... 158**
**3.7 Discussion ..... 160**
EHT upscaling ..... 160
Addition of non-cardiomyocytes ..... 162
Addition of Endothelial cells ..... 164
Analysis of contraction kinetics ..... 166
EHT morphology ..... 167
Calcium transient analysis ..... 168
Conduction velocity analysis ..... 169
Conclusion ..... 170

**Chapter 4: Establishing rabbit infarct and heart failure models ..... 172**
**4.1 Development of rabbit Infarct model ..... 174**
**4.2 Echocardiographic evaluation ..... 178**

**4.3 Serial Sections to quantify infarct size ..... 181**
**4.4 Development of heart failure model ..... 184**
**4.5 Echocardiographic evaluation of infarct size ..... 186**
**4.6 Discussion ..... 188**
Why the rabbit model? ..... 188
Rabbit Myocardial Infarction Model Set up ..... 190
Heart failure model ..... 195
Summary ..... 197
**Chapter 5: Preclinical testing of upscaled engineered heart tissue ..... 199**
**5.1 Development of EHT in-vivo grafting model ..... 201**
**5.2 Revised immunosuppression protocol ..... 204**
**5.3 EHTs become vascularised ..... 206**
**5.4 Graft cellular retention tested at serial time points ..... 209**
**5.5 Capillary density at serial time points ..... 212**
**5.6 Feasibility of grafting onto infarcted hearts ..... 214**
**5.7 EHTs improve ventricular function ..... 217**
**5.8 Optical mapping experiments ..... 221**
**5.9 Arrhythmogenic potential of EHTs ..... 225**
**5.10 Discussion ..... 229**
Optimisation of in-vivo grafting protocol ..... 229
Immunosuppression ..... 229
Attachment method ..... 231
Prosurvival cocktail ..... 232
Cellular retention ..... 233
EHTs and arrhythmia ..... 235
EHTs and left ventricular function ..... 240
Conclusion ..... 242
**Chapter 6: Ex-vivo testing of a conductive polymer patch ..... 243**
**6.1 Conductive Polymers affect conduction delay ..... 245**
**6.2 - Conduction polymers do not appear to affect action potential duration ..... 247**
**6.3 Conduction velocity does not appear to be changed when applying the patch to infarcted hearts ..... 250**

**6.4 Conductive polymers do not appear to be pro-arrhythmic ..... 252**
**6.5 Discussion ..... 254**
Conductive polymers ..... 254
Future work ..... 257
Translational outlook ..... 258
Conclusion ..... 259
**Chapter 7: Final Discussion ..... 260**
**7.1 Introduction ..... 261**
**7.2 Are EHTs a suitable modality for the future of regenerative medicine? 261**
**7.3 Are iPSC-CM the correct cell type in regenerative medicine? ..... 263**
**7.4 Insights from rabbit EHT grafting ..... 265**
**7.5 Moving from animal to human experiments ..... 266**
**7.6 Conclusion ..... 271**
**7.7 Review of Aims ..... 271**
7.7.1 Characterisation of upscaled EHT ..... 271
7.7.2 Development of in-vivo rabbit EHT grafting model ..... 272
7.7.3 Development of rabbit in-vivo EHT myocardial infarction model ..... 273
7.7.4 Development of in-vivo rabbit heart failure model ..... 273
**7.8 Review of hypotheses ..... 274**
7.8.1 Engineered heart tissue will mature in-vitro over time ..... 274
7.8.2 The encapsulation of hiPSC-CM in the EHT will increase cell retention 274
7.8.3 EHT will provoke arrhythmia when grafted onto infarcted rabbit hearts. 274
7.8.4 EHT will improve function in an intermediate model of myocardial infarction ..... 274
7.8.5 A conductive polymer patch will alter myocardial conduction when grafted onto the epicardium ..... 275
**7.9 Limitations of current work ..... 275**
**7.9.1 In-vitro work ..... 275**
The addition of non-cardiomyocytes to EHTs ..... 275
Cell number ..... 275
Gene analysis / PCR ..... 276
**7.9.2 In-vivo work ..... 277**
Echocardiography ..... 277

Telemetry ..... 277
Translational Model ..... 277
**7.9.3 Ex-vivo work ..... 277**
Conductive polymer ..... 277
Optical Mapping ..... 278
**7.10 Concluding remarks ..... 279**
**8: Bibliography ..... 281**

## List of Figures

### Chapter 1: Introduction

Figure 1-1 Heart failure classification ..... 32

Figure 1-2: Compensatory mechanisms in heart failure ..... 35

Figure 1-3: Pathways activated in heart failure ..... 37

Figure 1-4: Normal calcium cycling ..... 38

Figure 1.5: Guidelines recommmendations for HFrEF ..... 41

Figure 1-6: Non-pharmacological therapy for advanced HFrEF ..... 42

Figure 1-7: Current regenerative medicine strategies under investigation ..... 47

Figure 1-8: Meta-analysis of cell therapy and effect on ejection fraction ..... 49

Figure 1-9: Cell distribution post bone marrow intra-coronary injection ..... 50

Figure 1.10: Pathway from reprogramming somatic cells to iPSC-CM ..... 64

Figure 1-11: Pathway from reprogramming somatic cells to iPSC-CM ..... 65

Figure 1-12: Sustained retention of hESC-CM in infarcted macaque heart ..... 67

Figure 1-13: EHT medium throughput platform ..... 70

Figure 1-14: Different types of engineered heart tissue in investigation ..... 71

Figure 1-15: Histology of iPSC-CM post grafting in small / large animals ..... 76

Figure 1-16: Implantation of a Cardiovascular Progenitor cells Fibrin based Patch . 80

Figure 1-17: Paradigm behind conductive polymers and conductivity ..... 82

Figure 1-18: Fabrication of PANI patch ..... 83

### Chapter 2: Materials and Methods

Figure 2-1: Engineered heart tissue silicone posts and Teflon spacers ..... 93

Figure 2-2: Macroscopic images of upscaled engineered heart tissue ..... 94

Figure 2-3: Principles of MUSCLEMOTION ..... 98

Figure 2-4: gCaMP6f ..... 101
Figure 2-5: Cell alignment ..... 103
Figure 2-6: Example of MEA electrode recordings ..... 105
Figure 2-7: Microelectrode array and plastic mesh / weight ..... 106
Figure 2-8: Troponin measurement macro ..... 107
Figure 2-9: Processing of CD31 stained images ..... 109
Figure 2-10: Graft capillary density calculation ..... 110
Figure 2-11: rabbit V-gel ..... 115
Figure 2-12: Merlin ventilator and Zoll defibrillator ..... 118
Figure 2-13: Image depicting coronary ligation suture ..... 119
Figure 2-14: EHT grafting protocol ..... 121
Figure 2-15: Reveal LINQ device ..... 123
Figure 2-16: Tracing of Reveal LINQ telemetry ..... 123
Figure 2-17: Indus Telemetry set up ..... 125
Figure 2-18: Telemetry transmitter ..... 126
Figure 2-19: Telemetry system dashboard ..... 127
Figure 2-20: Fractional area change measurement ..... 128
Figure 2-21: Image of abdominal aorta and inferior vena cava ..... 130
Figure 2-22: Heart attachment to cannula and perfusion system ..... 133
Figure 2-23: Optical mapping set up ..... 135
Figure 2-24: Electrocardiographic recordings of arrhythmia provocation protocols 139

**Chapter 3: Characterisation of upscaled engineered heart tissue**

Figure 3-1: EHT Contraction Kinetics over time ..... 146
Figure 3-2: EHT calcium kinetics ..... 148

Figure 3-3: EHT immunostaining ..... 150

Figure 3-4: EHT morphological alignment over time ..... 153

Figure 3-5: Addition of non-cardiomyocytes ..... 156

Figure 3-6: Conduction Velocities ..... 159

**Chapter 4: Establishing rabbit infarct and heart failure models**

Figure 4-1: Establishing the myocardial infarction procedure ..... 176

Figure 4-2: Echocardiographic confirmation of myocardial infarction ..... 180

Figure 4-3: Serial sections of infarcted tissue ..... 183

Figure 4-4: Serial sections of heart failure model ..... 185

Figure 4-5: Heart failure echocardiographic data ..... 187

**Chapter 5: Preclinical testing of upscaled engineered heart tissue**

Figure 5-1: Preliminary in-vivo grafting results ..... 203

Figure 5-2: Revised in-vivo grafting protocol ..... 205

Figure 5-3: EHT vascularisation ..... 208

Figure 5- 4: Troponin T retention at serial time points ..... 211

Figure 5-5: Graft vascularisation over time ..... 213

Figure 5-6: Feasibility of grafting onto infarcted hearts ..... 215

Figure 5-7: EHTs improve left ventricular function ..... 219

Figure 5-8: Ex-vivo optical mapping studies ..... 223

Figure 5-9: Arrhythmogenic potential of EHTs ..... 227

**Chapter 6: Ex-vivo testing of a conductive polymer patch**

Figure 6-1: Conductive polymers affect global conduction delay ..... 246

Figure 6-2: Conductive polymers do not appear to affect action potential duration 248
Figure 6-3: Conductive polymers do not appear to affect conduction velocity of infarcted hearts ..... 251
Figure 6-4: The conductive polymer patch does not appear to be pro-arrhythmic in nature ..... 253

## List of Tables

### Chapter 1: Introduction

Table 1-1: Common aetiologies of HFrEF ..... 34

Table 1-2: Recent trials involving BMNSCs and MSCs. ..... 57

Table 1-3: Summary of trials involving cardiac stem cells and cardiospheres ..... 60

### Chapter 2: Materials and Methods

Table 2-1: Master Mix solutions for engineered heart tissue ..... 96

Table 2-2: Arrhythmia provocation protocol scoring system ..... 140

# Chapter 1: Introduction

### 1.1 Heart Failure

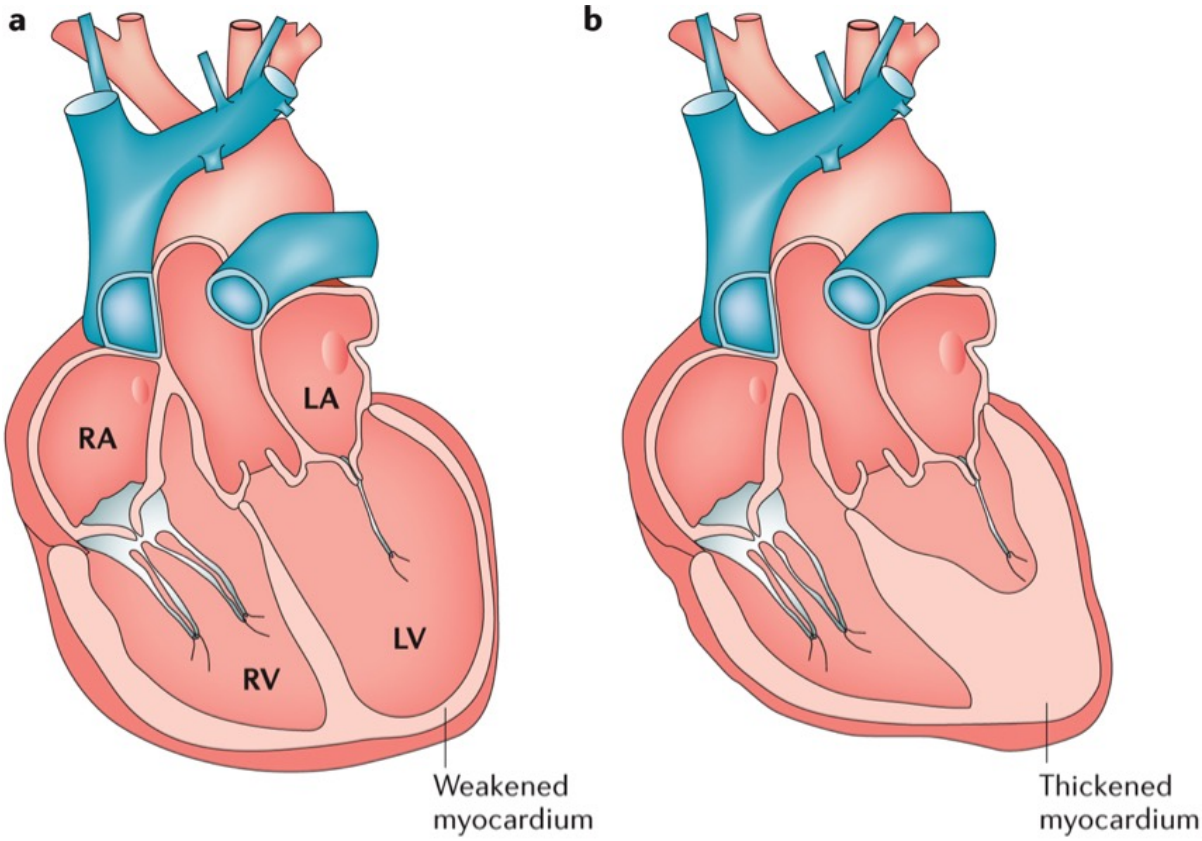
Heart failure is a complex clinical syndrome associated with considerable morbidity and a mortality rate higher than several common cancers including bowel and prostate.(Mamas *et al.*, 2017) It is associated with an enormous financial burden to healthcare systems, accounting for 1-2% of the NHS budget and estimated to cost over 100 billion dollars worldwide in healthcare costs each year.(Cook *et al.*, 2014) Despite decades of research, few effective treatment options exist, with a 5-year survival of only 50% once symptoms develop.(Taylor *et al.*, 2019)(Lozano *et al.*, 2012) Current treatments modalities are predominantly associated with slowing disease progression rather than reversing or treating the disease process. Therefore, recently, a great deal of research has been focussed on exploring numerous original strategies to regenerate the heart, spanning from exogenous stem cell therapy, which has reached human clinical trials to activating endogenous repair mechanisms which are still at the preclinical stage. This is because, unlike the dramatic improvements that have been seen in treating myocardial infarctions, this unfortunately has not been seen in heart failure, with stubbornly low and constant survival rates over the last 15-20 years.(Taylor *et al.*, 2019)

#### 1.1.1 Classification

The 2016 guidelines from the European Society of Cardiology define heart failure as a: “clinical syndrome characterized by typical symptoms (e.g. breathlessness, ankle swelling and fatigue) that may be accompanied by signs (e.g. elevated jugular venous pressure, pulmonary crackles and peripheral oedema) caused by a structural and/or functional cardiac abnormality, resulting in a reduced cardiac output and/or elevated intracardiac pressures at rest or during stress.”(Coats *et al.*, 2016) This

definition implies that heart failure still remains a clinical diagnosis with other tests used as confirmation (blood investigations and imaging). Heart failure can be grouped into heart failure with reduced ejection fraction (HFrEF) or heart failure with preserved ejection fraction (HFpEF). Broadly speaking, HFrEF is typically due to poor pump function due to weakened myocardium; for example, post myocardial infarction or dilated cardiomyopathy. In contrast, HFpEF is due to conditions that give rise to thickened and hypertrophied ventricles where systolic function is normal but the heart cannot relax properly (termed diastolic dysfunction).(Bloom *et al.*, 2017) Approximately 50% of patients diagnosed with heart failure have HFpEF and differentiating between the two is important (Figure 1-1). Heart failure with reduced ejection fraction is the older classification and the type that most clinicians are most familiar with. There are several prognostic medications and devices that improve survival. In contrast, despite numerous randomized clinical studies, heart failure with preserved ejection fraction does not currently have any treatment options that significantly improve hard end-points and treatment therefore is aimed at controlling the underlying cause (e.g. hypertension, atrial fibrillation). The recent European guidelines also have introduced heart failure with mid-range ejection fraction: this is primarily due to the lack of research in this area and possible overlap between HFrEF and HFpEF.(Coats *et al.*, 2016)

**Figure 1-1: Heart failure classification**




*A) Heart failure with reduced ejection is primarily due to poor systolic ventricular contraction because of weakened myocardium; B) Preserved ejection fraction heart failure is generally due to inefficient relaxation, causing diastolic dysfunction, which is generally due to thickened and hypertrophied myocardium. Reused with permission; Reference:* (Bloom *et al.*, 2017)

### 1.1.2 Epidemiology

Chronic heart failure affects approximately 2% of the world's population. There is a strong correlation regarding age and prevalence ranging from <2% in the under 60 year olds to >10% in the over 75s.(Bloom *et al.*, 2017) Well known associated conditions include: hypertension, coronary artery disease, cardiomyopathies, and valve disease. Currently, the lifetime risk of developing heart failure is 20%; however,

with the improvement in treated cardiovascular disease (e.g. STEMI), the prevalence is projected to increase by up to 25% in the next 20 years.(Metra and Teerlink, 2017) This epidemic will increase healthcare associated costs – by over 200% in the next 20 years.(Bloom *et al.*, 2017) Since healthcare associated costs already account for 2-3% of most healthcare systems in high income countries, it is critical to focus research on improving outcome and disease prevention.(Metra and Teerlink, 2017) Patients with heart failure have a mortality rate worse than several cancers and have considerable morbidity with frequent hospital admissions. Device therapy and medical therapy have improved mortality but average rates range from 6-7% per year in stable patients with a dramatic increase to 25% or more per year if hospitalised for heart failure.(Metra and Teerlink, 2017)

### 1.1.3 Aetiology of HFrEF

Coronary artery disease is the predominant driver of developing HFrEF, being responsible for nearly 2 out of every 3 cases, whilst the predominant attributable risk factor however is hypertension (Table 1-1). Other cardiovascular causes include: 1) cardiomyopathies; 2) myocardial infarction; 3) myocarditis; 4) valvular heart disease whilst non-cardiovascular causes include endocrine disorders including thyroid dysfunction, systemic diseases including sarcoidosis and SLE, alcohol, or more recently oncological drugs.(Bloom *et al.*, 2017) The initiating event that culminates in a deterioration in pump function can be acute in onset; for example, myocardial infarction, myocarditis, Takotsubo syndrome. In contrast, it can be chronic or insidious in onset; for example, heart failure due to pharmacotherapy including doxorubicin / anthracyclines or the development of non-ischaemic dilated cardiomyopathy. In some cases, the symptoms of heart failure (shortness of breath,

orthopnoea, paroxysmal nocturnal dyspnoea) can manifest years after the initial insult. (Taylor *et al.*, 2019)

**Table 1-1: Common aetiologies of HFrEF**

| Cardiovascular | Non-cardiovascular |
|---|---|
| Coronary artery disease | Endocrine (Thyroid) |
| Hypertension | Systemic (SLE, Sarcoid) |
| Myocardial infarction | Alcohol excess |
| Cardiomyopathies | Cocaine |
| Myocarditis | Chemotherapy |
| Valvular heart disease | |

*Common causes of heart failure with reduced ejection fraction.*

### 1.1.4 Pathophysiology of HFrEF

The pathophysiology of heart failure with reduced ejection fraction is multifaceted and complex but usually however begins with a "primary myocardial insult"; either from a ruptured plaque (MI), the development of dilated cardiomyopathy or the progression of coronary artery disease. The initial insult then leads to a progressive reduction in left ventricular function. This leads to several compensatory mechanisms (myocardial, neurohormonal, endothelial pathways), which aim to restore function, but eventually the compensatory mechanisms perpetuate the disease process leading to heart failure with a worsening of symptoms.(Coats *et al.*, 2016) The insult initially causes an upregulation of the sympathetic nervous system

and renin-angiotensin-aldosterone system. Vessel vasoconstriction occurs via endothelin and cytokine mediated pathways. These are beneficial and compensatory initially, with improvements in myocardial contractility and cardiac output; however, chronically the effects are deleterious, leading to apoptosis, fibrosis, and left ventricular remodelling (Figure 1-2). Sudden cardiac death, often due to lethal ventricular arrhythmias is often a final common pathway.(Lozano *et al.*, 2012)

**Figure 1-2: Compensatory mechanisms in heart failure**

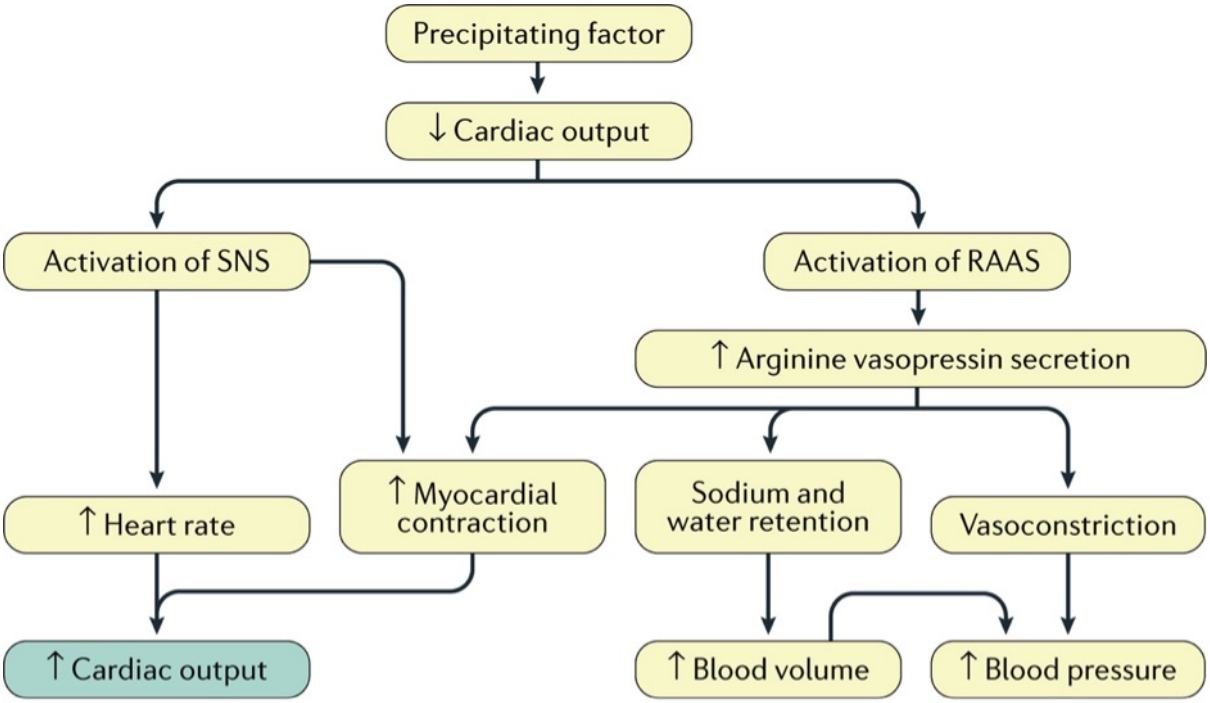



*Diagram illustrating compensatory improvements to improve cardiac output post myocardial injury leading to a reduction in cardiac output. Reused with permission; Reference:* (Bloom *et al.*, 2017)

The reduction in cardiac output post myocardial injury is the primary driver of activating the renin-angiotensin-aldosterone system. This leads to arginine vasopressin secretion from the posterior pituitary gland, which improves blood volume and blood pressure by vasoconstriction and sodium and water retention.(Bloom *et al.*, 2017) It also directly increases inotropy, which also is increased by activation of the sympathetic nervous system, which additionally increases chronotropy. Long standing sympathetic stimulation causes β-adrenoreceptor downregulation, which consequently results in a blunted response of the myocardium to catecholamines, which translates into decreased inotropy and a reduction in ventricular function. As well as a reduction in ventricular contraction, a chronic sympathetic state can lead to the development of pathological arrhythmias and sudden cardiac death. The heart failure syndrome causes chronic stimulation of RAAS leading to increased angiotensin II and aldosterone levels, which results in the development of myocyte hypertrophy and interstitial fibrosis or adverse ventricular remodelling (Figure 1-3).(Bloom *et al.*, 2017)

**Figure 1-3: Pathways activated in heart failure**

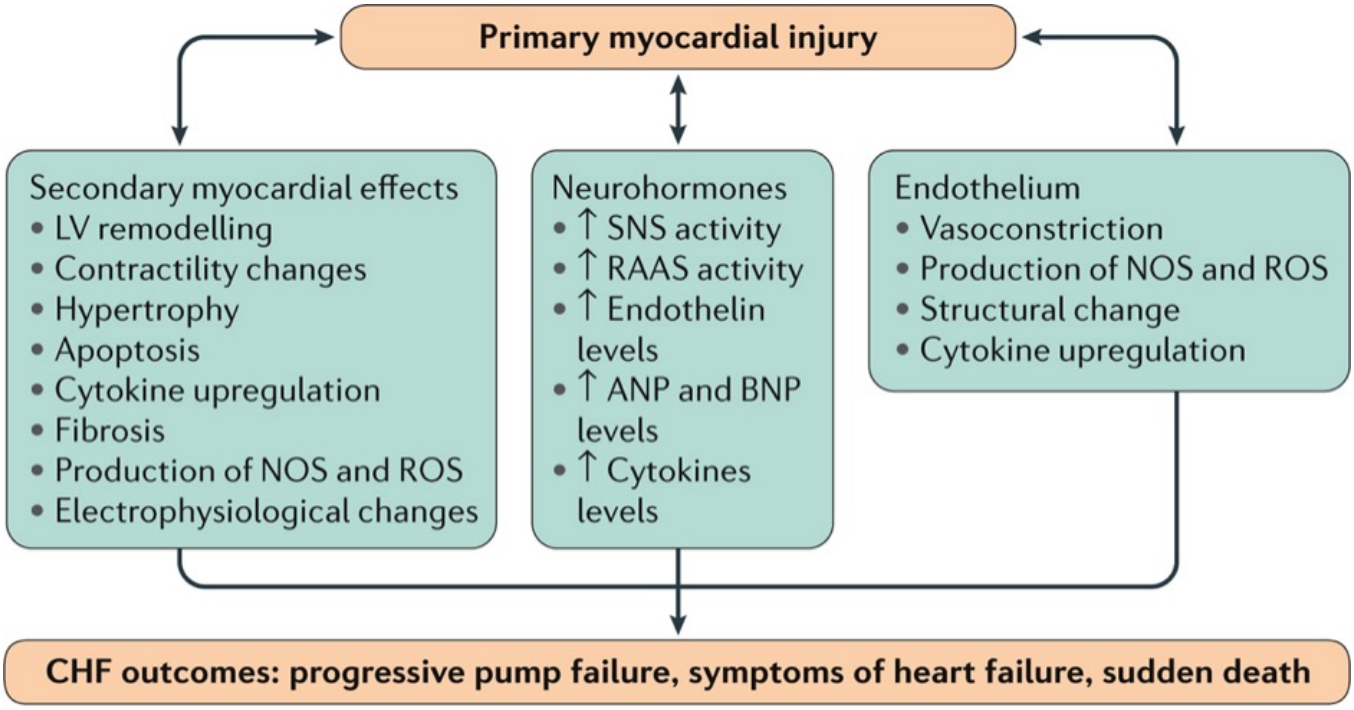



*Diagram illustrating the pathways activated in heart failure post primary myocardial injury. LV: left ventricle, SNS: sympathetic nervous system, RAAS: renin–angiotensin–aldosterone system, BNP: natriuretic peptide B; CHF: congestive heart failure; NOS: nitric oxide synthase; ROS: reactive oxygen species.*

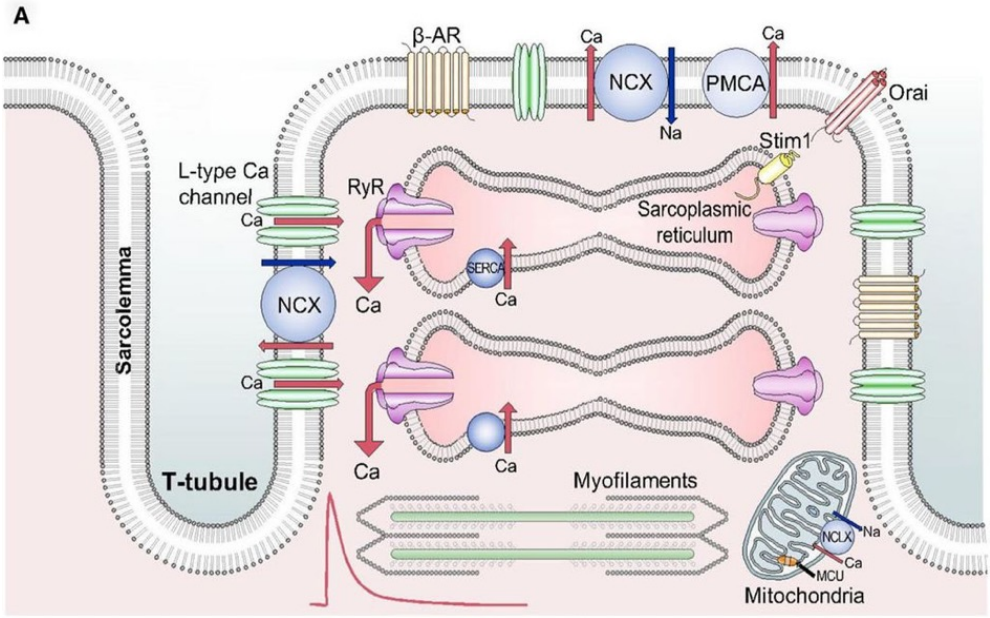
*Reused with permission; Reference:* (Bloom *et al.*, 2017)

The correlation between the initial myocardial insult and the actual progression of disease and the development of HFrEF is multi-layered and intricate.

There are changes that occur at genetic / molecular / protein and cellular levels with aberrant calcium handling and metabolic alterations. (Taylor *et al.*, 2019) They are generally thought to occur secondary to paracrine factors released from remaining dysfunctional cells and the cell death that occurs post cardiac injury. Among the contractile changes that occur there is an overall reduction in myosin / myofibrils along with a reduction in myofibrillar ATPase. In addition, there is a shift from B

myosin heavy chain to A myosin heavy chain. Chronic heart failure also leads to myocyte loss from apoptosis, necrosis and autophagy. There is also increased collagen deposition and a shift to type I subtype.(Bloom *et al.*, 2017)

**Figure 1-4: Normal calcium cycling**




*Cardiac contraction consists of calcium induced calcium release. NCX: sodium-calcium transporter, Ca: calcium; RyR: ryanodine receptor; Na: sodium; SERCA; B-AR: beta-adrenoreceptor. Reused with permission; Reference:* (Eisner *et al.*, 2017)

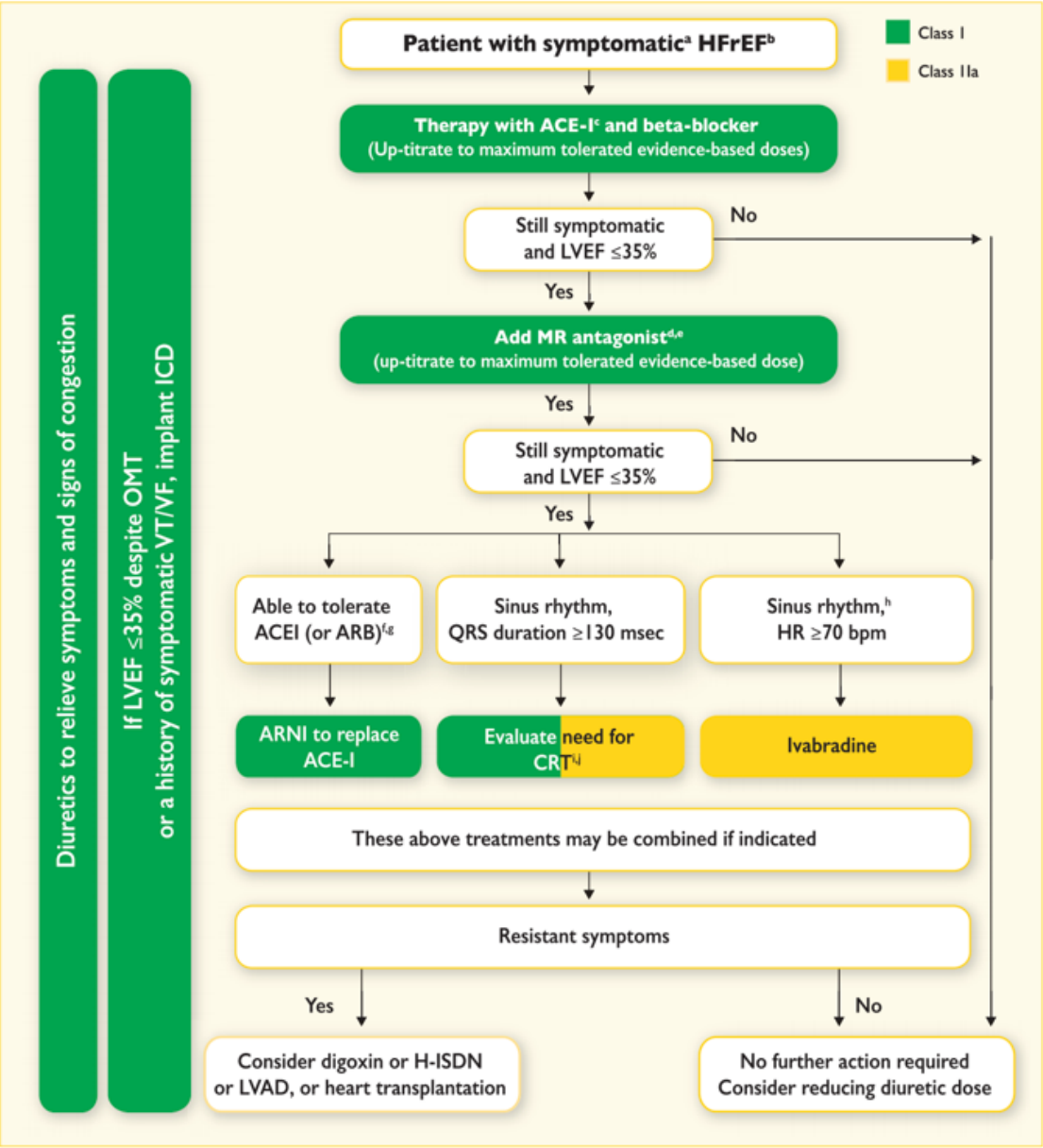
Calcium induced calcium release is the fundamental pathophysiological process that allows normal myocyte contraction (Figure 1-4). Firstly, cytosolic calcium binds to the L-type calcium channels which then triggers calcium release from the sarcoplasmic reticulum via the ryanodine receptors, which then allows myofilament contraction due to a conformational change in the tropomyosin complex.(Eisner *et al.*, 2017) Restoration of sarcoplasmic calcium is via SERCA dependent calcium channels and normalisation of cytoplasmic calcium is also achieved by sarcolemmal calcium-Na

transporters.(Eisner *et al.*, 2017) In heart failure, intracellular calcium is often accumulated due to dysfunction in SERCA and calcium extrusion via the sodium-calcium transporters. (Coats *et al.*, 2016) The calcium transients are often prolonged leading to early or delayed after depolarisations which can promote arrhythmogenesis. In addition, abnormalities occur in membrane bound sodium and potassium channels which further prolong action potential duration and promote arrhythmogenesis. (Coats *et al.*, 2016) In terms of metabolism, aberrations have been reported including a switch to a greater dependence on glucose and decrease in oxidative phosphorylation due to mitochondrial dysfunction. Although all the aforementioned aberrations have been reported, the timing in relation to one another and the initial myocardial insult is still not yet well known.(Bloom *et al.*, 2017)

### 1.2 Medical Therapy

Neurohormonal antagonists remain the cornerstone for managing systolic heart failure. Treatment with ACEi and beta-blockers should be initiated at relatively low doses but then be aggressively up-titrated to the maximum tolerated evidence based dose.(Figure 1-5) If symptoms persist, and the ejection fraction is below 35%, a mineralocorticoid antagonist can then be added. In recent years, relatively newer medications have become available and are now being incorporated into the guidelines based on the results of randomised data. These include ivabradine, an $I_f$-channel inhibitor, that causes a reduction in resting heart rate via the SA node and should be prescribed to patients who remain symptomatic with a resting heart rate >70bpm,  Recently, a newer medication (sacubitril/valsartan [angiotensin II receptor – neprilysin inhibitor; ARNI]) has appeared which has shown superiority over conventional ACEi (enalapril) including a reduction in all-cause mortality, cardiovascular death as well as improvement in symptoms. Diuretics do not affect prognosis but are primarily used to prevent fluid overload and symptomatic control. Digoxin has some benefit for symptomatic control and reduced hospitalization but no effects on hard endpoints.(Coats *et al.*, 2016)

**Figure 1-5: Guidelines recommendations for HFrEF**

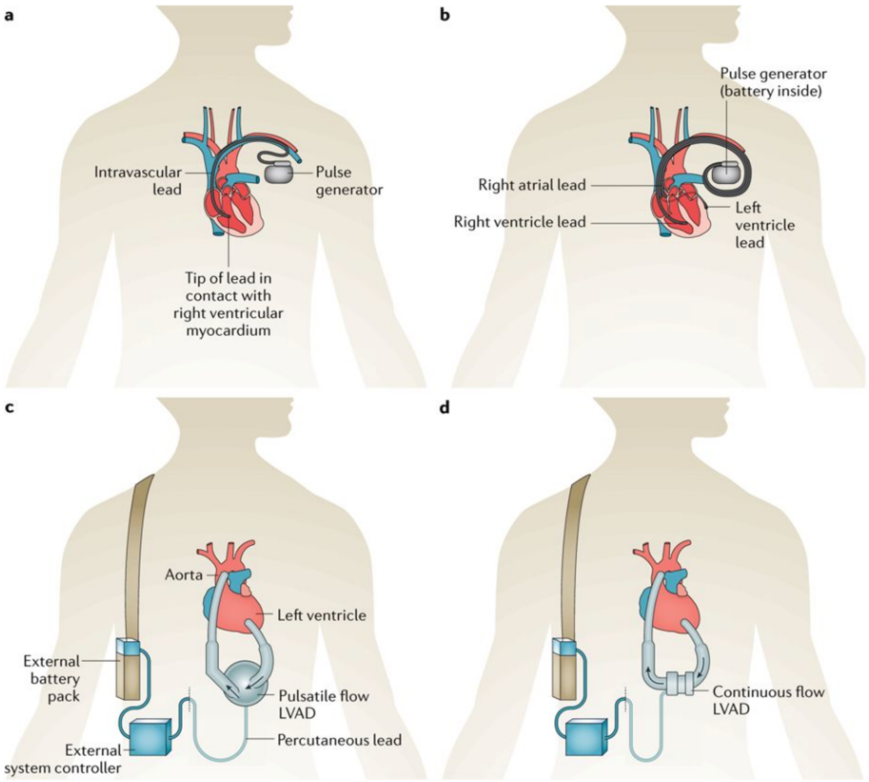



*ESC Heart failure treatment pathway. ARB, angiotensin receptor blocker; ARNI, angiotensin II receptor–neprilysin inhibitor; BP, blood pressure; COR, class of recommendation; C/I, contraindication; CrCl, creatinine clearance; CRT, cardiac resynchronization therapy; CRT-D, CRT defibrillator; ICD, implantable cardioverter defibrillator; LBBB, left bundle branch block; LVAD, left ventricular assist device; LVEF, left ventricular ejection fraction; MI, myocardial infarction; NSR, normal sinus rhythm; NYHA, New York Heart Association. Reused with permission; Reference:* (Coats *et al.*, 2016)

### 1.3.1 Non-pharmacological therapies

Non-pharmacological strategies for HFrEF are generally targeted for use in advanced heart failure patients with symptoms refractory to maximal medical therapy. Device therapy ranges from implantable cardioverter defibrillators (ICDs), which can be inserted for both primary and secondary prevention reasons in patients with HFrEF to left ventricular assist devices which can be used as a bridge to cardiac transplant or in some cases a destination therapy (Figure 1-6). (Coats *et al.*, 2016)

**Figure 1-6: Non-pharmacological therapy for advanced HFrEF**




*A) Implantable cardioverter defibrillators; B) cardiac resynchronisation therapy; C) pulsatile flow left ventricular assist device; D) continuous flow LVAD. Reused with permission; Reference:* (Bloom *et al.*, 2017)

### 1.3.2 Implantable cardiac defibrillators

Implantable cardiac defibrillators are predominantly implanted to prevent the sudden cardiac death due to lethal ventricular arrhythmias that are often the final common pathway in heart failure. An ICD can detect and treat pathological ventricular arrhythmias via the delivery of an electric shock or via anti tachycardia pacing. European guidelines recommend ICD therapy in all patients with an ejection fraction ≤35% despite optimal pharmacological therapy, but generally only if life expectancy >1 year and relatively good baseline function. (Coats *et al.*, 2016).

### 1.3.3 Cardiac resynchronization therapy

Cardiac resynchronisation therapy (CRT) improves morbidity and mortality in patients with a broad QRS interval and HFrEF. Guidelines recommend CRT to symptomatic patients with a prolonged QRS duration (≥130 ms) who are in sinus rhythm with EF≤35% despite maximal medical therapy. It has been proven that CRT promotes reverse remodelling in many patients but up to 30% of patients are non-responders to therapy. Possible reasons include type of conduction disturbance (LBBB better responders), extensive scar and lead placement. (Coats *et al.*, 2016)

### 1.3.4 Mechanical circulatory support

Advanced heart failure occurs when optimal medical therapy and device therapy is no longer effective and patients have treatment refractory heart failure. These patients suffer from persistent symptoms, often at rest, and are frequently admitted to hospital for protracted periods of time and have considerable morbidity and a high mortality rate. Options in these patients include mechanical circulatory support and cardiac transplantation. Critical to future management is the identification and early

referral of these patients to a specialist tertiary centre for initiation of advanced management pathways since quality of life and mortality may be improved if advanced treatment is started earlier in the disease process. (Bloom *et al.*, 2017)

### 1.3.5 LVADs

Guidelines initially recommended left ventricular device therapy as a bridge to cardiac transplantation, but due to favourable results with LVAD therapy regarding reverse remodelling and the paucity of available donors, it is now considered as a destination therapy in some circumstances. Newer device iterations include continuous flow LVADs, which have improved survival as well as symptoms and quality of life when compared to first generation pulsatile flow LVADs. Continuous LVADs can be further subdivided into axial flow devices (HeartMate II™ [Thoratec Corporation, San Diego, CA]) and centrifugal flow ([HeartWare® (HeartWare International, Framingham, MA] or HeartMate 3™ [Abbott Laboratories, Lake Forest, IL]). (Bloom *et al.*, 2017)

LVADs are usually reserved for advanced heart failure patients' dependent on inotropic support, but some observational data has shown that continuous LVAD therapy may be of benefit earlier in the disease process. The mortality rate even after continuous LVAD insertion is not insignificant with data from an European Registry publishing 1-year survival rates of 72% and 2-year of 62.8%.(de By et al., 2015)

### 1.3.6 Transplantation

Heart transplantation is still the treatment of choice for patients with advanced refractory heart failure and offers the best chance of survival and improving quality of life. Inclusion criteria consists of patients' being dependent on inotropic support or those with poor exercise capacity despite maximal medical therapy. Prognostic scores exist and should be considered when assessing eligibility. Due to the relative lack of donors and risk of invasive therapy, several contraindications exist including excessive obesity, severe pulmonary hypertension, advanced renal failure, active substance abuse and history of recent or active malignancy. Data from the International Society for Heart and Lung Transplantation (ISHLT) has reported 1 year survival rates of over 80% and median survival rates of 11 years.(Lund *et al.*, 2016)

### 1.3.7 Limitations of non-pharmacological therapy

Despite LVADs convincing evidence of improving morbidity and mortality, they are not without risk of complications. For example, serious haematological complications including haemolysis and thrombosis, GI bleeding, stroke and right ventricular failure can occur seriously affecting morbidity.

The situation is similar with cardiac transplantation. Early mortality rates (<30 days) are predominantly related to graft failure / rejection whilst later cases (5 years) are related to the development of malignancies and allograft vasculopathy. The need for constant immunosuppression is primarily responsible for complications and this has improved with newer immunosuppressive regimes; however, hypertension and renal failure are relatively common (HTN 91% at 5 years, 68% at 10 years for renal dysfunction). Allograft vasculopathy increases over time from around 25% at 1 year

to 50% at 10 years. (Yusen *et al.*, 2014; Bloom *et al.*, 2017)

Despite the impressive results of cardiac transplantation when compared to medical and device therapy, unfortunately due to the lack of donors, there will never be enough donor hearts and newer treatment modalities are urgently needed to help target the disease process.

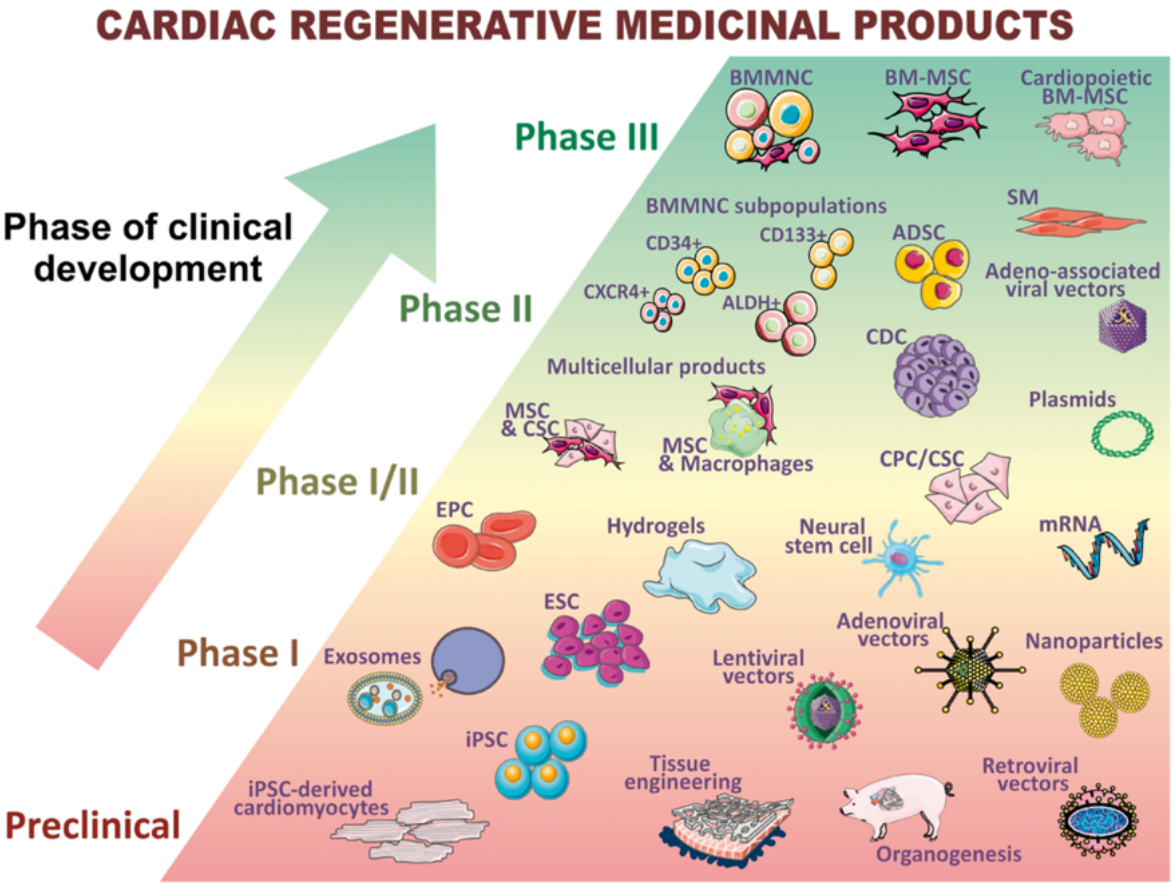
Overall, the lack of improvements in mortality rates (50% survival at 5 years) despite the introduction of non-pharmacological therapies spawned the development of the cardiac regenerative medicine field, with the aim of regenerating or restoring myocardial function and therefore reversing the disease process.

### 1.4 Regenerative Medicine

In the last 15 years, a vast amount of research has been focussed on exploring numerous novel biological therapies to try and repair damaged hearts. Some treatment modalities have already reached clinical trials (up to phase III); for example, exogenous administration of autologous / allogenic stem cell therapies including unfractionated bone marrow mononuclear stem cells (BMNSCs). In contrast, more radical and newer paradigm treatment modalities including reactivating endogenous myocyte repair mechanisms or direct reprogramming methods, are still being investigated in pre-clinical studies. It has now become clear that cellular therapy alone may be insufficient for a sustained improvement in function and therefore recent research has been focussed on combining cells with biomaterials to enhance cell retention and improve efficacy. For example, tissue engineering, which is the encapsulation cells in a hydrogel or scaffold in-vitro to

create 3-D constructs has been shown to be a promising method in preclinical models (Figure 1-7).

**Figure 1-7: Current regenerative medicine strategies under investigation**




*Current regenerative medicine strategies under investigation. Bone marrow mononuclear cells have reached phase III trials. In contrast, induced pluripotent stem cell derived cardiomyocytes are largely at the preclinical stage. Reused with permission; Reference:* (Fernández-Avilés *et al.*, 2017)

### 1.4.1 Exogenous stem cell therapy

Exogenous administration of cells was initially thought to improve myocardial function via a multitude of different mechanisms including transdifferentiation or reactivating endogenous repair mechanisms; however, it has become apparent that

the most likely mechanism of improvement is paracrine in nature. Numerous cell types have been researched in chronic heart failure that include: 1) skeletal myoblasts, which were one of the first to be investigated; 2) BMNSCs (which have been most extensively investigated in humans); 3) mesenchymal stem cells; 4) endogenous cardiac stem cells and 5) more recently pluripotent stem cell-derived cardiomyocytes (derived from either human adult or embryonic origin).

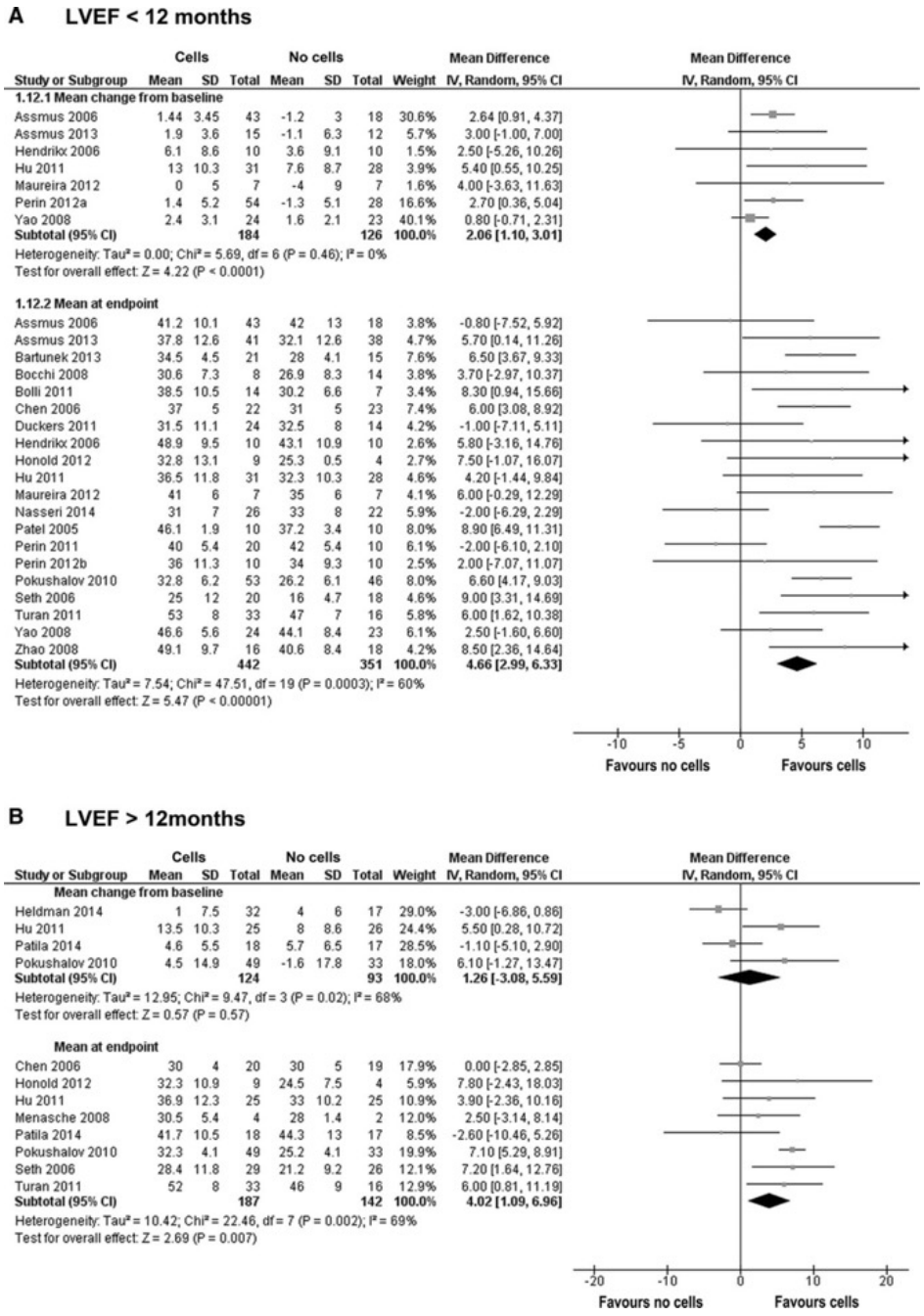
The first clinical trials were undertaken after the results of numerous encouraging pre-clinical studies were published; however, the results of exogenous stem cell therapy for chronic heart failure have been disappointing.(Fisher *et al.*, 2015)(Madonna *et al.*, 2016) Only minor improvements in function (Figure 1-8) and other structural parameters along with symptoms have generally been seen in the clinical trials and it may be related to the lack of cell retention seen with existing delivery methods (intra-coronary / intra- myocardial). To date actual cardiac regeneration (de novo myocardium) has not reliably been shown in any study so far.(Madonna *et al.*, 2016; Fernández-Avilés *et al.*, 2017)

The poor cell retention is likely due to several factors including:

1) Cell washout after injection with high concentrations found in spleen and liver (Figure 1-9),
2) Unfavourable and toxic environment of the myocardium,
3) Upregulation of apoptotic pathways,
4) Ischaemia of cells due to inadequate supply of blood / nutrients,
5) Matrix detachment,
6) Immunological rejection (Chong and Murry, 2014)(Don and Murry, 2013)

**Figure 1-8: Meta-analysis of cell therapy and effect on ejection fraction**

.

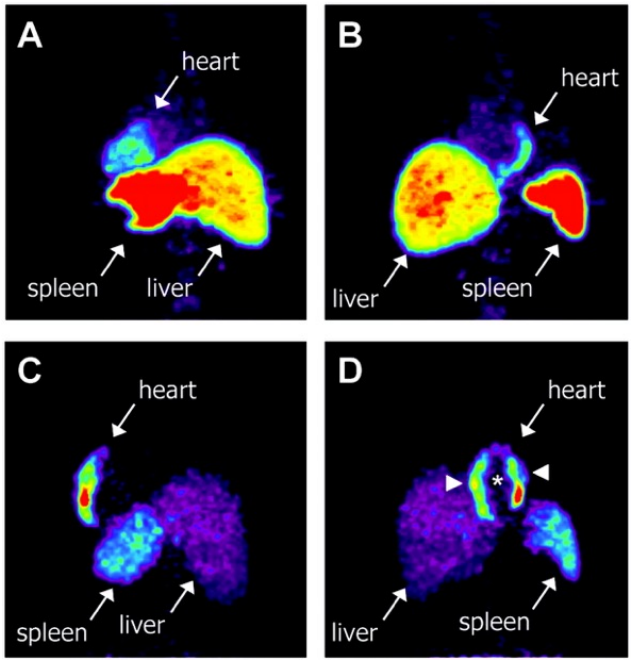



*Forest plot of effect of exogenous stem cell therapy for the treatment of heart failure. Reused with permission; Reference:* (Fisher *et al.*, 2015)

Data from numerous preclinical and clinical studies imply that the exogenous stem cells secrete numerous cytokines / growth factors that promote angiogenesis,

provide beneficial paracrine signalling to the diseased heart, or even activate endogenous CPCs leading to transdifferentiation into de-novo myocytes. However, recent data regarding cardiac stem cells has been conflicting and it has now become apparent that endogenous cardiac stem cells are found in much lower numbers than previously thought and have minimal cardiogenic potential.(Neidig *et al.*, 2018)(Zhang *et al.*, 2018)(Maliken and Molkentin, 2018) Additionally, numerous landmark publications have been recently withdrawn from a prominent researcher in the cardiac stem cell field. This has cast doubt on endogenous regeneration using cardiac stem cells in general and has also tarnished the reputation of the field with the wider general public.(Maliken and Molkentin, 2018)(Chien *et al.*, 2019)

**Figure 1-9: Cell distribution post bone marrow intra-coronary injection**




*Bone marrow distribution after intracoronary injection in human infarcted hearts. (18F-FDG–labelled autologous bone marrow cells). Left posterior oblique (A) and left anterior oblique (B) views of a human patient 65 minutes post injection into left circumflex coronary artery. Cells detectable in the lateral wall of the heart (infarct*

*centre and border zone), liver, and spleen. Left posterior oblique (C) and left anterior oblique (D) views of chest and upper abdomen of another patient 70 minutes post injection into left anterior descending coronary artery. CD34-enriched cells detected in the anteroseptum of heart, liver and spleen. Cell homing occurs in infarct border zone (arrowheads) but not centre (asterisk). Reused with permission; Reference: (Hofmann et al., 2005)*

### 1.4.2 Clinical Data

To date, most human clinical data has involved relatively small, phase I/II, open-label studies which therefore naturally have been underpowered for hard endpoints including mortality. In addition, many were unblinded without adequate sham control arms, which makes them subject to inherent biases. A meta-analysis of 31 studies (1521 patients), elegantly describes this situation.(Fisher *et al.*, 2015) The overall analysis found not only reported improvements in symptoms (NYHA class) and LVEF but also the hardest endpoint of mortality. However, when accounting for biases due to poor trial design, no benefits were seen in any endpoint studied in the double-blinded trials.(Fisher *et al.*, 2015) Depending on the type of cell, the clinical experience is varying but several phase III trials are currently ongoing and will provide a more reliable answer regarding the efficacy of cell therapy using current delivery methods and cell types.

### 1.4.3 Skeletal myoblasts

This cell type was one of the first to be studied and reach clinical translation. There was great enthusiasm from the clinical community due to the autologous nature (skeletal muscle progenitor cells) and the relative similarity to cardiomyocytes. In

addition, the relative ease in which they could be expanded ex-vivo made them potentially ideal for replacing lost muscle. After several encouraging pre-clinical studies, human clinical data were neutral / negative with reports of pathological ventricular arrhythmia in the treatment arm.

The landmark trial involving skeletal myoblasts was the Myoblast Autologous Grafting in Ischemic Cardiomyopathy (MAGIC) Trial. MAGIC was a randomized, placebo-controlled trial that investigated the efficacy of myoblasts in ischaemic heart failure patients undergoing cardiac surgery (CABG) at varying doses (400 [33 patients] or 800 million [34 patients]) against a placebo controlled arm (30 patients). (Menasché *et al.*, 2008)

Importantly, cells were injected intramyocardially during CABG and every patient had implantable cardiac defibrillator devices inserted. At follow-up, the primary endpoint of change in LVEF was not met and pathological ventricular arrhythmias were observed in the cell treated groups. Because of the data from this trial, skeletal myoblasts are not the favoured cell type, the lack of efficacy may be due to inadequate electrical coupling due to the lack of adequate gap junctions contained in the myoblasts and the absence of transdifferentiation to cardiomyocytes (which was once believed to occur).(Henning, 2011)(Fernández-Avilés *et al.*, 2017)(Madonna *et al.*, 2016)

### 1.4.4 Bone marrow mononuclear cells

Found within the bone marrow, there are a variety of stem cell populations including hematopoietic, endothelial progenitor cells, and mesenchymal stem cells, all in small

quantities. These can be obtained by biopsy, isolated and then purified upon which they can be administered to humans as BMNSCs. BMNSCs are the cell type that has the most human clinical data, and the majority are in patients with ischaemic rather than non-ischaemic DCM. Several phase III trials are ongoing (Table 1-3). A recent meta-analysis including 20 randomized controlled trials (1255 patients) reported only minor improvements in symptomatic status and LVEF in bias resistant studies.(Fisher *et al.*, 2015) Although no major adverse events have been reported, theoretical concerns exist regarding ventricular arrhythmias due to a potential mismatch in electromechanical coupling between the donor cells and host myocardium.(Fukushima *et al.*, 2007)

FOCUS-CCTRN (Effect of transendocardial delivery of autologous bone marrow mononuclear cells on functional capacity, left ventricular function, and perfusion in chronic heart failure) was a phase II randomized, double-blind, placebo-controlled study that administered BMNSCs (intramyocardial injection) to symptomatic chronic ischaemic heart failure (LVEF ≤45%) patients (n=61 cell therapy vs n=31 sham procedure). Although the trial was negative a minor LVEF improvement was seen in the cell treated group with reduction in sham group, and there was a correlation with the proportion of CD34+ and CD133+ cells contained in BMNSC samples. This is important since certain types of BMNSCs may be more efficacious than others, and therefore more specific / purified cells may need to be administered to improve efficacy.(Perin *et al.*, 2012)

For example, ixmyelocel-T which is primarily a BMNSC population, but relatively higher population of M2 macrophages and CD90+ mesenchymal stem cells when

compared to standard unfractionated BMNSCs. ixCELL-DCM (phase II) investigated the product and randomized 126 patients (n=60 cell therapy; n=66 placebo) with ischaemic cardiomyopathy ineligible for further revascularization. The trial was technically positive regarding the composite endpoint of all-cause death, cardiovascular admissions to hospital, or unplanned clinic visits to treat acute decompensated heart failure.(Patel *et al.*, 2016) Notably however, the trial was relatively small and larger trials are needed to definitively answer the question of efficacy. In contrast to ischaemic cardiomyopathy, exogenous cell therapy has also been studied in the acute myocardial infarction setting with persistent LV dysfunction. The idea is that the stem cells may prevent heart failure in high risk patients as they are recovering from a myocardial infarction by limiting infarct size via antiapoptotic, pro-angiogenic and anti-inflammatory paracrine factors. Numerous small studies have reported feasibility; however, efficacy will be assessed in the phase III (The Effect of Intracoronary Reinfusion of Bone Marrow-derived Mononuclear Cells on All-Cause Mortality in Acute Myocardial Infarction) BAMI Trial (NCT01569178). Patients with persistent heart failure (LVEF<45%) post successful primary PCI for acute ST elevation myocardial infarction will be treated with autologous BMNSCs via intracoronary injection. It was initially designed to recruit 3000 patients and therefore be the first trial involving exogenous cell therapy adequately powered for hard endpoints including all-cause mortality as its primary endpoint, with cardiac death and rehospitalisation included as secondary endpoints. However, recruitment into the trial has been slow and now the projected final number of patient included based on data from the clinicaltrials.gov website (checked June 2019) is 350 patients with a projected study completion date of October 2019.

### 1.4.5 Mesenchymal stem cells

MSCs can be obtained from a variety of sources including bone marrow, umbilical cord blood and adipose tissue. Relatively fewer clinical trials are available when compared to BMNSCs; however, phase III trials are currently in progress (Table 1-2). One of the landmark studies involving autologous MSC administration to patients with heart failure was the Cardiopoietic stem Cell therapy in heart failURE (C-CURE) phase II trial. Although the numbers of patients receiving MSCs was low (n=21), no adverse events were observed there was a marked improvement in EF (+7% [27.5% to 34.5%], $p < 0.0001$), end-systolic volumes and six-minute walk test. However due to inadequate bias resistant features in trial design (open label with no sham procedure), data should be interpreted with caution. (Bartunek *et al.*, 2013)

Whether autologous or allogenic cells are used is a matter of debate, since allogenic will be more easily available to administer; for example, allogenic cells could potentially be an off the shelf product that has undergone extensive testing prior to administration. In contrast, immunological reactions could occur if allogenic cells are administered. This was investigated in The Percutaneous Stem Cell Injection Delivery Effects on Neomyogenesis Pilot (POSEIDON) study, which administered autologous (16 patients) or allogeneic (15 patients) MSCs via intramyocardial injection of varying doses (20-200million). Importantly, there were no adverse reactions, and positive signs of efficacy including infarct size reduction and ventricular parameter improvements were seen. (Hare *et al.*, 2012) Further data are eagerly awaited to assess efficacy. The Prospective Randomized Study of Mesenchymal Stem Cell Therapy in Patients Undergoing Cardiac Surgery (PROMETHEUS) trial was the first of its kind to ascertain the effects of localised

injection of autologous MSCs into and around scar tissue that was unsuitable for revascularisation during coronary artery bypass grafting surgery. After 18 months' follow-up, there was an overall increase in LVEF which corresponded with reductions in scar tissue. Additionally, this was mirrored with enhanced contractile performance at the cell injection sites. Since only data from 6 patients were published from a potential total of 45, further data is awaited.(Karantalis *et al.*, 2014)

The Phase III trial (The Safety and Efficacy of Autologous Cardiopoietic Cells for Treatment of Ischemic Heart Failure (CHART-1, NCT01768702) trial was a double-blind placebo-controlled phase III trial involving 240 patients. The primary end-point was a composite of morbidity and mortality, quality of life questionnaire changes, and objective measures of exercise capacity and left ventricular parameters.(Bartunek *et al.*, 2017) The primary outcome was neutral, however; an exploratory analysis showed signals of benefit in patients with elevated end-diastolic volumes (200-370mls). Ongoing phase III trials are investigating allogenic cells (Rexlemestrocel-L; NCT02032004) and further studies are planned but not yet recruiting (CHART-2, NCT NCT02317458). These will provide a more definitive answer to the efficacy of this cell type in the treatment of heart failure.

**Table 1-2: Recent trials involving BMNSCs and MSCs.**

| Trial | Phase | Details | Patients | Aetiology | Primary endpoint | Results |
|---|---|---|---|---|---|---|
| **BMNCs** | | | | | | |
| BAMI | phase III | Randomised, open label | 350 | Ischaemic | All-cause mortality | NA |
| ixCELL-DCM | phase II | Randomised, double-blind | 126 | Ischaemic | Composite (All-cause death, cardiovascular admissions / unplanned clinic visits) | Composite end point met |
| REGENERATE-DCM | phase II | Randomised, double-blind | 60 | Non-ischaemic | LVEF | Improvement in LVEF, NYHA, NT-pro BNP |
| FOCUS-CCTRN | phase II | Randomised, double-blind | 92 | Ischaemic | LVESV, maximal oxygen consumption, SPECT reversibility | Neutral |
| REPAIR-AMI | phase III | Randomised, double-blind | 204 | Ischaemic | LVEF | Improvement in LV function |
| **MSCs** | | | | | | |
| CHART-1 | phase III | Randomised, double-blind | 157 | ischaemic | Composite (inc mortality, QOL, LVESV) | neutral |
| POSEIDON | phase I/II | Randomised, open label | 30 | Ischaemic | Safety | Low incidence of events |
| C-CURE | phase II | Randomised, open label | 48 | Ischaemic | LVEF | Improvement in LV function |
| PROMETHEUS | Phase I/II | Randomised, double-blind | 6 | Ischaemic | Safety / LVEF | Improvement in LV function |

*A summary of recent and important human clinical trials involving bone marrow mononuclear stem cells and mesenchymal stem cells. Most trials published have been phase I/II; however, phase III trials are ongoing.*

### 1.4.6 Resident cardiac progenitor stem cells

Resident cardiac progenitor stem cells (CPCs), consist of a very minor fraction of the total cardiomyocyte population (estimates vary but <1%) and are subdivided based on the expression of various cell surface markers (c-kit, Isl-1, Sca-1). Cardiospheres are the term given to a mixed population of CPCs. Clinical studies involving c-kit cells and cardiospheres have been reported; however, the scientific community is reeling from the after effects of the recent retraction of over 30 papers from a prominent researcher in the field in 2019.(Chien *et al.*, 2019) Additionally, a recent murine study using dual genetic lineage tracing indicates that the heart may lack an endogenous cardiomyocyte producing cell in adult hearts. (Y. Li *et al.*, 2018) Therefore, clinical data regarding endogenous cardiac progenitors must be interpreted with caution.

### 1.4.7 c-kit Cardiac stem cells

The SCIPIO (Administration of Cardiac Stem Cells in Patients With Ischemic Cardiomyopathy) was the first and most reported phase I, randomized, open label trial involving autologous administration of c-kit+ cardiac stem cells via intracoronary injection to patients with ischaemic heart failure.(Bolli *et al.*, 2011) Cells were initially obtained from right atrial appendage samples during open heart surgery, which were then expanded ex-vivo and then administered months after the initial surgery. Twenty patients underwent cell therapy and an impressive improvements in left ventricular function were found after one year follow-up. It is important to state that the trial was largely discredited a number of years ago after investigations and expressions of concern by an independent research group and editorial board of the Lancet journal a number of years ago. Eventually in 2019 after extensive

investigation, the paper was finally retracted by the Journal. (‘Expression of concern: The SCIPIO trial’, 2015)

### 1.4.8 Cardiosphere-derived stem cells

The CADUCEUS (Cardiosphere-Derived Autologous Stem Cells to Reverse ventricular dysfunction) phase I trial involved the feasibility of autologous cardiosphere-derived stem cell therapy administration to patients with ischaemic heart failure (Table 1-3).(Makkar *et al.*, 2012) 17 patients received cell therapy versus 8 patients in the control group. Instead of obtaining samples via open heart surgery, samples were taken by right ventricular endomyocardial biopsy; however, on average 10 biopsies were taken per patient to obtain enough tissue for cells.(Sanganalmath and Bolli, 2013) Data suggests that data from CDCs are more readily obtained and expanded from atrial but not ventricular biopsies. (Chan *et al.*, 2012) Biopsies in general however, raise the risk of complications including the development of arrhythmia occurring but on the other hand avoids the need for a sternotomy. At follow-up, even though there were improvements in viability coupled with a reduction in scar mass; there was however no improvement in EF / end systolic dimensions when compared to the control group.

**Table 1-3: Summary of trials involving cardiac stem cells and cardiospheres**

| Trial | Phase | Details | Patients | Aetiology | Primary endpoint | Results |
|---|---|---|---|---|---|---|
| **CDCs** | | | | | | |
| CADEUCUS | phase 1 | Randomised, open label | 31 | Ischaemic | Composite of multiple endpoints including MACE, MRI ventricular assessment | Increase in viable mass observed by MRI |
| **Cardiac Stem Cells** | | | | | | |
| SCIPIO | phase 1 | Randomised, open label | 33 | Ischaemic | Adverse events including death, ventricular tachycardia; MRI ventricular assessment | *WITHDRAWN* |
| CONCERT-HF | phase II | Randomised, double blind | 144 | Ischaemic | Death, heart failure admissions, LV function | *WITHDRAWN* |

*A summary of recent trials involving cardiac stem cells and cardiospheres. Trials involving this type are still at the phase I/II stage.*

### 1.5 Novel cell types and hurdles

As well as lack of cell retention used with existing delivery methods, the lack of efficacy seen in clinical trials may also be related to the cell number used (2-200 million) since approximately 1-2 billion cells are destroyed in a human myocardial infarction.(Laflamme and Murry, 2005) Efforts to upscale differentiation have improved rapidly, but it may not be feasible with current cell types e.g. bone marrow cells or cells obtained from cardiac biopsies. Induced pluripotent stem cell derived cardiomyocytes (iPSC-CMs) hold great promise, and can successfully and relatively easily be upscaled to the cell number required to effectively replace the number of lost myocytes post myocardial infarction. Additionally, to date, they are the only cell type available that can create bonafide “cardiomyocytes” from an adult source.

### 1.5.1 Pluripotent stem cells

Pluripotent stem cells can be obtained from human adult cell (hiPSC-CMs) or embryonic stem cells (hESC-CMs) and both cell types have a theoretically nearly unlimited proliferation potential. hiPSC-CMs have the added advantage of being a potential autologous source and therefore lower immunogenicity issues. In addition, hiPSC-CMs do not have the ethical issues surrounding the use of embryonic cell types. Other theoretical concerns involve teratoma formation and uncontrolled cell differentiation although pre-clinical studies have not convincingly reported this so far.(Weinberger et al., 2016)(Chong et al., 2014)

The creation of iPSC-CMs was invented by Yamanaka et al who consequently won the Nobel prize after his discovery. By administering just 4 transcription factors (Oct4, Sox2, cMyc, Klf4) to adult somatic cells, they could be reprogrammed into a pluripotent stem cell state (Figure 1-10).(Takahashi et al, 2006) The induced pluripotent cells could then be differentiated into numerous cell types including cardiomyocyte like cells.(Yoshida and Yamanaka, 2017) Historically, retroviral mediated transduction of the 4 transcription factors was used to reprogram the adult somatic cells to newly created iPSCs that exhibit phenotypic and functional properties similar to embryonic stem cells.(Abou-Saleh *et al.*, 2018)(Sadahiro, 2019) At present, several approaches are used to generate iPSCs and can broadly be grouped into integrating and non-integrating methods.

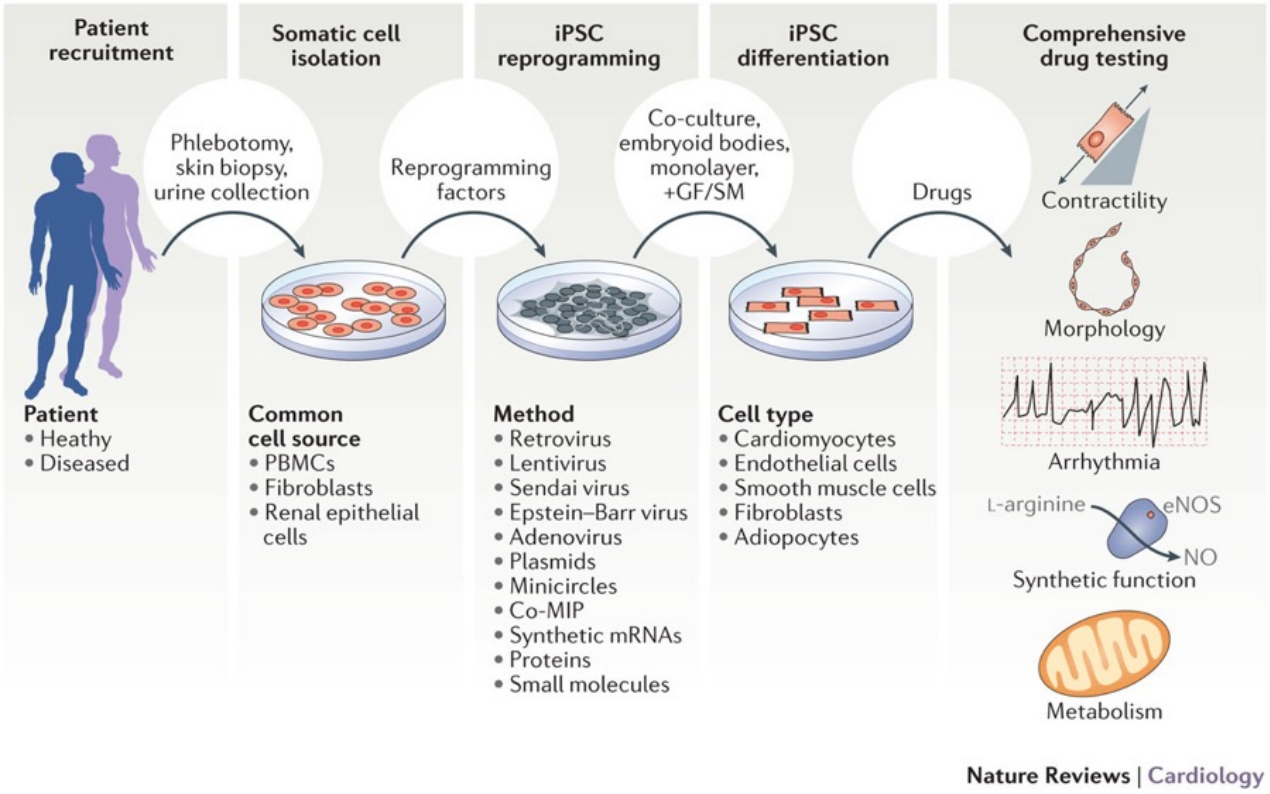
The viral integrating method was the first to be successfully utilised (retroviral or lentivirus) and deliver the OKSM factors and transgene delivery enabled random insertion into the genome with iPSC colonies appearing 3-4 weeks post integration. (Abou-Saleh *et al.*, 2018)(Sadahiro, 2019) A caveat of using this technology was the

permanent integration of the transgene into the genome, which could result potential reactivation at a later date, affecting gene expression, DNA methylation, pluripotency and even tumour formation. (Sadahiro, 2019) The issues with permanent integration were partially overcome using Cre-Lox recombinase system which mediated excising the integrated genes, but efficiency remained low and additionally persistent viral vectors remained at sites of integration. (Abou-Saleh *et al.*, 2018)(Sadahiro, 2019) The persistent caveats with integrating technology were overcome by using non-integrating viruses such as sendai virus and adenoviruses, where high levels of expression of exogenous genes are found without integration. Non-viral non-integrating methods include plasmid DNA, minicircle DNA, RNA delivery and protein delivery. (Abou-Saleh *et al.*, 2018)(Sadahiro, 2019) Although these methods seem promising, generally the reprogramming efficiency is relatively low when compared to viral methods. Current method to improve efficiency include small molecules and specific compounds including chromatin modifiers and regulators of the cell signalling pathway. (Abou-Saleh *et al.*, 2018)(Sadahiro, 2019)

Once somatic cells have been reprogrammed to a pluripotent state the next stage is to differentiate them into cardiomyocyte like cells. Similarly to reprogramming methods, differentiation protocols have improved rapidly over time. The current differentiation protocols are targeted (as opposed to spontaneous with low efficiency rates of approx. 10% using embryoid bodies) and try to recapitulate the fetal processes that occur to generate cardiomyocytes and termed directed cardiac differentiation.(Kehat *et al.*, 2001) (Sadahiro, 2019) For example, temporal activation and inactivation of specific foetal pathways including Wnt, BMP, and Nodal / Activin convert PSCs to hiPSC-CMs.(Mummery *et al.*, 2012)(Kattman *et al.*, 2011)(Ren *et*

*al.*, 2011) And now with more experience of manipulation and using defined conditions including metabolic selection, protocols have become much more efficient.(Burridge *et al.*, 2014)(Loh *et al.*, 2016)(Lian *et al.*, 2012)(Tohyama *et al.*, 2017)(Sadahiro, 2019)  Things that seemed almost inconceivable just a few years ago have become a reality. For example, where only a few million could be differentiated previously with relatively low efficiency, up to 1 billion cells have been created in a single differentiation using 1 litre 3D suspension spinner flasks.(Chen *et al.*, 2015)(Kehat *et al.*, 2001) Other modalities to improve differentiation and upscaling include the use of microcarriers which increase surface area per unit volume.(Q. Li *et al.*, 2018)

**Figure 1-10: Pathway from reprogramming somatic cells to iPSC-CM**




*Pathway to reprogram somatic cells into induced pluripotent stem cells. Once reprogrammed they can be differentiated into numerous cell types including cardiomyocytes. Reused with permission; Reference:* (Chen, Matsa and Wu, 2016)

### 1.5.2 The caveat of immaturity

One of the caveats of this technology is that the cells are immature or fetal-like with notable absences of various adult like parameters including lack of t-tubules. In addition, energy production is typically more glycolytic as opposed to fatty acid ß-oxidation(figure 1-11).(Yoshida and Yamanaka, 2017) Variations in troponin I and myosin heavy chain isoforms are also present. There are also relatively low levels of SERCA, phospholamban and calsequestrin when compared to mature cardiomyocytes. These limitations are important to appreciate when using iPSC-CMs for cardiac regeneration and research has focussed on maturing them using a

variety of means including mechanical or electrical stimulation, hormonal stimulation, or leaving them for long cultivation times in 3D culture. (Yoshida and Yamanaka, 2017) However, whether or not maturity is desirable for in-vivo grafting is a matter of debate since immature cells are more resistant to hypoxia and therefore are of benefit in the early integration phase, and in-vivo maturation of cells has been described previously. (Weinberger *et al.*, 2016; Weinberger, Mannhardt and Eschenhagen, 2017)

**Figure 1-11: Pathway from reprogramming somatic cells to iPSC-CM**

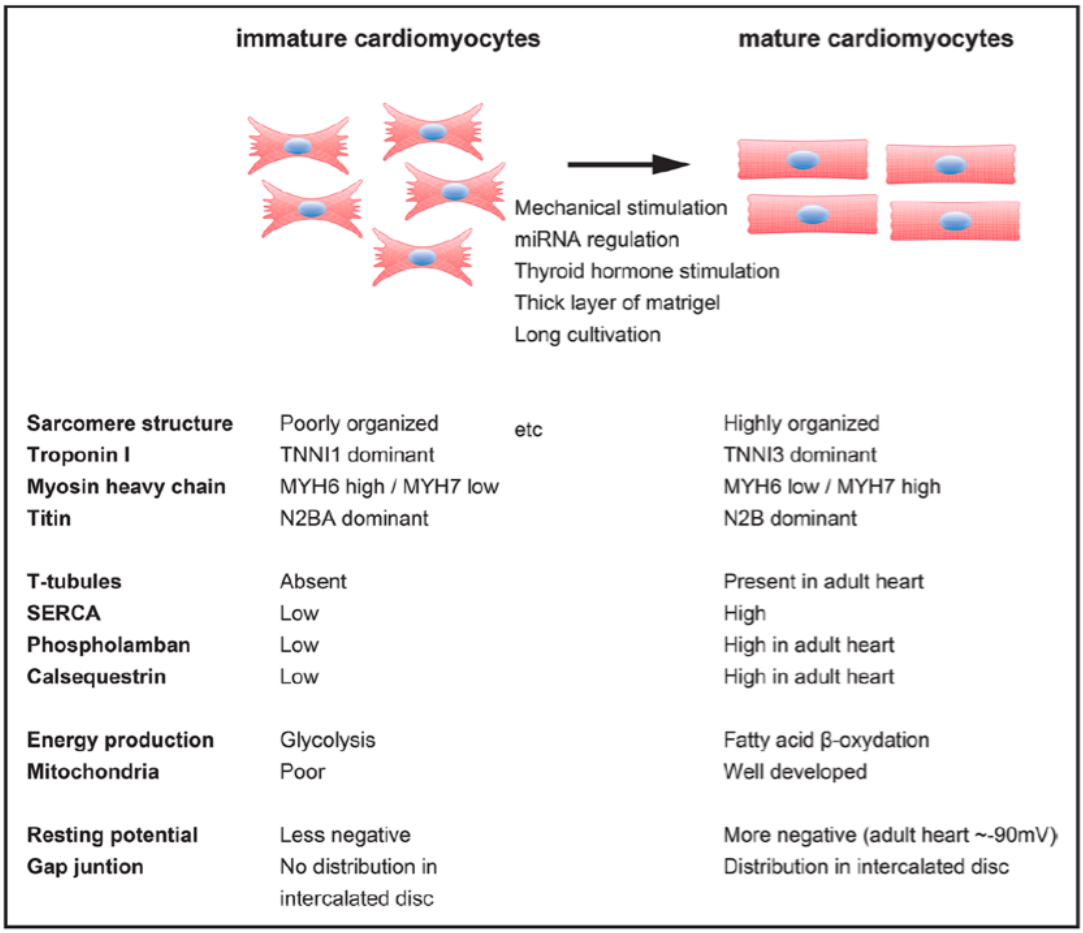



*Image depicting differences between relatively immature human-induced pluripotent stem cell derived cardiomyocytes and adult mature cardiomyocytes. Reused with permission; Reference:* (Yoshida and Yamanaka, 2017)

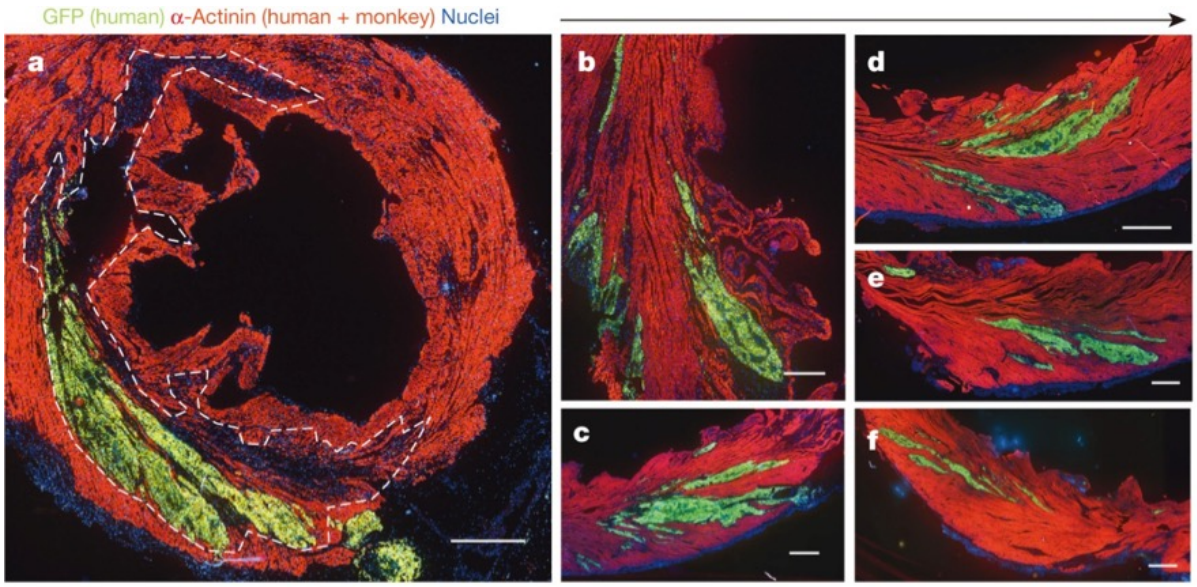
### 1.6 Preclinical and first in man data

The efficacy of both hESC-CM and hiPSC-CMs has been shown in numerous small animal models. hESC-CM studies published over 10 years ago have shown efficacy in both murine and rat models of myocardial infarction.(van Laake *et al.*, 2007)(Caspi *et al.*, 2007)(Laflamme *et al.*, 2007) Similar findings have been reported by several groups using iPSC/hiPSC-CMs injected into infarcted murine and rat hearts with favourable improvements in ventricular function reported.(Mauritz *et al.*, 2011)(Nelson *et al.*, 2009) More recent small animal studies have looked at combining cell delivery with biomaterials to help improve efficacy.(Chow *et al.*, 2017)

Pre-clinical studies have now reached macaque level and have shown the feasibility of using grafts of up to 1 billion cells in size using both hESC-CM and iPSC-CM. (Chong *et al.*, 2014)(Liu *et al.*, 2018)(Shiba *et al.*, 2016) Cells were cryopreserved and administered by intramyocardial injection in an ischaemia reperfusion model (Figure 1-12). Although grafts were perfused by host vasculature and evidence of electromechanical coupling occurred, non-fatal ventricular arrhythmia was reported in the first few weeks post grafting.(Chong *et al.*, 2014) The sustained retention (up to 3 months) using an intramyocardial injection method of delivery with evidence of electromechanical coupling is an exciting prospect that had not been convincingly shown in a large animal model prior to the publication of this trial. Similar findings of sustained retention, electromechanical coupling, and the development of arrhythmia formation were reported using allogenic iPSC-CMs when injected into macaques. (Shiba *et al.*, 2016)The resurgence of pathological ventricular arrhythmia, although relatively well tolerated is a major concern when moving to first in human trials.

**Figure 1-12: Sustained retention of hESC-CM in infarcted macaque heart**

*Confocal images of infarcted macaque hearts and intramyocardial grafting of hESC-*




*CM (14 days images). A-F) Sustained retention of donor hESC-CM co-expressing green fluorescent protein. Alpha-actinin (red) is macaque in origin. (B-F) Additional images in peri-infarct region demonstrating significant hESC-CM engraftment. Scale bars 1000μm. Reused with permission; Reference:* (Chong *et al.*, 2014)

There is however one phase I trial using hiPSC-CMs that has recently be approved in Japan (Osaka University). Instead of intramyocardial injection, hiPSC-CMs will be seeded into a “sheet” in-vitro and attached to the epicardial surface (patch method). Cells will be administered to 3 patients using the cell sheet technology and each patient will receive approximately 100 million cells. The trial will assess feasibility, the development of arrhythmia, tumorigenicity and changes in ventricular function. The cells will be from an allogenic source and long term engraftment will not be possible since immunosuppression will only be given for a period of one month and therefore will die due to immune rejection.

### 1.7 Usefulness of biomaterials as an adjunct to cellular therapy

The use of biomaterials in cardiac regeneration is a promising regenerative medicine strategy to overcome the limitations of exogenous cell therapy. They can provide a scaffold for cellular maturation in-vitro, act as a carrier for growth factors and provide a shield to the grafted cells in the hostile environment post in-vivo grafting. Numerous biomaterials have been under investigation from either natural (fibrin, collagen, alginate) or synthetic sources (polylactic-co-glycolic acid, polyurethane). Natural biomaterials have the advantage of being highly biocompatible and therefore are less inflammatory post in-vivo grafting. The tissue engineering field of cardiac regeneration is predominantly focussed on creating bonafide muscle in-vitro (using cells and biomaterials) that could replace the muscle that is lost post myocardial infarction, provide structural support to the failing heart, enable increased cell retention and therefore prolonged paracrine release. The ideal biomaterial needs to have properties that facilitate the easy growth of cells and therefore the development of functional cardiac tissue. The focus of this part of the introductory chapter will explore the use of engineered heart tissue (fibrin based) and conductive polymers as a regenerative medicine tool.

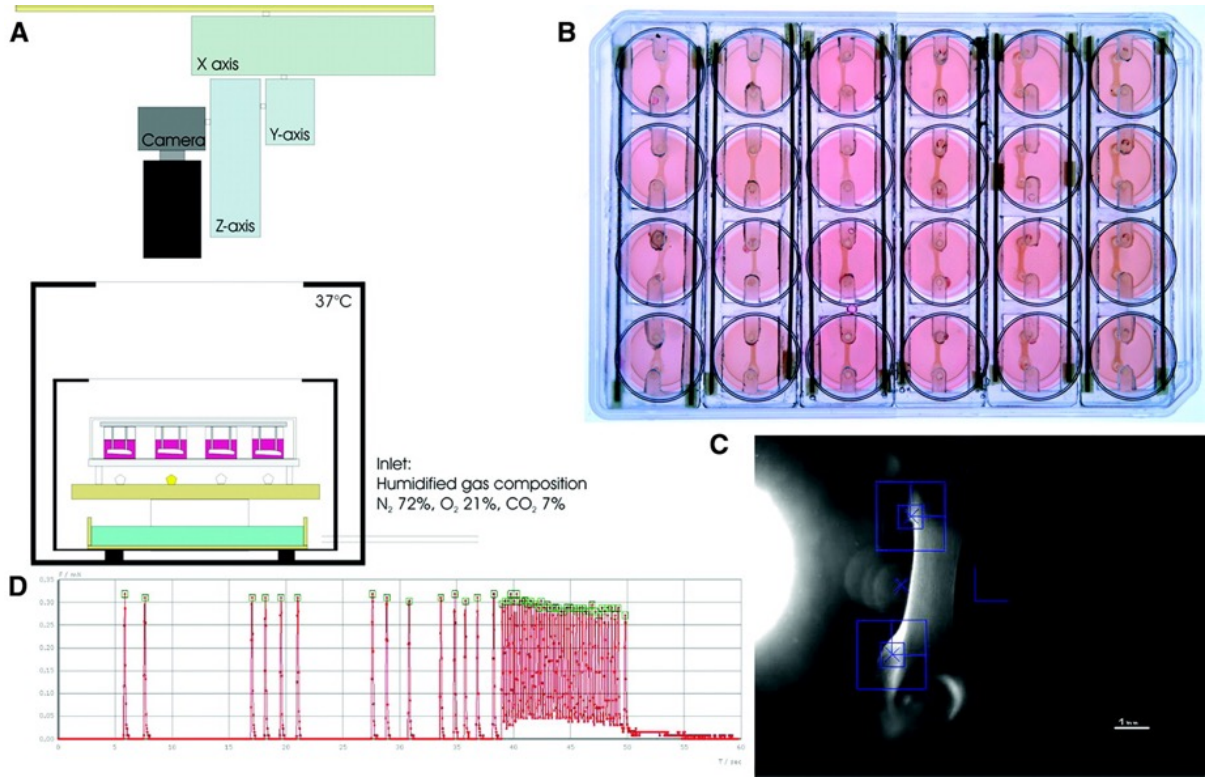
#### 1.7.1 Engineered Heart Tissue

EHT was pioneered last century by Prof Thomas Eschenhagen.(Eschenhagen *et al.*, 1997) There have been remarkable improvements over the last 20 years, the first primitive EHT used glass tubes and Velcro, while the most recent EHT use flexible silicone posts, and many can be made in one batch using a medium through put method (Figure 1-13).(Hansen *et al.*, 2010) In this method, EHTs are housed in a 24 well plate, and a “white box” video recording system used to monitor for evidence of

EHT maturation via improvements in force measurements calculated from the degree of silicone post deflection during EHT contraction. (Figure 1-13).

It is well-known that if adult cells are removed from their 3D extra cellular matrix, they de-differentiate into an immature state. This is the major concept behind tissue engineering by combining cells (cardiomyocytes +/- non-cardiomyocytes) in an extracellular like matrix.(Zimmermann *et al.*, 2006; Kensah *et al.*, 2013) The cells in the matrix elongate and become more mature like when compared to 2D monolayer culture. The grafting of EHT enables long term cell retention and may improve cell survival and integration by shielding cells from a hostile environment, while facilitating attachment of a graft to the epicardial surface. EHT combines stem cell derived cardiomyocytes (at present most commonly hiPSC-CMs) into a 3D fibrin matrix. The spontaneous activity of the cells and flexible posts provides a continuous auxotonic load which helps align the cardiomyocytes. This has been shown to improve several maturation markers including gene expression, calcium transients and contraction kinetics.(Kensah *et al.*, 2013)(Tiburcy *et al.*, 2017)(Zimmermann *et al.*, 2006) EHTs have a multitude of uses from disease modelling, drug toxicology studies to cardiac regeneration with the idea of replacing lost myocytes in failing hearts.

**Figure 1-13: EHT medium throughput platform**



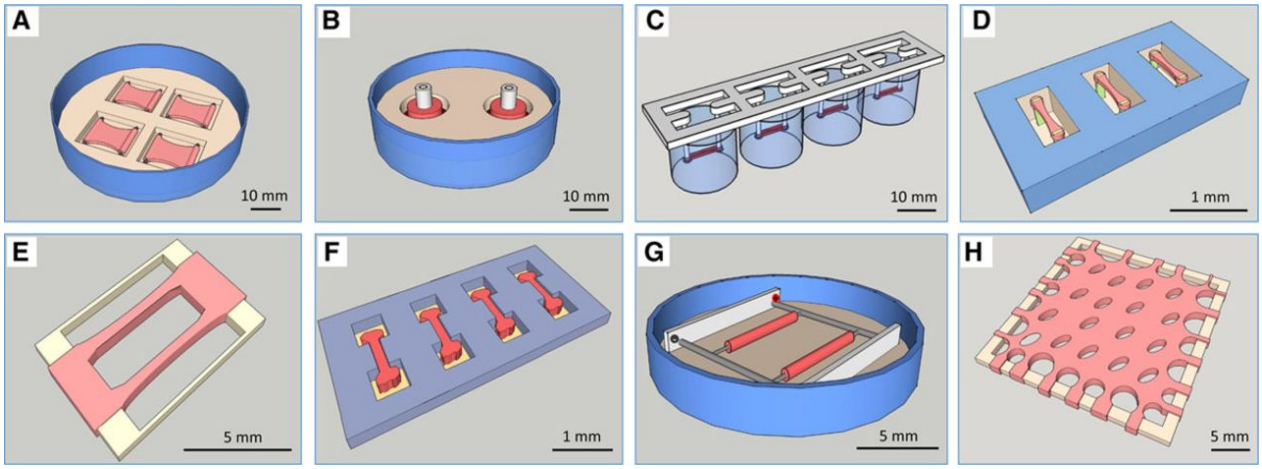

*A) Diagram of cell culture incubator along with camera; B) 24 well plate containing EHTs; C) Software that detects EHT and silicone posts deflections; D) Graph of force measurements. Reused with permission Reference:* (Hansen *et al.*, 2010)

### 1.7.2 Progression

The first generation EHT from the landmark paper by Eschenhagen used embryonic cardiomyocytes from chicken mixed with collagen to act as an extra cellular matrix.(Eschenhagen *et al.*, 1997) EHT displayed heart muscle like characteristics including a positive force frequency relationship and similar calcium handling characteristics. The next generation EHTs were circular and used neonatal rat heart cells and collagen I, mixed with Matrigel (basement cell membrane secreted by Engelbreth-Holm-Swarm mouse sarcoma cells) which improved maturation,

alignment and force production.(Zimmermann *et al.*, 2002) In 2010, a medium through put protocol was developed to improve consistency between constructs, again using rat neonatal cells and a 3D fibrin based hydrogel, utilising the fibrinogen and thrombin reaction to create fibrin.(Hansen *et al.*, 2010)(Sala *et al.*, 2017). The hydrogel forms around the posts, and since EHT contraction kinetics mature over time in-vitro, a certain level of force attainment can be used to guide the quality of constructs prior to grafting experiments. The advantage of using fibrin is that it is a natural and biocompatible so any possible inflammatory reaction is minimised. Numerous different types of EHTs are under investigation including cardiobundles, cardiac patches and micro heart tissues. (Figure 1-14)

**Figure 1-14: Different types of engineered heart tissue under investigation**




*Various hydrogel based engineered heart tissue (EHT) approaches. A) EHT on velcro-covered rod; B) circular ring shaped EHTs; C) fibrin-based EHTs; D) fluorescent pillars holding micro tissues; E) cardiobundles on PDMS frame; F) micro heart tissue; G) cardiac biowires; H) cardiac patch. Reused with permission; Reference:* (Weinberger, Mannhardt and Eschenhagen, 2017)

### 1.7.3 Improvements over monolayers

It is now generally accepted that 3D cell culture (especially with hiPSC-CMs) has numerous benefits over 2D monolayers. It has been shown that 3D EHTs have more adult myocyte like responses when compared to cells cultured in monolayers including larger catecholamine responses, larger sodium currents, and higher levels of adult gene expression.(Lemoine *et al.*, 2018)(Uzun *et al.*, 2016)(Tiburcy *et al.*, 2017) It has now been shown that some degree of mechanical or electrical stimulation is needed to help in maturation, either by electrically pacing the construct or providing auxotonic load by using flexible pillars.(Ronaldson-Bouchard *et al.*, 2018)(Tiburcy *et al.*, 2017)(Weinberger, Mannhardt and Eschenhagen, 2017)(Breckwoldt *et al.*, 2017) However, it is widely accepted that the hiPSC-CMs contained within the construct are still more fetal like as opposed to adult myocardium, even with 3D culture.(Yoshida and Yamanaka, 2017)(Ronaldson-Bouchard *et al.*, 2018) This is important since any tissue that is created in-vitro must resemble the target tissue to make it a successful strategy. Other strategies including the addition of hormonal or growth factors, using different culture techniques or adding non-cardiomyocytes including fibroblasts or endothelial cells.(Zimmermann *et al.*, 2006; Tulloch *et al.*, 2011; Hirt *et al.*, 2012; Kensah *et al.*, 2013; Godier-Furnémont *et al.*, 2015; Jackman, Carlson and Bursac, 2016; Tiburcy *et al.*, 2017; Ronaldson-Bouchard *et al.*, 2018) All strategies appear to show improvements but advances are still way behind adult myocardium in multiple parameters. One of the most robust measures of maturation is force production. To put things in perspective – the first generation primitive EHT has force productions of approximately 0.3mN/mm$^2$ which is far lower than adult myocardium. With the invention of bioreactors, vitamin C, the addition of non-cardiomyocytes (fibroblasts),

an increase in static stress levels of 4.4mN/mm$^2$ were recorded. However, this is still significantly lower than adult myocardium (up to 20mN/mm$^2$). (Kensah *et al.*, 2013)

Construct remodelling occurs over time in-vitro and is predominantly because of fibroblasts / non-cardiomyocytes. The addition of fibroblasts have been shown to improve force production and improve cell retention post grafting. The optimal fibroblast: cardiomyocytes ratio was reported to be approximately 1:1; however, only 30% fibroblasts were added at baseline, indicating that non-cardiomyocytes proliferated. Other studies have used 1:10 ratios of fibroblast to cardiomyocytes whilst others have not used any non-cardiomyocytes in their constructs.(Tiburcy *et al.*, 2017)(Weinberger *et al.*, 2016)

A recent Nature publication has reported the development of specific adult like muscle characteristics not previously reported in other EHT studies. In this paper, iPSC-CM were subjected to early electrical stimulation (day 7) with a relatively intense pacing protocol (up to 6 Hz). Remarkably, at 28 days, specific adult myocardial characteristics including transverse t-tubules, mature adult like calcium handling, oxidative phosphorylation metabolism and positive force frequency relationships were reported. However, despite the remarkable findings, even this "state of the art" EHT still had conduction velocities and force productions inferior to human adult myocardium with conduction velocities of 25.8cm/s (50-70cm/s in human adult myocardium) and force productions of 2-3 mN/mm$^2$ (20mN/mm$^2$ in adult myocardium).(Ronaldson-Bouchard et al., 2018). In addition, the EHTs in this study were relatively small in cell number (2 million cells) and even with the advanced adult like morphology described in the paper, the conduction velocities reported were still

relatively similar to other groups that have published on this topic.(Tiburcy et al., 2017). Other groups have reported higher forces ($22.4 \pm 0.9$ $mN/mm^2$), but only when presenting the data as force per cross sectional area.(Shadrin et al., 2017)

### 1.7.4 Regenerative medicine application

EHT are an exciting potential new treatment option and could become a viable and novel strategy that directly targets the irreversible cell death that occurs in the heart failure syndrome. EHT consisting of hiPSC-CM could be grafted onto the host to directly replace lost muscle and provide a cell dependent continuous release of paracrine factors. Additionally, the graft may provide structural support to the failing left ventricle. (Naito *et al.*, 2006; Zimmermann *et al.*, 2006; Mannhardt *et al.*, 2016).

EHT placement currently requires an open thoracotomy to place the EHT onto the epicardial surface of the left ventricle. Therefore, currently this precludes the use of this technology in myocardial infarctions which are predominantly treated in a minimally invasive way. The first patients that are likely to be treated are patients undergoing coronary artery bypass grafting who have ischaemic heart failure since the procedure is performed by open sternotomy and therefore EHT can be grafted onto scar tissue concurrently.

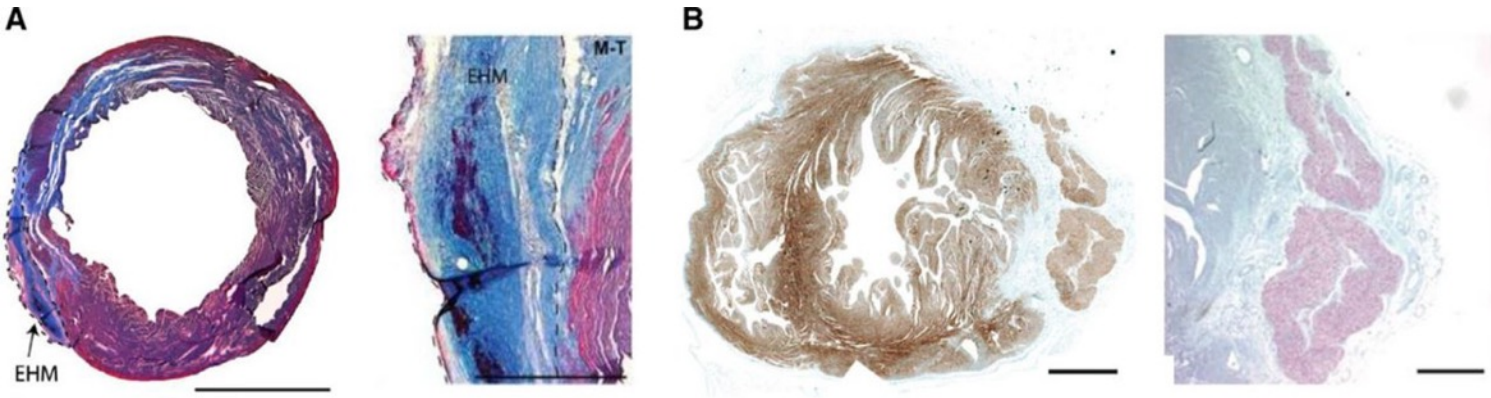
Preclinical data of efficacy, as assessed by ventricular function has been shown in numerous small and large animal models. The seminal paper by Zimmerman et al showed evidence of electromechanical coupling and improvements in systolic function, and favourable effects on ventricular remodelling as well as increased wall

thickness in the infarcted areas in a rat MI model.(Zimmermann *et al.*, 2006) The same group reported efficacy in a heart failure guinea pig models using fibrin based EHTs with improvements in fractional area change by approximately 30% at 1 month post grafting. (Weinberger *et al.*, 2016) Similar improvements have been shown using cell sheet technology as well as fibrin based EHTs in swine animal models (Kawamura *et al.*, 2017)(Gao *et al.*, 2018) The concept of EHT has now reached first in man trials but several hurdles still need to be overcome if EHT is ever to become a viable and effective therapeutic strategy.

### 1.7.5 Upscaling

One of the main issues precluding clinical use is the lack of patches available at a clinically relevant size suitable for human use. For example, while retention of grafts containing human cardiomyocytes have been shown in a guinea pig model at one month (figure 1-15), approximately 1-2 billion cells are lost in a myocardial infarction. Whilst it has been shown that multiple EHTs can be fused to make larger constructions (15mm diameter / 1-4mm in length) and relatively large EHTs (5-7million) were grafted onto a guinea pig model of cryoinjury (figure 1-15), this is still insufficient for human use.(Weinberger *et al.*, 2016)(Zimmermann *et al.*, 2002)(Zimmermann *et al.*, 2006) Feasibility of larger EHTs (up to 10 million cells) has been shown in a swine model but much larger EHTs (e.g. 10cm x 10cm) may be needed to contain the cell number required to effectively replace the muscle that is lost post infarction.(Gao *et al.*, 2018)(Shadrin *et al.*, 2017)(Huang *et al.*, 2018).

**Figure 1-15: Histology of iPSC-CM post grafting**




*A) Axial section showing engineered heart muscle (EHM) attached to epicardial surface. B) Engineered heart tissue attached to epicardial surface stained for troponin (left image) and human specific marker ku80 (right image). Reused with permission; Reference: (Weinberger, Mannhardt and Eschenhagen, 2017)*

### 1.7.6 Vascularisation

EHT vascularisation is essential to maintain graft viability since the average inter-capillary distance is just 20μm and clinically relevant grants would likely need to be several mm / cm in depth. Therefore, it is likely that the grafts used may need to have a vascular network formed in-vitro prior to grafting. Research has focussed on co-culture with endothelial cells / progenitors with or without the addition of fibroblasts, microfluidic systems and 3D bioprinting methods. However, further work is needed since to date a fully prevascularized network of vessels has not been shown in any EHT.(Huang *et al.*, 2018)(Nakane *et al.*, 2017)(Redd *et al.*, 2019)(Kolesky *et al.*, 2016)

### 1.7.7 Electromechanical integration

To fully replace the muscle that is lost in heart failure, and for it to be effective at

contributing to improving function, electromechanical integration is a prerequisite. It has been noted on several preclinical studies that a non-cardiac tissue predominantly fibrotic layer (200-300μm) exists between the graft and the host.(Weinberger et al., 2016)(Shadrin et al., 2017) Although a small number of grafts have been reported to electromechanically integrate, the general lack of coupling is most likely due to the non-cardiomyocyte layer precluding connexin coupling between the graft and host.(Weinberger et al., 2016)(Shadrin et al., 2017) The non-cardiac tissue may in part be due to an inflammatory process (xenograft transplantation), and this may be significantly less with an allograft or autograft EHT.

### 1.7.8 Immunosuppression

Although an autologous source of cells are desirable, at present allogenic sources which require immunosuppression (even if HLA matched), are the likely cells to be used in the early clinical trials. Allogenic sources typically are extensively tested to ensure reliability and efficacy and also can be potentially used as an “off the shelf” product dispensed from HLA matched iPSC-CM banks. While immunosuppression protocols have improved over time; nevertheless, severe side effects occur with long term use which may be an issue for regulatory approval. (Huang et al., 2018)(Riolobos et al., 2013) One potential way to overcome this would be by utilising CRISPR/Cas9 technology to “knockout” various potential triggers for the host immune system thereby circumventing the need for immunosuppression. For example, a recent study involving murine and human iPSCs, which underwent major histocompatibility complex (MHC) class I and II gene inactivation and CD47 overexpression, became hypoimmunogenic and were able to survive up to 50 days when implanted into fully MHC mismatched allogeneic mice.(Deuse et al., 2019)

Using an autologous source would minimise the use of immunosuppression; however, currently the logistics of obtaining donor cells and differentiating them is costly and time intensive. In addition, cells from an autologous source would not have been extensively tested in the same way as a GMP grade allogenic cell line.

### 1.7.9 Ventricular arrhythmia

The development of ventricular arrhythmia has always been a concern since the MAGIC trial involving skeletal myoblasts. It is possible however that this may be related to the mode of delivery since several recent publications regarding EHTs have not report any pathological arrhythmias despite durable and long lasting improvements in function and retention.(Gao *et al.*, 2018)(Shadrin *et al.*, 2017) In contrast, intramyocardial delivery seems more associated with the development of pathological ventricular arrhythmia, which appear to be generated from focal mechanisms originating from the graft cells.(Chong *et al.*, 2014)(Liu *et al.*, 2018)(Giannini *et al.*, 2017)(Romagnuolo *et al.*, 2019)

### 1.7.10 Teratoma formation

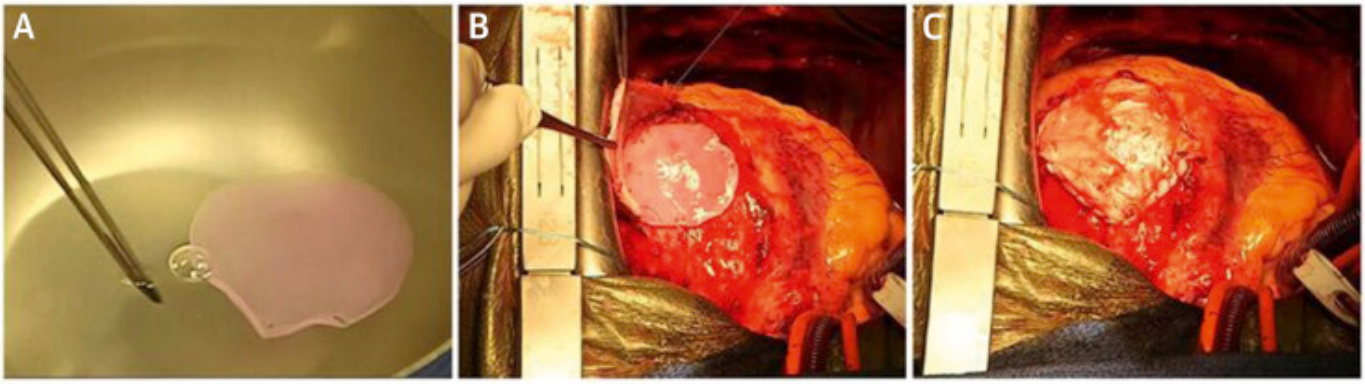
Finally, using EHT consisting of iPSC-CMs has the potential risk of unwanted cell differentiation and teratoma formation. This concern was as a result of teratoma formation post undifferentiated pluripotent cell implantation into immunosuppressed mice.(Minami and Murry, 2007) Teratomas and unwanted cell differentiation have however not been reported in several studies so far despite long term engraftment.(Chong *et al.*, 2014)(Weinberger *et al.*, 2016)(Liu *et al.*, 2018)

### 1.7.11 Clinical data

The concept of EHT has reached first in man trials. A patch of human embryonic

stem cells (SSEA-1+, Isl-1+) was delivered to 6 patients contained in a fibrin scaffold to patients with severe ischaemic advanced heart failure (EF<35%) and an indication for surgical coronary revascularisation.(Figure 1-16) The patch was attached to the epicardial surface with the use of autologous pericardium. Since cells were from an allogenic source, immunosuppression was given with ciclosporin and mycophenolate mofetil for one month. Out of 6 patients, 1 died soon after the operation due to comorbidities. Out of the remaining 5, none experienced ventricular arrhythmias and there was no evidence of teratoma or off target adverse proliferation. Although improvements in function were reported in the patch treated segments, all patients had undergone concurrent coronary artery bypass grafting, which may be a confounder. In addition, this was a phase 1 clinical trial with small numbers of patients reporting feasibility only.(Menasché *et al.*, 2018) Approval for another phase I Japanese study using cell sheets containing hiPSC-CM has recently been granted and is due to treat 3 patients over the course of one year. A common theme in these two trials is the short period of immunosuppression, removal of which inevitably causes the death of all cells in the graft. The short period of immunosuppression may be due to regulatory hurdles but nevertheless long-term immunosuppression is essential with current allogenic cell lines if a muscle replacement strategy is favoured over short term paracrine mediated repair.

**Figure 1-16: Implantation of a cardiovascular progenitor cell fibrin based patch**




*A) Cell containing fibrin patch during a final wash in a physiological serum-filled container, just prior to implantation over infarcted area. B) Patch placed onto epicardial area of infarcted region. C) An autologous pericardial flap is sutured around the infarcted area and then folded over the fibrin patch with the aim of pericardial growth factors to the patch. Reused with permission; Reference:* (Menasché *et al.*, 2018)

### 1.7.12 Other uses: Drug Screening

Since the description of the medium throughput method, EHTs can be made consistently with relatively low variability. The fact that they display several characteristics of human muscle, and can be made from hiPSC-CMs, makes them potentially suitable for drug screening / toxicology studies.(Hansen *et al.*, 2010)(Mannhardt *et al.*, 2016) For example, cardiotoxicity is currently an important issue, especially with the emergence of the cardio-oncology subspecialty, and the cardiotoxic nature of numerous oncological drugs.(Eder *et al.*, 2014)(Eder *et al.*, 2016)(Mannhardt *et al.*, 2017) Additionally, it has been shown that EHTs can be used for testing new anti-arrhythmic medications.(Lemoine *et al.*, 2017)(Lemoine *et*

*al.*, 2018) This new type of in-vitro testing may limit the failures that are so often seen when research progresses from the pre-clinical to clinical stage.

### 1.7.13 Disease modelling

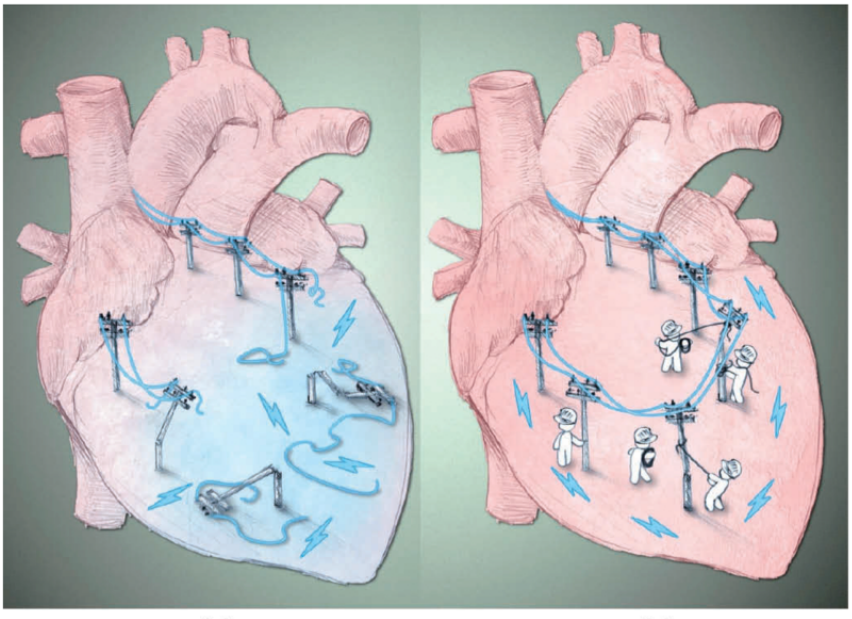
Since EHTs behave like heart tissue, great interest has been given to studying the effects of various heart diseases in EHTs derived from hiPSC-CMs. For example, recent work has focussed on hypertrophic cardiomyopathy and contraction abnormalities have been reported in EHTs derived from cells containing the Myosin Binding Protein-C defect (shorter relaxation and contraction times) when compared to controls.(de Lange *et al.*, 2012)(De Lange *et al.*, 2013)(Stöhr *et al.*, 2013) EHTs in conjunction with CRISPR/Cas9 editing can help model disease conditions in more detail. For example, analysing EHTs consisting of cells which have had point mutations corrected in myosin heavy chain 6; for example, ACTC1 or PRKAG2 mutations that cause HCM, or mutations that truncate the massive protein titin which cause DCM.(Hinson *et al.*, 2015)(Ben Jehuda *et al.*, 2018)(Mosqueira *et al.*, 2018)(Smith *et al.*, 2018) Other recent work has modelled conditions including Takotsubo and other various inherited cardiac conditions including long QT syndrome.(Borchert *et al.*, 2017)(Schwartz *et al.*, 2019) The advantage of this method is that hiPSC-CM can be modelled in-vitro and the ethical use of animals is circumvented.

## 1.8 Biomaterials - Conductive polymers

Due to the limitations with stem cell grafting, even with the use of biomaterials (arrhythmia / lack of coupling), research has focussed on the use of conductive polymers to help aid integration and potentially improve cell survival.

Clinically, they could be used as a vehicle for pluripotent stem cell delivery to mitigate arrhythmia risk during the early integration phase which may reduce arrhythmia and improve cell retention. (Cui, Yang and Li, 2016) The paradigm behind the use of conductive polymers is to correct the impaired conduction that occurs in areas of scar after a myocardial infarction (Figure 1-17). Conductive polymers are attractive since they can be relatively easily synthesised, contain intrinsic electrical properties and can potentially be biocompatible and biodegradable. The conductivity of the polymers is due to the conjugated backbone formed by a series of single and double bonds in an alternating fashion. (Cui, Yang and Li, 2016)

**Figure 1-17: Paradigm behind conductive polymers and conductivity**




*A) Scar tissue formation post myocardial infarction disrupts homogenous electrical signal propagation, increasing the risk of arrhythmia development; B) Conductive polymers may smooth over heteregenous conduction by reconnecting damaged areas with existing healthy myocardium, repairing damaged electrical pathways.*

*Reproduced (open access) from Reference: (Cui, Yang and Li, 2016)*

There are many conductive polymers including polypyrrole, polyaniline (PANI), poly(3,4-ethylenedioxythiophene) (PEDT, PEDOT), polyazulene (PAz), and polythiophene derivatives. Of these, PANI has recently been shown to have prolonged electrical properties when doped with phytic acid on the surface of a chitosan film (figure 1-18). The chelation between phytic acid and chitosan led to a conductive patch that had retained electroactivity, low surface resistivity and oxidised form after 2 weeks' incubation.(Mawad *et al.*, 2016) Ex-vivo experiments using myocardial slices and rat hearts revealed that the heart immediately changed the electrophysiology of the heart, speeding up conduction over areas of infarcted tissue. In contrast, the opposite was found on healthy hearts. Further in-vivo work is needed in larger animal models to see whether combining conductive polymers with hiPSC-CMs mitigates arrhythmia, improves coupling and cell retention before clinical translation occurs.

**Figure 1-18: Fabrication of PANI patch**

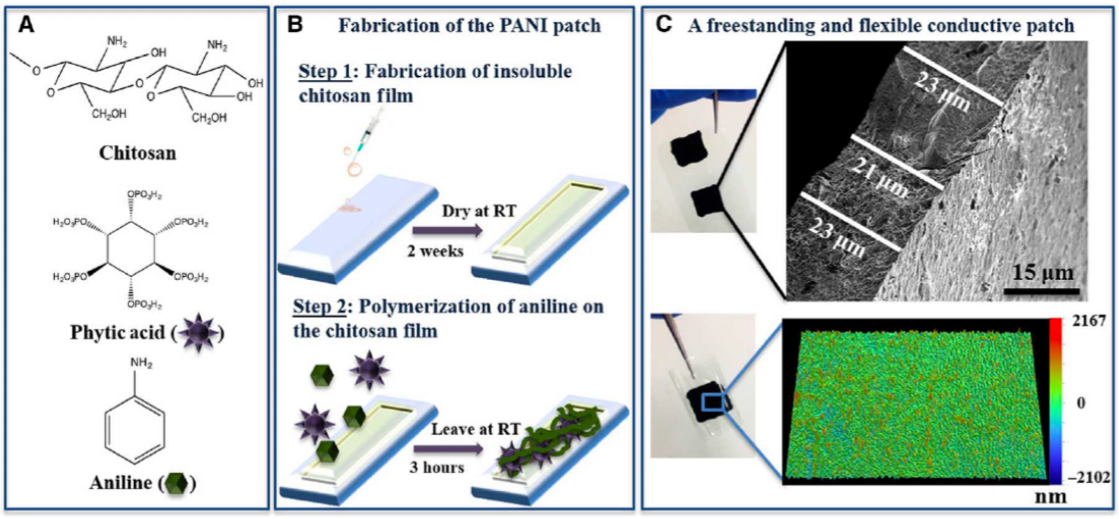


*Diagram showing how a PANI patch is made. A) Chemical components of chitosan, phytic acid and aniline; B) Manufacturing steps include fabrication of an insoluble chitosan film followed by polymerization of aniline on the chitosan film; C) Scanning electron microscopy image of a cross section of the patch (top). Surface topography of the patch recorded using an optical profilometer. Reprinted with permission from AAAS. Reference: (Mawad et al., 2016)*

## 1.9 Other regenerative medicine strategies

### 1.9.1 Gene therapy

Stromal cell-derived factor-1 (SDF-1) promotes tissue repair in a multitude of ways including vasculogenesis, endogenous stem cell recruitment and prolonging survival. STOP-HF was a phase II trial involving the administration (intramyocardial) of non-viral DNA plasmid gene therapy encoding stromal cell-derived factor-1 (JVS-100) to patients with heart failure (ischaemic). Although the primary endpoint was not met (change in six-minute walk test and quality of life questionnaire after 4 months), there were signals of benefit with improvements in LV function in the most advanced heart failure patients (LVEF<26%).(Chung *et al.*, 2015)

## 1.10 Future regenerative strategies

### 1.10.1 Cell cycle re-entry

It is well known that fetal cardiomyocytes actively divide as opposed to the relatively terminally differentiated adult myocardium. Therefore, this strategy is predominantly focussed on reverting adult cells back into a fetal like cell. In adult rat cardiomyocytes, certain cell cycle pathways and cyclin-dependent protein kinases have decreased expression whilst some cell cycle inhibitors are upregulated.(Lin and

Pu, 2014)(Ahuja, Sdek and MacLellan, 2007) Forced expression of certain cell cycle regulators to try and promote cell cycle re-entry and division has had mixed results. For example, transgenic expression of cyclin D2 formed *denovo* cardiomyocytes. In contrast, AAV delivery of E2F-1 causes apoptosis.(Hassink *et al.*, 2008)(Agah *et al.*, 1997) Certain paracrine factors including IGF-1 and p38 mitogen-activated protein kinase inhibition have also resulted in cardiomyocyte proliferation in small animal models.(Welch *et al.*, 2002)(Engel *et al.*, 2005) Similarly, Neuregulin-1, which is known to have an important role in fetal cardiomyocyte proliferation and adult cell survival has shown some signals of benefit in a phase I clinical trial.(Odiete, Hill and Sawyer, 2012)(Jabbour *et al.*, 2011) Micro RNAs, which can be administered as synthetic small molecules / AAV are known to regulate multiple gene pathways and have recently been implicated in cell cycle division.(Gabisonia *et al.*, 2019)(Olson, 2014) For example, 590 and 199a augment neonatal cardiomyocyte proliferation and promote healing of adult cells after infarction.(Eulalio *et al.*, 2012) The microRNA-17-92 group also promote proliferation(Chen *et al.*, 2013); in contrast, microRNA-15 causes the reverse effect.(Porrello *et al.*, 2013) A recent swine study by the Giacca group, showed convincing evidence of cardiomyocyte de-differentiation and proliferation by administering microRNA-199a to infarcted swine. Treatment was associated with improvements in global and regional contractility and a reduction in scar size. Notably however, the uncontrolled expression of 199a resulted in sudden arrhythmic death in the majority of animals. Further work is needed regarding dosage and expression but nevertheless this work is novel and in a large animal model.(Gabisonia *et al.*, 2019)

### 1.10.2 Direct reprogramming

A more recent radical idea of cardiac regeneration is to directly reprogram existing resident non-cardiomyocytes (fibroblasts) into cardiomyocytes. This could circumvent the potential issues regarding tumorgenicity and low engraftment rates with exogenous cell therapy. This has been achieved in mice using retroviral delivery of specific cardiac transcription factor genes: tbx5, Mef2c, Gata4, and in a murine myocardial infarction model improved function with a consequent reduction in infarct size.(Qian et al., 2012)(Ieda et al., 2010) Several other studies have also reported the fibroblast – cardiomyocyte direct conversion.(Wada et al., 2013)(Nam et al., 2013) A recent study was able to reprogram cells using a non-integrating Sendai virus, which was also associated with an improvement in cardiac function in a murine model.(Miyamoto et al., 2018) Numerous challenges lie ahead before clinical translation occurs. For example, direct targeting, increasing conversion efficacy and improving the cardiomyocyte like cells to make them more adult like are several obstacles that need to be overcome.(Fernández-Avilés et al., 2017)(Lin and Pu, 2014)(Hashimoto, Olson and Bassel-Duby, 2018)

## 1.11 Conclusion

It is now becoming apparent that the heart is no longer fully differentiated but an organ with potential regenerative capabilities. The regenerative medicine field is expanding rapidly, phase III clinical trials are ongoing involving exogenous cell administration, whilst other newer modalities involving endogenous repair mechanisms are at still at the preclinical stage. Further preclinical work is needed in all areas to understand the mechanism of improvement and develop novel ways of overcoming the existing limitations of each modality. Only then will effective but safe repair of patients with ischaemic heart disease be possible.

**Aims and hypothesis of current study**

The study of engineered heart tissue in this PhD has two main parts. The first part involves the in-vitro characterisation of the upscaled engineered heart tissue patch. This will be assessed using force measurements, contraction kinetics, calcium transients and hiPSC-CM alignment. The second part involves in vivo grafting experiments using an intermediate rabbit model to assess feasibility on control hearts and efficacy on infarcted hearts.

Additionally, an upscaled conductive polymer patch will be tested ex-vivo on control and infarcted rabbit hearts to ascertain whether the effects seen in smaller animal models can be replicated in a larger animal with a thicker ventricle (i.e. whether a polymer attached to the epicardial surface can affect myocardial electrical wavefront propagation).

### 1.12.1 Hypotheses:

- Engineered heart tissue will mature in-vitro over time when attached to their silicone supports
- The encapsulation of hiPSC-CM into EHT will increase cell retention over currently used delivery methods
- EHT will provoke arrhythmia when grafted onto infarcted rabbit hearts
- EHT will improve function in an intermediate model of myocardial infarction
- A conductive polymer patch will alter myocardial conduction when grafted onto the epicardium

### 1.12.2 Aims:

- Characterisation of EHT in-vitro (calcium transients, hiPSC-CM alignment, contraction kinetics
- Development of in-vivo rabbit model (control experiments)
- Development of in-vivo rabbit myocardial infarction model
- Development of in-vivo rabbit heart failure model
- Ex-vivo optical mapping of rabbit hearts with and without conductive polymer

# Chapter 2: Materials and Methods

## 2.1 Introduction

This chapter will describe the materials and methods used to obtain the data presented in this thesis. The specific techniques used range from: 1) *in-vitro* methods including stem cell differentiation and the formation of engineered heart tissue; 2) *in-vivo* methods including the development of the myocardial infarction and heart failure rabbit models; and 3) *ex-vivo* Langendorff / optical mapping experiments.

## 2.2 In-vitro methods

### 2.2.1 Cell maintenance and differentiation of hiPSC

*Cells were kindly differentiated by Dr Thomas Owen / Pragati Pandey / Thusharika Kogoda / Brian Wang / Oisin King.*

Undifferentiated stem cells (IMR-90, gCaMP6F [provided courtesy of Conklin laboratory]) were maintained in culture with mTeSR/TeSR-E8 (Stem Cell Technologies) and were then split (1:15) ratio by using versene (Thermo Fisher Scientific). Firstly, a six well plate was gently washed and incubated with versene (1ml in each well) for 8 min. The versene was then carefully aspirated and then replaced with 1ml of fresh media. The cells / media mix (RPMI B27 / 10% FBS) was then carefully dislodged from the plate using a pipette and then added to RPMI B27 / FBS containing 10mM of Rock inhibitor (Y-27632, Stem cell technologies). The cells were then plated with 2ml in each well. Differentiation was started when iPSCs had reached 80-90% confluency. Firstly, CHIR 99021 (6μM [Tocris Bioscience]) was added at day 0. On day 2, media was changed to RPMI-B27 minus insulin. On day 3, WNT-C59 2.5μM (Tocris Boiscience) was added, and then on day 4, RPMI-B27

minus insulin was then readded. Cells were maintained in this media until beating occurred at approximately day 8-10. To obtain iPSC-CM, at day 11 metabolic selection with glucose free media was started and continued until day 15. This is because iPSC-CM can utilise lactate as an energy source.(Burridge *et al.*, 2014) At day 15 cells were replated and maintained in RPMI-B27 containing insulin until isolated.

### 2.2.2 Cardiomyocyte isolation

Day 15-29 hiPSC-CMs were firstly removed from the 6 well format using Collagenase II (Thermo Fisher Scientific) at 200U/ml contained in HBSS (Thermo Fisher Scientific), HEPES (Thermo Fisher Scientific), BTS (4-Methyl-*N*-(phenylmethyl)benzenesulfonamide, Tocris), Rock inhibitor (Y-27632, Stem cell technologies). Firstly, the cell media was aspirated and then the cells washed with calcium (-) HBSS twice at 37 $^{o}$C. The collagenase solution was then added to each well (1.5ml each 6-well). The 6 well was then incubated for 2.5-3.5 h at 37 $^{o}$C. The cells were then placed into a falcon tube and equal volumes of RPMI and DNAse (1 in 500 concentration) added. The cell suspension was then centrifuged for 15min at 100g. Cells were then resuspended in 10mls of media and counted using an automated cell counter. Cells were then recentrifuged and resuspended in 10ml NKM media (Fetal calf serum 10%, 1% glutamine, 1% penicillin/streptomycin, DMEM [Thermo Fisher]).

### 2.3 Engineered Heart Tissue

*EHTs were predominantly created with Dr Thomas Owen.*

#### 2.3.1 First generation

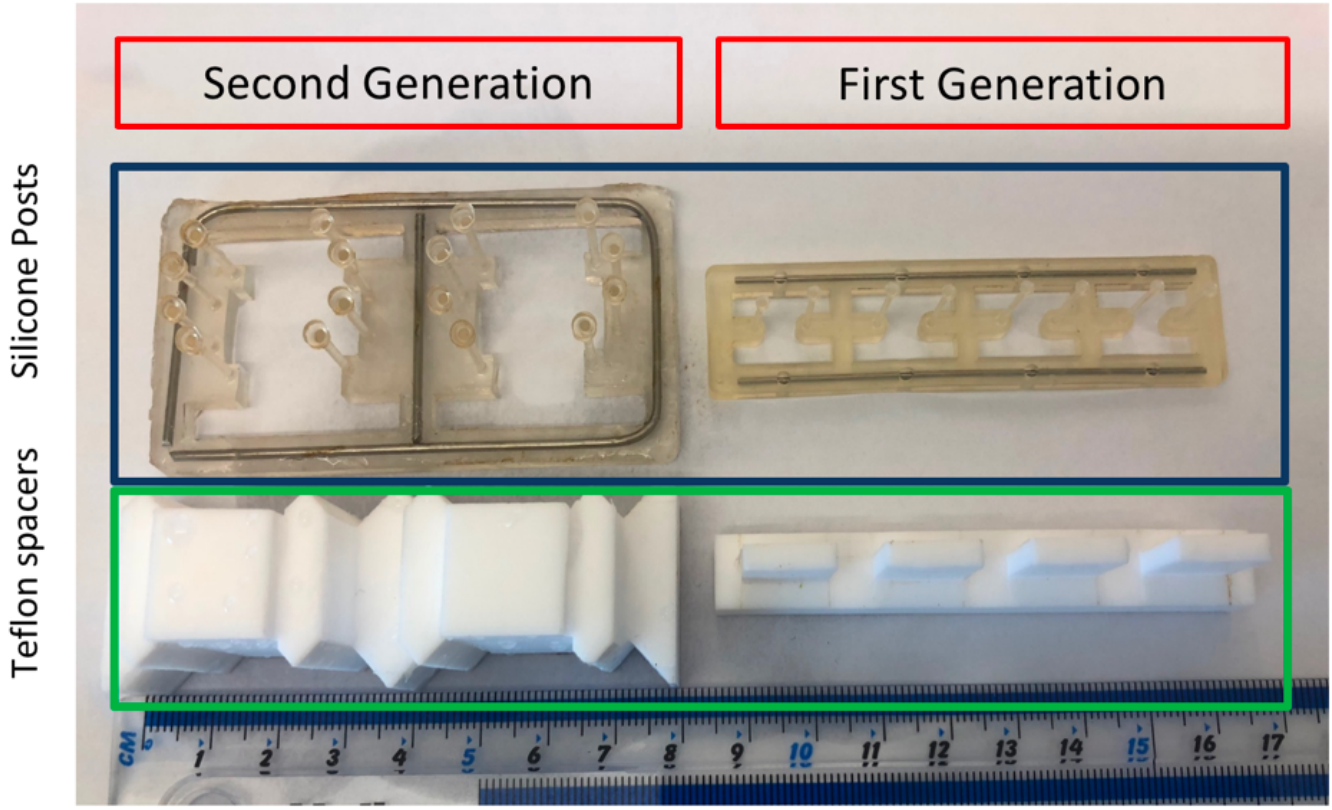
First generation EHTs were manufactured as previously described.(Breckwoldt *et al.*, 2017) Firstly, 1.6ml of 2% liquid agarose (in PBS) was placed into each well of a 24-well plate. Then a Teflon spacer (Figure 2-1) was quickly placed to form a casting mold for the master mix solution, and then after 10-15min, once the agarose had cooled and solidified, the spacers were removed.

The master mix consisted of: 1) hiPSC-CM $1x10^6$ 2) fibrinogen (Sigma 200mg/ml); 3) 2 x DMEM; 4) aprotinin (Sigma-Aldrich); and 5) NKM media. The master mix was prepared on ice and then pipetted 15 times to ensure the fibrinogen and other reagents were equally distributed in the solution. Thrombin stock (Evicel, 800-1200 U/ml) was firstly diluted to a concentration of 1:10 (in 60% PBS and 40% water) and then 3µl placed into individual PCR tubes (1 tube for each EHT). 100µl of the master mix was then quickly mixed with one thrombin aliquot, and then pipetted into the agarose casting molds.

The 24-well plate with fibrin gels was then placed in the incubator for 90 min (37$^{o}$C, $CO_2$ 7%, $O_2$ 40%, humidity 100%). Each well was then hydrated with 300µl of warm EHT media (DMEM, 10% horse serum [Gibco 26050], 1% penicillin/streptomycin [Sigma], 0.1% human insulin [Sigma], 0.1% aprotinin [Sigma]) and a further 30 minute incubation. Finally, the EHTs were transferred to a new 24-well plate with 2ml EHT media in each well. The media was changed on Monday, Wednesday and Fridays for maintenance (2ml each time). The silicone racks and Teflon spacers

were washed thoroughly in boiling demineralised water and then autoclaved prior to reuse (Figure 2-1).

**Figure 2-1: Engineered heart tissue silicone posts and Teflon spacers**



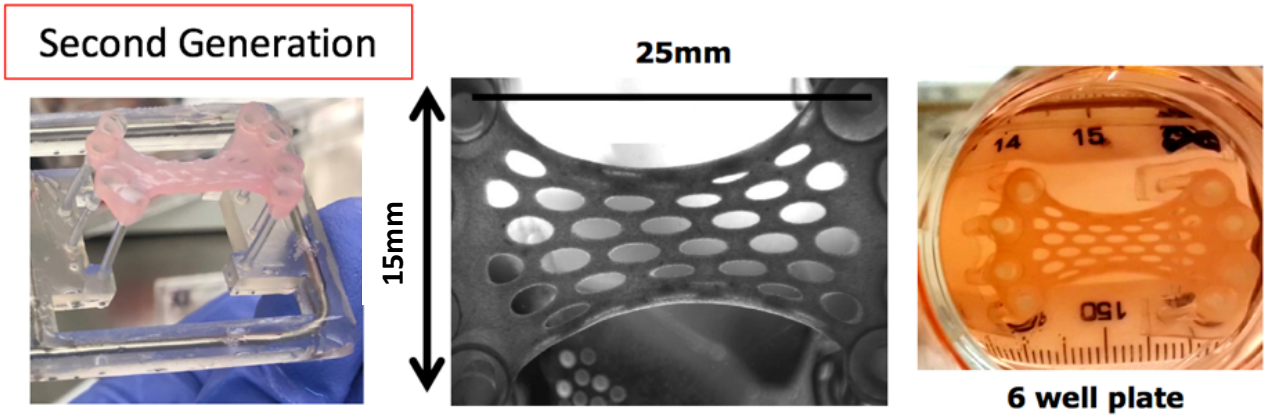

*Significant upscaling was achieved moving from first generation EHTs to second generation EHTs. This was achieved by an increase in the size of both the posts and Teflon spacers used to create the EHTs. Upscaling achieved by collaborating with Prof Thomas Eschenhagen's group.*

### 2.3.2 Second generation

The manufacturing process of the upscaled EHT with master mix, fibrinogen and thrombin reaction is largely similar to and adopted from first generation EHT. Firstly, sterile silicone nets were added to 8ml sterile 5% pluronic (Sigma-Aldrich) for at least 15 min. Whilst the nets were immersed in the pluronic solution, the Teflon spacers

were placed into a fresh 6 well plate and 8ml of sterile liquid agarose added to each well (Figure 2-1). Whilst the agarose was cooling down, the EHT master mix (table 2-1) was made on ice. The silicone nets used to make holes in the EHT were then washed in PBS once and then shaken lightly. After the agarose has solidified, the spacers were removed and the silicone net positioned into the mold. The silicone posts were then placed into the mold and the feet carefully placed into the correct position. The thrombin was then added to the master mix and quickly pipetted up and down using a 2ml pipette to ensure that it was mixed evenly throughout the master mix. The master mix was then pipetted directly into the agarose mold. Any air bubbles were then quickly removed with a 1ml pipette and the master mix checked to ensure even dispersion. The 6 well plate was then placed into the incubator for 45 min. After 45mins, 2-3 ml of warmed media was then added to the well for hydration and then the 6 well plate placed into the incubator for a further 15 min (Figure 2-2). After a total of 60mins, the silicone posts were then carefully removed from the mold and placed into a fresh 6 well containing 8-10mls of prewarmed media. EHTs were fed with 8-10mls of media each day.

**Figure 2-2: Macroscopic images of upscaled engineered heart tissue**




*Macroscopic images of upscaled EHT. Upscaling achieved by collaboration with Prof Thomas Eschenhagen's group.*

### 2.3.3 EHT stock solutions

1) EHT media:

   Typically made and stored in 50ml Falcon tubes at 4 $^{o}$C:

   - 5ml Horse serum (10%),
   - Insulin 50µl (0.1%, 10µg/ml),
   - Aprotinin 50µl (0.1% of 33µg/ml),
   - 500µl (1% penicillin/streptomycin).
   - 45ml DMEM + / +.

2) Aprotinin:

   - Add 33mg per 1ml of sterile cell culture grade water. Aliquoted into 50µl PCR tubes and then stored in freezer at -20 $^{o}$C.

3) Fibrinogen:

   - 200mg/ml (sterile) in pre-warmed 0.9% Sodium Chloride solution
   - Add 72.1µl aprotinin (33mg/ml stock) to 25ml fibrinogen solution
   - Mix, aliquot into 100µl and store at -20 $^{o}$C.

4) Thrombin:

   - 100U/ml made up in 60% sterile PBS and 40% sterile water.
   - Aliquot and store -20 $^{o}$C.

5) 10x DMEM solution:

   - dissolve 670mg DMEM powder in 5ml cell culture grade water,
   - sterile filter and store at +4 $^{o}$C.

6) 2x DMEM:

- 2ml 10x DMEM solution
- 2ml Horse serum 2ml,
- 0.2ml of penicillin / streptomycin
- 5.8ml cell culture grade water
- sterile filter and store at +4 $^{o}$C.

7) NKM media

- 10% inactive fetal calf serum
- 1% glutamine (200mM)
- 1% penicillin/streptomycin
- DMEM

**Table 2-1: Master Mix solutions for engineered heart tissue**

| Reagents | Stock Concentration | Working Concentration | For 1 EHT |
|---|---|---|---|
| hiPSC | - | | 15 - 20,000,000 |
| 2x DMEM | - | 2x | 93.5 µl |
| Matrigel | 100% | 10% | 170 µl |
| Y-27632 | 100% | 0.10% | 1.7 µl |
| Fibrinogen | 200 mg/ml | 5 mg/ml | 42.5 µl |
| Thrombin | 100 U/ml | 3 U/ml | 51 µl |
| Sum of supplements | | | 358.7 µl |
| Cell volume (µl) | | | 1000.00 µl |
| NKM to add (µl) | | | 341.30 µl |
| Total volume (µl) | | | 1700.00 µl |

## 2.4 In-vitro engineered heart tissue characterisation

### 2.4.1 Contraction kinetics

*Contraction Kinetics were recorded and analysed with the help of Daphne Pantou and Mr Pragati Pandey.*

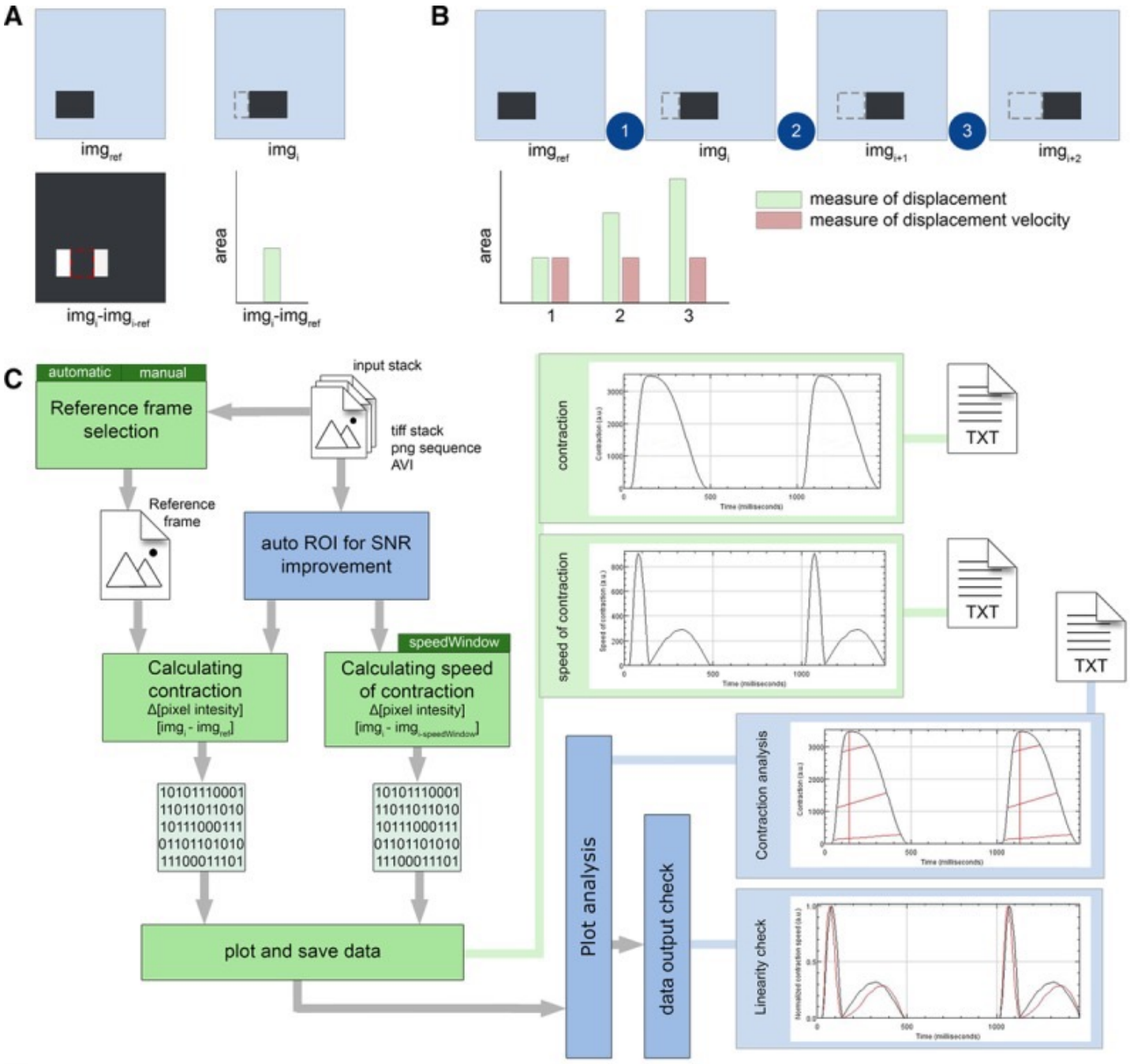
Contraction kinetics were calculated using an open source software tool (MUSCLEMOTION) from videos obtained from a Basler camera (acA720-520µm) at 100 frames per second.(Sala *et al.*, 2017) The software enables the calculation of movement from high frame per second movies and determines the dynamic changes in pixel density that is present between each image frame and presents the data as a relative change in movement during cardiomyocyte contraction and relaxation. The principle underlying the algorithm is the assessment of contraction by the quantification of the absolute change in pixel intensity between a reference frame and frame of interest:

$$\left| img_i - img_{ref} \right| = img_{result}$$

In any given frame, each pixel of interest is subtracted from the reference pixel and the difference is represented in absolute number format. Black pixels correspond to low values or unchanged pixels. In contrast, white values indicate greater change (figure 2-3A). Mean pixel intensity of the whole image is calculated next and is a quantitative measure of how much the pixels have moved compared to the reference frame with higher numbers of white indicating more movement. If a series of images were analysed relative to the same ref image, the output is presented as accumulative change or displacement over time (figure 2-3B). The software also improves signal to noise ratio from video recordings, automated ref frame selection

and built in checks to ensure data validity (figure 2-3C). The software is used on open source ImageJ.

**Figure 2-3: Principles of MUSCLEMOTION**




*A) Method of measuring pixel intensity difference by subtracting $img_{ref}$ from $img_i$, which is then followed by measuring the nonzero region post image subtraction. B)*

*Method of using pixel intensity difference to quantify displacement and displacement velocity. C) Diagram depicting the overview of MUSCLEMOTION. Reused with permission. Reference: (Sala et al., 2017)*

### 2.4.2 Calcium transients

*Calcium transients were analysed / recorded with the help of Dr Thomas Owen*

Calcium transient recordings from hiPSC-CMs were obtained using genetically encoded calcium indicators, specifically gCaMP6F hiPSC-CMs (provided courtesy of the Conklin laboratory and obtained by Dr Sam Kitanan). A brief overview regarding genetically encoded calcium indicators and the gCaMP6F line will be described.

### 2.4.3 GECI

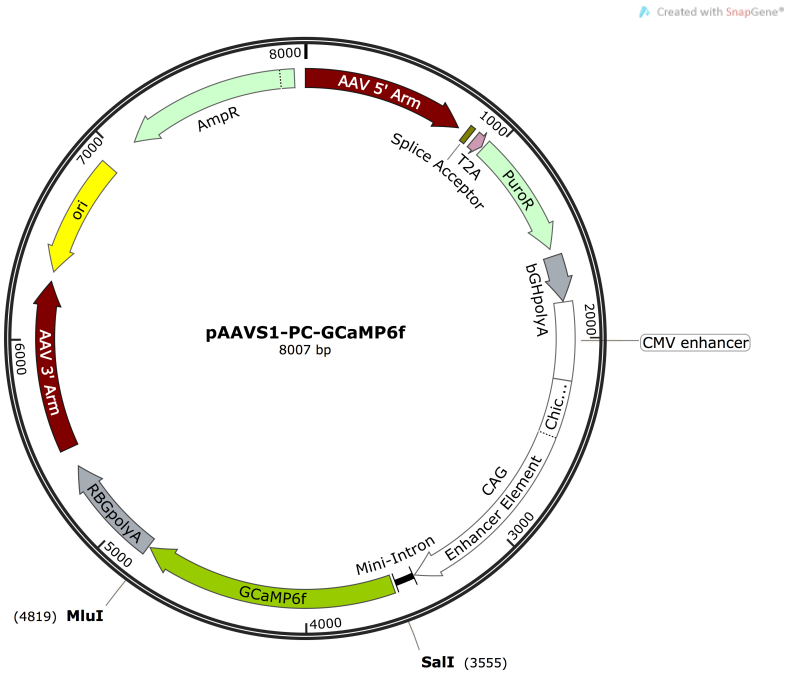
GCaMP is a genetically encoded calcium indicator that was initially pioneered in 2001 (Nakai, Ohkura and Imoto, 2001), after several groups were investigating the use of green fluorescent protein based calcium probes. GCaMP is formed by the fusion of green fluorescent protein, calmodulin and the M13 peptide of myosin light chain kinase.(Mandegar *et al.*, 2016) Firstly, Green fluorescent protein is circularly permutated, which results in the fusion of N- and C- termini. This creates a new terminus in the central portion of the protein to which calmodulin and M13 were fused. In calcium depleted states, circularly permutated fluorescent proteins were poorly fluorescent. When calcium binds to calmodulin, there is a conformational change and the hinge region is able to bind certain peptides on target proteins including M13. There is also a structural shift that results in fast deprotonation of the chromophore and an increase in fluorescence intensity.(Wang *et al.*,

2008)(Akerboom *et al.*, 2009)

The plasmid insertion technique of gCaMP6F was carried out via TALEN (transcription activator-like effector nucleases) which is one of the most precise and "cleanest" editing methods currently available, and when compared to retroviral methods and CRISPR is associated with a lower change of random/off target effects.(Boch, 2011)(Boettcher and McManus, 2015) This translates into a lower likelihood of silencing occurring due to editing errors. GCaMP was expressed via a CAG promoter which is a hybrid construct, consisting of the cytomegalovirus (CMV) enhancer fused to a chicken beta-actin promoter which enables reliable and constant expression (figure 2-4).

The GCaMP containing plasmid was inserted into the Adeno-Associated Virus Integration Site 1 (AAVS1), which is the most widely used safe harbour locus (figure 2-4). It is relatively easily and efficiently targeted, and supports robust and stable, long-term transgene expression without any untoward effects on the modified cells.(Qian *et al.*, 2014)(Smith *et al.*, 2008)

**Figure 2-4: gCaMP6f**




AAVS1 locus, CMV enhance and gCaMP6 insertion.

(Reference: https://www.addgene.org/browse/sequence/135875/)

### 2.4.4 Calcium Transient Analysis

*Calcium transient analyses were analysed / recorded with the help of Dr Thomas Owen*

Videos of EHTs containing gCaMP6F hiPSC-CMs were obtained using a Zeiss AxioObserver Microscope with a minimum frame rate of 250 frames / second. Intensity profiles were plotted and transient kinetics extracted and analysed manually using Clampfit software. The time to peak (ms) was obtained by analysing the difference between baseline time and peak voltage. Curve decay characteristics were calculated at time to 50%, 75%, and 90% decay from peak voltage using

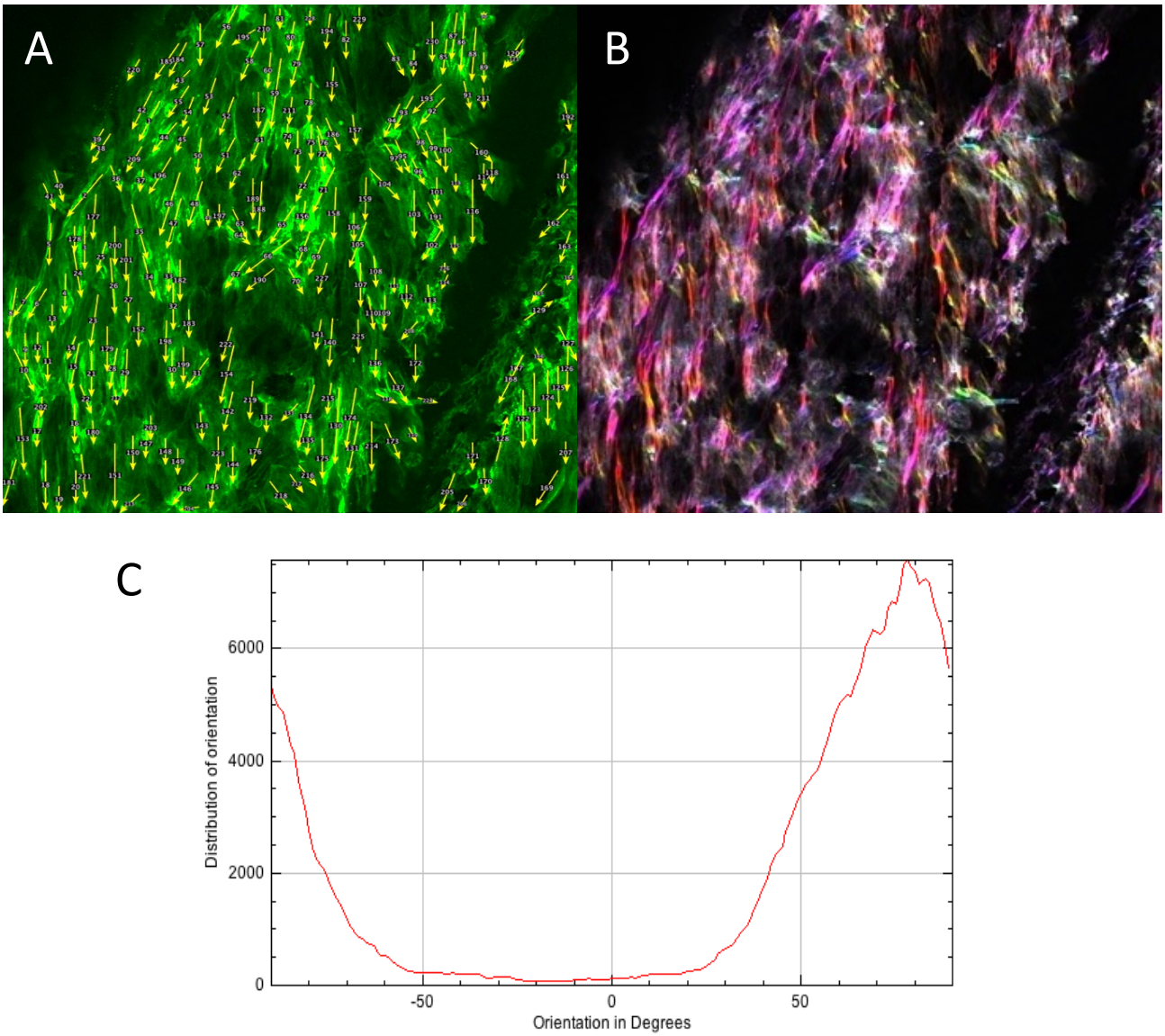
manual calculation with Clampfit software. EHTs were loaded with BDM (30 mmol/L) prior to calcium transient analysis to minimise the effect of motion artefact.

### 2.4.5 Cell Alignment

*Cell alignment images were analysed with the help of Dr Thomas Owen and Daphne Pantou*

The alignment of hiPSC-CMs contained in the EHT were assessed at varying time points during the in-vitro maturation phase. EHTs were stained for troponin T and DAPI and confocal images obtained on an inverted Zeiss LSM-780 confocal microscope. A dedicated macro was used to assess alignment (Orientation J, Biomedical Image Group (BIG), EPFL, Switzerland). The macro produces a histogram of the image which calculates the overall alignment of the troponin positive cells (previously immunostained) contained in the EHT (figure 2-5 B/C). In addition, the cumulative angle change between troponin T stained cells was assessed manually using Image J (Macro tool created by Mr Stephen Rothery, figure 2-5A).

**Figure 2-5: Cell alignment**




*a) EHT stained with troponin T (488 channel). The overall alignment or cumulative angle change between the cells was determined by manually analysing the vectors of the cells (Yellow Arrows); b) Automated processed image of troponin T stained EHT using Orientation J macro; c) Histogram produced by Orientation J macro.*

### 2.4.6 Conduction velocities

*Conduction velocity recordings were obtained with help from Dr Fillipo Perbillini and Mr Fotios Pitoulis.*

Conduction velocities of engineered heart tissue was assessed using a dedicated multi-electrode array (MEA) system (Multichannel Systems, Reutilingen, Germany). This system permits the recording of extracellular field potentials in a synchronised manner in real time. An MEA plate was made up of 60 microelectrodes arranged in an 8 x 8 matrix (no corner electrodes). The specific distance between electrodes was 700μm whilst the diameter of the electrode was 100μm which equates to a recording area of approximately 4.9 × 4.9 $mm^2$.

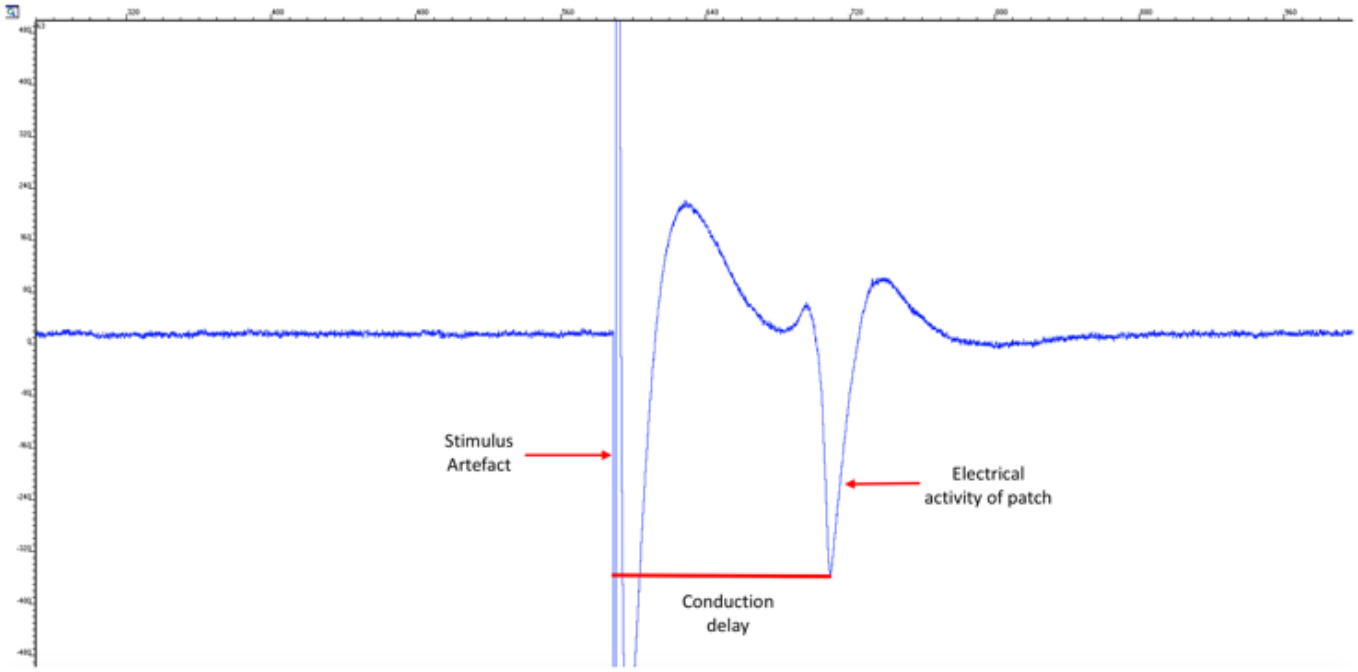
Firstly, the engineered heart tissue was removed from the posts and gently placed onto the MEA surface. It was held in place with a custom built plastic mesh and a small metal weight placed on top to ensure adequate contact between the EHT and MEA dish (figure 2-7A/B). The EHT was continuously perfused with oxygenated Tyrode's solution, heated to 37 $^oC$. MEA recordings were taken with (bipolar stimulation, 0.5-2Hz, 1ms width, 2 Volts) and without point stimulation from one of the MEA electrodes for approximately 10 seconds. Raw data from each MEA plate was first amplified by a filter amplifier and then digitised at a sampling rate of 50 kHz (MC Card hardware). It was then recorded on dedicated software (MC Rack).

Conduction delay was then calculated from both the stimulus artefact and the steepest part of the activation complex, enabling conduction velocity to be calculated from the following formula:

$$\text{Conduction Velocity (mm/s)} = \frac{\text{Distance µM (point of stimulation of electrode X)}}{\text{Activation complex time - Stimulus artefact time (ms)}}$$

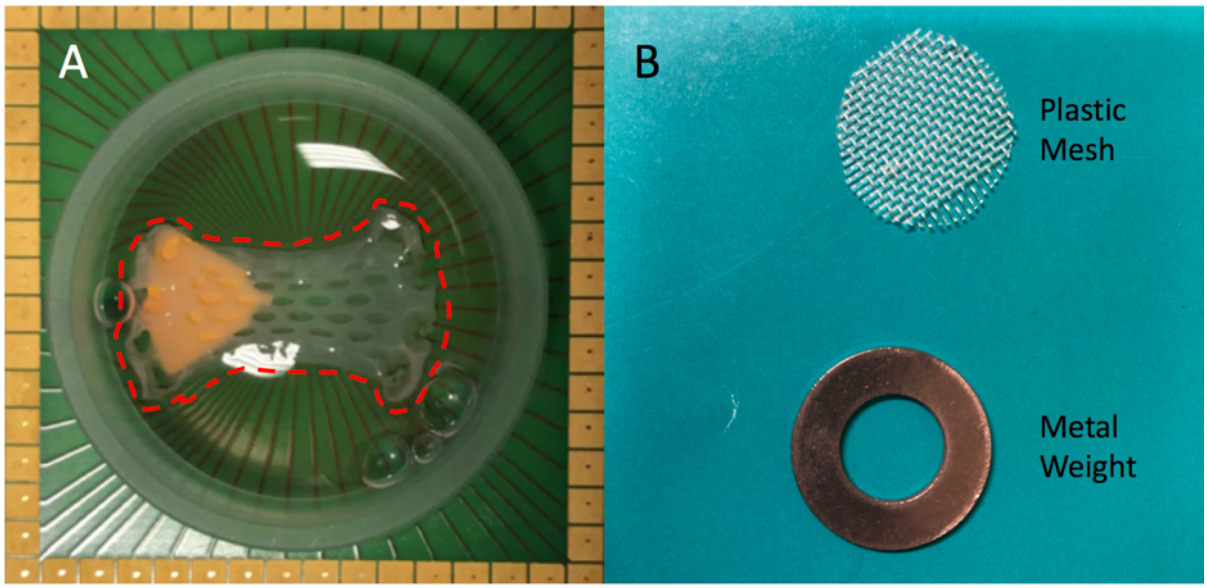
An illustration of conduction delay measurements was shown in the below figure 2-6. MATLAB (Mathworks) script was used to analyse data and generate activation maps conduction velocities as previously described.(Watson *et al.*, 2019)(Chowdhury *et al.*, 2018)

**Figure 2-6: Example of MEA electrode recordings**




*Stimulus artefact and electrical activity of patch. Conduction velocity can be calculated from the distance between the stimulus artefact and electrical activity of the patch (conduction delay).*

**Figure 2-7: Microelectrode array and plastic mesh / weight**




*A) Microelectrode array dish with EHT on the surface, EHT is outlined with red dotted lines; specific distance between electrodes is 700µm whilst the diameter of the electrode is 100µm which equates to a recording area of approximately 4.9 × 4.9 mm2 at the centre of the dish. Yellow triangle points to centre of dish. B) Plastic Mesh and weight used to enhance contact between EHT and MEA surface electrodes. The mesh is placed over the EHT, upon which the weight is placed over the mesh.*

### 2.4.7 Calculation of Troponin T Retention in Graft

*Retention analyses were primarily carried out by Daphne Pantou and Pragati Pandey.* A custom-made macro (developed by Mr Stephen Rothery) was used to calculate the percentage of troponin positive staining in the graft relative to day 0 controls. Image analysis was carried out on wax stained troponin positive sections using 3,3′-Diaminobenzidine (DAB) staining. A brief description of the macro will be described. Firstly, an EHT image is stitched, and then converted to 8 bit (figure 2-8A). It is then smoothed, the contrast enhanced, background subtracted and Gaussian blur applied. A line is then drawn around the EHT in Image J (figure 2-8B), after which the threshold for the tissue is set (Fig 2-8C). The macro then splits the

DAB signal (colour deconvolution) from the EHT (Fig 2-8D). The EHT troponin positive area (DAB threshold set) is then provided in numeric form (figure 2-8E/F).

**Figure 2-8: Troponin measurement macro**

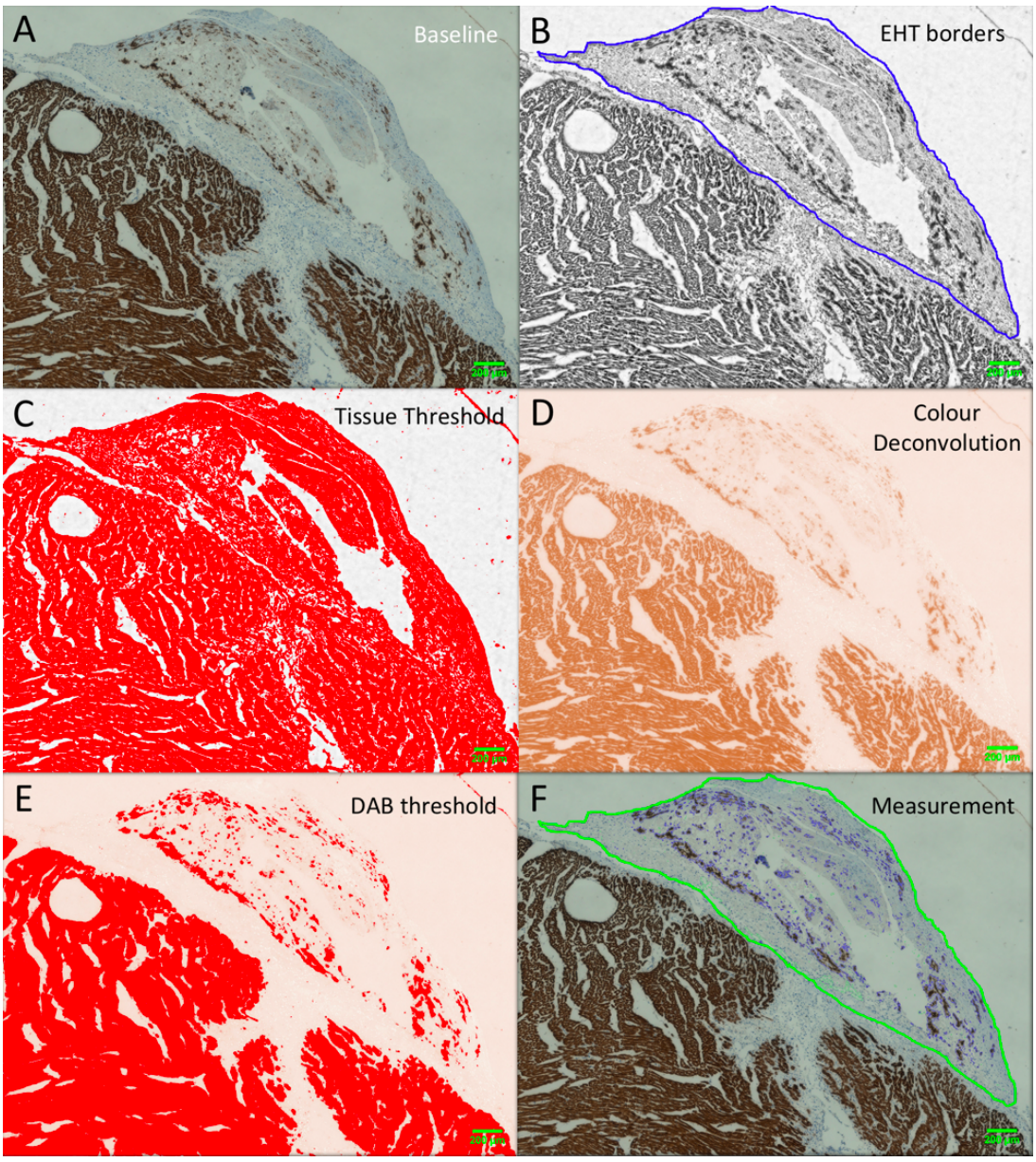



*Figure illustrating the steps in the macro to calculate area of troponin positive signal in the EHT. Macro is applied in Image J. Steps include drawing around the EHT borders (A); followed by setting tissue threshold (C); colour deconvolution (D) and then setting threshold of troponin signal. The two signals are then measured as a fraction (F).*

### 2.4.8 Capillary density calculation

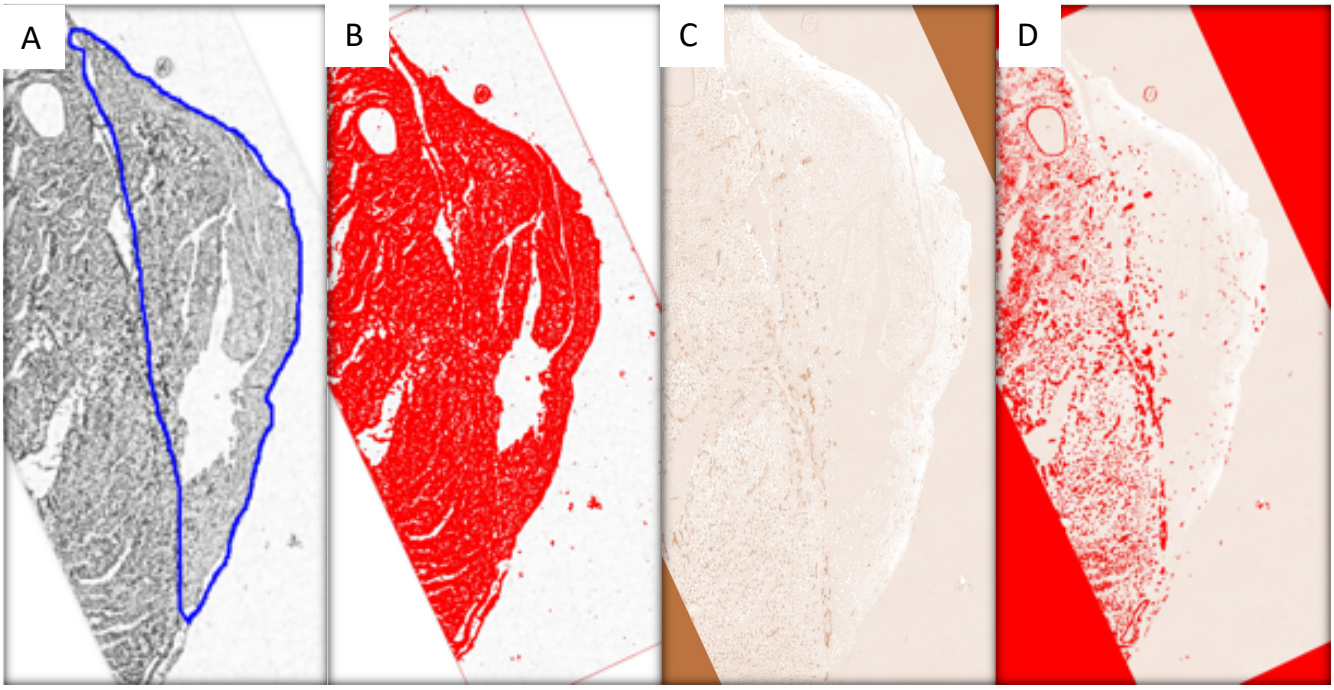
*Capillary density analyses were carried out with the help of Daphne Pantou and Pragati Pandey.*

Capillary density in the EHT was calculated using the Cell Counter plugin (Author: Kurt De Vos, University of Sheffield) in Image J. Firstly, staining was carried out on 5µm wax embedded sections that were previously fixed in PFA and processed as described previously.

Subsequently, sections were stained with the CD31/PECAM-1 antibody (Novus Biologicals, JC/70A, NB600-562SS) and visualised with 3-3-diaminobezedine (DAB) staining. Nuclei were counterstained with haematoxylin. 20x magnification images of the whole graft / ventricular host border zone were then taken on a Zeiss AxioObserver Microscope and analysed on Image J.

Initially, the image was processed in a similar way to the troponin stained sections by firstly stitching the image, converting to 8 bit, smoothing, contrast enhancement, background subtraction and then Gaussian blur applied. A line was then drawn around the EHT in Image J (figure 2-9A) and the threshold for the tissue set (figure 2-9B). The macro then splits the DAB signal (colour deconvolution) from the EHT (Fig 2-9C), and the CD31 positive staining in the EHT is then shown (figure 2-9D).

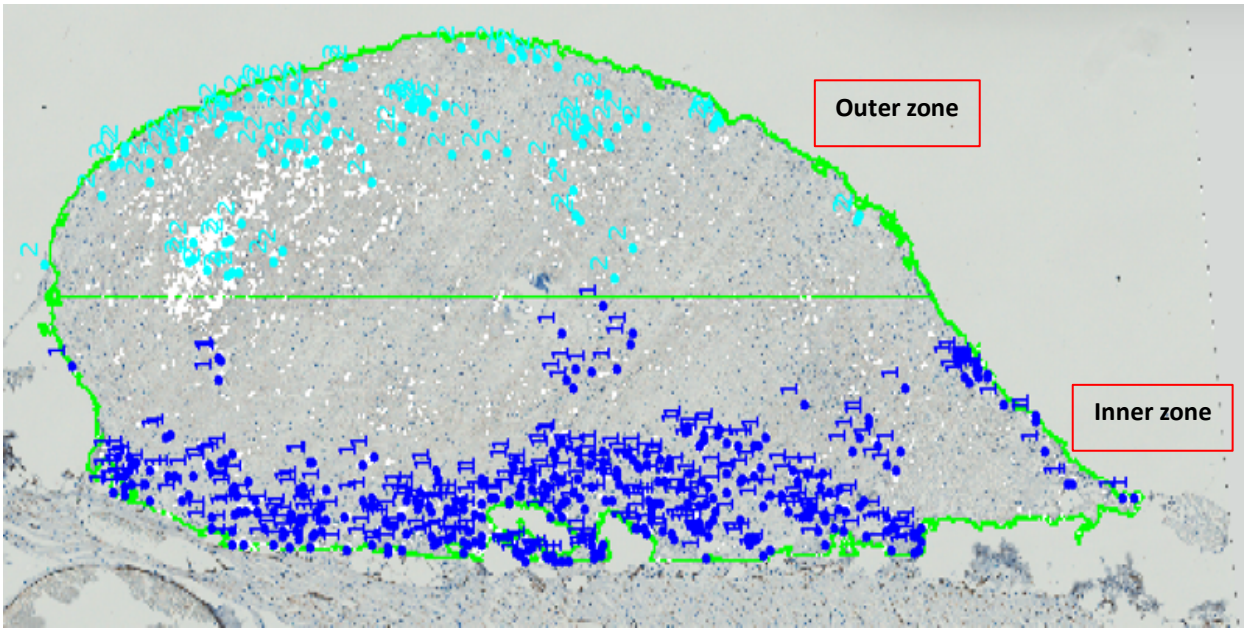
**Figure 2-9: Processing of CD31 stained images**




*A) The outline of the EHT is drawn around the processed image; B) Threshold for total tissue; C) Colour deconvolution; D) Presence of CD31 staining*

The number of CD31 cells were then manually counted in the EHT graft using the Cell Counter plugin and then divided by the EHT area and capillary density presented as number of CD31/PECAM-1 positive cells per $mm^2$. Further analysis included analysing capillary density in the inner and outer borders of the EHT using a custom-made Macro (Author: Mr Stephen Rothery, figure 2-10).

**Figure 2-10: Graft capillary density calculation**




*A custom made Macro (Credit: Mr Stephen Rothery) was used to calculate capillary density in the inner and outer zones of the EHT graft. Inner zone CD31 positive cells were manually counted and appear in dark blue. Each dark blue dot represents a CD31 positive cell. In contrast, light blue CD31 positive cells were in the outer zone. Each light blue dot represents a CD31 positive cell. Straight green line is the border zone between the inner and outer half of the EHT.*

## 2.5 Immunohistochemistry

*Immunohistochemistry was performed with help from Daphne Pantou and Pragati Pandey*

### 2.5.1 OCT embedding protocol

Samples were fixed in 4% PFA for 24 h. Then fixed samples were placed in a 30% sucrose solution in PBS for a further 24 h or until the sample sunk to the bottom of the container indicating appropriate dehydration. Samples were then placed into a preformed mold, embedded in Optimal Cutting Temperature (Tissue-Tek)

compound, then frozen in dry ice cooled isopentane and stored at -80 $^{o}$C. Sections were then cut on a cryotome at 10μm intervals.

### 2.5.2 Immunostaining protocol

Firstly, sections were permeabilized with 0.5% Triton X-100 (in PBS) at room temperature for 30 min. This was followed by a blocking step of 1 h with 4% FBS at room temperature. Samples were then incubated with a primary antibody at 4 $^{o}$C overnight, which was then followed by a secondary antibody for 1 h in a dark room at room temperature. Hoechst (1 in 1000) was then added for 10 min. Between each step, 3 PBS washes of 5 min were carried out. Vectashield (Vector Laboratories Ltd, UK) was used to mount the samples and the cover slip sealed with nail varnish. Confocal imaging was carried out using a dedicated Zeiss LSM-780 microscope.

### 2.5.3 Paraffin staining protocol

After optical mapping experiments, whole hearts were fixed for 24 h in 4% paraformaldehyde (PFA) and then cut into sections (2-4mm thickness) and temporarily stored in 70% alcohol solution. Samples were then processed and 5μm wax embedded slides created (Courtesy: Ms Lorraine Lawrence). The paraffin immunohistochemistry protocol was a 2-day protocol (See supplementary appendix for flow chart protocol). Firstly, dewaxing was performed by 2 x 15 min in Neoclear® (Sigma Aldrich), followed by rinsing (2 x 30 seconds) in 100% absolute alcohol. Endogenous peroxidases were then blocked by incubating sections in methanolic hydrogen peroxide for 10 min. Antigen retrieval was then performed by boiling the sections in citrate buffer (ph6) for 10 min in total (4 x 2.5 min). The sections were then rinsed with tap water, followed by phosphate buffered saline (PBS). A PAP pen was then applied around the section, followed by blocking in 5-10% goat serum in

PBS for 1 hour. This was then followed by the primary antibody and incubated overnight at 4 $^{o}$C. The slides were then washed with 3x5min triton buffer (0.1% Triton X-100 in PBS at pH 7.4) followed by secondary antibody 1 hour in PBS without serum. This was then followed by 3 x 5-minute wash with Triton buffer. The Vectastain ABC HRP kit (Vector labs) was then applied for 30 min. After 30 min the slides were washed with 3x5 min of the Triton buffer and then the DAB peroxidase kit (Vector labs) applied for 2-10min. Afterwards the slides were washed in running tap water for 10minutes to neutralise the DAB. The slides were then immersed in 200µl of Vector® Haematoxylin counterstain (Vector Labs) per sample for 5-10 min. The sections were then dipped 10x with deionized / distilled water and then the sections were left in running tap water for 5 min. The sections were then dipped 10 times in 70% alcohol and then transferred to a container with running tap water for a further 5 min. Finally, the sections were dipped 10 times with deionised / distilled water. Dehydration was then carried out with alcohol of varying concentrations (70% alcohol for 30 seconds [10 dips]; 95% alcohol for 30 seconds [10 dips]; 100% absolute alcohol for 45 seconds [10 dips]; 100% absolute alcohol [10dips]). Clearing was then performed with Neoclear® (7.5 min x 2). Finally, slides were mounted with DPX mountant (Sigma-Aldrich) and then a coverslip applied and left to dry for a minimum of 1 hour.

### 2.5.4 Myocardial Histology

*Histological staining was primarily performed by the research technician Lorraine Lawrence at the South Kensington campus at Imperial College London.*

Histological staining was primarily used to visualise and quantify infarct size and

morphology when developing the rabbit model of myocardial infarction and heart failure.

### 2.5.5 Haematoxylin and Eosin (H&E)

Firstly, wax embedded sections were deparaffinised and rehydrated as described previously. Slides were then washed briefly and immersed in Harris Haematoxylin solution for 5-8 min. Slides were then washed in running tap water for 5 min, then dipped in an acid / alcohol mixture (1% hydrochloric acid / 70% ethanol) and then counterstained with eosin for a further 2 min. Slides were then quickly washed in tap water and then dehydrated in alcohol solutions of varying concentrations (70%, 90%, 100%, 100%) for 30 seconds followed by Neoclear (2 x 7.5 min). Finally, coverslips were applied after mounting with DPX mounting medium (Sigma – Aldrich).

### 2.5.6 Sirius Red

Firstly, wax embedded sections were deparaffinised and rehydrated as described previously. Slides were then washed briefly and submerged in Harris Haematoxylin solution for 5-8 min, followed by a wash for 10min in running tap water. This was then followed by immersion in picro-sirius red for 60 min. Slides were then washed in acidified water (2 x washes in Acetic acid [5ml in 1litre of distilled water]). Dehydration was then performed with ethanol at varying concentrations (70%, 90%, 100%, 100%), followed by clearing with Neoclear (2 x 7.5 min). Finally, slides were mounted with DPX mountant and a coverslip applied.

## 2.6 In-vivo methods

### 2.6.1 Animal husbandry

Every procedure was performed according to the standards for the care and use of animal species written in the “Guide of the Care and Use of Laboratory Animals” (NIH publication No. 85-23. Revised 1996). In addition, experiments conformed to the dedicated requirements as set by the UK home office (ASPA 1986; Amendments Regulations 2012) which incorporates the EU directive 2010/63/EU. All the protocols carried out had prior approval from the Animal Welfare and Ethical Review Body of Imperial College London, UK.

### 2.6.2 Rabbits

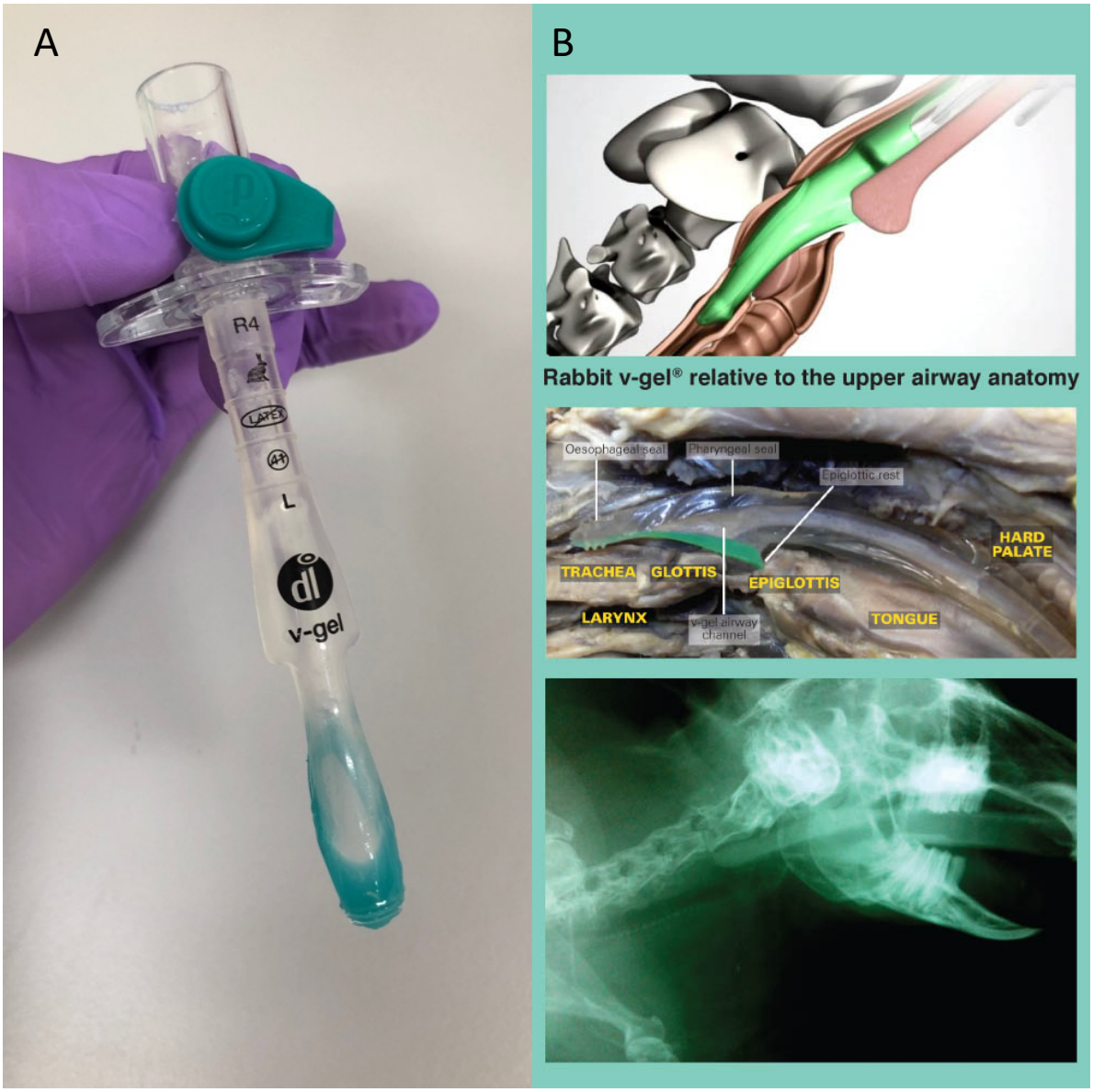
All rabbit experiments were carried out on male sex New Zealand white species at 2.5-3.5kg. Rabbits were obtained from Envigo Laboratories (Huntington, UK) and housed in the Centre for Biological Services (CBS) at Imperial College London for a minimum 14 days’ acclimatisation period (mandatory) before any recovery procedure. Terminal procedures were ideally carried on the day of arrival or could be carried out within the acclimatisation period if necessary. Rabbits were housed 1 per pen, and exposed to a 12-hour light dark cycle with maintenance temperature of 21 $^{o}$C.

### 2.6.3 Terminal, non-recovery

For terminal non-recovery procedures, rabbits were initially sedated with ketamine (7.5mg/kg) and medetomidine hydrochloride (0.125mg/kg) and then administered isoflurane gas via a facemask (1-2%). After 5-10 min animals were intubated using a V-gel tube® (figure 2-11) and then administered isofluorane at a higher concentration

(3-5%). A merlin small animal ventilator was used for periprocedural anaesthetic ventilation (figure 2-12).

**Figure 2-11: rabbit V-gel**




*A) macroscopic image of rabbit V-gel device used to inserted into oral cavity; B) upper panel: cartoon depicting V-gel (in green) location on intubation. The device covers the oesophagus while enabling airway ventilation via the trachea. It is inserted once the rabbit has been appropriately sedated. Middle panel: further diagram illustrating v-gel airway seal. Lower panel: X-ray image of intubated V-gel. Figure B obtained from: [http://www.millpledge.com/vgel-c6x13966364](http://www.millpledge.com/vgel-c6x13966364)*

An incision was then made in the left 4th intercostal rib of and the heart exposed after making an incision through the pericardium. An incision was then made in the centre of the abdomen (linea alba) and the descending aorta and inferior vena cava visualised. The aorta was then cannulated with an 18G green canula and 150-200ml of ice cold cardioplegic solution (Harefield Hospital Formulation; composition mmol/L: Na 147; K 84; Mg 80; Ca 2; Procaine 5; Chloride 400) administered. Just prior to administration of cardioplegia, an incision was made in the IVC to prevent intracardiac pressure build up during fluid administration. Additionally the IVC and aorta distal to the insertion of the green cannula were clamped to prevent antegrade passage of the cardioplegic solution. After cessation of heart beating, the heart was then explanted and placed into cold cardioplegic solution with heparin (12units / ml). Care was taken to preserve the aorta to the level of the aortic arch so that Langendorff experiments could be performed. *Credit: Dr Sean Bello helped me perform the first terminal procedure utilising the intrabdominal vessels to administer cardioplegia.*

### 2.6.4 Myocardial infarction

*Mr Michael Dunne taught me the rabbit model at Glasgow University. Modifications to their protocol were made and developed at Imperial College London.*

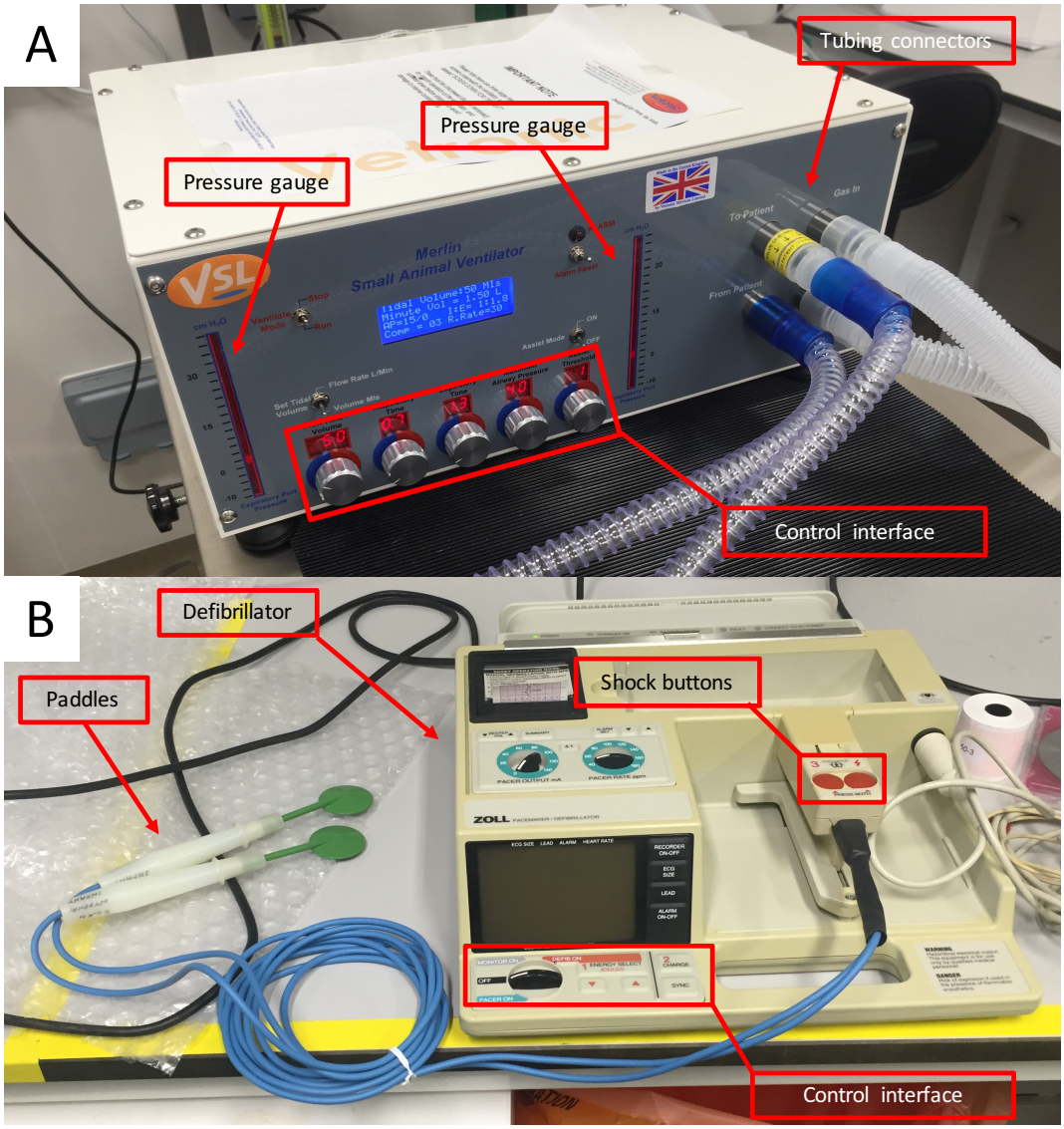
After sedation with ketamine (7.5mg / kg) and medetomidine hydrochloride (0.125mg/kg), the rabbit was first shaved to prepare the operating area. The rabbit was then intubated with a V-gel and placed on its right side (protocol similar to non-recovery). Ventilator settings were titrated according to weight (10-15mls per kg for tidal volume, 35-50 breaths per minute). Capnography (end tidal C02 monitoring) was performed via the V-gel using an Impact III device (Vetronic, Devon, UK).

Rimadyl 4mg/SC was then administered subcutaneously, Antisedan administered intramuscularly (IM) as the same dose as domitor (0.125mg/kg) and antibiotics administered subcutaneously (Baytril 10 mg / kg). A 26 Gauge purple cannula was placed in the ear to allow administration of periprocedural medication and fluids. 1ml of Marcaine was then administered along the head of the 2nd, 3rd, 4th, 5th and 6th intercostal spaces on the caudal edge of the head of the rib (0.2ml each rib). An incision was then made through the 4th intercostal rib space and the heart exposed. A small incision was made in the pericardium along the atrioventricular border and then perpendicular to the atrioventricular border towards the atrium. This was so the heart can be removed easily from the pericardial sac. The heart was then temporarily removed from the pericardial sac using a Blunt Snook Hook and a 4.0 Prolene suture placed through the apex of the heart which provides stability and manoeuvrability. A 4.0 prolene suture was then placed through the obtuse marginal artery around 5-7mm from the atrioventricular border to create the infarct. The infarct was clearly visualised distal to the suture due to the discoloured darker tissue as a result of oxygen starvation (figure 2-13).

Prior to ligation a bolus of quinidine hydrochloride (10mg) was administered via the cannula in the ear vein. Two further boluses of quinidine were administered at 10mins and 20mins post ligation (5mg each bolus). If the heart developed ventricular fibrillation an initial 3J shock was delivered to the heart (Zoll refurbished human grade defibrillator, figure 2-12). If needed a short period of cardiac massage was given until cardiac output was restored. If further shock are needed due to ventricular fibrillation 5 Joules were administered. If cardiac output was not restored, adrenaline can be administered via the cannula in the ear vein (0.25mg/ml) in 0.25-5ml boluses.

Approximately 25mins post ligation, the patch (EHT or sham) was sutured onto the chest using a 7.0 prolene suture (Ethicon) at each of the 4 corners of the patch. All animals that underwent patch insertion were pretreated with 5 days of oral ciclosporin (10mg/kg) and intramuscular methylprednisolone (2mg/kg) 2 days prior to surgery.

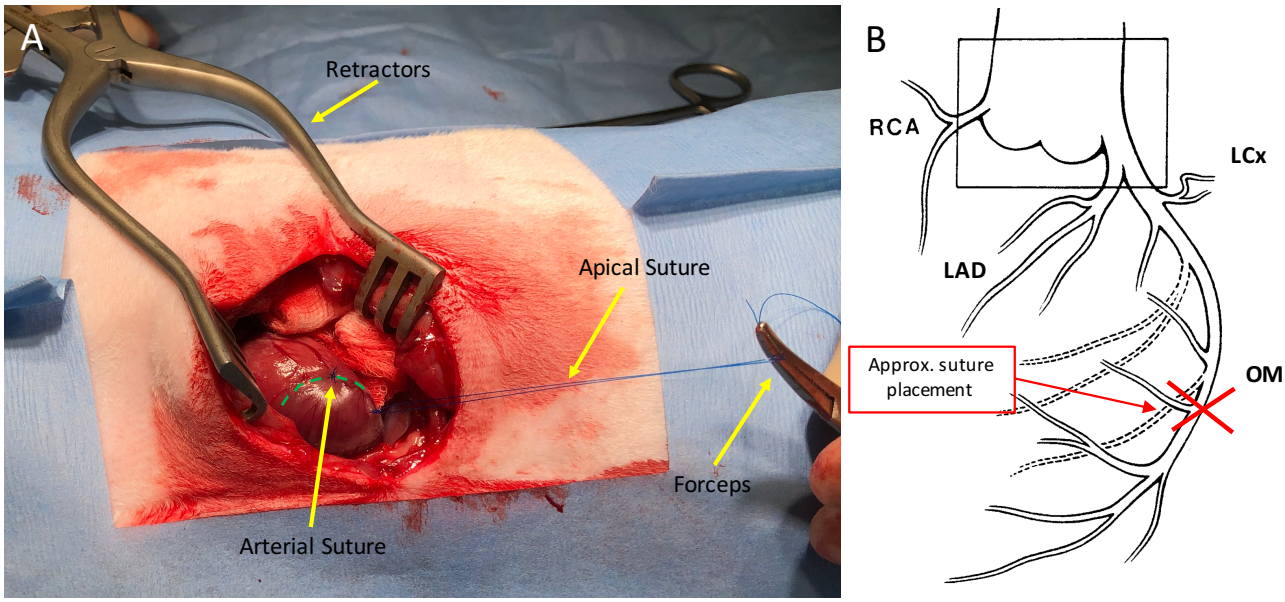
**Figure 2-12: Merlin ventilator and Zoll defibrillator**




*Macroscopic image of small animal ventilator and refurbished Zoll medical defibrillator. Refurbished human paediatric paddles were used for internal cardiac defibrillation.*

The heart and EHT were carefully placed back into the pericardial sac. The ribs were closed using 1.0 Ethicon Monocryl sutures (Johnson and Johnson) and the muscle layer closed with 3.0 Ethibond Excel (Johnson and Johnson) sutures. The skin layer was closed with Polysorb 2.0 sutures (Coviden). Carprofen (2mg/kg SC) was administered intraoperatively. Additionally Vetergesic (0.05mg/kg) was administered IM on the day of surgery and then two further doses administered on the first day post op. 20ml of saline was given subcutaneously to replace 3rd space losses. Antibiotics (Baytril 10mg/kg SC) and Rimadyl (2mg/kg SC) were continued for 5 days.

**Figure 2-13: Image depicting coronary ligation suture**




*A 4.0 Prolene suture was placed around the marginal artery and permanent ligation causes the infarct. An apical suture (4.0 Prolene) was placed to enable the heart to be remove from the pericardial sac and stabilised. Fig B – diagram depicting approximate suture placement in marginal artery. Modified from Reference:* (Podesser *et al.*, 1997).

### 2.6.5 Heart failure model

The index procedure is identical to the myocardial infarction surgery described in methods 2.6.4. However, with the heart failure model the animal was allowed at least 4 weeks to recover post myocardial infarction so that the scar was established and the infarct matured. The second procedure was identical to the first except the rib incision was however through the 5$^{th}$ intercostal space to avoid the adhesions present from the first incision via the 4$^{th}$ intercostal space. Any adhesions that have formed on the epicardial surface / pericardium were then carefully debrided. The patch was then be sutured to the epicardial surface with a 7.0 Prolene suture at each of the 4 corners. The rest of the surgery including rib, muscle and skin closure was the same as per myocardial infarction surgery.

## 2.7 EHT grafting protocol

The in-vivo EHT grafting protocol begins approximately 2 months prior to surgical attachment of the EHT (figure 2-14). It begins with the in-vitro differentiation and maturation of the iPSC-CMs, followed by creation of the EHTs approximately 21-28 days prior to grafting. Since the EHTs consist of human iPSC-CMs (Xenograft), immunosuppression was started prior to grafting. Initial experiments used a relatively low dose of ciclosporin (5mg per kg administered orally (PO), 2 days before) and methylprednisolone 1.5mg/kg administered intramuscularly (IM) 48 h before. However, the final protocol consisted of 10mg /kg ciclosporin (PO) 5 days before and 2mg /kg methylprednisolone (IM) 48 h before. The animals were grafted on day 0. Periprocedural antibiotics were given SC (Batyril 5mg/kg) and continued for 5 days after surgery. EHTs were grafted onto control, at the time of myocardial infarction rabbits and approximately one month after infarction (heart failure model).

Immunosuppression was given until the day of explant. The final study protocol was one month; however, during the optimisation phase, hearts were explanted from one week onwards. Some animals were explanted at day 0 to act as controls (EHT grafted onto heart followed by euthanisation). To help improvement engraftment rates of the hiPSC-CMs, EHTs were subjected to heat shocking and a pro-survival cocktail as previously described (Laflamme et al. 2007). Briefly, EHTs were heat shocked to 43 °C for 60 min 24 h before grafting. The pro-survival cocktail consisted of ZVAD (100 mM, benzyloxycarbonyl - Val-Ala-Asp (O-methyl) - fluoromethyl ketone, Calbiochem) Bcl-XL BH4 (cell-permeant TAT peptide, 50 nM, Calbiochem), ciclosporin (200 nM, Wako Pure Chemicals), IGF-1 (100 ng/ml, Peprotech) and pinacidil (50 mM, Sigma). IGF1 and ciclosporin were administered 24 h before, with the remaining medication on the day of grafting (1 hour before).

**Figure 2-14: EHT grafting protocol**

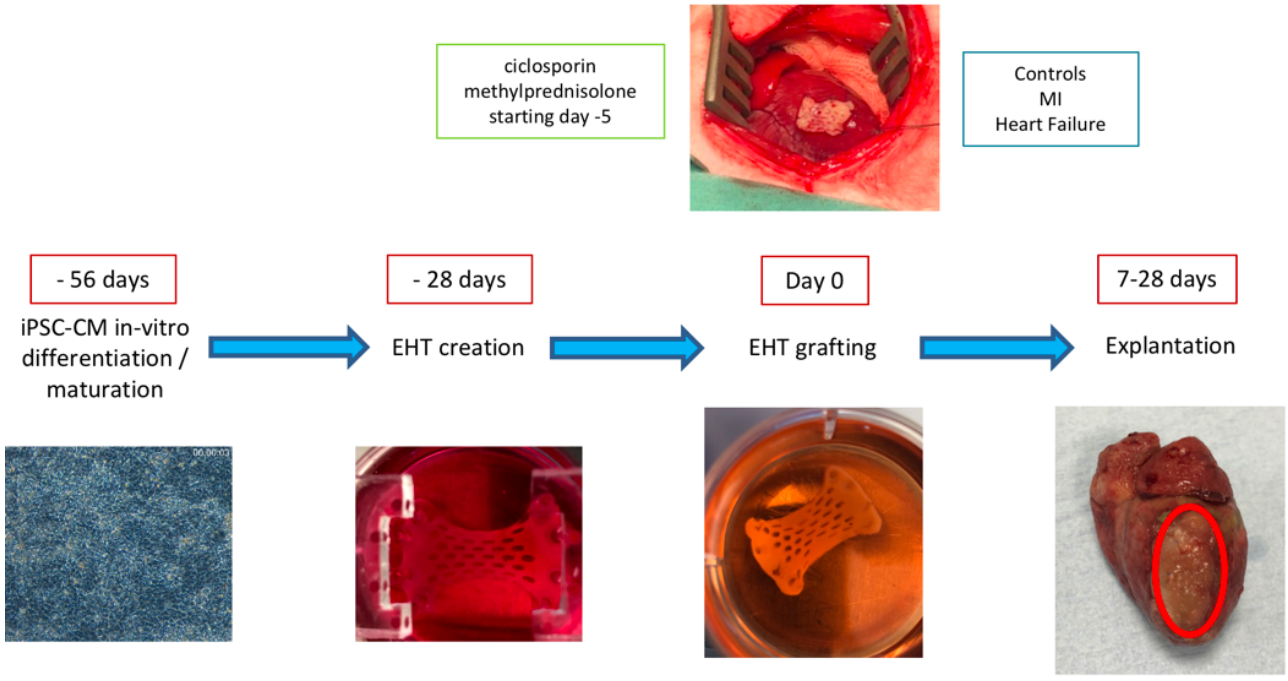



*Figure illustrating EHT grafting protocol which begins approximately 2 months prior to day 0.*

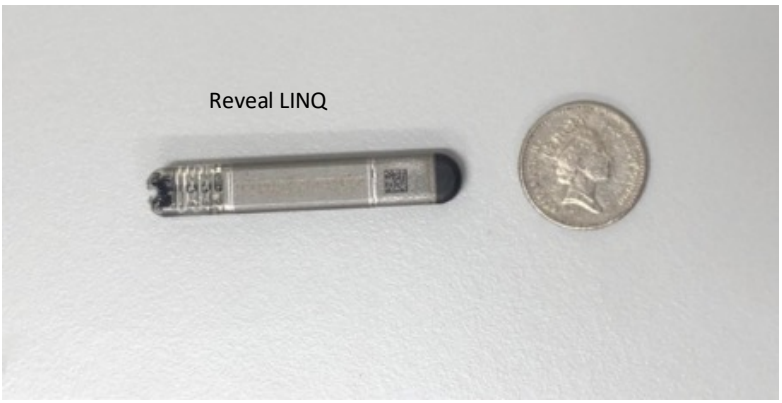
## 2.8 Telemetry

Telemetry recordings were primarily used to assess the arrhythmogenicity of the EHT graft. Two different telemetry devices were used to assess arrhythmic burden during this thesis: 1) Reveal Linq (Medtronic, figure 2-15) and 2) Indus small animal telemetry system (USA). The Indus small animal system was used in the latter experiments (esp sham patch vs EHT) and was a dedicated system obtained to enable continuous automatic intermittent recordings throughout each study period and therefore was more suitable for grafting experiments.

### 2.8.1 Reveal LINQ telemetry

The Reveal LINQ telemetry device (Medtronic) is a human grade remote monitoring device that is primarily used on patients with infrequent arrhythmia symptoms with a battery life of up to 3 years. It has both a manually activated recording mode and automatic arrhythmia detection above and below a certain heart rate. The device was inserted subcutaneously at the end of surgery in the left side of the chest tunnelled away from the rib incision site. Manually activated recordings were taken at random intervals each day (average four times per day at 7.5 min recording each episode).

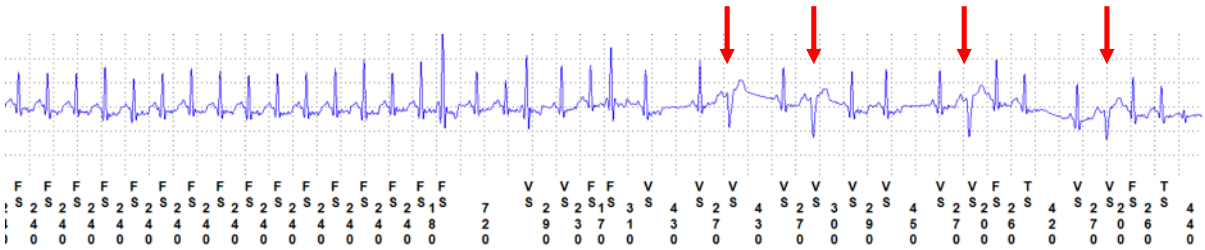
**Figure 2-15: Reveal LINQ device**




*A macroscopic image of a reveal LINQ device next to a 5 pence coin.*

An example of a recording taken from a recording in one rabbit is shown below (figure 2-16):

**Figure 2-16: Tracing of Reveal LINQ telemetry**



*Representative trace showing 4 ventricular ectopics.*

All traces were manually analysed by an experienced cardiologist (R.J) for episodes of pathological arrhythmia and any ambiguous traces analysed by another experienced cardiologist (F.Ng).

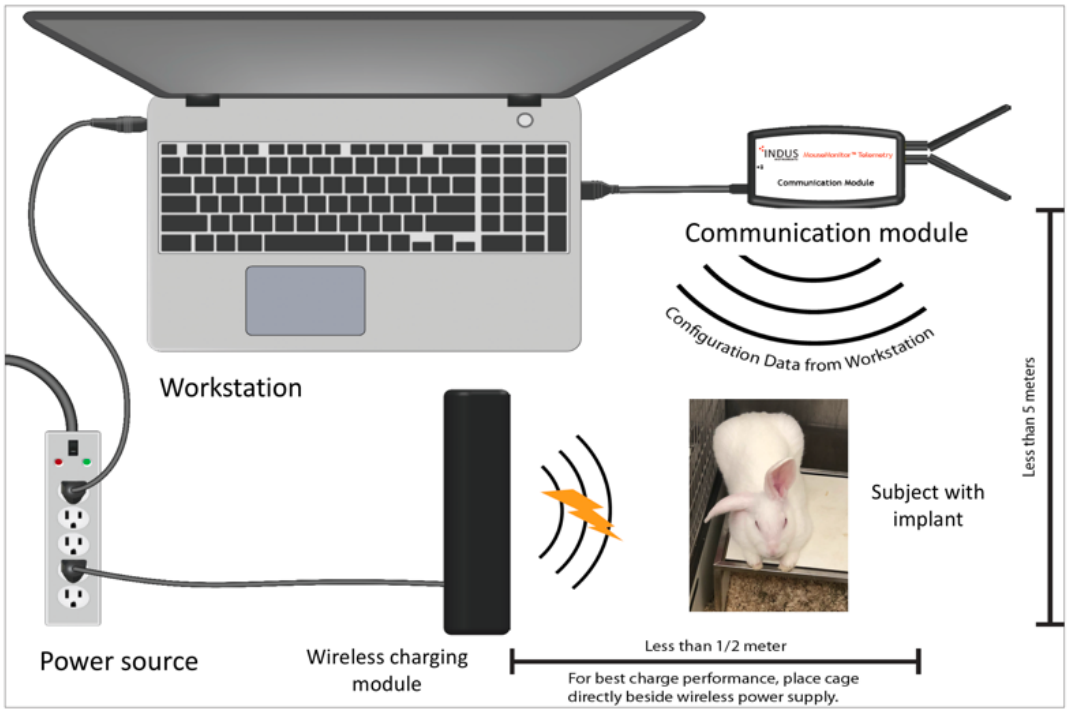
### 2.8.2 Indus Instruments Telemetry System

The Indus Instruments small animal implantable telemetry system (Scintica, USA) is

a dedicated preclinical telemetry device that consists of 4 main core components: 1) Telemetry communication module; 2) Wireless charging station; 3) Wireless implant; and 4) Data acquisition software (figure 2-17).

The telemetry communication module was connected to a laptop (HP ProBook 450 G6) and allows the recording of several implants (up to 100) simultaneously from up to 5 metres away. The wireless implant can record data on temperature, ECG, activity (including circadian rhythm and general movement) and heart rate variability. The wireless charger was typically placed under a cage and charges devices up to 5cm away from it. However, the original telemetry system was designed for mice and rats with significantly smaller cages. Therefore, to preserve battery life of the device, intermittent recordings of 30 seconds every 5 min were taken so that the battery life of the device was sufficient for the study period (up to 1 month). The electrode lead length was 20cm, but flexible and can be cut so that it can fit correctly in the chest. The heart rate reporting frequency was 1Hz when active. The battery life off the charge is 5 days when used continuously and there is an on-board data capacity of 1 gigabyte. The device is reusable and cleaned / disinfected with 1% Tergazyme enzymatic detergent solution (for 30 min) and Metrex MetriCide 14 (10 h) between uses. The figure below demonstrates the telemetry set up.

**Figure 2-17: Indus Telemetry set up**

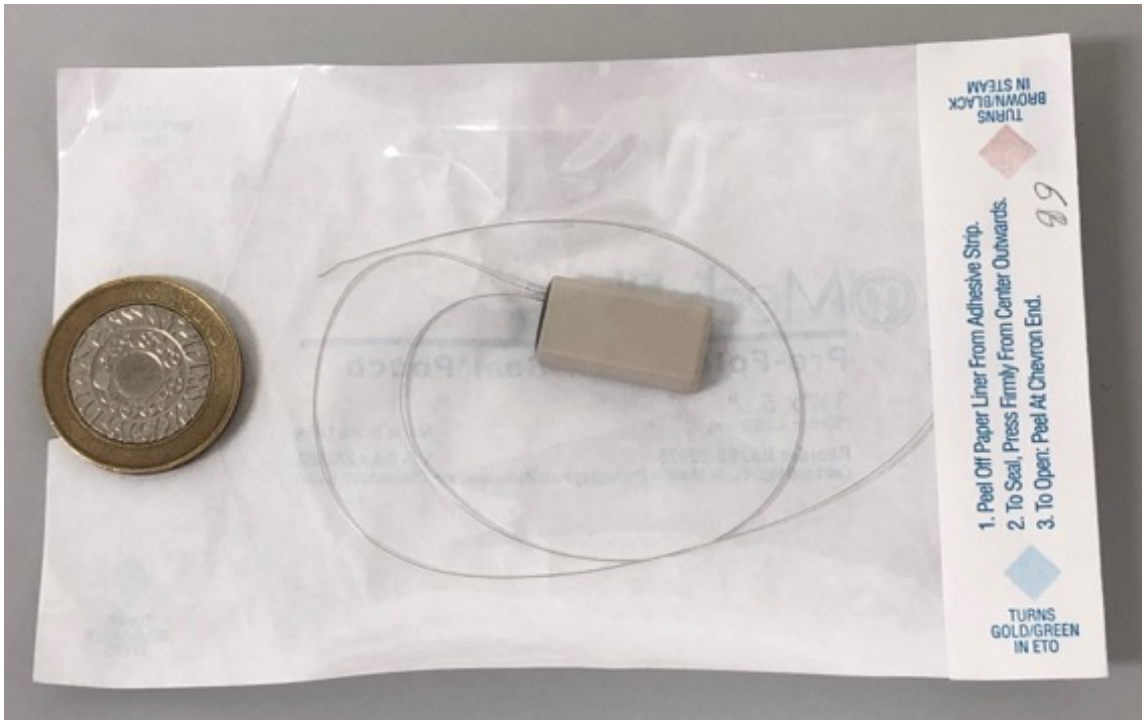



*Adapted from Indus Telemetry system user manual*

### 2.8.3 Implantation

The wireless implant was inserted subcutaneously after the closure of the muscle layer (figure 2-18). The body of the device was tunnelled under the subcutaneous tissue into the abdomen and the two electrode leads sutured to the left and right side of the chest with a 6.0 Prolene suture. Adequate ECG recording traces were checked prior to final electrode lead placement and suturing and moved accordingly until a satisfactory trace was visualised on the monitor. The device was set to record at either a 512/1024Hz sampling frequency with input voltage range of ±5mV. The device was set to record intermittently (30 seconds every 5 min).

**Figure 2-18: Telemetry transmitter**

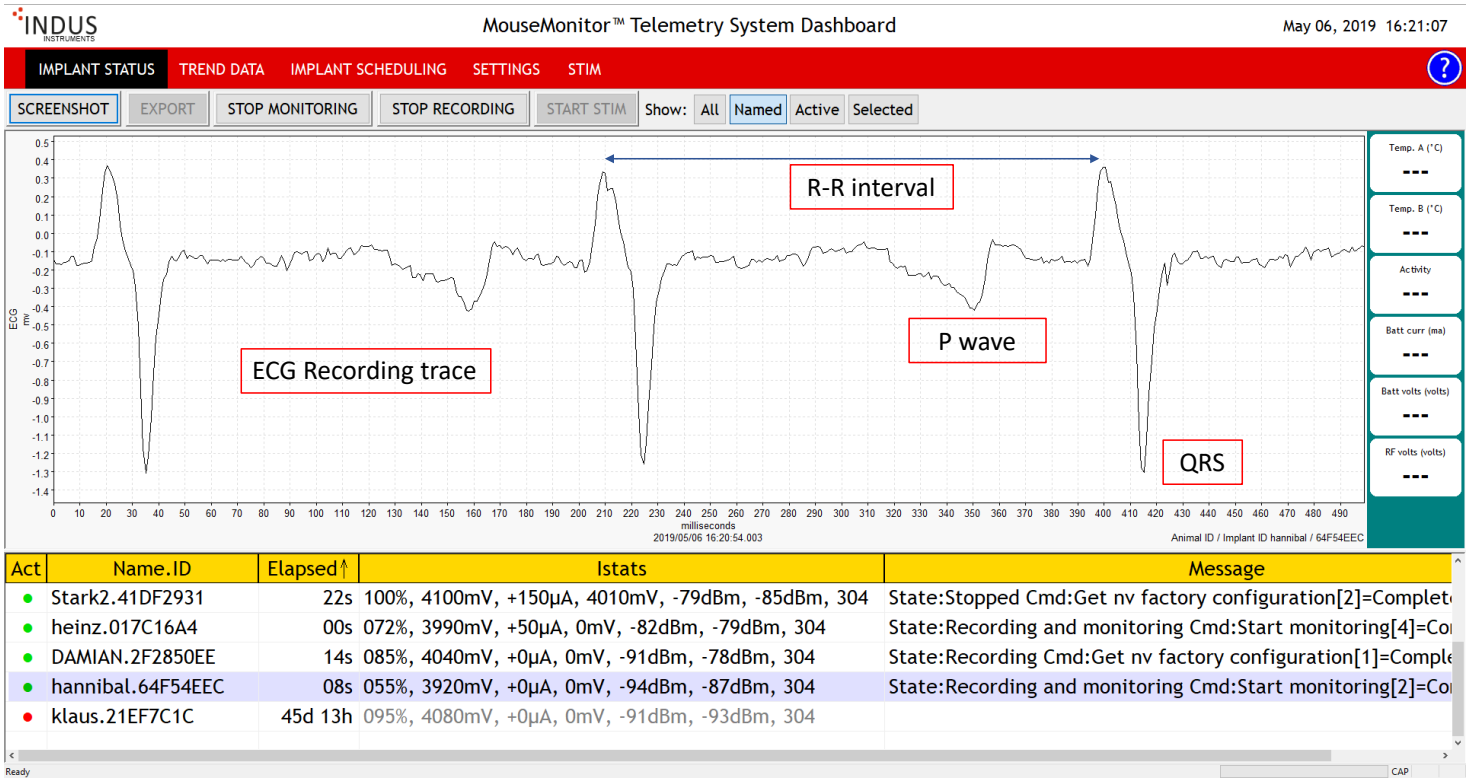



*Telemetry device with two electrode leads approximately 20cm in length*

### 2.8.4 Indus Recording Software

During the study period the telemetry device was checked regularly to ensure that the ECG signal was sufficient for analysis. A typical recording is shown in figure 2-19. Data is shown regarding the telemetry devices and whether they were active (green) or not active (amber or red circle). Data is also provided in real-time if the monitoring button is set. Data regarding battery life is also shown. To preserve battery life data was downloaded for analysis after the study period and not continuously. All files were manually downloaded and manually analysed on Microsoft Excel. As per the Reveal LINQ data, all data was analysed by an experienced cardiologist (R.J) and any discrepancies checked with another experienced cardiologist (F.Ng).

**Figure 2-19: Telemetry system dashboard**




*Screenshot of the Indus Telemetry System dashboard showing ECG trace and the status of the telemetry devices transmitting to the communication modules.*

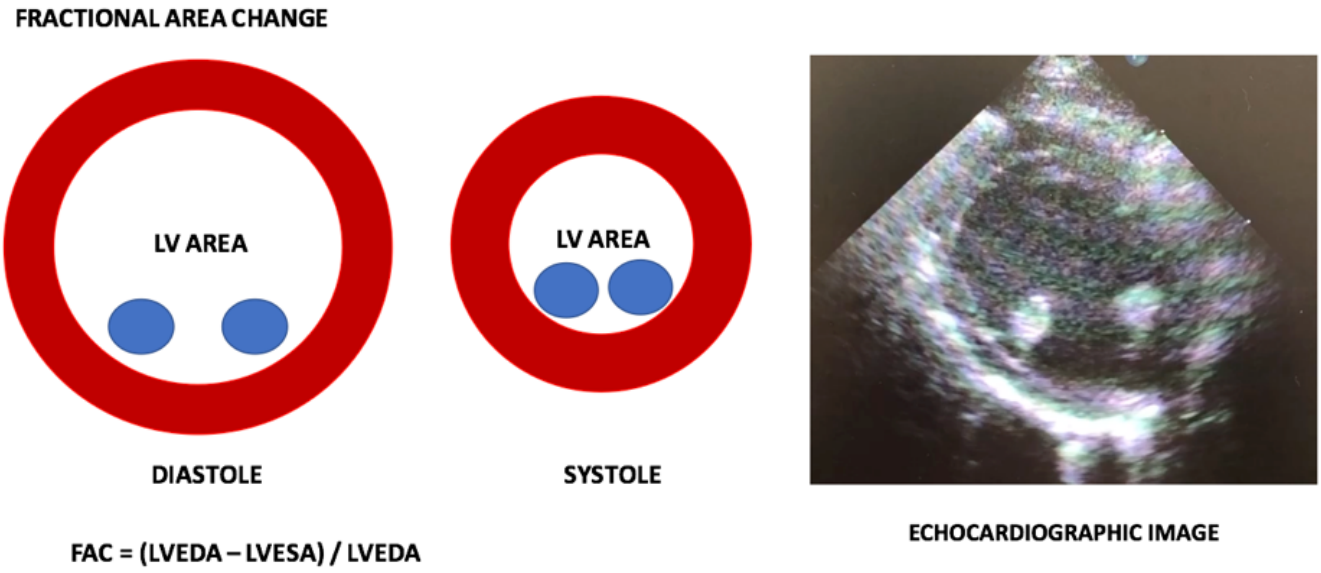
## 2.9 Echocardiography

*Echocardiographic measurements were taken by myself and to minimise bias analysed blinded by two different experienced imaging fellows (Dr Mayooran Shanmuganathan and Dr Daniel Stuckey)*

Echocardiography was the prime modality for assessing cardiac function in this PhD. It has numerous advantages over other imaging modalities. For example, it is non-invasive and can be performed relatively easy when compared to MRI or CT scanning. Echocardiography relies on the principles of ultrasound waves to create a real-time image of the cardiac cycle. Images were obtained by an experienced

sonographer on a refurbished IE33 machine (clinical grade). All analyses were performed by 2 independent reviewers blinded to the treatment groups. Data were obtained from the parasternal long axis and parasternal short axis views. Recordings included left atrial size, wall thickness and fractional area change. M-mode recordings were primarily used for assessing ventricular size whilst conventional 2D imaging used for assessing fractional area change (figure 2-20).

**Figure 2-20: Fractional area change measurement**



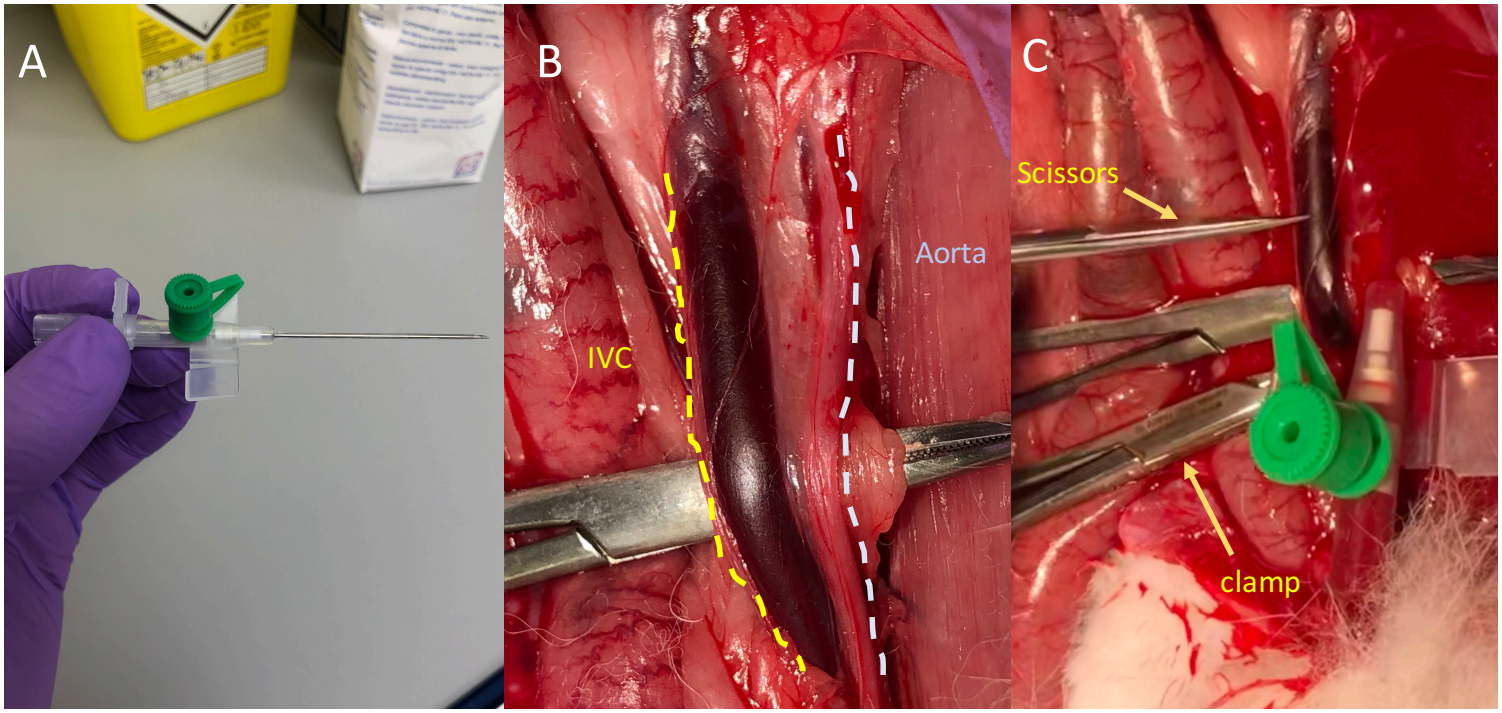

*Left: Diagram depicting fractional area change and equation from end diastolic to end systolic area taken from the parasternal short axis view. Right image – 2D image of left ventricle at mid ventricular level showing papillary muscles. LVEDA: left ventricular end diastolic area; LVESA: left ventricular end systolic area; LV: left ventricle.*

### 2.10 EHT explanation protocol

At the end of the in-vivo study protocol, hearts were explanted so that ex-vivo experiments could then be performed. Optical mapping experiments were affected

by ischaemic tissue, and therefore to preserve viability a cardioplegic arrest protocol was devised. Firstly, rabbits were sedated with ketamine (7.5mg/kg) and medetomidine hydrochloride (0.125mg/kg), and then intubated with a V-gel. Isofluorane was then administered via the V-gel and mechanical ventilation carried out using a small animal ventilator (10-15mls/kg at 35-50 breaths per minute; Merlin laboratories). The heart was then explanted under terminal anaesthesia but prior to that cardioplegia solution was administered via the abdominal aorta. An abdominal laparotomy was carried out and the abdominal aorta and inferior vena cava exposed with blunt dissection. A 18G cannula (Vygon, UK) was then inserted into the abdominal aorta to allow slow retrograde infusion (over 3-5 min) of 300-400ml of cold (4°C) heparinized (12units/ml) cardioplegia solution (Harefield Hospital formulation, Terumo BCT, UK; composition mmol/L: Na 147; K 84; Mg 80; Ca 2; Procaine 5; Chloride 400). After insertion of the arterial line, the aorta and inferior vena cava were clamped distally (to the catheter). Then using scissors, the inferior vena cava was clamped proximally (figure 2-21). This permits the free flow of blood and cardioplegia out of the circulatory system during cardioplegia administration thereby preventing an increase in intracardiac pressure. After infusion of cardioplegia the heart was excised carefully and transferred into a container containing cold (4°C) heparinised cardioplegia solution, and then to the laboratory for experiments.

**Figure 2-21: Image of abdominal aorta and inferior vena cava**




*A) macroscopic image of 18G cannula; B) Macroscopic image of IVC and aorta that has been blunt dissected and exposed; C) A pair of forceps clamp both the IVC and aorta distal to the cannula insertion site. Scissors were used to cut the IVC proximal to the clamp (forceps).*

## 2.11 Ex-vivo methods

### 2.11.1 Ex Vivo Isolated Rabbit Heart Perfusion

The experiments in this thesis use the isolated rabbit heart preparations in 2 main ways. First, to study the interaction and coupling between engineered heart tissue and the myocardial host by assessing propensity for arrhythmia formation by performing programmed electrical stimulation, and also to assess for the presence of synchronous electrical activity between the graft and the host (electrical coupling). The second way was to study the effect of a conductive polymer patch on both regional and global myocardial conduction velocities and the propensity for arrhythmia formation after the patch had been applied to the epicardial surface. These experiments were performed on a dedicated Langendorff Perfusion Apparatus.

### 2.11.2 Langendorff Perfusion Apparatus

For ex-vivo optical mapping experiments, a constant flow system was used since hearts were mechanically uncoupled to reduce motion artefact and therefore the diastolic suction wave that normally occurs and facilitates coronary perfusion with cardiac contraction is lost. The Langedorff perfusion system used contains a water bath and a series of insulated tubes and water jacketed reservoirs (Radnoti, USA) to enable the perfusate to be maintained between 36.5-37.5 $^{o}$C. The system contains a 5μm filter and a numerous one-way valves and 3 way taps to administer drugs and a bubble trap proximal to the custom built aortic cannula to prevent air emboli. The Tyrode's solution (128.2mM NaCL,1.3mM $CaCl_2(2H_20)$, 4.7mM KCl, 1.05 $MgCl_2(6H_20)$, 1.19mM $NaH_2PO_4(H_20)$, 20mM NaHCO3, 11.1mM Glucose) was first placed into a water jacketed 2 litre reservoir (Radnoti, USA) where it was oxygenated

(95% 02) and heated for at least 30 min prior to use. The calcium chloride in the Tyrode's solution was added after oxygenation (with 5% C02) in the reservoir to prevent calcium precipitation. The Tyrode's solution was perfused through a peristaltic pump (Radnoti, USA) at a flow rate typically 40-60ml/min at a pressure of between 40-70mmHg.

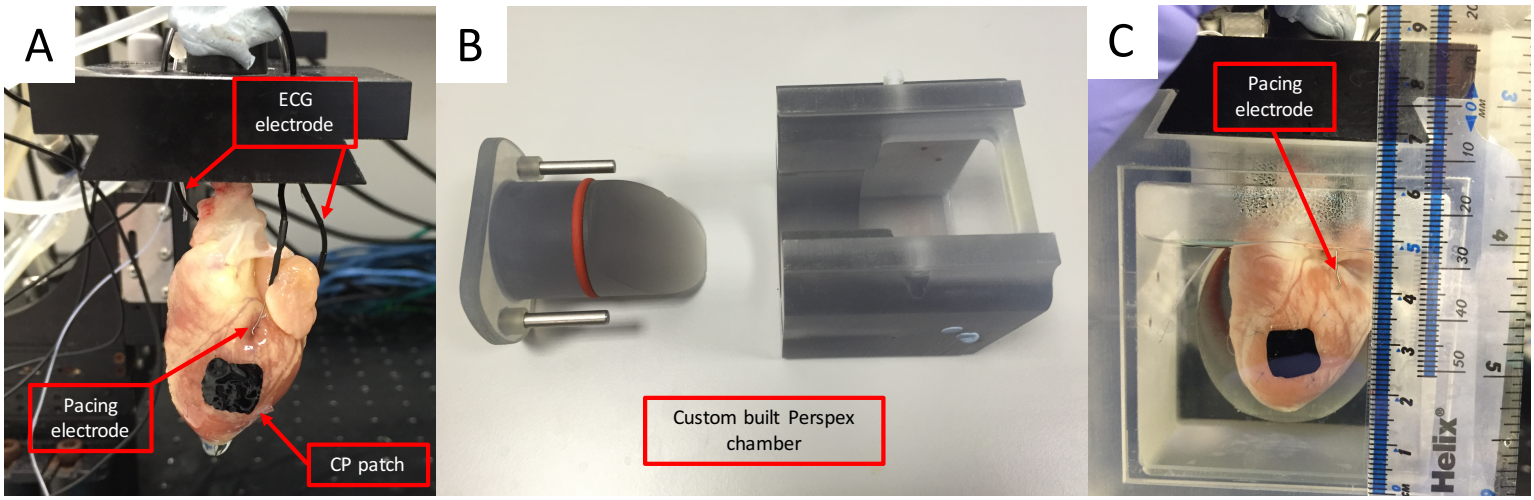
### 2.11.3 Heart isolation protocol

First, the hearts were explanted and placed into ice cold cardioplegia as previously described in methods section 2-10. The lungs and surrounding tissue were then quickly dissected to expose the ascending aorta. The ascending aorta was then mounted onto a 2.5 mm diameter steel cannula (Custom made, courtesy of Mr Paul Brown, Physics department, Imperial College London) which had previously been attached to the perfusion circuit apparatus. During attachment the perfusate was slowly perfused onto the aorta to ensure no air bubbles were present in the aorta during attachment (and therefore to prevent air emboli).

It was first held in place on the cannula with a surgical clip, and then a 3.0 silk suture was placed around and tied to the ascending aorta and cannula to ensure fixation (Ethicon, UK). The heart was then retrogradely perfused with oxygenated Tyrode's solution at 45-49 $^{o}$C at a rate of between 40-70ml / min to maintain a perfusion pressure of 40-70mmHg inside a custom made optical mapping Perspex chamber (Custom made, courtesy of Mr Paul Brown, Imperial College, figure 2-22) to enable the heart to be at a constant physiological temperature (36.5-37.5 $^{o}$C). The perfusion pressure was monitored throughout the experiments and the flow rate adjusted accordingly.

All hearts were subjected to a 15-20-minute acclimatisation period. The pacing electrode was then placed onto the epicardial surface just inferior to the left atrium at the base of the left ventricle. A reference electrode was then placed on the metal cannula. Two ECG electrodes were placed into the Perspex chamber to create a field potential which was connected via a BioAmplier (ADInstruments, USA) to a dedicated data acquisition system (Powerlab 8/35, AD Instruments, USA). ECG recordings were then visualised using LabChart 7 (ADInstruments, USA). Hearts were excluded from further study if after the stabilisation period: 1) the HR was less than 150bpm or greater than 350bpm; 2) there was persistent signs of ischaemia on ECG recordings; or 3) there had been sustained arrhythmia during the last 5 min of stabilisation. After the stabilisation period, experiments continued as per methods section 2.12.

**Figure 2-22: Heart attachment to cannula and perfusion system**




*A) Heart suspended on custom made cannula B) Custom made Perspex chamber; C) Heart in chamber with physiological solution. CP patch: conductive polymer patch.*

## 2.12 Optical Mapping

### 2.12.1 Principles

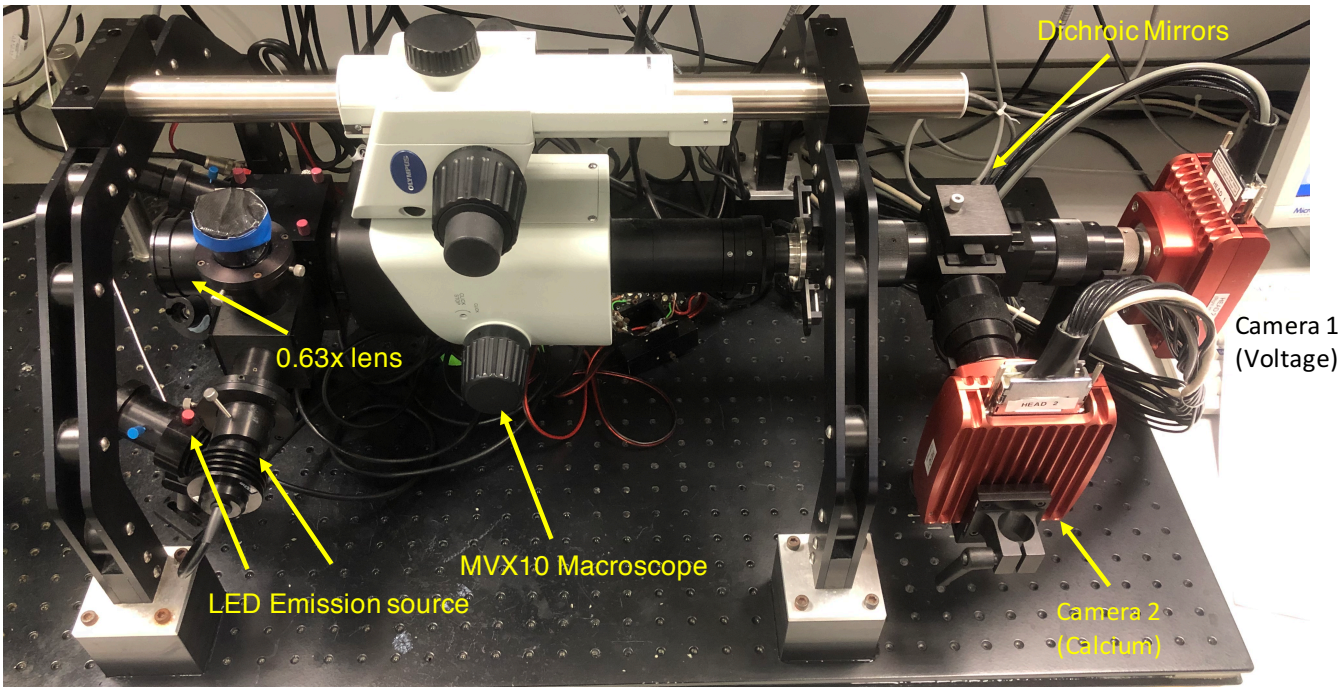
Optical mapping is a technique whereby fluorescent calcium or voltage dyes enable real time recordings of optical signals from surface of the intact heart in a non-contact way. Voltage dyes bind the outer myocyte cell membrane and the emission spectra is then altered depending on transmembrane voltage. RH237, a voltage dye is excited by a LED light at a certain wavelength (535nm) if it falls within the specific excitation spectra. When it returns to its original, pre-excited state it emits a photon of light at a longer wavelength (660nm). Emitted photons were then detected by a sensor such as a photodiode array from a CMOS camera, which is then quantified into degree of fluorescence per unit time. Calcium sensitive dyes work in the same way except the dye is intracellular since it is bound to cytosolic calcium.

### 2.12.2 Hardware configuration

Optical mapping recordings were made and carried out on a custom made dual CMOS (complementary metal-oxide semiconductor) camera system (Cairn Research Labs, UK; figure 2-23). This allowed high spatial (100μm pixel size) and temporal (average sampling rate of 1000 frames / second) resolution. Excitation light was produced by a series of LEDs (Cairn Research Labs, UK) with removable filters and depending on which dye used emitted light at a certain wavelength (2.12.1). Emitted light from the epicardial surface was then passed through a 0.63x objective lens (Nikon, UK) and a macroscope (MVX10 Olympus, UK) for fine focusing. The emitted light then travels through a dichroic mirror and was detected by two CMOS cameras (one voltage, one calcium). The dichroic mirror splits the light depending on light wavelength. The CMOS cameras (Red Shirt Imaging LLC, USA) contain a

sensor size of 128x80 pixels, giving an effective pixel size of 100µm. All recordings were taken in a dark room to enable accurate epicardial surface recordings.

**Figure 2-23: Optical mapping set up**




*Optical mapping hardware. Emitted light is detected by two CMOS cameras. The MVX10 macroscope is used for zooming and focussing.*

## 2.13 Experimental protocols

### 2.13.1 Conductive polymer work

After a 15-20 minute stabilisation period, the heart was loaded with a bolus injection (40 µL injected into the perfusate over 30 s, i.e. diluted in 2 mL of saline) of the voltage sensitive dye RH237 (Molecular Probes, OR USA) dissolved in DMSO (Thermofisher). To eliminate motion artefact, hearts were initially perfused at a constant rate with the excitation contraction uncoupler Blebbistatin (30 µM) to arrest movement and was then maintained at a rate between 10-20 µM depending on myocardial contractions. 530nm light emitting diodes were used to excite the epicardial surface and recording signals were obtained during ventricular pacing (left ventricular base) at varying cycle lengths (typically at 200ms [300 bpm]; 7-15 mA). The conductive polymer patches were sutured onto the epicardial surface of the heart using an 8-0 Prolene suture in each corner and appropriate contact ensured between the polymer and epicardium. Recordings were taken with and without the conductive polymer attached. A custom MATLAB script was then used to analyse data including voltage signal characteristics, conduction velocity and create activation maps. Calculations of conduction velocity were based on methods previously described.(Laughner *et al.*, 2012)

### 2.13.2 Engineered heart tissue mapping

*Optical mapping was carried out at Imperial College London and University of Glasgow (UoG). Dr Catherine Mansfield taught me how to use the optical mapping system at Imperial College London. Dr David Pitcher and myself performed the EHT mapping experiments. Mapping experiments at UoG (n=3) were carried out by Dr Rachel Myles and Dr Quentin Lachaud. Data were analysed by myself and*

*additionally by Dr Rachel Myles (UoG) who was blinded to treatment allocation. Dr Rachel Myles helped me with interpretation of the data and presentation of the data in Figure 5-8.*

***Glasgow Protocol***

Hearts were mounted in a custom chamber and a volume-conducted pseudoECG was monitored from the chamber. A bipolar platinum stimulating electrode was placed on the epicardial surface at the apical border between the LV/RV, when indicated in the protocol, ventricular pacing was performed using a 1ms square pulse at twice diastolic threshold. Blebbistatin (10 μM) was added to the perfusate to minimise motion artefact during optical recording. Where indicated by the protocol heart were loaded with a single bolus of 25uL of RH237 (1mg/ml, Molecular Probes, OR) for Vm mapping. Wide-field epicardial optical imaging was performed with dual CMOS system mounted on a THT macroscope (Micam05, SciMedia, Costa Mesa, CA) with a 20mm$^2$ field of view resulting in a spatial resolution of ~200μm$^2$/pixel. All signals were sampled at 1kHz and recordings made for up to 10s. Hearts were illuminated by LED light sources centred at 475nm (Cairn, UK) and emitted light was collected using a 1x objective lens (Leica, Japan) and split with a dichroic mirror at 662nm. The shorter wavelength moiety, containing the gCaMP6F signal, was bandpass filtered between 575 ±15nm and focussed onto the CMOS sensor. The longer wavelength moiety, containing the RH237 signal (where applicable) was long pass filtered at >715nm for $V_m$ imaging. All optical data were processed with a single iteration of a 3x3 Gaussian spatial filter before being analysed using custom software (Optiq, Dr Francis Burton, UoG).

***Imperial Protocol***

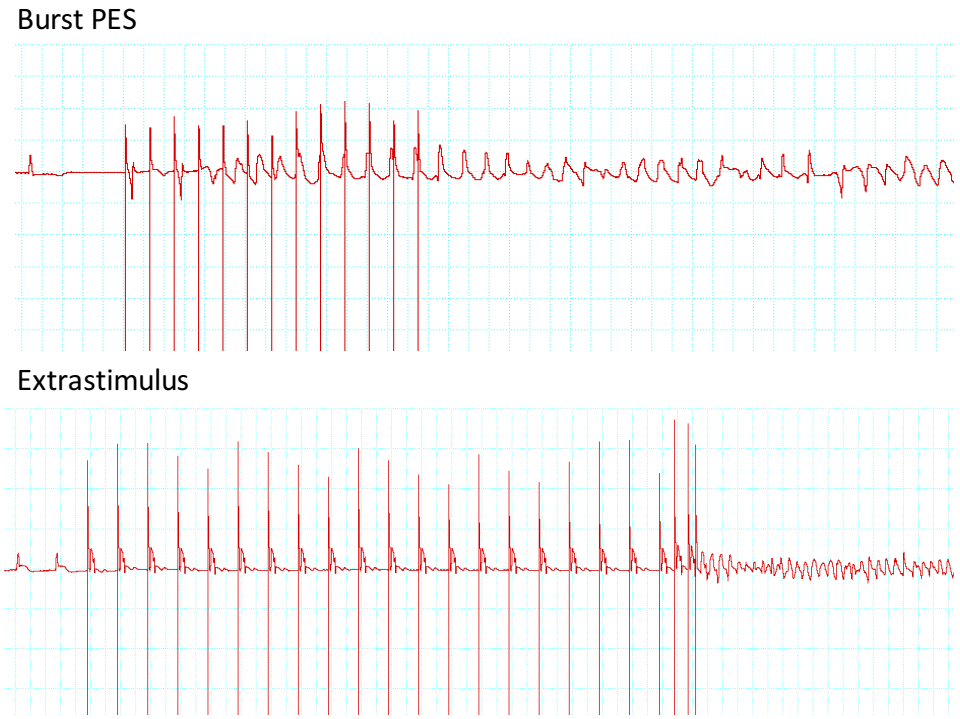
A 450-470nm LED light source (Cairn, UK) excited the epicardial surface containing the EHT. This was then viewed through a 495nm excitation dichroic to image the calcium transients originating from gCaMP6F hiPSC-CM in the EHT. If spontaneous signals were not observed the ventricular surface was paced at varying cycle lengths and the EHT was point stimulated with a platinum electrode at 1-2.5Hz. If either a spontaneous or stimulated signal were then observed, hearts then proceeded to undergo a series of ventricular / EHT pacing protocols to ascertain evidence of electrical coupling, by synchronising to the surface ECG.(Shadrin et al., 2017) In a subset of hearts, dual mapping of both voltage (Di4ANEPPS at 1 ml of 5 μM) concentration and calcium was used to further assess for electrical coupling. The two-different emission of gCaMP6F and di-4-ANEPPS were separated with a excitation dichroic mirror of 495 nm, and a 610 long pass emission filter.(Shadrin *et al.*, 2017)

### 2.13.3 Programmed electrical stimulation protocols

Extrastimulus programmed electrical stimulation protocols were performed ex-vivo to measure susceptibility to the development of arrhythmia and carried out using a MicroPace electrical stimulator (MicroPace, Auckland, New Zealand). First, a pacing electrode was placed at the base of the left ventricle and paced with a 20 beat S1 drive train (cycle length 200ms, 300bpm, stimulus 10mA), which was then followed by an extrastimulus with an initial S1-S2 interval of 130ms (figure 2-24). The S1-S2 interval was then successively decreased by 5ms intervals automatically until either an arrhythmia was induced or it fell on the refractory period. If a sustained arrhythmia was obtained the protocol was stopped. If no significant arrhythmia was obtained, a

further extrastimulus (S3) was introduced. This was then followed by an additional third extrastimulus if needed (S4). With the introduction of each extra stimulus, the coupling intervals were reduced by 5ms each time until ventricular refractoriness occurred. If no arrhythmia was provoked with S1-S4, burst pacing was instituted at a cycle length of between 70-130ms for 50 beats (Fig 2-24).

**Figure 2-24: Electrocardiographic recordings of arrhythmia provocation protocols**




*Top panel – electrocardiogram of burst PES (programmed electrical stimulation protocol) resulting in ventricular fibrillation; lower panel – electrocardiogram of extra stimulus (S1-S4) protocols resulting in ventricular fibrillation.*

All ECG monitoring and arrhythmias induced were visualised and recorded on CHART 5.5 software using a dedicated data acquisition system (Powerlab; AD Instruments, Sydney, Australia). The susceptibility of each heart to the development of ventricular arrhythmia was categorised using an arrhythmia inducibility score based on the principles as described previously.(Bélichard *et al.*, 1994) Ventricular tachycardia was defined as non-sustained if >6 but <14 and sustained if >15 were provoked. VF was classified as sustained if >1 second was provoked. Arrhythmias induced on burst pacing were viewed as less arrhythmic than if on extra-stimulus protocols (Table 2-2).

**Table 2-2: Arrhythmia provocation protocol scoring system**

| Arrhythmia provocation protocol scoring system | |
|---|---|
| **Induced arrhythmia** | **Score** |
| **Sustained VT / VF on S1S2** | **7** |
| **Non-sustained VT / VF on S1S2** | **6** |
| **Sustained VT / VF on S1-S3** | **5** |
| **Non-sustained VT / VF on S1-S3** | **4** |
| **Sustained VT / VF on S1-S4** | **3** |
| **Non-sustained VT / VF on S1-S4** | **2** |
| **Any VT / VF on burst pacing protocol** | **1** |
| **No arrhythmia induced** | **0** |

*Arrhythmia provocation protocol scoring system. A score of 0-7 was given depending on susceptibility to arrhythmia formation.*

### 2.15 Statistical analysis

The data obtained from all experiments were analysed using GraphPad Prism 6

software (GraphPad Software). Unless prespecified, all data are presented as mean ± SEM with $p<0.05$ indicating statistical significance. The D'Agostino & Pearson omnibus normality tests were applied to the data prior to performing analyses. When distribution was normal, Student's t-test statistical analyses were performed. Between group comparisons were calculated using one-way ANOVA and post-test ad hoc Tukey's test used to assess for differences between 3 or more groups. When distribution was not normal, or if ordinal variables were being compared Kruskal–Wallis test was performed. *=$p<0.05$, **=$p<0.01$, ***=$p<0.001$.

# Chapter 3: Characterisation of upscaled engineered heart tissue

## Introduction

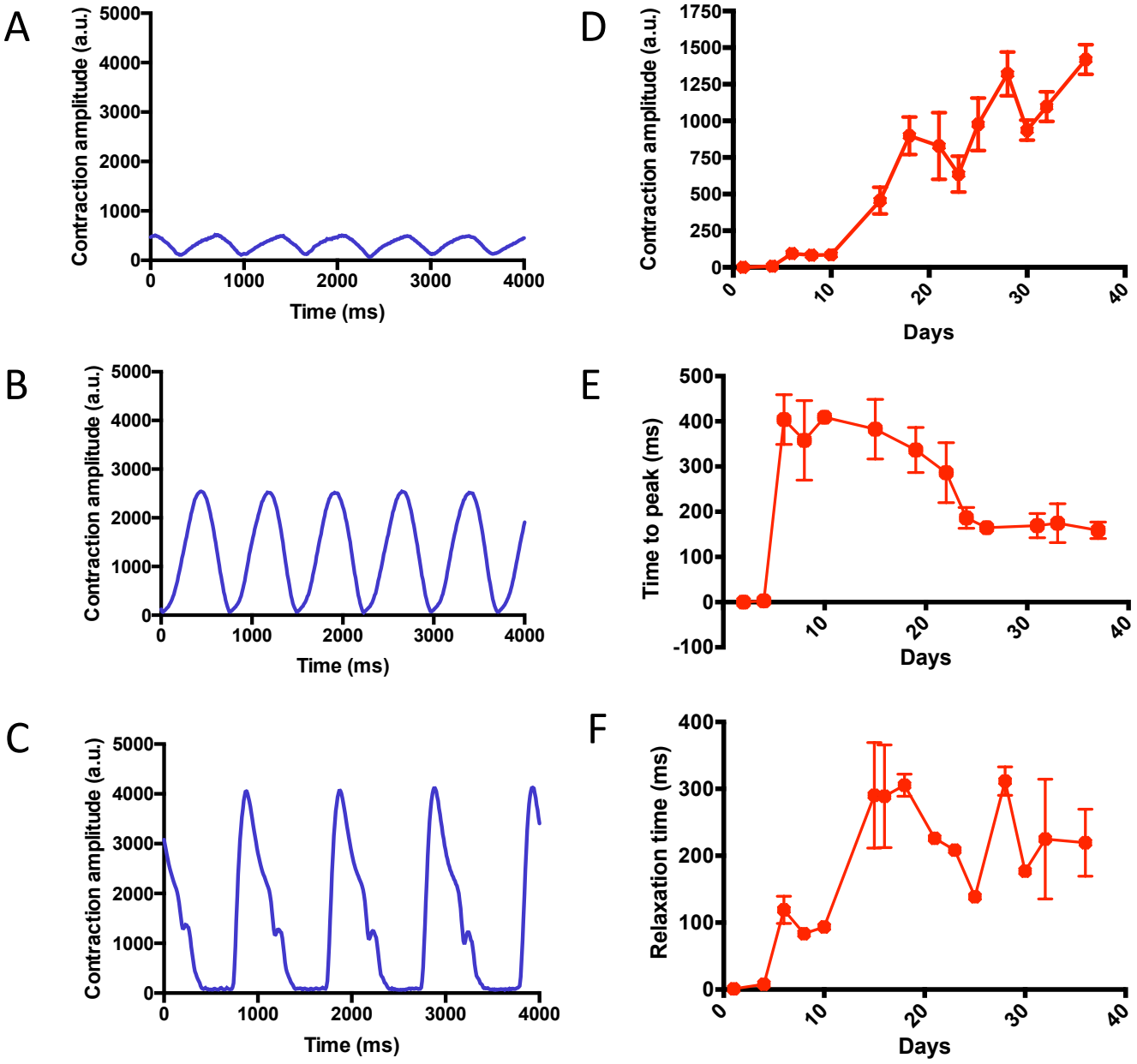
The first chapter of the results section describes the characterisation of the upscaled EHT. The upscaling of EHT was carried out in close collaboration with Prof Eschenhagen's group who designed the upscaled posts, Teflon spacers and silicone nets and provided them to the Harding group who created the constructs for the experiments used in this thesis. One of the hypotheses of this thesis was that they would show evidence of maturation over time in-vitro. A wide range of maturation markers were assessed including contraction kinetics, calcium transients and cell alignment. Contraction kinetics were analysed using open source software (Muscle Motion; Methods 2.4.1).(Sala et al., 2018) Calcium transients were analysed using EHTs containing genetically encoded calcium indicator (GCaMP) hiPSC-CMs and cell alignment was based on immunostaining of troponin T positive cells. It is well known that smaller EHTs used in our laboratory mature in force over time and it is also a good way of assessing the quality of the constructs for in-vivo grafting experiments.(Breckwoldt *et al.*, 2017) If the constructs did behave in a similar way to the smaller first generation EHT then constructs would be suitable for in-vivo grafting. The first generation EHT that we use in our laboratory consisted of up to 0.5 - 4 million cells per EHT, and the volume of master mix used to create a single EHT was 100μl. The volume of Mastermix in the newer generation EHTs was 1.7ml (17 times greater), giving a theoretical cellular capacity of anywhere between 8.5 - 68 million cells. A number of different ranges of cells were used from 10 – 50 million and it was found that the most reliable balance between force and capacity for media use in the 6 well plate, which could contain a maximum of 10mls of media in each well, was between 15-20 million cells per EHT. In contrast, Prof Eschenhagen's group use between 12-15million hiPSC-CMs per EHT.(Unpublished)

### 3.1 In-vitro characterisation of upscaled engineered tissue

The first step in the characterisation of newer generation EHT was to assess maturation of the constructs by analysing the contraction kinetics of the hiPSC-CM EHTs over time. Since the newer EHTs were kept in a 6-well plate (as opposed to 24 well plate) and significantly larger than first generation EHT, the existing hardware used for measuring force / contraction kinetics was not compatible. Therefore, a dedicated recording system was designed and 3D printed (courtesy of Mr Pragati Pandey) and high frame rate videos recorded on a Basler camera (See supplementary appendix). Videos were analysed using MUSCLEMOTION software as described in the methods section 2.4.1. Recordings were taken on average at least 3 times per week (Monday, Wednesday, Friday; Daphne Pantou, Pragati Pandey primarily performed the recordings / raw data analysis of contraction kinetics). EHTs were subjected to dynamic rocking culture to enhance maturation as previously described.(Jackman, Carlson and Bursac, 2016) The contraction amplitude increase of the EHTs, relative to day 0, was relatively low up to day 10. Unsynchronised contractions of EHTs could clearly be seen microscopically (days 1-7 at 5x magnification) initially and then later visualised macroscopically (day 7 onwards; representative graph in Figure 3-1A). After approximately 7-10 days, the myocytes in the EHT started to synchronise, and this was mirrored by increases in EHT contraction amplitude (Figure 3-1B). From 15-35 days, as synchronisation improved further, there were additional increases in contraction amplitude (Figure 3-1C; average of early peak contraction (<2 weeks) amplitudes 87.9$\pm$5.8a.u. versus later averages (>2 weeks) 952$\pm$304a.u.; $p<0.001$, n=6 in each group, Figure 3-1D). Regarding time to peak contractions, measurements were detectable at day 6 (404 $\pm$ 55ms), which then progressively decreased over time (significant difference from day

22 onwards when compared to day 6 measurements; Figure 3-1E). EHT relaxation times indicated that stable recordings were obtained from day 15 (290.5 $\pm$ 79ms) and there was significant variability in recordings taken at later time points.

**Figure 3-1: EHT Contraction Kinetics over time**

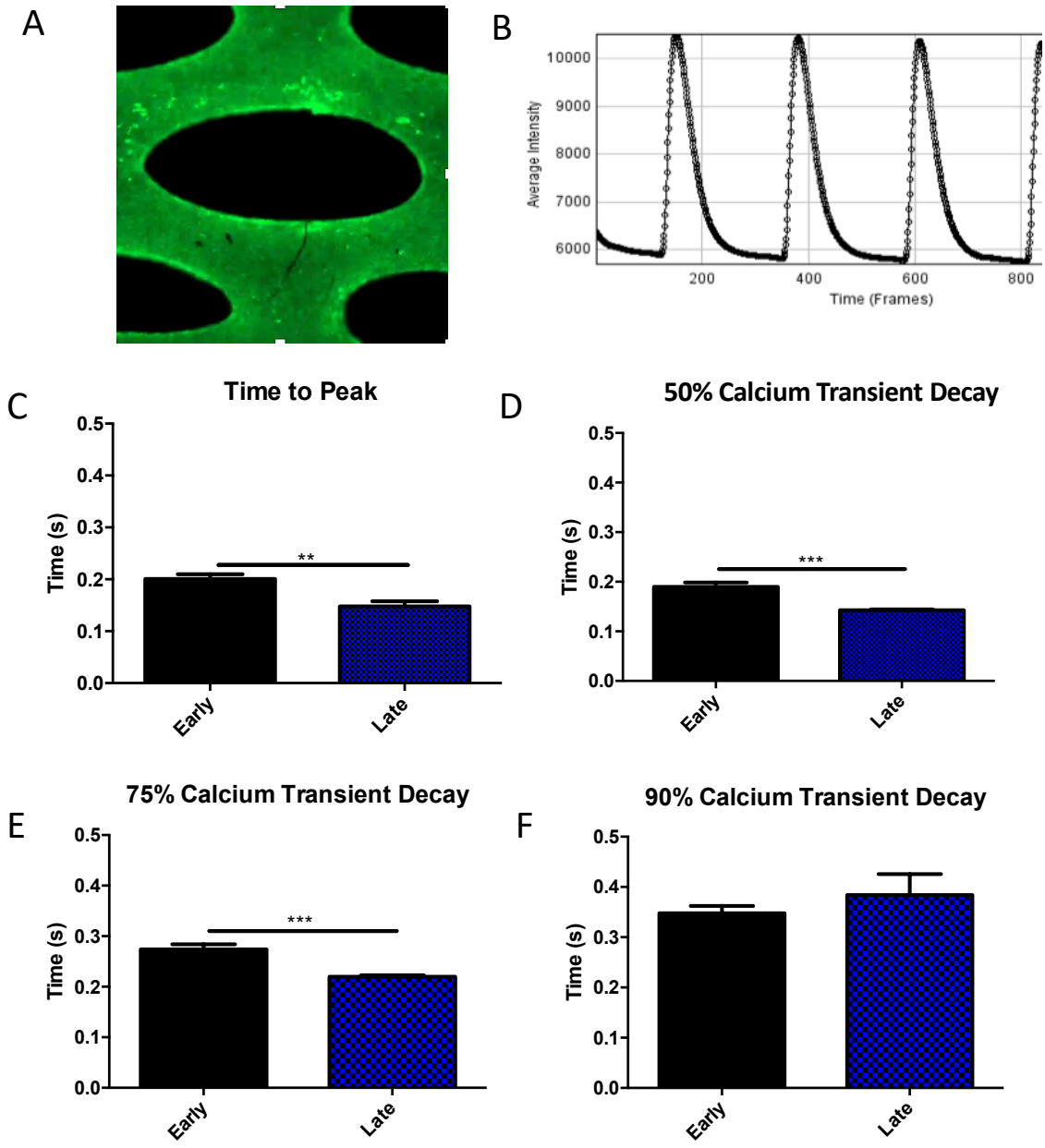



*A) Representative contraction amplitude of an EHT at day 7. B) Same EHT at day 18 C) same EHT at day 28 prior to grafting. D-F) Contraction amplitude (D), time to peak (E) and relaxation times (F) for n=6 EHTs. Data presented at mean ± SEM.*

### 3.2 EHT calcium transient analyses

The observed improvements contraction kinetics suggested evidence of EHT maturation in-vitro. It is known that hiPSC-CM display a relatively immature fetal like phenotype when compared to adult cardiomyocytes. (Denning *et al.*, 2016) Calcium handling is one of the hallmarks of maturation and therefore experiments were performed on EHTs at different time points to ascertain whether there was evidence of improvement of calcium handling characteristics over time. Optical mapping was performed on EHTs consisting of GCaMP6F hiPSC-CMs (kindly provided by Conklin Laboratory, USA). GCaMP is a genetically encoded calcium indicator developed from the fusion of green fluorescent protein, calmodulin and M13 from myosin light chain kinase. This enabled repeated real time imaging of calcium transients without the use of dye which can damage cells or be pumped out of cells over time (Figure 3-2A/B). Full details are described in methods section 2.4.2-2.4.4. Live imaging of EHT calcium transients was performed on EHTs perfused with Tyrode's solution and loaded with BDM to prevent motion artefact. Calcium transients were then compared between recordings taken from early (4 - 14 days) and late EHTs (29 - 42 days). Calcium transients analysed from later EHTs showed evidence of more mature calcium handling characteristics including faster time to peak measurements (201± 0.8ms [n=5] vs 148 ± 1ms [n=6], p = 0.004; Fig C), faster 50% calcium transient decay measurements (190 ± 0.8 [n=5] vs 143 ± 0.2ms [n=6], p = 0.0003; Fig D) and quicker 75% (274 ± 1ms [n=5] vs 220 ± 0.2ms [n=6] , p =0.0003; Fig E) calcium transient decay times. In contrast, there was no significant change in time to 90% calcium transient decay (347 ± 1.5 ms [n=5] vs 384 ± 4 ms [n=6]; p = 0.50; Fig F).

**Figure 3-2: EHT calcium kinetics**

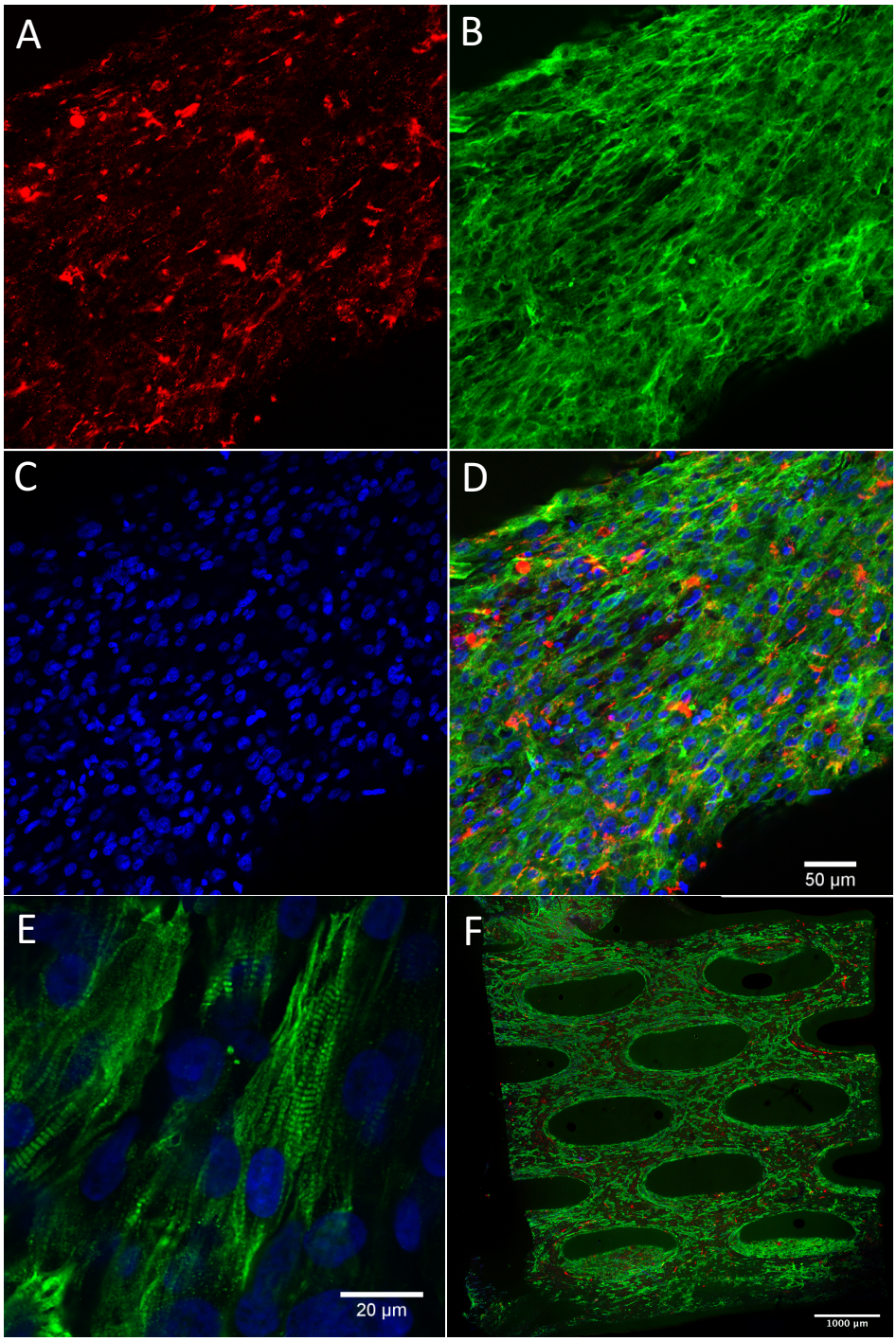



*A) 5x magnification image of EHT consisting of gCAMP hiPSC-CMs. The intensity of the green channel is directly related to calcium release from the sarcoplasmic reticulum and hiPSC-CM contraction. B) A representative calcium transient recording from a region of interest on the surface of the EHT. C) Bar chart comparing time to peak of early and late EHTs D) Bar chart of 50% calcium transient decay; E) Bar chart of 75% calcium transient decay; F) 90% calcium transient decay.* **=p<0.01, ***=p<0.001. *Data presented at mean ± SEM. Unpaired t-test used to test for significance.*

### 3.3 Upscaled EHT immunohistochemistry

The gradual improvements in contraction kinetics and calcium transients imply that the larger EHTs (similar to the first generation EHTs) show enhanced maturation kinetics over time in vitro when: 1) attached to silicone posts providing auxotonic load, and 2) using dynamic rocking culture. Previously dynamic culture conditions have improved the quality of EHT constructs (e.g. increased conduction velocity / force production), and associated with an upregulation of mTOR but not ERK1/2. Rocking culture conditions were insensitive to mechanosensitive channel blockers indicating that increased nutrient availability rather than mechanical stimulation was the main mechanism behind the upregulation of mTOR. (Jackman, Carlson and Bursac, 2016) The next step was to perform optimisation of the antibody staining of EHTs so that specific morphological characteristics could be obtained. Full details regarding staining are in the methods section 2.5.2 and the supplementary appendix. Firstly, when the EHTs (consisting of hiPSC-CMs) had developed synchronised and mature contractions at > 28 days, sections of EHT were stained in whole mount preparations. Firstly, they were fixed in PFA for 24 hours, followed by a 3 day staining protocol. Sections were then immunostained for Vimentin (Fig 3-3A, D), Troponin T (Fig 3-3B,D,E,F) and nuclear stained with DAPI / Hoechst (Fig 3-3C,D). As can be seen, fibroblasts were present in relatively small numbers (when compared to troponin T positive cells) and equally distributed through the EHT. Troponin T staining revealed evidence of troponin positive cells equally distributed throughout the EHT and higher magnification images revealed well organised sarcomeres. Nuclear staining, using DAPI, revealed that the cells were relatively well compacted together and equally distributed in the hydrogel matrix.

**Figure 3-3: EHT immunostaining**



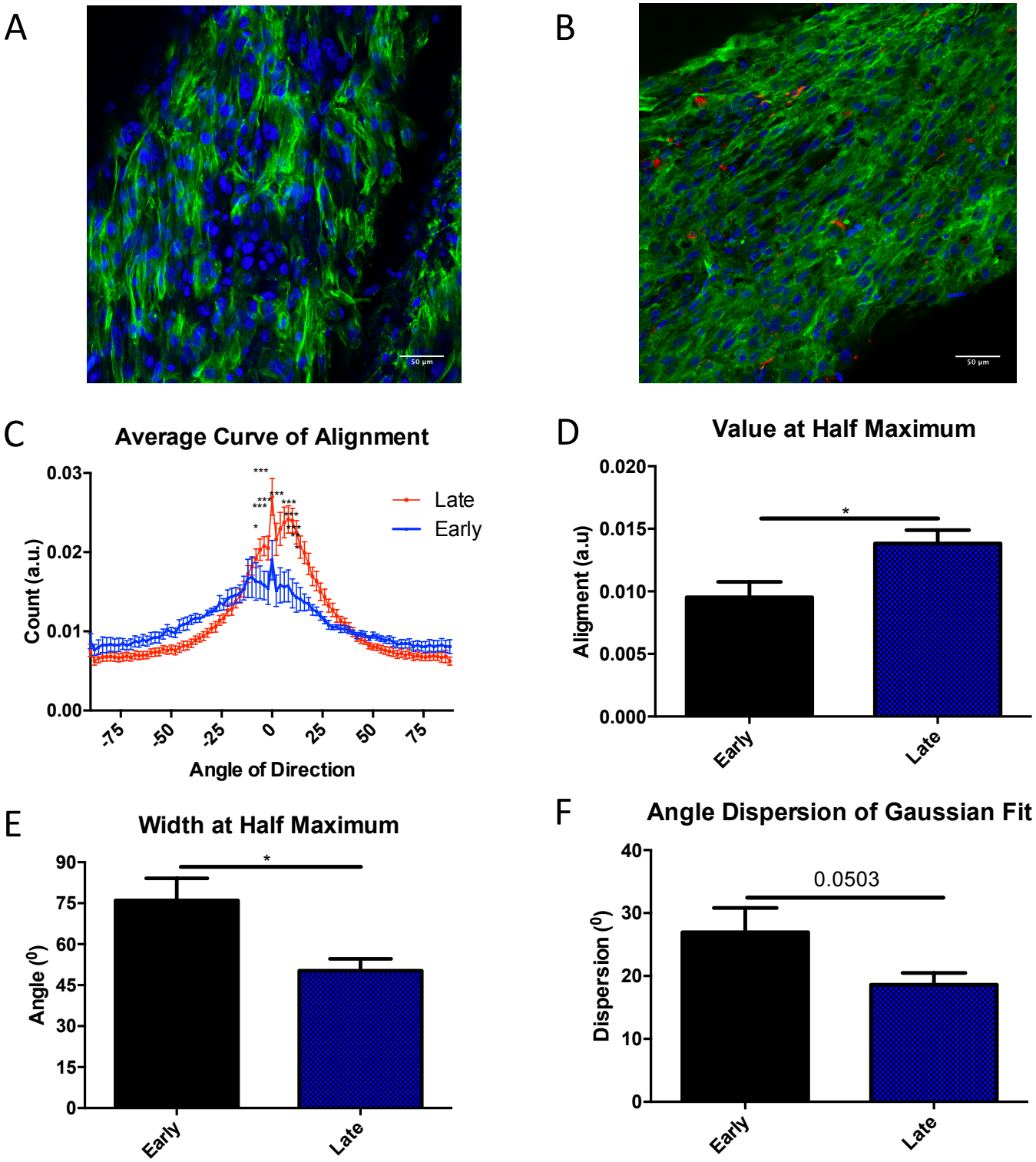

*A-D) Confocal staining of EHT at 10 x magnification. Red channel – Vimentin [A], green channel – troponin T [B], blue channel – DAPI nuclei [C], Composite image [D]. E) 40 x magnification of EHT, green channel = troponin T. Sarcomeres can be seen. Blue channel – DAPI nuclear stain. F) 5x image of troponin T stained EHT. The characteristic holes in the EHT can be seen. Scale bar in D is applicable to A-C.*

### 3.4 Upscaled EHTs align over time

Since it was observed that EHTs developed improvements in contraction kinetics over time and the immunostaining protocol has been optimised, the next step was to perform immunostaining experiments of early and late EHTs to ascertain whether there was any change in cardiomyocyte alignment over time. It is well known that cardiomyocytes elongate and become aligned in 3D EHT Culture on a smaller scale and resemble a more adult like phenotype. Firstly, EHTs were fixed and stained with troponin T at two different time points (Early < 2 weeks, Late > 4 weeks). Nuclei were stained with DAPI. Immunoconfocal images were then obtained and analysed using the Orientation J macro (Images analysed with help from Ms Daphne Pantou / Dr Thomas Owen). Full details regarding analysing cell alignment can be found in the methods section 2.4.5. Representative confocal images of an early EHT (troponin T) are shown in Figure 3-4A, whilst representative images of a late EHT (troponin T) are shown in Figure 3-4B. Later EHTs had troponin T positive cells that were more aligned (Figure 3-4C) with significantly greater values at half maximum (0.01±0.001a.u. [n=4] vs 0.014 ± 0.001a.u. [n=8], p=0.03 Figure 3-4D) and significantly lower widths at half maximum (Figure 3-4E; 76± 8.1a.u. [n=4] vs 50.3± 4.4a.u. [n=8], p=0.01) when compared to early EHTs. There was a trend towards a decreased angle of dispersion between early and late EHTs (Figure F; 27 ± 3.9 [n=4] vs 18.6 ± 1.9 [n=8], p=0.05). As well as analysing the cumulative angle change using a macro, the cumulative angle change was manually calculated between 50 randomly picked troponin T positive cells on confocal images of early and late EHTs. The results obtained by this method were consistent with the results obtained using the Orientation J macro, with more aligned cells found in EHTs fixed at a later time point (cumulative angle change 2702 ± 778 [n=4] early group vs 922 ± 186 [n=5];

p=0.04) . Together, these results imply that as EHTs develop more coordinated and greater force contractions over time, the troponin T positive cells become more aligned.

**Figure 3-4: EHT morphological alignment over time**



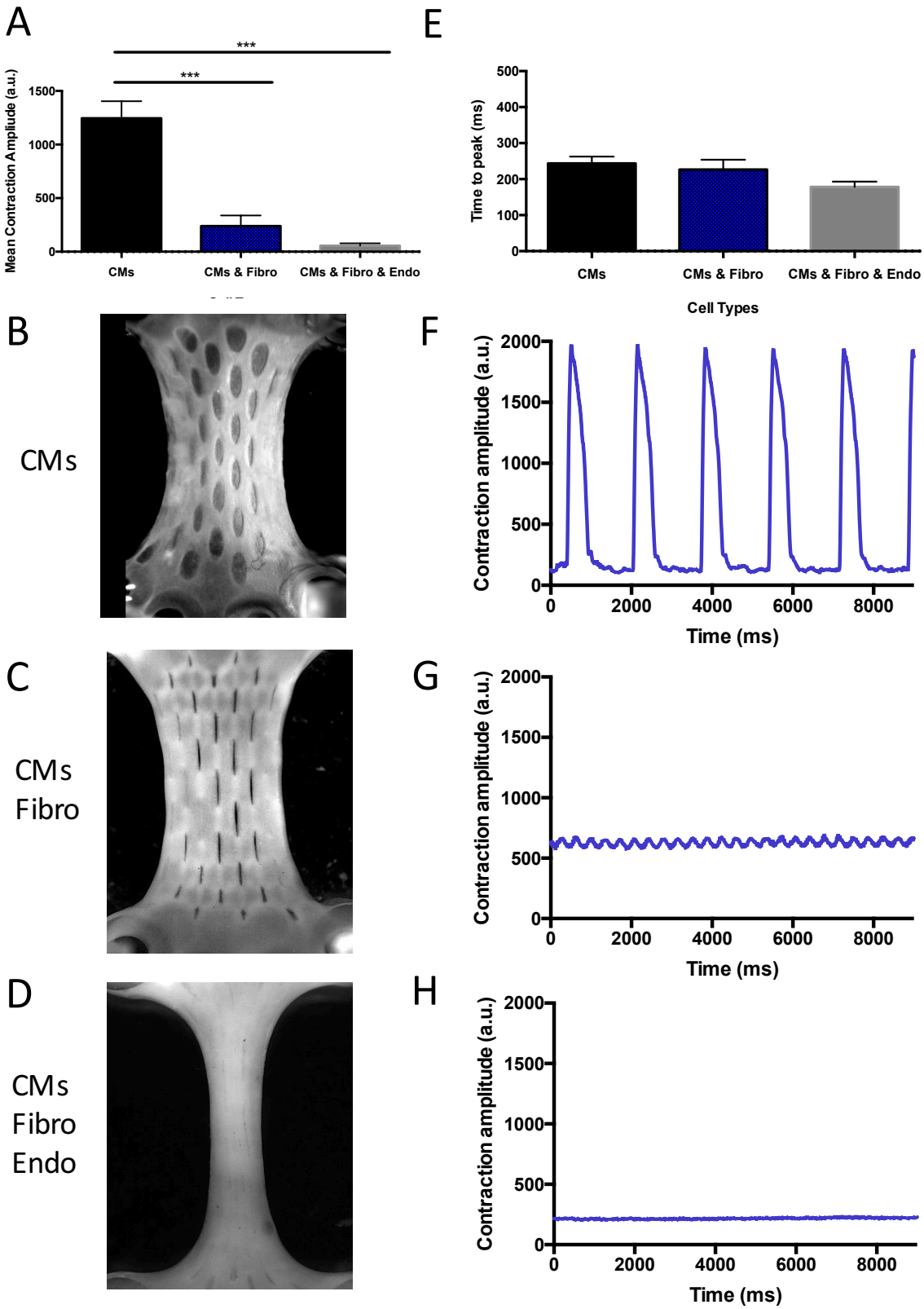

*A) 20x magnification of EHT stained with troponin T (green channel) and DAPI nuclei (blue) of an "early" EHT; B) 20x magnification of EHT stained with troponin T (green) and DAPI (blue) of a "late" EHT; C) Graph showing the angle of direction between*

*troponin T stained cells of early and late EHTs; D) Bar graph depicting the value at half maximum and E) the width at half maximum and F) angle dispersion between early and late EHTs (Gaussian Fit). N=4 early group versus n=8 late group.* *=p<0.05, **=p<0.01, ***=p<0.001. *Data presented at mean ± SEM and 2-way ANOVA (C) and unpaired t-test (D-F) statistical methods used.*

### 3.5 Non-cardiomyocyte addition to EHT Mastermix

Since the addition of non-cardiomyocytes has been shown to improve integration and survival of grafts in-vivo previously and also improved force productions, we experimented with the addition of fibroblasts and endothelial cells as well as hiPSC-CMs. However, we found that the addition of non-cardiomyocyte cells at a value of 10% (fibroblasts) and 5% (endothelial cells), caused a significant reduction in contraction amplitude (Figure A) when compared to EHTs containing hiPSC-CMs alone (1246±158au [n=5] CMs only; 240±98au [n=5] CMs + Fibros; 56±26au [n=3] CMs + Fibros + Endos, $p<0.0005$ for CMs vs CMs/Fibro and CMs vs CMs/Fibro/Endos). Calculations were obtained from measurements averaged from approximately day 15 (range 15 – 46) onwards when the EHTs were synchronised. In addition there was a large reduction in the diameter of the EHT in the x-axis (Figure B-D) when compared to constructs consisting of solely hiPSC-CMs (Figure F-H). In contrast, there was no significant change in time to peak measurements between the EHTs created with and without non-cardiomyocytes (Figure E). 243±20ms CMs only, 227±28ms CMs/Fibros, 178±15ms CMs/Fibros/Endo; p=ns). Since it is well known that EHT rely on auxotonic load (generated by deflecting the posts) for maturation, and the fact that the best force production and morphology (Figure B, F) was obtained with hiPSC-CMs only, it was decided that EHT production would consist of solely hiPSC-CMs at a value of between 15-20million cells per EHT.

**Figure 3-5: Addition of non-cardiomyocytes**

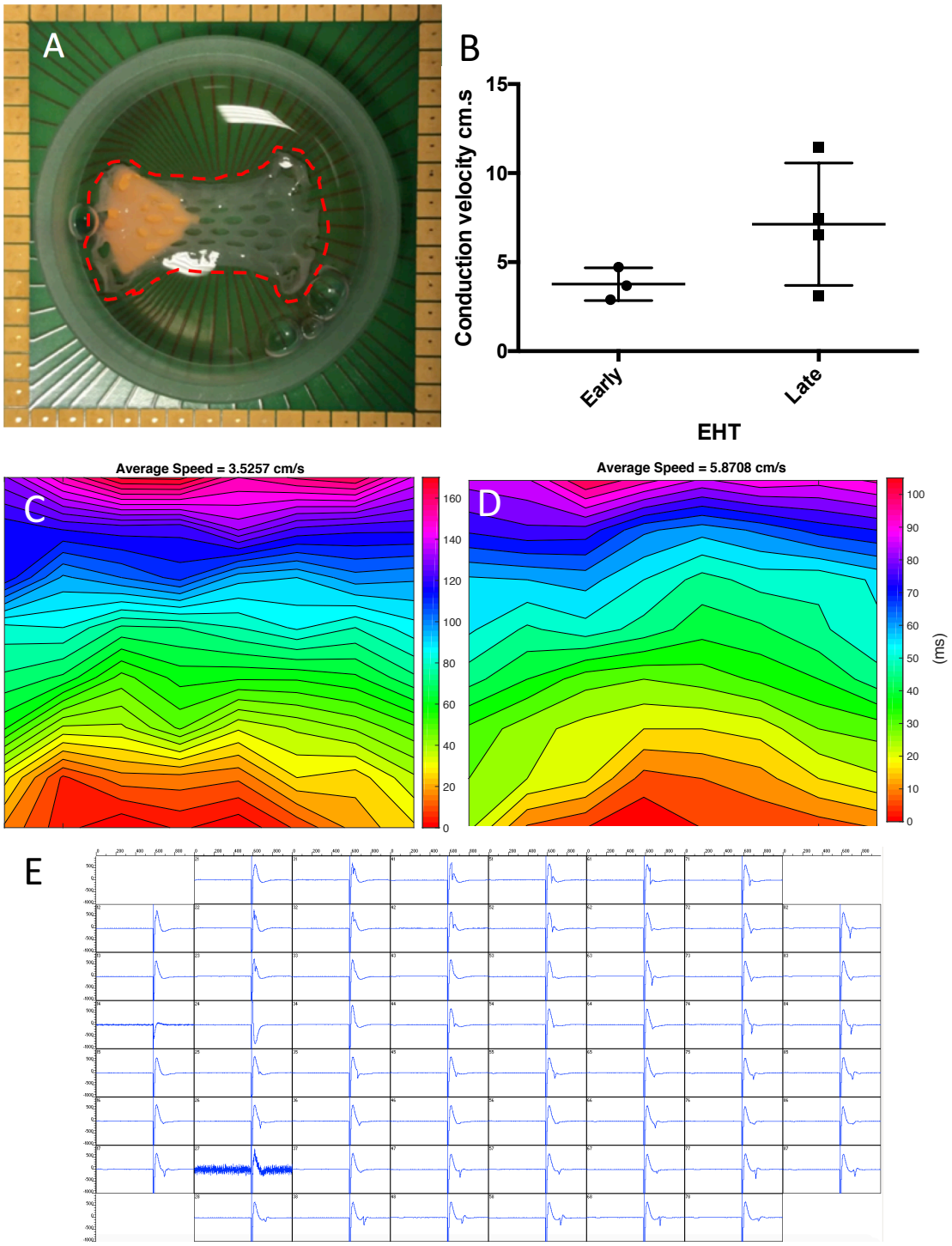


*A) Bar chart comparing EHTs consisting of either: 1) hiPSC-CMs only (n=5); 2) hiPSC-CMs and fibroblasts (n=5); or 3) hiPSC-CMs, fibroblast and endothelial cells (n=3). B) Macroscopic image of EHT consisting: of hiPSC-CMs only; C) hiPSC-CMs / fibroblasts (n=5); D) hiPSC-CMs, fibroblasts and endothelial cells (n=3). E) Bar chart comparing time to peak values of EHTs consisting of hiPSC-CMs (n=5), hiPSC-CMs / fibroblasts (n=5) or hiPSC-CMs, fibroblasts or endothelial cells (n=3). F) Representative graph of contraction amplitude of an EHT containing hiPSC-CM only; G) hiPSC-CM / fibroblast EHT; H) hiPSC-CMs, fibroblasts, endothelial cells. CMs – hiPSC-CMs, Fibro – fibroblasts, Endo – endothelial cell. *** = $p < 0.001$. Data presented as mean ± SEM.*

### 3.6 EHT conduction velocity calculation

The improvements observed in contraction kinetics, cardiomyocyte alignment and calcium transients imply that EHT matures over time in-vitro. Conduction velocity is an important parameter in tissue engineering since any EHT must resemble the host tissue as much as possible to enable effective electromechanical coupling and therefore mitigate the risk of potential arrhythmia formation due to electrical mismatch. Therefore, EHT conduction velocities were recorded at different time points (early <2 weeks and late >4 weeks) from the surface of the patch using a micro electrode array dish (Figure 3-6A). Full details regarding conduction velocity measurements are described in the methods section 2.4.6. In addition, recordings were taken either from spontaneous signals or paced signals via point stimulation at a frequency of 1-2Hz. Recordings were taken with and without BDM to prevent motion artefact. Representative activation maps from early EHTs (figure C) and late EHTs (Figure D). A representative MEA recording from an EHT undergoing point stimulation is shown in Figure E. Conduction velocity analysis from early and late EHTs revealed that there was no significant difference in the conduction velocities obtained from early or later EHT time points (3.8 ± 0.5 [early, n = 3] cm/s vs 7.1 ± 1.7 [late, n=4] cm/s; p=ns). Notably, the numbers in each group were small and likely underpowered to detect a significant difference in conduction velocity over time. There was however an absolute improvement in the conduction velocity in late EHT group of 3.364 ± 2.080 cm/s, indicating a possible trend. Further recordings were attempted but an inadequate signals was obtained for analysis, possibly due to the insulating layer of fibrin or the holes within the EHT so different methods of conduction velocity measurements are needed to obtain more reliable recordings.

**Figure 3-6: Conduction Velocities**




*A) Macroscopic image of EHT on microelectrode array dish. B) Graph comparing the conduction velocities of early and late EHTs (cm per second). C) Representative activation maps of early (C) and late (D) EHTs. E) Representative raw data MEA recordings generated from MC_RACK 2 software. Data presented at mean ± SEM. N=3 in early group; n=4 in late group. Data analysed with unpaired t-test.*

## 3.7 Discussion

The main findings of the first results chapter are: 1) EHTs were successfully upscaled and characterised in-vitro; 2) EHTs showed evidence of maturation over time in-vitro as assessed by contraction kinetics, calcium transients and cardiomyocyte alignment.

### EHT upscaling

EHT was pioneered by Eschenhagen et al last century, and has undergone a rapid evolution with numerous successive iterations, with the most recent medium throughput method protocol published in 2017. (Breckwoldt *et al.*, 2017) These, "first generation" EHTs, whilst showing several characteristics associated with human cardiac muscle as well as being relatively easily manufactured, are not suitable for human clinical translation. This is due to insufficient cell number and size, since over a billion cells are lost in a myocardial infarction; in contrast, the maximum a first generation EHT can contain is approximately 4 million hiPSC-CMs, with average size of 10mm x 1mm x 1mm. Therefore, if EHT is ever to become a viable therapeutic product, much larger constructs are needed.

The upscaling process of the larger EHTs used in this study was predominantly achieved by increasing the size of the silicone posts in the x and y axes, as well as increasing the number of feet (from 2 to 8). The Teflon spacers used to create the cavity for the mastermix were also significantly larger in size. Additionally, the use of silicone nets to create small holes in the EHT were utilised to improve cellular distribution and to allow for effective delivery of media throughout the EHT (upscaling achieved with close collaboration with Prof Eschenhagen's group in Hamburg

University, Germany). The actual manufacturing process regarding dissociation of hiPSC-CMs, mastermix preparation and fibrin based extracellular matrix was similar to first generation EHTs, except that the volume of master mix was 17 times larger (100ul versus 1.7ml). This translated into a markedly increased potential cell containing capacity with a theoretical maximum of 68 million (17 x 4 million [largest number contained in first generation EHT]). The optimum cell number for the EHTs used in this study was between 15-20 million hiPSC-CMs. In contrast, the optimum cell number for smaller first generation EHT is approximately one million cells per EHT, which translates into 17 million for the larger EHTs (17 x Mastermix volume), which means that the cell density between first generation EHTs and the newer larger version used in this thesis was similar. Identifying the correct cell number per patch and therefore cardiomyocyte density is not always straightforward. For example, in a recent study by the Bursac group, they found that a relative decrease in the number of cells in their “cardiopatch” from 1 million to 0.5 million cells, i.e. halving the density of cells, resulted in thinner constructs but a large increase in cell size (of up to 30%). (Shadrin et al., 2017) Interestingly, this was associated with higher contractile force production per input CM, significantly faster twitch kinetics and improvements in conduction velocities. However, it must be stated that overall force production, not taking into account dimensions, was greater with the EHTs containing more cells. It is possible that hiPSC-CMs need a sufficient space to elongate and mature in-vitro. Twenty million cells per EHT is still below the number required for clinical translation but future work could look at increasing cell number or increasing the size of the EHTs further. Regarding larger EHTs, the Zimmerman group reported engineered heart muscle patches of sizes up to 35x34mm containing up to 40 million cardiomyocytes.(Tiburcy *et al.*, 2017) Interestingly, and similarly to

our group, the patches did not increase in thickness significantly (average thickness 0.5±0.1 mm).(Tiburcy *et al.*, 2017) In a study by Gao et al, patches of 4cm x 2cm were reported with approximately 8 million cells (4 million hiPSC-CMs, 2 million hiPSC-ECs, and 2 million hiPSC-SMCs). The patches in this study were thicker but still relatively thin when compared to a native human ventricle (average EHT thickness 1.25mm versus 6-10mm in human ventricle).(Gao *et al.*, 2018) To increase EHT thickness further it is likely that a fully in-vitro prevascularised network would be needed to supply the specific nutrients and oxygen both in-vitro and in-vivo in order to prevent hypoxia, cell death and a necrotic core from forming. Recently, however, the Zimmerman group has stacked together multiple individual EHTs in layers to create fused EHTs up to 1cm in diameter and containing up to 800 x $10^6$ myocytes (Zimmerman presented at ESC 2019, unpublished).

**Addition of non-cardiomyocytes**

The addition of non-cardiomyocytes to engineered heart tissue is primarily to replicate the target tissue it is trying to emulate. Cardiac muscle consists of approximately 30% cardiomyocytes followed by 70% non-cardiomyocytes. (Tirziu, Giordano and Simons, 2010) The addition of fibroblasts to hiPSC-CMs has been shown to improve force contractions and increase the cardiotherapeutic potential of EHT grafts in small animal models.(Iseoka *et al.*, 2017)(Tiburcy *et al.*, 2017) This is thought to occur by providing an extracellular matrix as well as providing supportive paracrine factors for maturing hiPSC-CMs. (Li, Asfour and Bursac, 2017) The relative concentrations of fibroblast to cardiomyocyte ratio is also a matter of debate with studies adding between 10-50%.(Tiburcy *et al.*, 2017)(Iseoka *et al.*, 2017)(Pfannkuche *et al.*, 2010)(Kensah *et al.*, 2013) For example, in a study by the

Zimmerman group, they calculated that a cardiomyocyte to fibroblast ratio of 70% : 30% was optimal for the construction of force-generating loops. (Tiburcy *et al.*, 2017) This ratio was also associated with reduced variability in the functional maturation of EHTs, and a higher mean actinin fluorescence per cell, indicating higher sarcomeric content per cell. In addition, lower levels of immature myocyte cell markers were found. In a paper from the Bursac group, the differentiation protocol used after metabolic selection and replating yielded hiPSC-CMs ranging from 71–98%, with the remaining average of ~14% made up primarily of smooth muscle cells and fibroblasts with virtually no endothelial cells. (Shadrin *et al.*, 2017) They did not specifically add fibroblasts or endothelial cells to their master mix. Despite this, EHTs after 3 weeks of in-vitro culture demonstrated progressive vascularisation after 2 weeks when implanted onto nude mice. Our differentiation protocol (based on metabolic selection with the Burridge protocol) yields approximately 95% hiPSC-CMs, and in the EHTs that did not specifically contain intentionally added fibroblasts, vimentin staining was still positive and present throughout the graft. (Burridge *et al.*, 2014) Since studies have added fibroblasts at concentrations ranging from 10-30%, we decided to add fibroblasts at a relative low 10% concentration and endothelial cells at a 5% concentration. The results we obtained were significantly different to previously published studies regarding the addition of non-cardiomyocytes to the EHT protocol . (Kensah *et al.*, 2013; Tiburcy *et al.*, 2017) We found that only weak contractions of the EHTs were visible at 4 weeks, and there was a severe reduction in the diameter of the EHT in the x-axis. A reduction in the x-axis has been shown in other groups but this was associated with an increase in force production, although to some extent this may be due to the reporting of force per unit area ($mm^2$). (Kensah *et al.*, 2013)(Jackman, Carlson and Bursac, 2016) There are several

possible reasons for this. For example, it could be that the concentration of non-cardiomyocytes could be incorrect and lower numbers were needed. However, we only used 10% in our preliminary experiments and when compared to the literature when some studies have reported 30% as the optimum number, we started at a relatively low concentration. In addition, it could be the length of time left in in-vitro culture. Fibroblasts continue to proliferate in-vitro whilst hiPSC-CMs do not. EHTs were kept up to 6 weeks in culture, when compared to only a week in some studies; and therefore even though the initial concentration was relatively low the final concentration would have been higher.

**Addition of Endothelial cells**

The addition of endothelial cells or endothelial progenitors has also been shown to improve graft cellular retention. The main goal of adding endothelial cells is to try and manufacture a fully vascularised graft in-vitro so that the tissue can integrate and vascularise more easily. This is hoped to therefore prevent cell death from hypoxia. For example, in a study by Sekine et al, neonatal rat cardiomyocytes were cocultured with GFP-positive rat derived ECs, which then formed cell networks within cardiomyocyte sheets, resulting in increased in-vitro production of vessel forming cytokines. (Sekine et al., 2008) When the EC positive EHTs were implanted onto a myocardial infarction model, increased capillary density was found and the blood vessels originating from the graft bridged into the myocardium and connected with the capillaries of the host heart. Adding relatively high concentrations of ECs increased cardiac function when compared to sham controls (assessing by fractional shortening). (Sekine et al., 2008) More recently, work has focussed on investigating the use of stem cell-derived ECs to create highly vascularized constructs in-vitro. For example, by utilising capillary tubes around a patterned and perfusable

microvascular network in-vitro. (Redd *et al.*, 2019) The implantation of the in-vitro pre-pattern perfused grafts with vascular networks resulted in better integration in rats, with higher cardiomyocyte and vascular densities found when compared to non-perfused grafts. (Redd *et al.*, 2019) A pre-formed vascular network may be especially pertinent with larger grafts or those several millimetres thick. Since the diffusion capacity of tissue is around 300μm, it is possible that thick grafts may have a necrotic core post grafting. This is because EHTs are attached to the epicardial surface (not injected intramyocardially or intracoronary) and therefore the graft will predominantly rely on diffusion until a primitive capillary network is formed. Data from several studies involving EHTs made solely from iPSC-CMs have been reassuring in small animal models. (Weinberger *et al.*, 2016) For example, Weinberger et al showed that grafts containing 5-7 hiPSC-CMs million cells, were well integrated with vasculature supplied by the host. (Weinberger *et al.*, 2016) It must be noted however that this study involved guinea pigs and the grafts were less than a millimetre thick. Data from large animal models (swine) have used patches of clinically relevant dimensions (4cm x 2cm x 1.25mm), containing hiPSC derived endothelial cells, cardiomyocytes and smooth muscle cells containing up to 8million iPSC derived cells (4 hiPSC-CMs, 2 hiPSC-ECs, 2 hiPSC-SMCs). (Gao *et al.*, 2018) Patches were implanted on a surgical model of myocardial infarction. The troponin retention in graft at 4 weeks was approximately 11% and there were improvements reported in left ventricular function, infarct size, myocardial wall stress, myocardial hypertrophy, and reduced apoptosis in the periscar border zone myocardium. Whether or not the addition of non-cardiomyocytes is essential in larger grafts remains to be seen.

In summary, the addition of non-cardiomyocytes seems like a logical step forward. It must be stated however that since no differentiation protocol at present is 100% efficient at producing hiPSC-CMs there will also be non-cardiomyocytes present in the graft if additional steps are not undertaken to purify the hiPSC-CMs. For example, as can be seen in the staining of EHTs in Figure 3-3A, fibroblasts were present in the graft even though they were not specifically added during manufacture. The non-cardiomyocytes present in every differentiation at varying degrees (including fibroblasts) would continue to expand and multiply in-vitro. Preliminary experiments did not appear to show any advantage to adding non-cardiomyocytes, with severe shrinkage of the constructs, but future work should vary the doses of fibroblasts used and also ascertain whether adding endothelial cells only is advantageous. In addition, the level of non-cardiomyocytes in each hiPSC-CM differentiation could be calculated and then the required non-cardiomyocytes added to make up the correct ratio.

**Analysis of contraction kinetics**

After optimisation of cell number and type, the next step was to characterise the EHT. Force measurements and contraction kinetics were one of the most important parameters used to assess maturation of the smaller EHTs. The existing equipment for measuring the contraction amplitude with the smaller EHTs consisted of custom made software and a white box using a high definition camera to analyse post deflection. Then by using the Young's Modulus of the silicone posts, the amount of deflection of the post can be worked out using a formula to convert it to $mN/mm^2$. However, since the newer EHTs were much larger and were kept in 6 well plates, a new way of measuring contraction kinetics had to be devised. The recently published

MUSCLEMOTION software, which essentially uses an algorithm to calculate changes in pixel intensity was open access and readily available and has been used by our collaborators in Germany. (Sala *et al.*, 2018) We utilised a Basler camera to obtain high definition and frame rate images and analysed the videos using the macro from Image J. The software worked relatively consistently but it was essential to have the camera at a fixed distance from the 6 well plate, record videos with a frame rate >100 frames per second and also record the videos on a surface without significant vibrations with a consistent intensity of light. We used a light source approximately 10-15cm from the 6 well plate. In addition, to get accurate recordings we had to remove the lid of the 6 well plate, and therefore had to perform measurements in the sterile hood. Although we were able to track EHTs over time and show that overall the contraction amplitude improved over time and the time to peak decreased over time, the units measured were arbitrary units and not in $mN/mm^2$. Accurate force measurements, using a force transducer, are needed to compare the grafts with human tissue. Future work will include devising a way to accurately measure paced and unpaced force contractions and force frequency relationships of the large grafts.

**EHT morphology**

3D culture in the EHT format is known to be associated with several morphological changes that are associated with maturation. For example, morphologically the cells elongate, show evidence of mature cardiac troponin I expression, and display a ventricular like isoform (ventricular (MLC2v)) along with abundant connexin 43 expression. (Shadrin *et al.*, 2017; Kensah *et al.*, 2013; Tiburcy *et al.*, 2017; Gao *et al.*, 2018) The larger EHTs used in this thesis displayed improvements in contraction kinetics with increases in contraction amplitude and time to peak. Morphologically we

assessed maturation by assessing cardiomyocyte alignment (Troponin T cells) over time at two time points. It was found that older EHTs subject to 3D culture and mechanical kinetic energy were more aligned with less cumulative angle change between the troponin T positive cells. This is plausible since it is well known that the myocytes elongate and become aligned over time in 3D culture in relatively smaller EHTs. (Mannhardt *et al.*, 2016) Further work is needed to characterise morphological changes including the expression of ventricular specific isoforms, ki67 expression, connexin distribution and also electron microscopy to detail the patches at an ultrastructual level (distribution of Z-bands, M-bands, T-tubule like structures).

**Calcium transient analysis**

As well as improvements in alignment, and contraction kinetics, improvements in calcium handling were also seen between early and late EHTs. In general, hiPSC-CMs have relatively immature calcium handling mechanisms, with the notable absence of t-tubules and more reliance on caveolae. (Yoshida and Yamanaka, 2017) In addition, calcium reuptake into the sarcoplasmic reticulum is less well developed when compared to adult cardiomyocytes. Experiments indicated that there were significant reductions in time to 50% and 75% decay but not time to 90% decay. These findings have also been replicated in previous hiPSC-CM studies. For example, Rao et al found that culturing iPSC-CMs on structured substrates caused significant reductions in time to peak calcium transient amplitude and time to 50% decay, but no difference in time to 90% decay. (Rao *et al.*, 2013) Notably, this occurred when pacing at 1Hz which is the same as our protocol. In that study, they found that culturing on microgrooved PDMS substrates also improved SR calcium release when performing caffeine experiments. Similar to our findings they also found greater evidence of alignment along with sarcomeric organisation. In a study

by Leonard et al, it was found that EHTs subjected to afterload had better calcium kinetics than those that were unloaded, with improvements in time to peak and 50% decay. (Leonard *et al.*, 2018) The fact that time to 90% decay was not altered, may be due to the persistent relative immaturity of hiPSC-CMs; for example, lack of improvements in SR reuptake. Further calcium based experiments are needed to elucidate this further.

**Conduction velocity analysis**

The next step was to assess the conduction velocity of the EHTs to ascertain whether the changes in contraction amplitude, alignment and calcium transients were associated with improvements in conduction velocity. Although we observed a numerical increase in conduction velocity, there was significant heterogeneity in the conduction velocities measured in the late EHTs and the numbers of EHTs in both groups was small. Therefore, it is likely that the two groups were underpowered to detect a true difference. The mean conduction velocity in the late EHT group was 7.1 ± 1.7 cm/s [late, n=4]. This is lower than some groups have reported previously. For example, conduction velocities of up to 25 ± 0.9 cm/s were recently reported (Ronaldson-Bouchard et al., 2018) The EHTs in this study were subjected to an intense electrical stimulation regime of up 6Hz in a graded fashion, which was started at a relatively early time point (Day 1). Electron microscopy showed impressive detail of adult like morphology including t-tubules, aligned sarcomeres with I/A-bands, M-lines, Z-lines, desmosomes, and intercalated discs. It must be stated however that the EHT used in this paper were much smaller than the EHTs used in this thesis (6mm x 1.8mm and 2 million cells), and whether these impressive results can be replicated in larger constructs remains to be seen. For our large

EHTs, we did not use electrical stimulation but dynamic culture, which has been shown to mature EHTs better than standard culture. (Jackman et al, 2016) Groups using dynamic rocking have reported conduction velocities of between 14.1±1.0 cm/s and 25.8 cm/s which is lower than adult but higher than we have reported. (Jackman et al. 2016; Shadrin *et al.*, 2017; Gao *et al.*, 2018) It must be noted that again the EHTs used in those studies were significantly smaller than ours containing fewer hiPSC-CMs. Interestingly, a paper by the Bursac group, they found that EHTs containing a relatively lower density of hiPSC-CMs (0.5 million vs 1 million) improved conduction velocity, with levels of up to 40cm/s reported in the lower density EHTs, which is approaching adult levels (46.4cm/s). (Shadrin *et al.*, 2017) Future work could include varying the total cell number in the EHT and also the effects of electrical stimulation combined with dynamic rocking culture.

**Conclusion**

The results presented in this chapter indicate that EHTs were able to be successfully upscaled to a potentially clinically relevant size (2.5cm x 1.5cm x 1mm) containing approximately 15- 20million hiPSC-CMs. Since a billion cardiomyocytes are lost post myocardial infarction it is likely that a greater cell number will be needed. This could be overcome by using multiple patches per patient or by increasing the cell number in each patch. In general, there are two potential modes of improving function / cardiac repair – either by paracrine mechanisms or by contributing to cardiac contraction by replacing the lost cells. If the cells act by mainly a paracrine mechanism, it could be possible that a lower number of cells may be needed than is lost by a typical myocardial infarction.

Experimentally, we were able to show that the contraction kinetics of the EHTs improved over time: this was mirrored by increases in hiPSC-CM alignment, and more mature calcium handling characteristics. Future work could also analyse the changes in the EHT at an ultrastructual level, along with force measurements obtained using a force transducer so that accurate comparisons with human tissue can be made.

# Chapter 4: Establishing rabbit infarct and heart failure models

## Introduction

The results presented in this chapter pertain to the development of the rabbit infarct and heart failure models that could potentially be used to evaluate the feasibility of EHT grafting. Prior to any first-in-human EHT studies it is critical to assess safety and efficacy in preclinical models. A rabbit model was chosen since it has already been shown that EHTs improve ventricular function in small animal models and therefore the next step was to confirm these findings in larger animal models.(Weinberger *et al.*, 2016)(Zimmermann *et al.*, 2006) The rabbit model was an ideal bridge between small animals and larger animal like pigs and macaques that are considerably more expensive / have ethical limitations, and therefore are reserved for immediate preclinical testing. The rabbit also has numerous similarities to human myocardium.(Pogwizd and Bers, 2008) A myocardial infarction model was initially set up and validated. Although the MI model is a less clinically relevant model, a heart failure model would involve an extra surgery and additional thoracotomy. This would significantly increase the complexity of the model, with a greater probability of adhesions while being more stressful for the animal. Therefore the myocardial infarction was a suitable starting point as inevitably there would be a learning curve when performing complex preclinical surgery. It was decided that an infarct would be performed by permanent ligation using sutures since a consistent transmural infarct would be created. Infarcts were confirmed intraoperatively by tissue discoloration and ST elevation on ECG recordings and then quantified histologically (H+E / PSR). Echocardiography was used to assess for reductions in left ventricular function as well as post infarct chamber dilatation / remodelling. Once the myocardial infarction data had been successfully validated, a heart failure model was developed and feasibility assessed using similar methods.

### 4.1 Development of rabbit Infarct model

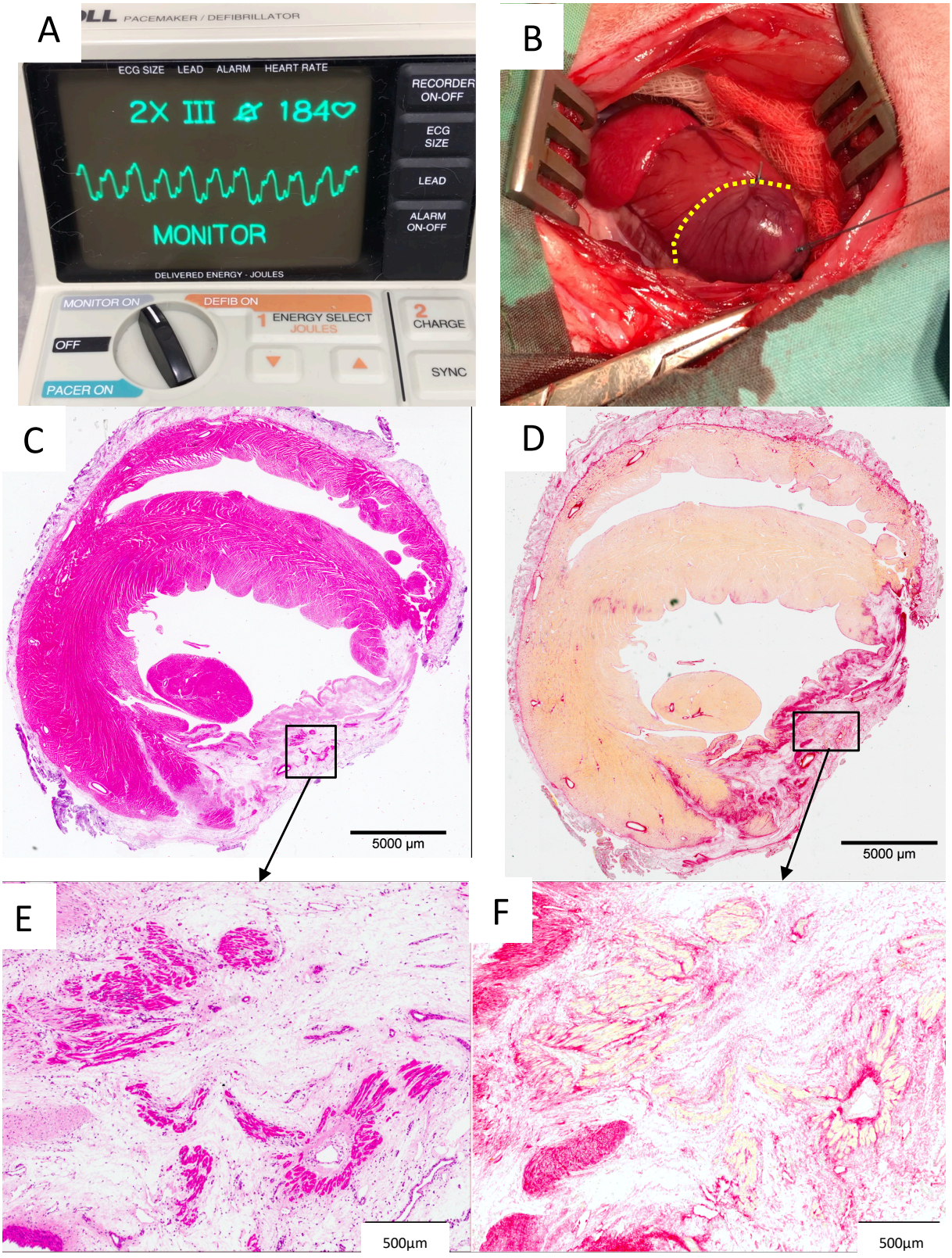
The rabbit myocardial infarction model was well established at our collaborating institution (Glasgow university) and it was therefore decided to first develop the myocardial infarction model at Imperial College after a period of training at Glasgow university (Credit Mr Michael Dunne, Animal Technician at Glasgow University). The heart failure model, although clinically more relevant would require two thoracotomies (i.e. an additional surgical procedure), and therefore be significantly more complex with the potential for greater perioperative morbidity and mortality. Furthermore, an additional surgical procedure could lead to the development of extensive adhesions limiting the feasibility of EHT grafting. To validate the MI model, 13 rabbits underwent ligation surgery. Three (23.1%) animals died: 1) the first was intraoperative due to intractable ventricular fibrillation and inadequate restoration of cardiac output; 2) another died within a 24 hour period due to acute heart failure and possible lung haemorrhage; and 3) another from probable sudden cardiac death 11 days post op after being found dead in his pen. Out of the 10 animals that survived the study period (explanted 40 $\pm$ 6.1 days post initial ligation), 7 hearts after explantation were used for ex-vivo optical mapping and conductive polymer work.

Full details regarding methodology are found in Methods section 2.6.4. Briefly, the myocardial infarction model was created by permanent ligation. The heart was firstly exposed during surgery and a suture placed around the marginal artery around 5-7mm from the atrioventricular border. Validation of the infarct was assessed intraoperatively by the presence of ST elevation on continuous ECG monitoring in all animals (Figure 4-1A). Since the rabbit has a relative lack of collateral circulation when compared to other species, after ligation of the artery, the infarcted tissue

could be clearly visualised as discoloured tissue distal to the suture entry point (Figure 4-1B). Six rabbits developed ventricular fibrillation post ligation, requiring intraoperative DC cardioversion and intracardiac massage to restore output. In 3 (out of 6 that went into VF) cases adrenaline was given to aid in restoring adequate cardiac output post defibrillation. Nine of the 10 hearts underwent sectioning and staining to quantify infarct size (results section 4.3), with the remaining animal used for myocardial slice work (in collaboration with Dr Fillippo Perbillini).

Representative histological sections of an animal that underwent myocardial infarction surgery are shown in Figure 4-1C-F. As can be seen from H+E staining of an axial section of the left ventricle at the level of the papillary muscles, infarcted tissue is relatively devoid of staining indicating necrotic tissue (Figure 4-1C). In the higher magnification image (Figure 4-1E), residual transmural islands of myocytes were evident, which is a characteristic finding post myocardial infarction in rabbits.(Walker *et al.*, 2007) PSR staining revealed areas of intense collagen deposition in the infarcted area (red colour; figure 4-1D/4-1F). This indicated the conversion of fibroblasts to myofibroblasts, which is typical of the remodelling process that occurs post myocardial infarction.

**Figure 4-1: Establishing the myocardial infarction procedure**




*A) Intraoperative ECG Evidence of ST elevation confirming full thickness infarction;*

*B) Intraoperative evidence of myocardial infarction with yellow line demarcating*

*border zone between infarcted and normal tissue; C) H+E stained axial section of rabbit heart at the level of the papillary muscles; D) PSR staining of serial section of rabbit heart at the level of the papillary muscles; E) High magnification image of black rectangle in C; E) High magnification image of black rectangle in D.*

### 4.2 Echocardiographic evaluation

Although intraoperative evidence of the infarct was confirmed by tissue visualisation post ligation and the presence of ST elevation on continuous ECG monitoring, a way of quantifying the degree of infarction was necessary. This was especially important for EHT grafting experiments to ascertain any possible improvement in cardiac function. Echocardiographic assessment was deemed the most valuable and practical way of quantifying change in function since it is non-invasive, readily available and can be used in theatre intraoperatively. Baseline recordings were taken after the animal was initially sedated just prior to intubation, and at the end of the operation prior to extubation to identify the presence of a regional wall motion abnormality. Out of the 10 animals that completed the study period, paired baseline and explant data was available for 7 animals (no echocardiographic recording equipment was available during the first 3 myocardial infarction surgeries). Representative echocardiographic images at baseline are shown in Figure 4-2A and at explant in Figure 4-2B.

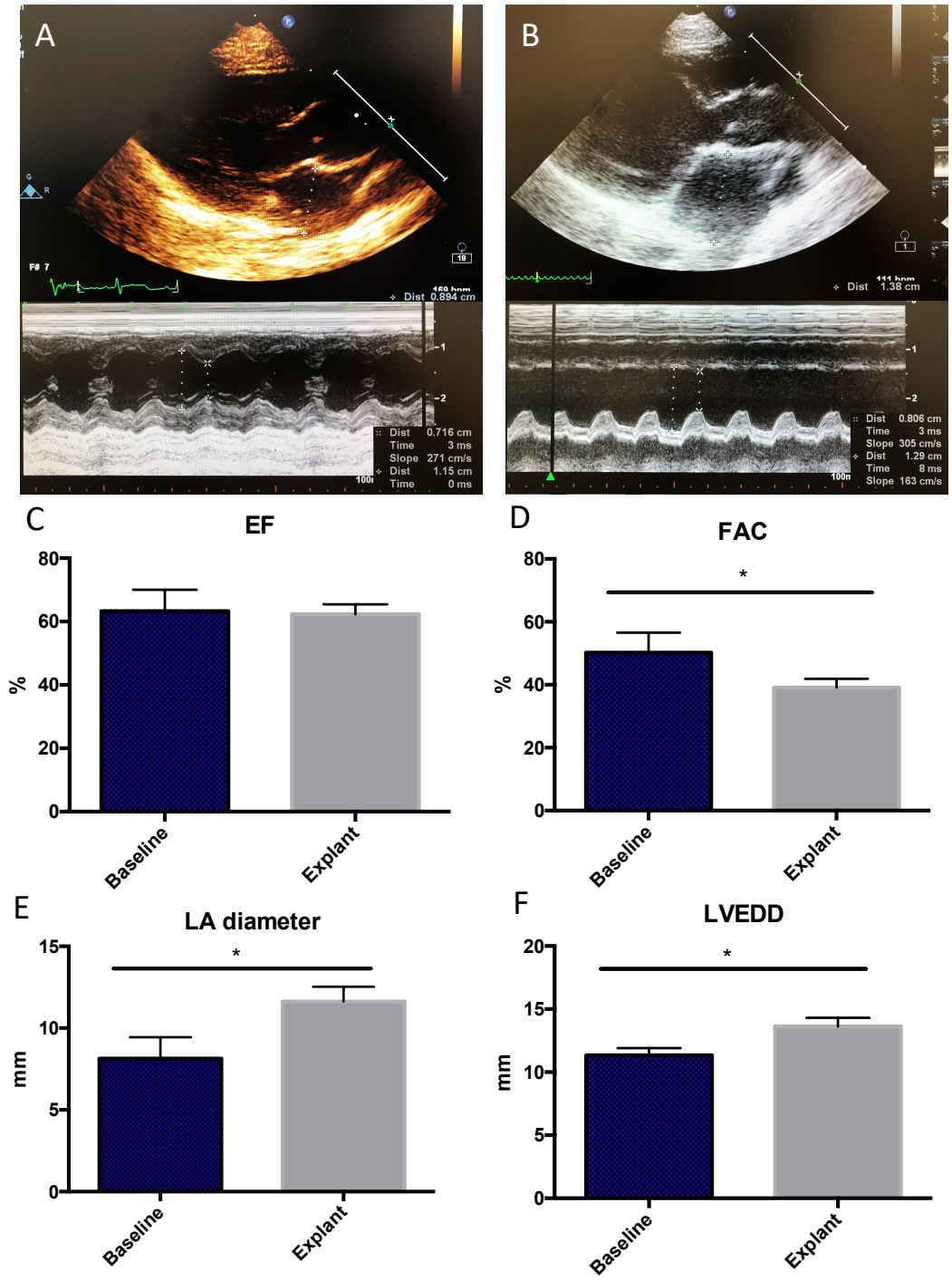
M-mode echocardiography was utilised in the beginning experiments but during later experiments it was discovered that fractional area change was a more reliable way of assessing infarct size. This was because M-mode recordings were obtained via line through the base of the ventricle through the anterior wall and inferior wall in the parasternal long axis view. Since the marginal artery predominantly supplies the lateral wall in rabbits, the M-mode derived ejection fraction recordings were not significantly affected (63.3 ± 2.5% [baseline] vs 62.3 ± 3.1% [explant], n=7; p=0.59, Figure 4-2C). By contrast, fractional area change on the other hand records the area change of the whole ventricle, so encompasses the contractions of all 4 walls

including the lateral wall (See methods section 2.9 for more details). This way of recording enabled the identification of the functional effect infarct more accurately (50.3 ± 2.4% [baseline] vs 39.1 ± 2.8% [explant], n=7; p=0.01, Figure 4-2D).

Typical remodelling features that occurred post myocardial infarction were also detected by echocardiography. For example, as can be seen in figure 4-2E, there was a significant increase in left atrial diameter between baseline and explants (8.1 ± 0.58 [baseline] vs 11.6 ± 0.9 [explant]; p=0.04), which indicated a chronic increase in left ventricular end diastolic pressure, which is commonly elevated post myocardial infarction. In addition, there was evidence of chamber dilatation, as assessed by left ventricular end diastolic diameter (11.3 ± 0.21mm [baseline] vs 13.6 ± 0.69mm [explant], p=0.01, figure 4-2F).

The validation of infarct size by echocardiography was an important step for future grafting work since ascertaining any improvements in function post grafting was to be one of the main study endpoints of assessing EHT efficacy.

**Figure 4-2: Echocardiographic confirmation of myocardial infarction**




2D echocardiography and M-mode recordings at baseline (A) and explant (B); C) ejection fraction (M-mode derived); D) fractional area change (FAC); E) left atrial (LA) diameter; and F). Left ventricular end diastolic diameter (LVEDD) at baseline and explant.

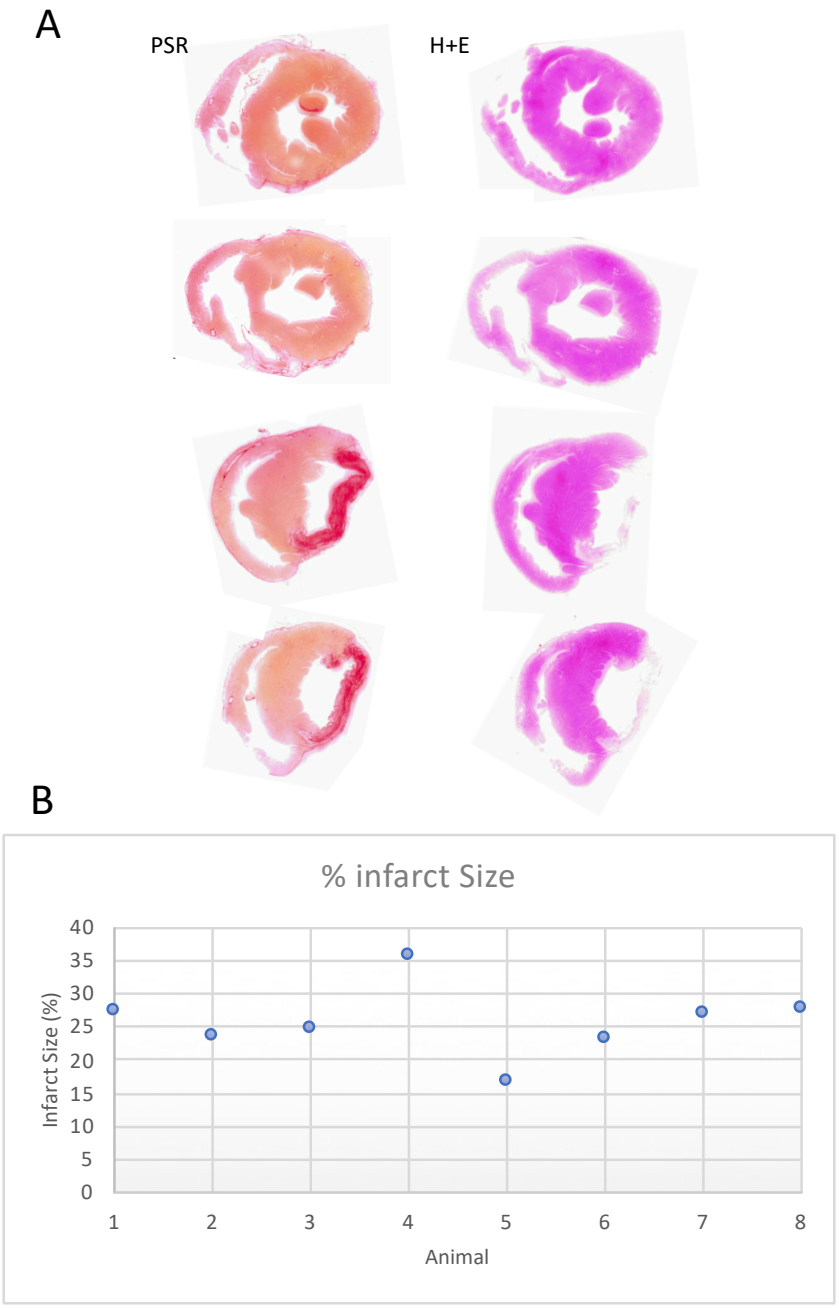
### 4.3 Serial Sections to quantify infarct size

Although echocardiography was an excellent tool for detecting regional wall motion abnormalities and assessing chamber remodelling, infarcts also had to be validated histologically to determine infarct size and infarct consistency between surgeries. Serial sections of myocardial infarction hearts were stained with H+E and PSR to quantify infarct size. Full details can be found in the methods section 2.5.4 – 2.5.6. Each serial section was cut at approximately 3-4mm intervals throughout the left ventricle (4/5 sections for each heart). Thinner sections could not be taken since the relatively larger ventricle required thicker tissue to enable reliable sectioning (performed and stained courtesy of Lorraine Lawrence).

A representative H+E / PSR staining of a section of a left ventricle is shown in Figure 4-3A. The calculated mean area of infarct, as percentage of total left ventricle was 23.39 ± 2.9% (n=9). Of note, the second animal that was operated on had a relatively low infarct size (4.47%). This was because the suture used to ligate had inadvertently come loose post ligation. Therefore in the subsequent surgeries, Prolene sutures were used instead of Polyester (braided, Ethibond Excel), which have more memory and are less resistant to becoming loose. A graph of the 8 animals (excluding the outlier with low infarct size) clearly shows that the infarcts were moderate in size and consistent between surgeries (Figure 4-3B). Moderate infarctions, caused by mid vessel occlusion were specifically chosen since it has been previously reported that proximal vessel occlusion as opposed to mid vessel occlusion has a much higher mortality rate due to intractable ventricular arrhythmia.(Coker, 1989)

In summary, the results in this chapter enable the reliable characterisation of the infarct both intraoperatively by ECG evidence and macroscopic visualisation (tissue discoloration), echocardiographic assessment and by histological staining. The infarcts created in this study were moderate in size, but were sufficiently identified by echocardiography and of consistent size between animals.

**Figure 4-3: Serial sections of infarcted tissue**

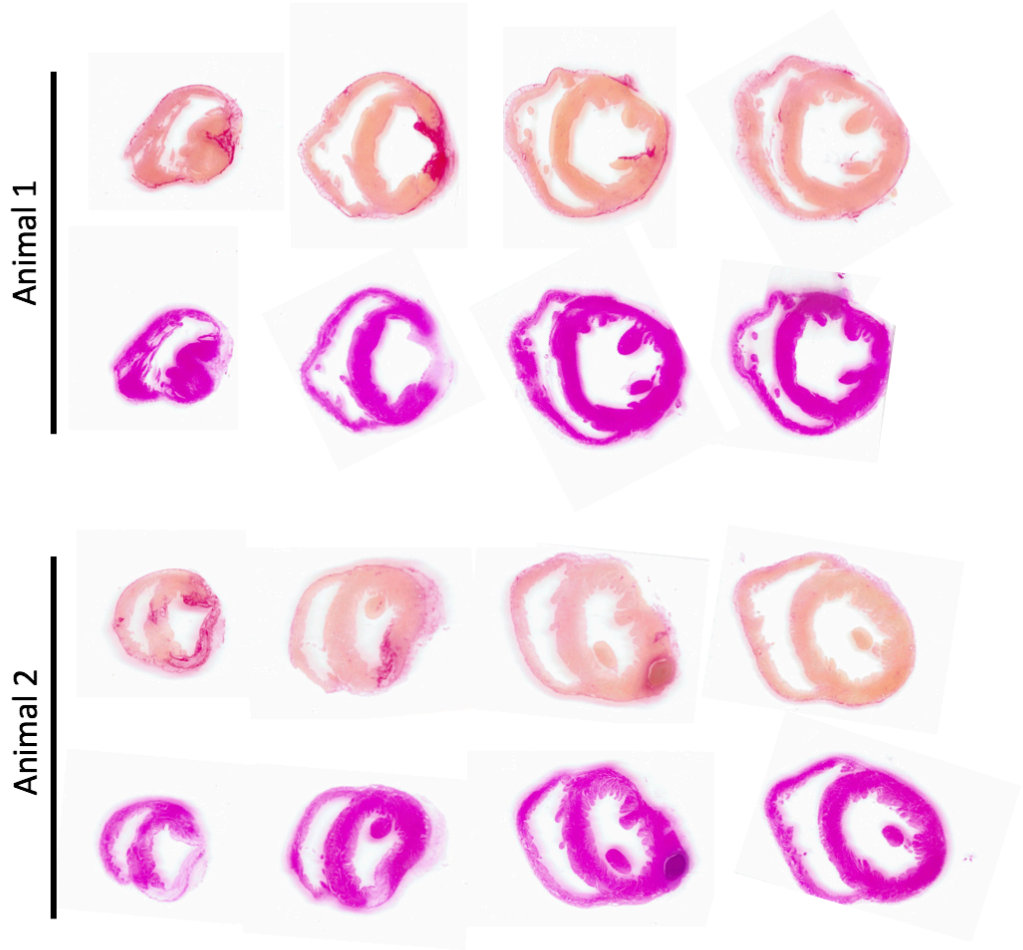



*A) Representative hematoxylin-eosin (H+E) and Picro Sirius Red (PSR) images of serial sections (at 3mm intervals) of a representative rabbit.. PSR – orange stain, areas of infarction (collagen staining) appear red. H+E – purple stain, corresponding areas of infarcted tissue are hypolucent indicating areas devoid of myocytes. B) Graph of infarct size of 8 consecutive animals.*

### 4.4 Development of heart failure model

After the successful set up and testing of the myocardial infarction model, the next step was to develop a more clinically relevant heart failure model for EHT grafting which would require two thoracotomies. The first thoracotomy was needed to create the infarct, and the procedure was performed in the same way as the myocardial infarction model (methods section 2.6.4). The second thoracotomy would then be performed after the infarct had matured, to enable EHT grafting onto the epicardial surface. Determining the time frame between the first and second thoracotomy was important since the myocardium undergoes a large inflammatory reaction during the recovery phase that can take up to 6 weeks to fully mature. This could potentially affect optical mapping studies and the clinical relevance of the heart failure model. Data from our collaborators indicated that reliable optical mapping studies could be performed after 4 weeks minimum and therefore an end point greater than this was chosen (39 $\pm$2.7 days between 1$^{st}$ and 2$^{nd}$ thoracotomy). The second surgery was performed via the fifth intercostal rib space to avoid the fourth intercostal rib that had been used to gain access to the heart during the index procedure. Feasibility of attaching a sham patch (fibrin only, cell free) was tested and successful in all animals. Four animals (80%) underwent immunosuppression beginning 5 days prior to the second surgery and continuing until explant. Significant adhesions, which were most likely due to inflammation from the previous infarction were seen in 3 out of 5 animals. These could be debrided in all animals prior to patch grafting. All animals survived the surgery and to explantation (third surgery; 29.6 $\pm$ 1.7 days). Histological analysis of 2 animals with full sectioning revealed that the infarct sizes were 13.8% and 18.6% (Figure 4-4).

**Figure 4-4: Serial sections of heart failure model**

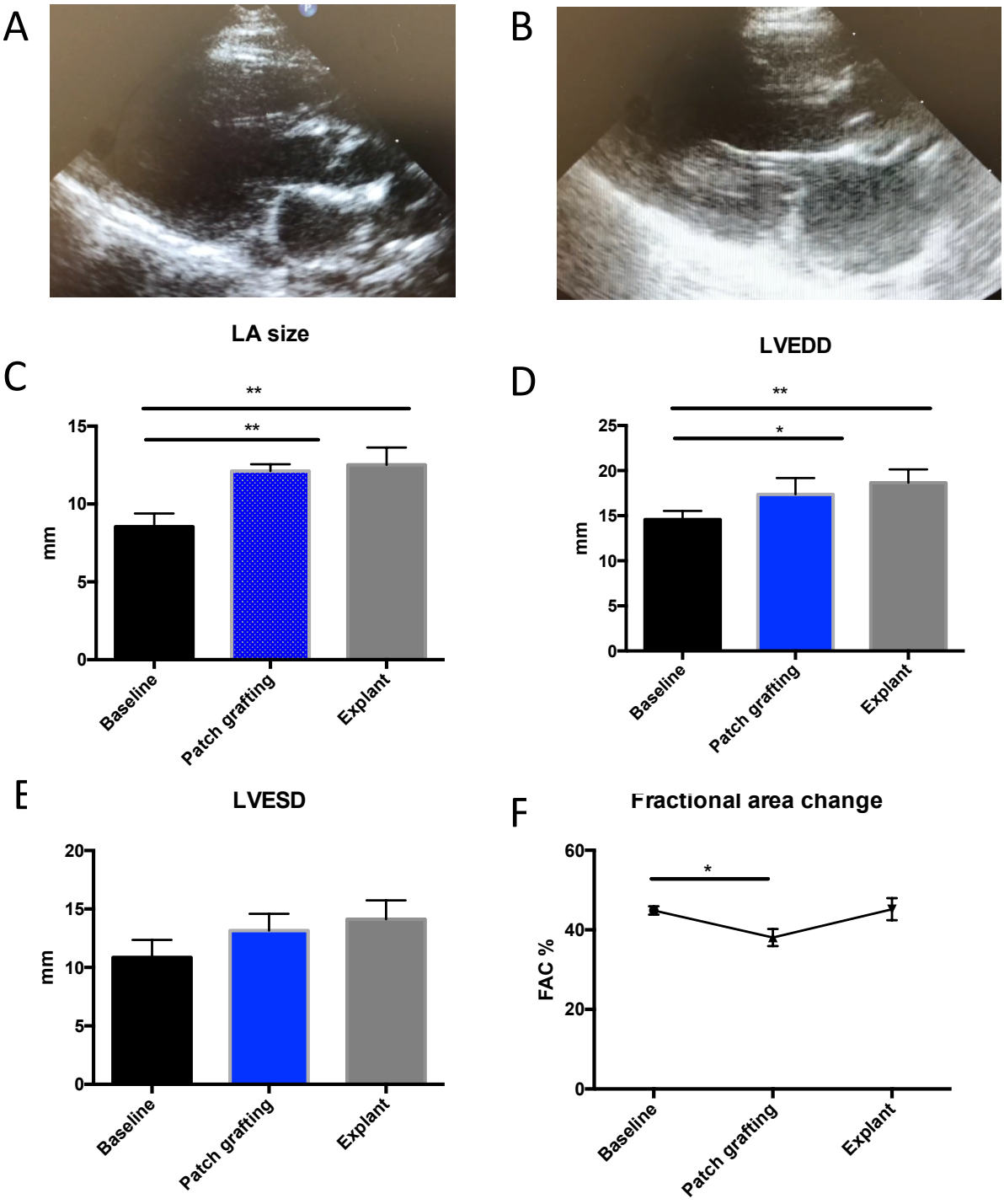



*Representative hematoxylin-eosin (H+E) and Picro Sirius Red (PSR) images of serial sections (at 3mm intervals) of 2 representative animals explanted >28 days post 2nd surgery. PSR – orange stain, areas of infarction (collagen staining) appear red. H+E – purple stain, corresponding areas of infarction are hypolucent indicating areas devoid of myocytes.*

### 4.5 Echocardiographic evaluation of infarct size

All 5 animals had intraoperative ECG evidence of ST elevation and macroscopic visualisation. Figure 4-5A is a representative image of a parasternal long axis view of an animal's baseline recording. Figure 4-5B is a representative example of the same heart two months after the initial surgery and prior to explantation. As can be seen the left atrial size has enlarged significantly which is a marker of chronic left ventricular end diastolic pressure overload. Mitral regurgitation due to papillary muscle rupture could show the same picture but no evidence of mitral regurgitation was found in any animal on colour echocardiography. This pattern was seen in the overall analysis, since the mean left atrial diameter increased from baseline (8.6 ± 0.4mm) to one month (12.1 ± 0.1mm; $p<0.005$ vs baseline) and then was relatively static from one month to explant (12.5 ± 0.4mm; $p<0.005$ vs baseline; Figure 4-5C). The increases in left atrial size were mirrored with increases in left ventricular end diastolic diameter from baseline (14.6 ± 0.4mm) to one month (17.4 ± 0.8mm; $p<0.05$ vs baseline) and from one month to explant (18.7 ± 0.6mm, $p<0.005$ vs baseline; Figure 4-5D). Left ventricular end systolic diameter also increased during the study period (10.9 ± 0.6mm [baseline]; 13.2 ± 0.6mm [one month]; 14.2 ± 0.7mm [explant], $p=0.03$ overall; post hoc test p=ns; Figure 4-5E). Regarding function, fractional area change decreased from baseline (44.8 ± 1.1% [baseline] to 38.1 ± 2.1% [1 month], $p<0.05$), but then increased post fibrin patch to explant (45.2 ± 2.8%; Figure 4-5F, p=ns). Putting together these results, we were able to show the remodelling process that occurs post myocardial infarction, the feasibility of performing two thoracotomies, grafting of a fibrin patch and toleration of immunosuppression treatment.

**Figure 4-5: Heart failure echocardiographic data**




*A) 2D-echo in parasternal long axis view of a rabbit heart at baseline and B) just prior to explantation. Bar chart of left atrial (LA) diameter (C); Left ventricular end diastolic diameter (LVEDD) (D); left ventricular end systolic diameter (LVESD) (E), fractional area change (F) at baseline, second thoracotomy and explant.*

## 4.6 Discussion

The main findings of chapter 4 of this thesis are the successful transfer, validation and optimisation of the rabbit myocardial infarction model from Glasgow university and the development and feasibility testing of a rabbit heart failure model using cell free fibrin based EHT patches.

### Why the rabbit model?

Extensive preclinical testing of human stem cell grafting is essential to assess for safety and efficacy prior to phase I clinical trials. However, the in-vivo assessment of human stem cell transplantation in preclinical animal models has major limitations, including the xenograft nature and lack of clinical similarities of most preclinical myocardial infarction / heart failure models. However, animal PSC-CM equivalents will never be transplanted into humans or ever be the final therapeutic product. In the cardiac regenerative medicine field, the choice of animal, and whether small or large animal has numerous caveats. For example, the excitation-contraction coupling of myocytes is wide ranging between species, with rats having hearts rates 5-10 times the rates of humans, and therefore assessing integration with hiPSC-CM with lower basal beating rates is not ideal and could be problematic.(Van Laake *et al.*, 2008) In murine studies, hESC-CM grafts form a fibrous tissue layer, and cells which do couple have been reported to die by calcium overload.(Van Laake *et al.*, 2010) The fasting basal beating rates in small animals model may also overdrive any ectopic pacemaker activity and therefore may not be a fair representation of what will happen in the first translational studies.(Chong and Murry, 2014) Macaques have numerous human similarities, and feasibility has been reported with PSC-CM (intramyocardial injection), albeit with the development of ventricular arrhythmia, but

ethical issues and expense limits use in the United Kingdom.(Chong *et al.*, 2014; Liu *et al.*, 2018) Pig models, have many advantages including similar size hearts to human and similar coronary circulation, but expense and logistic difficulties means that they should be reserved for immediate preclinical testing.(Hughes *et al.*, 2015) Therefore, an intermediate model is needed to bridge the gap. A rabbit model was decided as suitable since it has numerous similarities to human myocardium and therefore very appropriate for engineered heart tissue grafting experiments.

For example, the human similarities include:

1) rabbit myocytes have similar mechanisms of repolarisation and action potential morphology;

2) β-myosin heavy chain is predominant in rabbits;

3) the sarcoplasmic reticulum contributes approximately 70% to calcium elimination and the Na+/Ca2+ exchanger contributes the remaining 30%;

4) the force frequency relation of myocardial contraction is positive.(Pogwizd and Bers, 2008)

Additionally, the rabbit heart failure/post myocardial infarction syndrome has human similarities with force-frequency relationship inversion, beta-adrenoceptor desensitisation, and histological evidence of residual transmural islands of cardiomyocytes tissue post myocardial infarction.(Ezzaher, el Houda Bouanani and Crozatier, 2017)(WALKER *et al.*, 2007)(Myles *et al.*, 2011)(N. *et al.*, 1990) In addition, unlike guinea-pig or dogs, which have extensive collateral circulation, the relative lack of collateral circulation enabled the creation an infarct of consistent size via marginal artery ligation.(Podesser *et al.*, 1997) The larger heart size is also more

appropriate for tissue engineering strategies than smaller animal models since the thicker ventricular wall will be differently affected by an epicardial graft as opposed to a very thin mouse ventricle.(Maxwell, Hearse and Yellon, 1987)

**Rabbit Myocardial Infarction Model Set up**

The rabbit model was set up at Imperial College after a period of training in one of our collaborating centres at Glasgow University. After successful training, purchase and set up of the required equipment including a Merlin ventilator, Zoll ex-clinical grade defibrillator, endotracheal tubes and set up of the rabbit housing pens, the first procedure was performed supervised by the animal technician from Glasgow university at Imperial College. Over the course of this PhD several refinements occurred that developed the procedure further and improved outcome. For example, the introduction of anaesthesia monitoring sheets, which enabled detailed periprocedural observations to be recorded and facilitate appropriate anaesthesia titrations intraoperatively. The introduction of rabbit V-gel laryngeal masks instead of endotracheal tube intubation using human paediatric equipment also facilitated intubation. Endotracheal intubation caused laryngeal trauma and in one animal the procedure had to be aborted due to failed intubation; V-gels were much less invasive and caused minimal damage to the trachea / oral region and no procedures were aborted due to lack of intubation. The introduction of end tidal $CO_2$ monitoring equipment facilitated the titration of anaesthesia and also helped confirm that appropriate cardiac massage was carried out when needed. All of these refinements lead to the successful initiation of the model and a mortality rate similar to that observed at Glasgow university.

The first myocardial infarction experiments underwent ligation only (no EHT attached to epicardial surface) and in some hearts, data were obtained from ex-vivo conductive polymer experiments. Confirmation of infarct was ascertained intraoperatively and postoperatively. Intraoperatively by the presence of ST elevation on continuous ECG monitoring and visualised macroscopically after ligation as discoloured tissue. Postoperative confirmation was by non-invasive echocardiography and histological staining. Further ways to assess infarct confirmation could have included serial blood troponin measurements or intraoperative left ventricular pressure measurements. Troponin measurements change over time and serial measurements in the perioperative period would have caused additional stress to the animal when recovering from a severe protocol operation. Cardiac MRI would have been a useful tool to assess infarct size, especially using late gadolinium enhancement, but the logistics of transporting the animal in the periprocedural period, the additional stress to the animal and the lack of availability of an MRI scanner at Imperial College precluded its use. In addition, the use of MRI is significantly more expensive than echocardiography.

The relative lack of collateral circulation as well as the consistent anatomy between animals meant that a reproducible infarct size was possible. The marginal artery was ligated, as opposed to the left anterior descending in rodents and mice, since the LAD is difficult to visualise in rabbits, tends to be deep within muscle and also covered by epicardial fat. The marginal artery on the other hand tends to be relatively thick and easily visualised on the epicardial surface. This meant that the ideal ligation site could be chosen prior to suturing (with 4.0 Prolene sutures).(Podesser *et al.*, 1997)

The choice of permanent ligation over an ischaemia-reperfusion model was decided since permanent ligation creates a transmural infarct with robust remodelling response and large infarct size.(Lindsey *et al.*, 2018) The critical aspects of performing permanent ligation include the fact that it may not be a clinically relevant model since timely reperfusion for acute myocardial infarction is performed in most hospitals in the Western world at the present time. With the advent of stenting and primary percutaneous coronary intervention, only 15-20% do not undergo timely reperfusion.(Lindsey *et al.*, 2018) However, since the first patients to be treated with the patch would have end stage heart failure (requiring open thoracotomy) as opposed to myocardial infarction, the ischaemia reperfusion model was not a priority.

The majority of infarcts were in the mild to moderate category. This was because larger infarcts cause more intraoperative mortality due to the inability to restore sinus rhythm after ventricular fibrillation.(Coker, 1989) Several measures were undertaken intraoperatively to improve outcome and mitigate risk. These included pharmacological methods by administering Quinidine gluconate salt via an ear vein. The main mechanism of ventricular fibrillation in our cohort of rabbit was due to ischaemia induced ventricular ectopics, which then caused the initiation of ventricular fibrillation when the ectopic fell on the  T wave (R on T phenomenon). This was noticed on continuous ECG recording. Quinidine gluconate is a class I antiarrhythmic which prolongs the action potential and effective refractory period, and is especially useful in reducing the incidence of ischaemia induced ventricular ectopics.(Coker, 1989) If ventricular fibrillation occurred, immediate cardiac massage was performed, which in some incidences reverted the arrhythmia back to sinus rhythm. If persistent VF occurred a DC shock of 3J was administered with minimal interruption of cardiac

massage. End tidal $CO_2$ monitoring was extremely helpful during this point since the effectiveness of cardiac massage was evidenced by a relatively normal end tidal $CO_2$ output. It was also noticed that the precarious periprocedural time was 25-30 minutes after coronary artery ligation. If the animal was in sinus rhythm after 25-30 minutes, no further instances of ventricular fibrillation occurred and the mortality rate in our cohort was low with only 2 animals dying (out of 13) after leaving the operating suite.

Other groups have reported the rabbit model of myocardial infarction, with a similar methodology to the one reported in this model.(Tan *et al.*, 2017) For example, Tan et al reported infarct methodology similar to ours using the marginal artery (OM) but instead coagulated the artery using a monopolar GD350-D high-frequency electric knife. (Tan *et al.*, 2017) This may reduce blood loss, however coagulation is permanent. By contrast, in our model, if the infarct was too large or small in our model, the suture could be removed and placed at another location more suitable. Additionally in the study by Tan et al, surgery was performed (on 35 rabbits) via a left parasternal approach instead of entering via the 4th intercostal space (in our model). The theoretical benefit of this approach is that the pleura is well protected and the risk of pneumothorax lower. In the intercostal approach the lung is purposely deflated to visualise the heart. We only had one mortality due to possible lung haemorrhage however. A downside of their parasternal approach is the left ventricle is not well visualised. Out of 35 animals, 2 died during anaesthesia, leaving 23 in their OM branch group and 10 in the sham group. Five animals died in the OM group giving a mortality rate of 21.7%. 2 died from intraoperatively due to cardiogenic shock, 2 due to VF immediately post operatively and 1 of unknown causes 48 hours

after surgery. There was a significant reduction in LVEF from baseline to 4 weeks after OM branch coagulation from 53% ± 4.9% to 33% ± 3.5% after 4 weeks (**P<0.01). The size of the infarcts as determined by serial sectioning of Masson's trichome staining 32.5 ± 4.9% (n=18) and moderate in size.(Tan *et al.*, 2017) Other groups have attempted LAD ligation but it is essentially done blind to LAD position and the mortality rate is very high. (Isorni *et al.*, 2015) (Tan *et al.*, 2017)

A downside of our approach is the potential harm associated with a thoracotomy and the pain and distress by invasive surgery. To that extent, a minimally invasive way of developing an infarct has been investigated.(Isorni et al., 2015) This has the ability to more closely resemble the infarct situation that is seen in humans, which is caused by plaque rupture and embolization of atherosclerotic debris or thrombosis in the coronary microcirculation. Furthermore, the integrity of the surrounding structures including the pericardium is preserved, which is also important in the healing process post myocardial infarction. In contrast, the closed surgical technique has limitations including the use of relatively expensive interventional radiology equipment and expertise to create an infarct from within the heart, and sometimes it is difficult to create reliable infarcts by precisely controlling the location and duration of ischaemia. Various minimally invasive ways have been reported, ranging from free coils (n=4), interlocking coils (n=4), balloon occlusion (n= 4), release of a thrombogenic sponge (n= 4), and injection of alcohol (n=8).(Isorni et al., 2015) Procedures were performed on relatively large rabbits (3.8kg – 4.4kg) and vascular access was performed via the right carotid artery. Overall feasibility was shown with varying success with 16 animals (out of 24) surviving to 3 weeks. The most reliable method was alcohol injection with transmural infarcts achieved in all animals and 6 out of 8

animals surviving to 3 weeks and a reduction in ejection fraction from 58.3 ± 2.6 to 47.0 ± 2.4% (P<0.001). (Isorni *et al.*, 2015) However, this produces an infarct which does not have the same epi/endocardial gradient and myocyte islands as the ligation, and therefore is less congruent with the human scar.

**Heart failure model**

The preclinical heart failure model for testing is critical since EHT in its present form requires open chest application and attachment to the epicardial surface, and therefore the first-in-human patients that will be eligible for treatment will be those undergoing traditional open chest (sternotomy) cardiac surgery. The current gold standard treatment modality for managing myocardial infarction is primary percutaneous coronary intervention which is performed by a minimally invasive route, either via the wrist (radial artery) or via the groin (femoral artery) and involves the insertion of a metallic stent delivered from inside the artery via a metal wire inside the coronary artery to open the blockage and restore flow to the infarcted artery. Therefore, the prerequisite for open surgical attachment of the EHT preclude the use of EHT in its present form for the treatment of myocardial infarction. Research (Harding / Stevens labs) is ongoing regarding the development of a new delivery route that could enable minimally invasive delivery routes in the future.

The first surgery was exactly the same as the myocardial infarction model via the 4th intercostal space. It was then decided to perform the second surgery via the 5th intercostal space. Determining the time point, was based partly on our project license – which stated 2 weeks between surgeries and advice from our collaborator in Glasgow regarding optical mapping studies. We decided to wait at least 4 weeks to

allow the animal to recover fully and the infarct to mature. Five days prior to the second surgery, animals were treated with immunosuppression, and during the second surgery a sham patch sutured to the epicardial surface. This was to assess feasibility of EHT grafting using the model. The patch was successfully attached to the surface and all animals survived to explant. However on explantation, 3 animals had extensive adhesions limiting the future potential integration of any grafted EHT with the host and of any ex-vivo optical mapping studies performed post grafting. It is important to note that there was a recovery of function overall in this group. Possible reasons could include the effect of the fibrin patch, the size of the infarct and the remodelling (compensatory hypertrophy) process that occurs in the months post myocardial infarction.(Konermann *et al.*, 1997) The recovery of ventricular function that we observed most likely would have been limited by creating larger infarcts initially. If we had ligated the OM branch more proximally, the infarct size would have been larger, with a greater reduction in ventricular function. Greater scar tissue would equate to less viable myocardium and therefore less compensatory hypertrophy during the remodelling process. This of course would need to be balanced against the increase in perioperatively mortality observed with creating larger infarcts.

Notably, in other EHT grafting studies, relatively shorter time periods between the creation of the infarct and grafting have been reported. For example, the Eschenhagen group grafted EHTs 7 days post myocardial infarction (induced by cryoinjury with an aluminium probe cooled in liquid nitrogen).(Weinberger *et al.*, 2016) In a landmark study involving the administration of 750 million hESC-CMs to non-human primates, an ischaemia reperfusion model was used (intra coronary

balloon occlusion for 3 hours), followed by intramyocardial injection 2 weeks afterwards. The fact that the first surgery was done in a minimally invasive way meant that only a single thoracotomy was needed to administer the cells.(Liu *et al.*, 2018) In a recent study involving swine, a myocardial infarction model was used, by temporary ligating the 1st and 2nd diagonal arteries for 60 minutes, upon which the grafts (EHTs) were then placed.(Gao *et al.*, 2018) However, all of these models have limitations from the clinical picture, since the human heart failure syndrome is a progressive condition and in many instances is the result of chronic pressure overload due to a previous ischaemic event. Therefore, some preclinical models in rat and mice have investigated the use of ischaemia reperfusion followed by aortic banding to induce a chronic increase in afterload to therefore develop heart failure in the most clinically relevant way.(Schwarzer, 2015) This method in a rabbit would be significantly more complex and time consuming as it could take several months to develop heart failure.

The development of a closed chest myocardial infarction model is particularly attractive for EHT grafting experiments due to the preservation of the surrounding tissues, particularly the pericardium, therefore minimising the development of adhesions and facilitating EHT grafting. Future work is ongoing at our collaborating centre in Glasgow with the aim of using interventional radiology equipment and the use of intracoronary balloons delivered via the carotid artery to occlude the coronary vessel.

**Summary**

The results of this chapter have validated both a preclinical model of myocardial

infarction and double thoracotomy model with an acceptable morbidity and mortality rate. The infarcts created were of mild to moderate size, created by permanent ligation at the mid ventricle level, and formed a basis for EHT grafting experiments. Feasibility of a double thoracotomy model was also shown, albeit with the development of significant adhesions in 3 out of 5 animals. The fact that fractional area change improved with the sham patch in the double thoracotomy arm may be due to the relatively small size of the infarcts, the remodelling process that occurs post myocardial infarction or that the sham patch may have provided some structural support to the infarcted ventricle. It must be stated that no preclinical model will ever be able to fully recreate the clinical situation, since patients often suffer from the effects of multiple long term comorbidities including hypertension and diabetes. Future, preclinical rabbit work which is ongoing with our collaborating centres will continue develop minimally invasive ways of creating the infarct to minimise the effects of adhesions and the effects of an additional thoracotomy. Additional future work could include an ischaemia reperfusion model, followed by aortic banding to induce chronic pressure overload that may more reliably reflect the human clinical syndrome of heart failure that is most common nowadays.

# Chapter 5: Preclinical testing of upscaled engineered heart tissue

## Introduction

This result chapter will describe the development of the rabbit in-vivo EHT grafting model and the results of grafting experiments onto control and infarcted hearts. The rabbit was chosen since it was a suitable intermediate between small (rat and mice) and larger animal models including macaque and swine. Several important steps needed to be developed and optimised including: 1) a reliable method of attaching the EHT to the heart; 2) an adequate immunosuppression protocol and; 3) a rabbit specific immunohistochemistry staining protocol. Glue was used initially used to attach EHTs because it was thought that it was less invasive but initial experiments revealed a lack of troponin cell retention. The final method was using fine Prolene sutures to directly attach the patch to the epicardial surface. Once a reliable protocol was devised, feasibility of EHT grafting was evaluated by a variety of methods including graft troponin T cell retention and vascularisation ($CD31/mm^2$) assessed at serial time points up to one month. These experiments were primarily performed on control hearts. Efficacy was then evaluated by assessing change in left ventricular function post hiPSC-CM EHT grafting onto infarcted hearts. Echocardiography was the modality used to assess for improvements in ventricular function over appropriate controls (myocardial infarction hearts grafted with fibrin cell free patches). Safety was also assessed by evaluating arrhythmia formation, both in-vivo using subcutaneous telemetry devices to check spontaneous arrhythmia burden and ex-vivo to check for propensity for arrhythmia formation after performing programmed electrical stimulation protocols on hearts perfused via Langendorff apparatus.

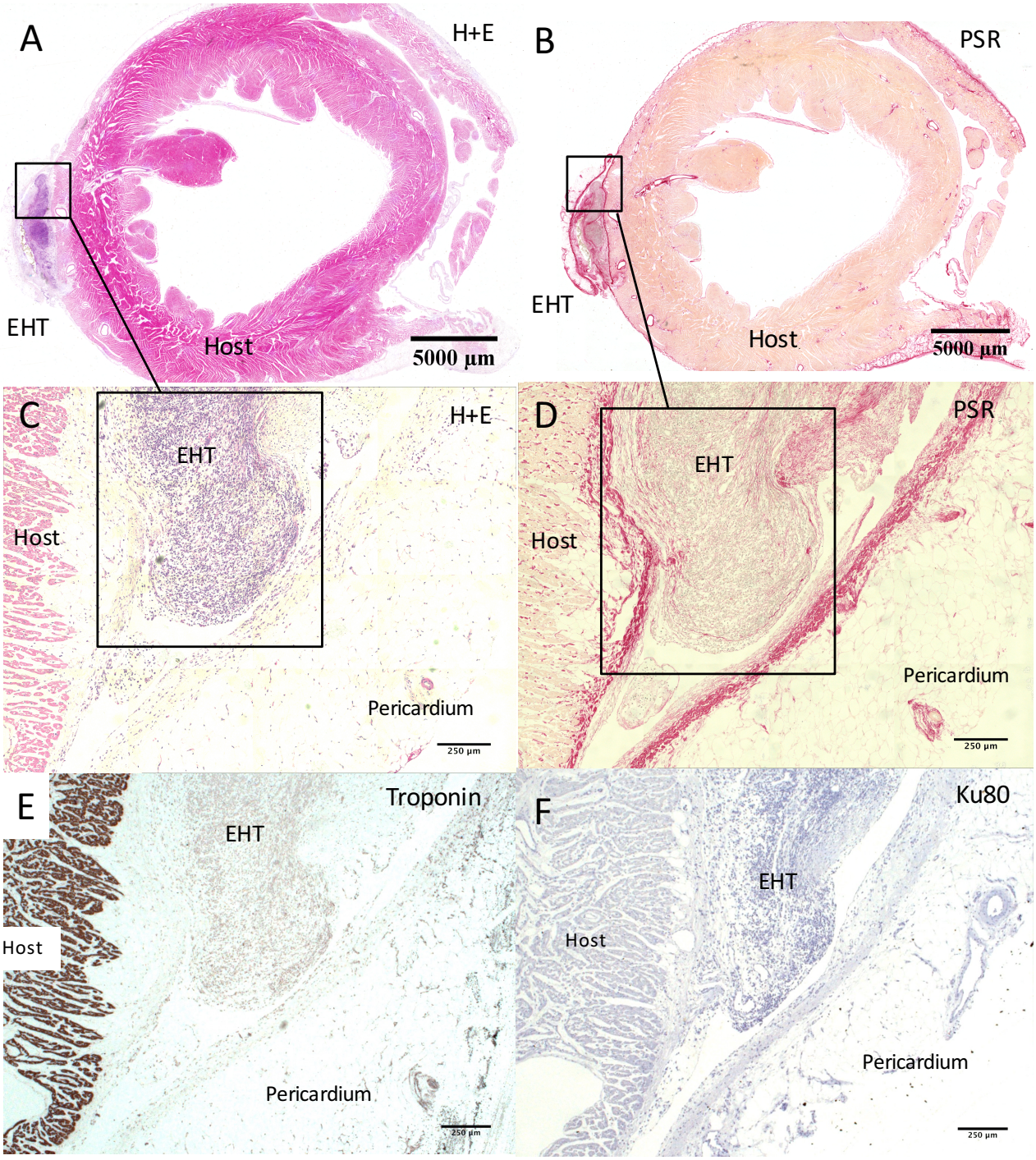
### 5.1 Development of EHT in-vivo grafting model

In the first experiments, the EHTs were attached to the epicardial surface of the heart using surgical Histoacryl glue. The idea behind using tissue adhesive was to facilitate attachment and minimise the injury caused by suturing onto myocardium. Although the method of fixation was relatively easy and the EHT was clearly attached to the epicardial surface after placement, after explant at one week there was no macroscopic evidence of the EHT present, which was also confirmed by antibody staining. It was thought the glue may create a barrier between the EHT and the host, or even encapsulate the graft so that nutrients and oxygen could not reach the cells in the graft. The glue also interfered with ex-vivo optical mapping experiments.

Therefore, method of fixation was switched to suturing at the 4 corners of the EHT (7.0 prolene). This caused some local damage to the area, but was a feasible method of attachment. At one week post grafting, after explant, the EHT was macroscopically visible on the surface of the ventricle. Histology staining with H+E (Figure 5-1A,C) clearly revealed evidence of a structure attached to the surface of the ventricle that was consistent with the macroscopic evidence of the EHT. On magnification, the structure was packed with nuclei (Figure 5-1C). The corresponding serial section stained with PSR revealed evidence of sparse collagenous material as evidenced by characteristic red staining (Figure 5-1B,D). Wax embedded serial sections were then stained for troponin and a human specific marker Ku80 since the cardiomyocytes used to create the EHT were human in origin. As can be seen in Figure 5-1E, the host was clearly stained brown indicating positive troponin staining. The EHT however was troponin negative. This was also

confirmed with the ku80 stain being negative throughout the host (as expected) and EHT (Figure 5-1F). The fact that the structure was relatively well preserved, the presence of relatively dense packed nuclei on H+E staining, and the lack of troponin and human specific nuclear marker cells on staining, strongly implicated an inflammatory process had occurred to the EHT. Due to the lack of infection, it was hypothesised that an immune mediated cellular rejection process had occurred and therefore the next steps were to optimise the immunosuppression protocol for subsequent grafting experiments.

**Figure 5-1: Preliminary in-vivo grafting results**



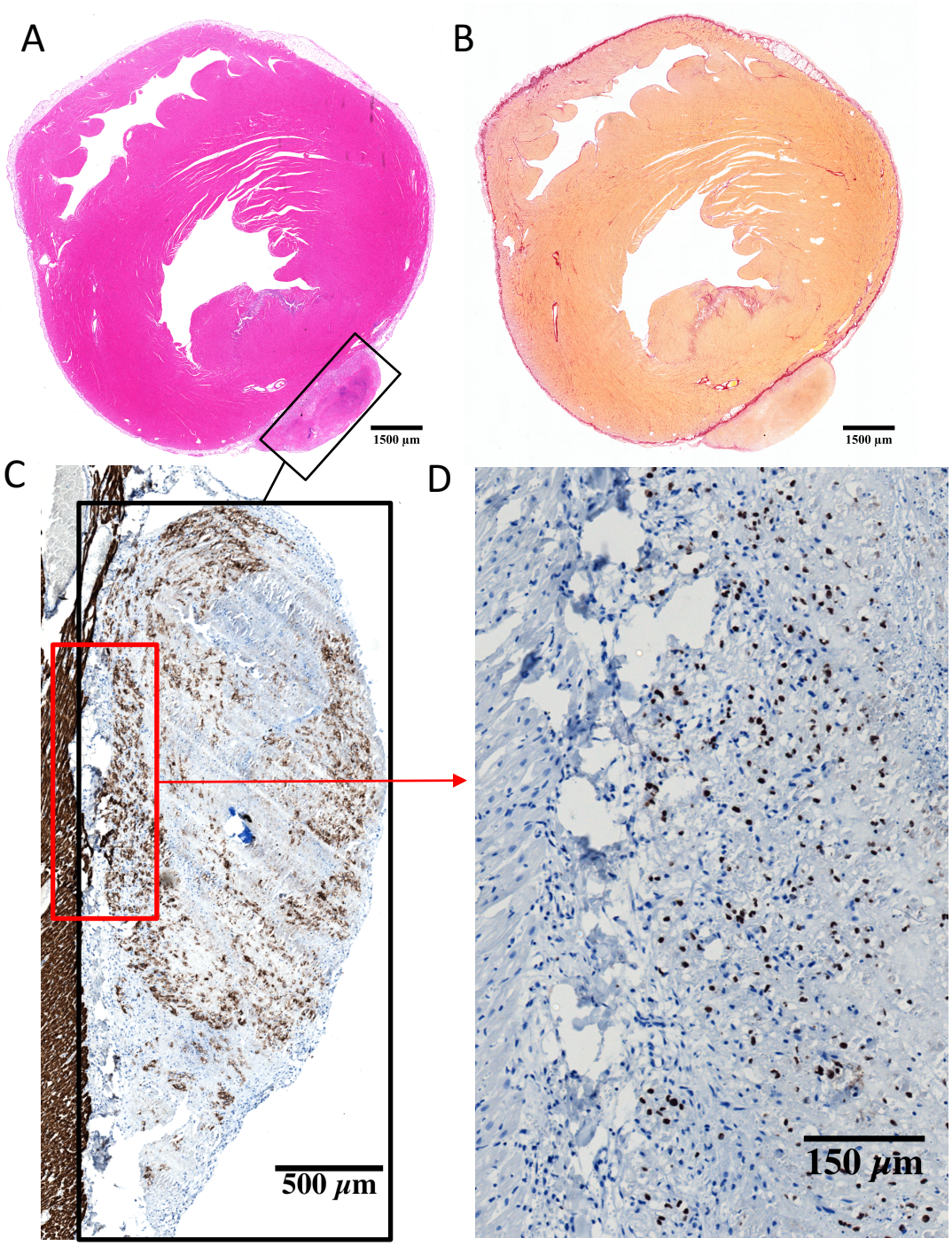

*A) 5x H+E stain axial section of rabbit heart. Small black rectangular box indicates an area of EHT that is magnified in "C". B) Corresponding serial section of rabbit / EHT stained with PSR; C) Magnified (40x) of black rectangle in A; D) Magnified PSR of black rectangle in B; E) Troponin stained section black rectangle in A/C showing positive staining in host but absence in graft. E) Ku80 staining of same region.*

### 5.2 Revised immunosuppression protocol

The first grafting experiments used ciclosporin (5mg / kg per day starting 2 days prior) and methylprednisolone (1.5mg/kg per day starting 2 days prior). In subsequent experiments the dose of ciclosporin was increased to 10mg, and since it was an oral preparation was administered 5 days prior to surgery. Additionally, the methylprednisolone dose was increased to 2mg/kg per day.

The newer protocol was then tested again on a control animal, with heart explant one week after grafting. After fixation and H+E staining it was evident that there was an EHT attached to the epicardial surface (Figure 5-2A). In contrast to Figure 5-1A, the graft was a similar stain to the host's ventricle instead of the darker colour (packed nuclei) of figure 5-1A. Additionally, PSR staining (Figure 5-2B) revealed a lower concentration of collagen (less red staining) when compared to Figure 5-1B. As can be seen in figure 5-2C there was evidence of troponin positive cells in the graft. In addition, the human specific marker ku80 revealed that the cells were human in origin (Figure 5-2D). Notably, the centre of the EHT was relatively devoid of troponin staining with a preferential location of the borderzone or surface closest to the epicardium. Nevertheless, we were able to show sustained retention post EHT grafting based on the new revised protocol of grating with sutures and high dose immunosuppression. The final part of the optimisation protocol involved the use of a pro survival cocktail,(Laflamme *et al.*, 2007) that was administered to the EHT media both 24 hours and 1 hour prior to grafting to shield the cells from the hypoxia due to lack of preformed blood vessel network in the graft and also to protect against cytokine damage.

**Figure 5-2: Revised in-vivo grafting protocol**




*A) H+E stained of 5x axial section of rabbit heart with EHT attached to epicardial surface (EHT is outlined approximately by the black box. B) PSR staining of rabbit heart and EHT. C) 20x magnification image of EHT. Both the host and the EHT contain troponin positive cells (brown stain). D) 40x zoomed in image of serial section of EHT. Numerous ku80 positive cells are present in the graft.*

### 5.3 EHTs become vascularised

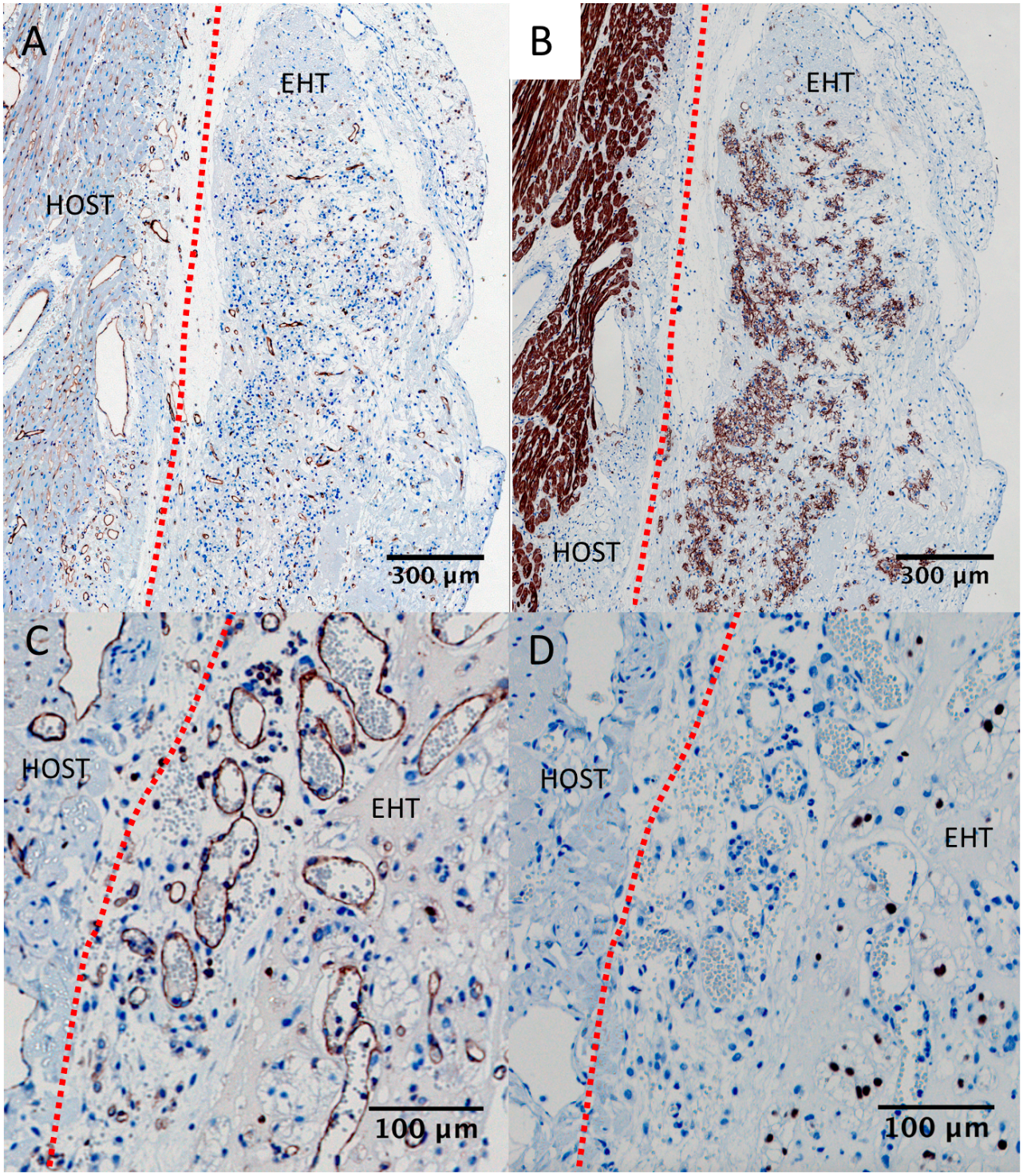
The development of the modified in-vivo grafting protocol resulted in sustained human troponin positive cell retention in the EHT graft and was an important step in the project. Several important observations were noticed that needed to be explored including: 1) how did the cells survive without an preformed in-vitro blood vessel network?; 2) did the grafts become vascularised in-vivo?; and 3) why was there an area in the centre of the graft relatively devoid of troponin cells?

To ascertain whether the grafts became vascularised in-vivo, CD31 positive staining was carried out on day 0 controls and 2 week animals. Day 0 controls showed no evidence of CD31 positive vessel formation. This was expected since only hiPSC-CMs were used in the master mix during EHT manufacture (98.3% GCamp line [12 wells from 4 differentiations], courtesy Daphne Pantou MSc student). In contrast, CD31 staining of EHTs that had been grafted in-vivo 2 weeks prior (Figure 5-3A) revealed that CD31 positive vessels were present throughout the EHT. The corresponding serial section in Figure 5-3B stained for troponin T showed that troponin positive cells were present throughout the graft. In contrast, the EHT centre was relatively devoid of troponin T in Fig 5-2C. This finding may have been due to the pro-survival cocktail was administered in 5-3B (but not in 5-2C), but this was not scientifically assessed since the effectiveness of pro-survival cocktail has previously been reported. (Laflamme *et al.*, 2007)

As can be seen in a higher magnification image from another animal (also explanted after 2 weeks; Figure 5-3C), numerous red blood cells were seen contained within the vessels. The next step was to ascertain whether the blood vessels were human

in origin or not (i.e. originating from the rabbit host). As can be seen in Figure 5-3D, the absence of the human specific ku80 marker present in the CD31 positive vessels, but present elsewhere in the graft thus confirmed the rabbit host origin of the vasculature. Therefore, data from this and the previous figure indicated that we could successfully graft hiPSC-CM EHTs onto a control heart of a rabbit, with sustained cellular retention in the graft and new vessel formation.

**Figure 5-3: EHT vascularisation**




*A) EHT attached to rabbit myocardium (20x magnification). Brown staining = CD31 positive; B) Serial section of A. Brown staining = troponin positive; C) EHT borderzone with host (63x). CD31 positive cells (brown); D) Serial section of C with Ku 80 (brown).*

### 5.4 Graft cellular retention tested at serial time points

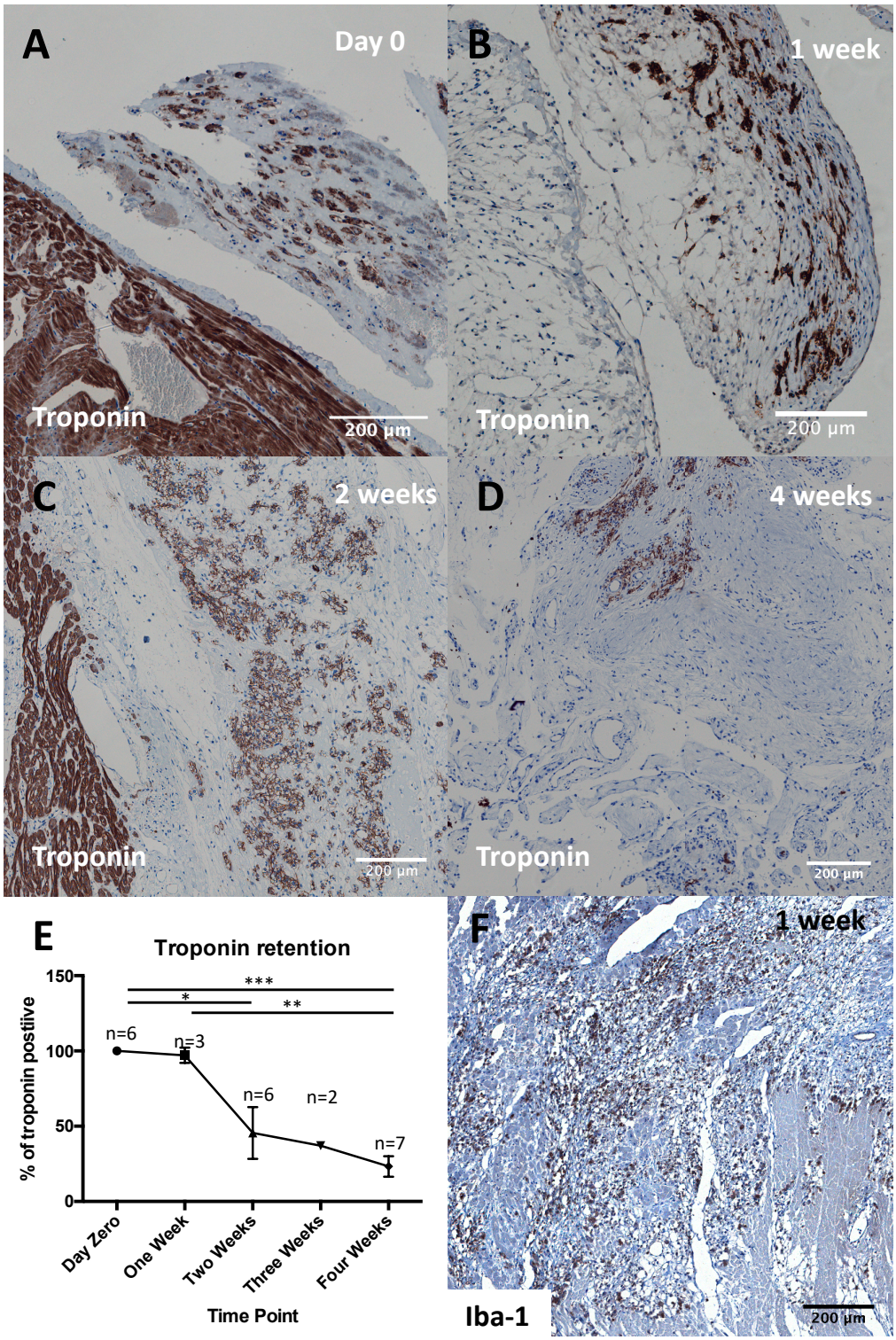
Since feasibility was successfully confirmed the next stage was to ascertain cell retention at longer time points since long term engraftment and replacement of lost muscle is one of the goals of using EHTs. Troponin retention was calculated using a custom made macro that analysed troponin T staining of grafts at serial time points at weekly intervals up to 4 weeks (Full details in methods section 2.4.7). Data were expressed as a percentage of troponin positive cells in the graft relative to day 0 controls (n=6, representative image of day 0 in Figure 5-3A). At day 0, the percentage of troponin positive cells within the graft relative to normal rabbit myocardium was 24.6 ± 5.6% (n=6).

Representative images of grafts explanted from control hearts are shown at 1 week (Figure 5-4B), 2 weeks (Figure 5-4C) and 4 weeks (Figure 5-4D). As can be seen in figure 5-4E, there was a relative preservation of troponin positive cells in the grafts from day 0 to 1 week (97.1 ± 5.1%, n=3, p=ns). At 2 weeks, the fraction of troponin positive cells was significantly reduced relative to day 0 (45.5 ± 17.1%, $p<0.05$, n=6). At longer time points, it was found that there was a progressive reduction in troponin T retention from 2 – 4 weeks and a 4 weeks the percentage of positive cells in the graft was 23.3 ± 6.8% (n=7, $p<0.001$ relative to day 0).

The next step was to work out why there was a reduction of cardiomyocytes in the graft at time points later than 1 week. Preliminary data of Iba-1 staining on a subset of hearts revealed that there was a strong presence of macrophage cells in the graft at week 1 (n=1; Figure 5-4F) and 2 weeks (n=1) which could possibly indicate the immune mediated rejection of cells. By contrast, Iba-1 positive cells were sparse at

the 4 week time point when few troponin positive cells remained in the graft (n=1; data not shown). Additionally there were no Iba-1 positive cells in hearts that underwent sham patch grafting at 4 weeks (n=1; data not shown).

**Figure 5-4: Troponin T retention at serial time points**



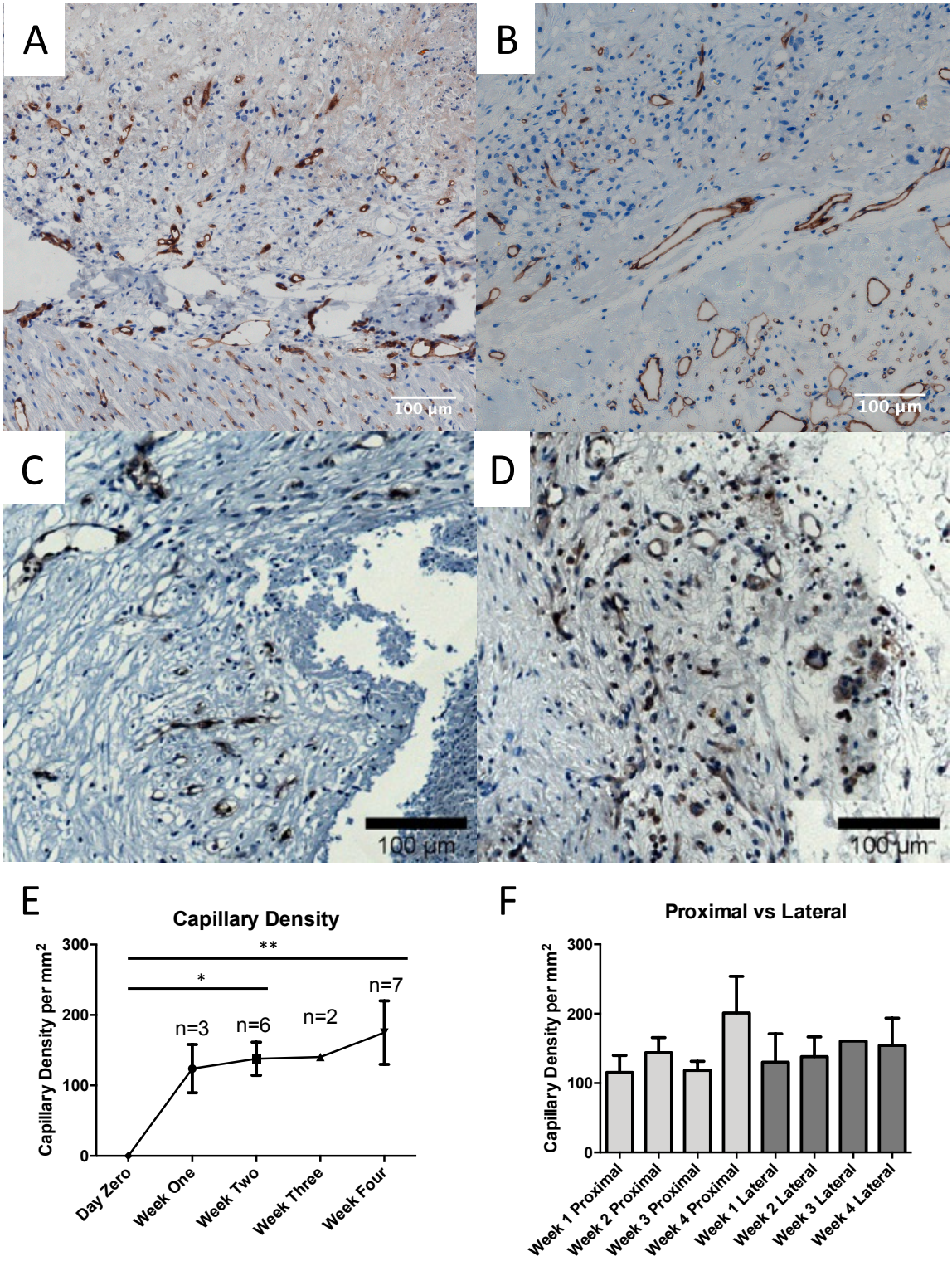

*Troponin T staining of graft at day 0 (A); 1 week (B); 2 weeks (C); 4 weeks (D). Graph of troponin T retention relative to day 0 (E). Iba-1 staining (brown) of EHT explanted at 1 week. All slides counterstained with haematoxylin (blue).*

### 5.5 Capillary density at serial time points

Since it was ascertained that the grafts became vascularised by the host and that troponin retention drops over time, it was critical to characterise the vascularisation process at serial time points up to one month (similar to troponin T retention experiments). Representative grafts of sections stained at serial time points are shown in Figures 5-5A-D (1 week - Figure 5-5A; 2 weeks - Figure 5-5B; 3 weeks - Figure 5-5C; and 4 weeks - Figure 5-5D). As can be seen in Figure 5-5D, the capillary density increased to 123.9 ± 34.3mm$^2$ at week 1 (n=3), and then 137.9 ± 23.5mm$^2$ at week 2 (n=6; $p<0.05$ relative to day 0). Capillary retention was then relative sustained and constant: from Week 3 capillary density 140.4 ± 35.4mm$^2$ (n=2) and week 4 density 175.1 ± 45.2mm$^2$ (n=7; $p<0.005$ relative to day 0).

Since the grafts were thicker and vascularised from the host, and there was evidence of a necrotic core in earlier grafting experiments, we decided to ascertain whether there were any differences between the inner and outer zones of the graft post grafting. This was calculated using a custom made macro (courtesy Mr Stephen Rothery). As per Figure 5-5F, there was no significant difference in the inner and outer zones in capillary density between any of the zones at all time points up to one month post grafting. (Week 1 proximal 115.4 ± 24.4mm$^2$ vs distal 130.1 ± 41.1mm$^2$; week 2 proximal 143.8 ± 21.8mm$^2$ vs distal 138.1 ± 28.6mm$^2$; week 3 proximal 118.4 ± 13.1mm$^2$ vs distal 160.6 ± 48.5mm$^2$; week 4 proximal 201.2 ± 52.7mm$^2$ vs distal 154.4 ± 39.2mm$^2$).

**Figure 5-5: Graft vascularisation over time**

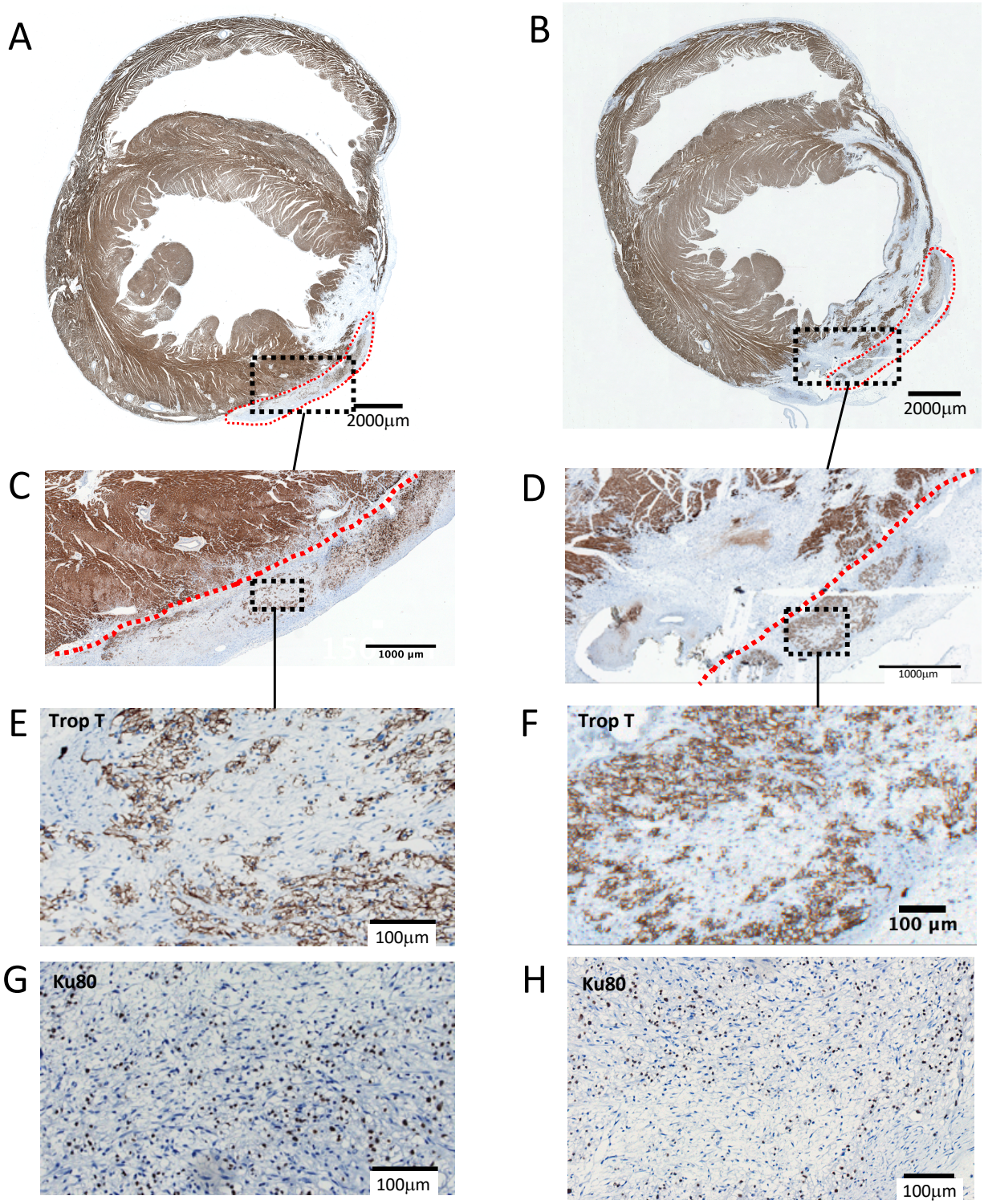



*CD31 staining at serial time points: 1 week (A); 2 weeks (B); 3 weeks (C); 4 weeks (D). Graph of EHT capillary density over time (E). Bar chart of capillary density of proximal and distal parts of EHT at serial time points (F).*

### 5.6 Feasibility of grafting onto infarcted hearts

The data obtained from the experiments presented in result sections 5.1-5.5 characterised several important findings from grafting experiments onto control hearts. One of the aims of this thesis was to test the efficacy of EHT grafting onto hearts that had undergone myocardial infarction, by ascertaining whether the graft improved ventricular function over a sham control group. Since the myocardial infarction model had been established and validated as per chapter 4 and feasibility of grafting was established onto control hearts, the next step was to test feasibility and efficacy of grafting onto infarcted hearts. It was decided that the patch would be sutured onto the epicardial surface during the index ligation procedure to avoid a second surgery. Determining the correct time point of EHT suturing post ligation was a balance between prolonging the anaesthetic time and the precarious 30 minute time point post ligation where there was a propensity for arrhythmia formation including ventricular fibrillation that could be exacerbated by additional suturing onto the epicardium. Therefore it was decided that no patch should be grafted less than 30 minutes post ligation and only if the animal was cardiovascularly stable. All patches were sutured onto the infarcted site and across the borderzone area. Feasibility of integration was first tested at earlier time points (1 - 2 weeks) with the aim of increasing to a 1 month time point. As can be seen in Figure 5-6 A-D, EHT was clearly seen attached to the heart (2 weeks post grafting) and troponin T staining was present in the graft (Figure 5-6E/F). Confirmation of human PSC-CMs in graft was shown by the presence of the human specific ku80 marker (Figure 5-6G and Figure 5-6H). The next steps were to ascertain any possible efficacy of grafting in terms of improving ventricular function when compared to control hearts.

**Figure 5-6: Feasibility of grafting onto infarcted hearts**




*A/B) Axial sections (5x) of infarcted heart stained with troponin and counted stained with haematoxylin. EHT attached to epicardial surface and outlined with red dotted lines. Small black rectangle indicates a section of the EHT attached to the epicardial*

*surface of the left ventricle and C/D) show the zoomed image of the rectangle stained with troponin T. E/F) Higher magnification of black rectangle shown in C/D. G/H) Ku80 staining of serial section of same black rectangle area (C/D) indicated numerous nuclei stained positive of ku80 (human specific nuclear marker).*

### 5.7 EHTs improve ventricular function

Echocardiography was the prime modality used to assess for the efficacy of EHT grafting in infarcted hearts and echocardiographic analysis was performed by an experienced cardiologist (MS) blinded to treatment arm. To accurately assess for any possible improvement in ventricular function, animals in the control group underwent thoracotomy and fibrin patch (cell free EHT patch) attachment using the same suturing method used with hiPSC-CM EHT. In total 14 animals underwent the study (n=7 EHT, n=7 sham patch grafting) and all animals survived to explant.

Looking at the group as a whole, as can be seen in Figure 5-7C there was a significant improvement in function in infarcted hearts that underwent EHT patch grafting (n=7) over sham patch grafting (n=7; absolute difference of 10.04 ± 3.1% fractional area change, $P<0.005$). In other words, the ejection fraction increased from 39.9 ± 2.6% to 47.4 ± 1.6% ($P<0.05$) in the treatment arm, whilst the ejection fraction was relatively static in the control arm (37.6 ± 1.8% [post ligation] to 37.4 ± 2.4% [explant], p=ns). A representative echocardiographic short axis view image (end systole) during the index procedure (ligation + patch) is shown in figure 5-7A. An echocardiographic image of the same animal is shown at one month in Figure 5-7B. The fractional area change increase in that animal was from 32.8% post ligation to 45.7% at explant (one month).

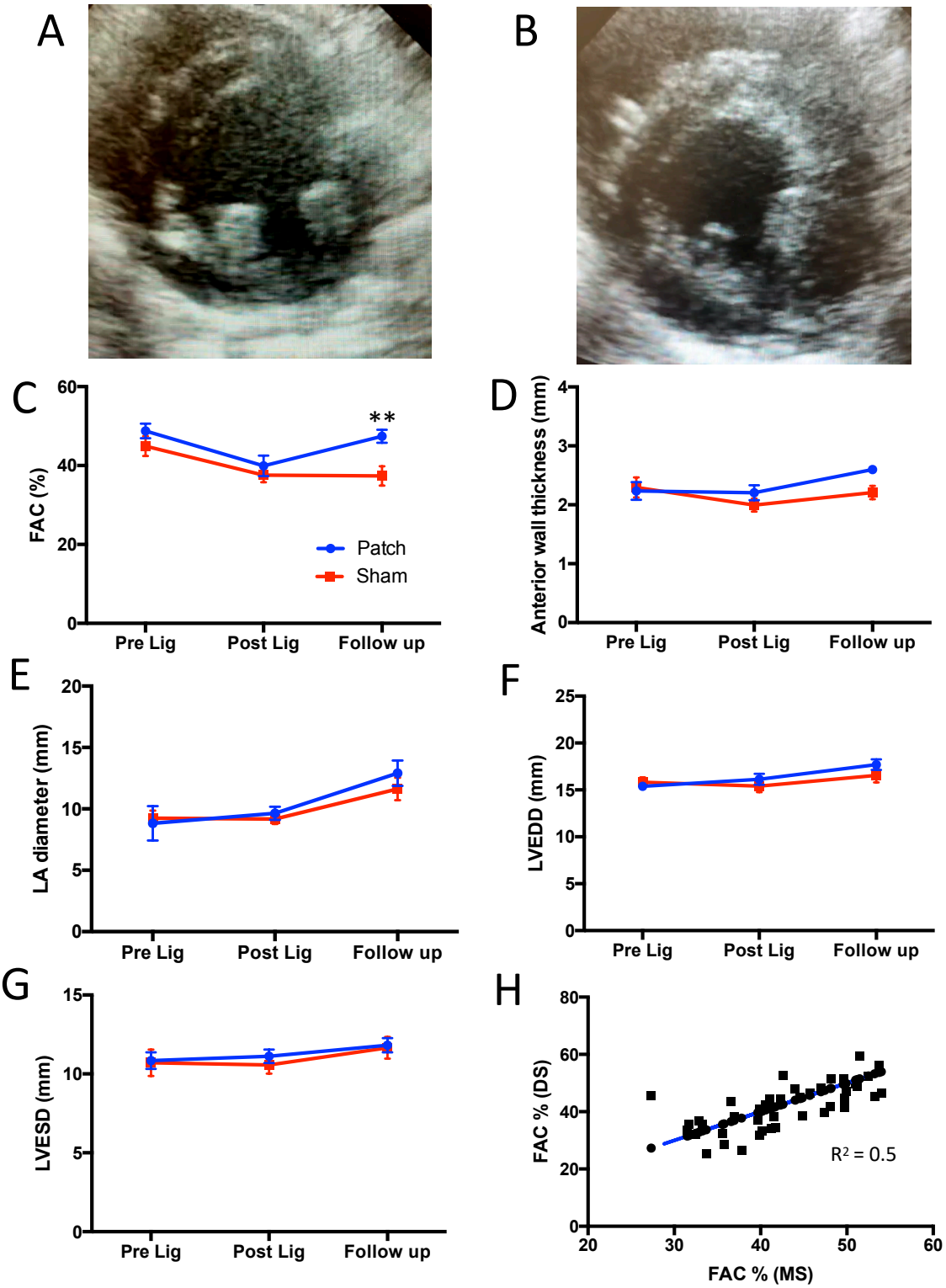
Regarding other parameters, there was a trend towards an improvement in left anterior wall thickness in the animals that underwent EHT grafting (2.2 ± 0.1mm [post ligation] vs 2.6 ± 0.1mm [explant]; p=0.057; Figure 5-7D) and a significant improvement in those that underwent sham patch grafting (2.0 ± 0.1mm [post

ligation] vs 2.2 ± 0.1mm [explant]; p=0.03; Figure 5-7D).

There were no significant differences in left atrial diameter (12.9 ± 1.0mm [patch] vs 11.6 ± 0.9mm [sham]; p=ns; Figure 5-7E), LVEDD (17.7 ± 0.6 cm [patch] vs 16.6 ± 0.8 cm [sham], p=ns; Figure 5-7F) and LVESD (11.8 ± 0.4cm [patch] vs 11.7 ± 0.7cm [sham], p=ns; Figure 5-7G) between EHT and sham control arms at the time of explant.

To ascertain the reliability of measurements, a second experienced preclinical imaging expert (DS) also blinded to treatment allocation measured the assessment and a correlation graph is shown in figure 5-7H. The $r^2$ value was 0.5 indicating good correlation between measurements and therefore confirming the validity of our analysis (Figure 5-7H).

**Figure 5-7: EHTs improve left ventricular function**




*A) Parasternal short axis view of infarcted heart post ligation (end systole); B) Same heart in same view 1 month post grafting (parasternal short axis; end systole). C-G) Baseline (pre ligation); post ligation and at follow-up graphs of: C) Fractional area*

*change; d) Anterior wall thickness; E) Left atrial (LA) diameter; F) left ventricular end diastolic (LVEDD) diameter;; G) left ventricular end systolic (LVESD) diameter; (n=7 patch group; n=7 sham group; 2-way ANOVA). H) correlation of fractional area change measurements between two echocardiographers blinded to treatment allocation.*

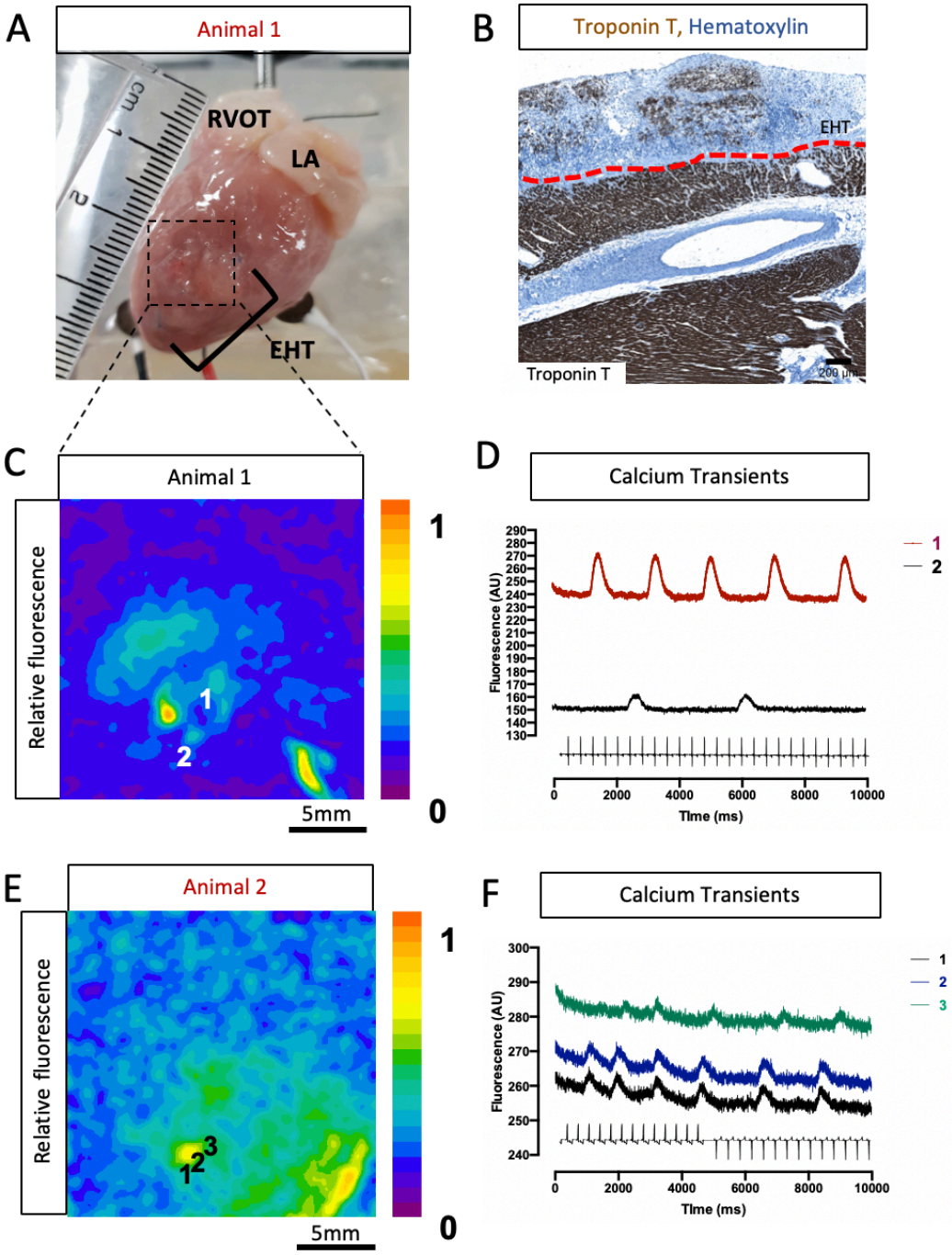
### 5.8 Optical mapping experiments

Electrical coupling of the grafted EHT to the host is one of the critical questions regarding EHT as modality of treatment in the regenerative medicine field (as opposed to intramyocardial injection). Ex-vivo optical mapping studies are able to provide important information regarding graft / host electrical interaction post in-vivo grafting experiments. Optical mapping experiments were performed at Imperial College and at our collaborating Institution (University of Glasgow). EHTs containing hiPSC-CM consisting of gCaMP6F cells were used. gCaMP6F contains GFP bound to calmodulin; which then emits a fluorescence during the rise in intracellular calcium associated with the action potential (Full details in Methods 2.4.2). Synchrony between this signal and the intrinsic rate or paced rate of the host could then be tested to ascertain whether there was any evidence of electrical coupling between the graft and host.

In total, 9 animals underwent ex-vivo optical mapping studies (Representative image Figure 5-8A). Hearts underwent immunostaining post mapping to check for troponin retention in the graft (Figure 5-8B). Data from optical mapping studies performed at Imperial College London (n=6) controls were analysed in a blinded manner by researchers at University of Glasgow. In 4 out of 9 hearts, there was evidence of spontaneous calcium transient activity found in the graft (n=1 week 1; n=1 week 2; n=1 week 3; n=1 week 4). A representative fluorescence map and calcium transient graph is shown in figure 5-7C/D. The spontaneous rates were slower than the intrinsic rate of the host (1 animal – 24bpm; $2^{nd}$ – 26bpm; $3^{rd}$ – 27bpm; $4^{th}$ – 78bpm; versus approximately 220 – 300bpm in host). In 1 of the animals (out of 4 with signal), there was a suggestion of entrainment during cessation of ventricular pacing, which could indicate possible evidence of electrical coupling to the host (Figure 5-

8E/F), although this observation was not sufficiently reproducible to allow a definite conclusion. In the remaining 3 hearts there was no evidence of electrical coupling. In a further 2 out of 5 without definite graft activity, possible activity from the graft was found, but it could not be distinguished from motion artefact definitively. In the remaining 3 hearts no EHT activity was found. Troponin staining analysis of the 5 hearts in which no definitive signal was found indicated that the % of troponin in the graft relative to day 0 was 16.3% (mapping week 4); 34.6% (mapping week 4); 13.6% (mapping week 4); 35.4% (mapping week 2); 2.1% (mapping week 2). In the hearts with a definitive signal (3 hearts with troponin T staining available out of 4) the percentage of troponin T in the graft was 84.1% (mapping week 1); 65.1 % (mapping week 3); 30.3% (mapping week 4).

**Figure 5-8: Ex-vivo optical mapping studies**




*A) Macroscopic image of EHT / rabbit heart explanted for opitical mapping one week post grafting; B) Troponin T staining (brown) of animal in A showing evidence of sustained troponin retention within the EHT, host / EHT separated by red dotted line; C) Fluorescence map of animal in A showing areas of activity within the EHT; D) Fluorescence of calcium transients of C (1-2); numbers correspond to numbers in C;*

*ECG trace of host animal below transients; E) Fluorescence map of animal 2 weeks post grafting showing areas of activity within the EHT graft; F) Respective fluorescence of calcium transients of E (1-3). ECG trace of host animal below calcium transients.*

### 5.9 Arrhythmogenic potential of EHTs

The arrhythmogenic potential of EHTs was assessed ex-vivo by performing programmed electrical stimulation using burst or extra stimulus based protocols (Figure 5-9A) on hearts that were Langendorff perfused and in-vivo using intermittent telemetry recordings (See methods section 2.8.3 / 2.13.3 for full details). The Langendorff perfusion system consists of a water bath and a series of insulated tubes and water jacketed reservoirs to enable the Tyrode's physiological solution to be maintained between 36.5-37.5 $^{o}$C. ECG electrodes were used to enable real time ECG recordings and a dedicated pacing electrode placed at the base of the left ventricle to perform the programmed arrhythmia provocation protocols.

Ex-vivo programmed electrical stimulation protocols revealed that there was no difference between control hearts and control hearts that underwent EHT implantation (mean arrhythmia inducibility score 4.7 ± 0.8 [control] vs 3.4 ± 0.6 [control / EHT]; p=ns; Figure 5-9B). In addition, there was no significant difference in arrhythmia inducibility score in infarcted hearts that underwent fibrin cell patch (sham) implantation or EHT implantation (mean arrhythmia inducibility score 5.6 ± 1.0 [MI/patch] vs 5.0 ± 0.6 [MI/sham]; Figure 5-9B)

Regarding in-vivo telemetry recordings, data from a subset of animals was available in animals that underwent EHT grafting onto control hearts (n=7), EHT grafting onto infarcted hearts (n=7), fibrin cell free patch (sham) grafting onto infarcted hearts. In the control / EHT group (n=7), no animal suffered from any clinically significant ventricular arrhythmias (sustained ventricular tachycardia [>30 seconds] / ventricular

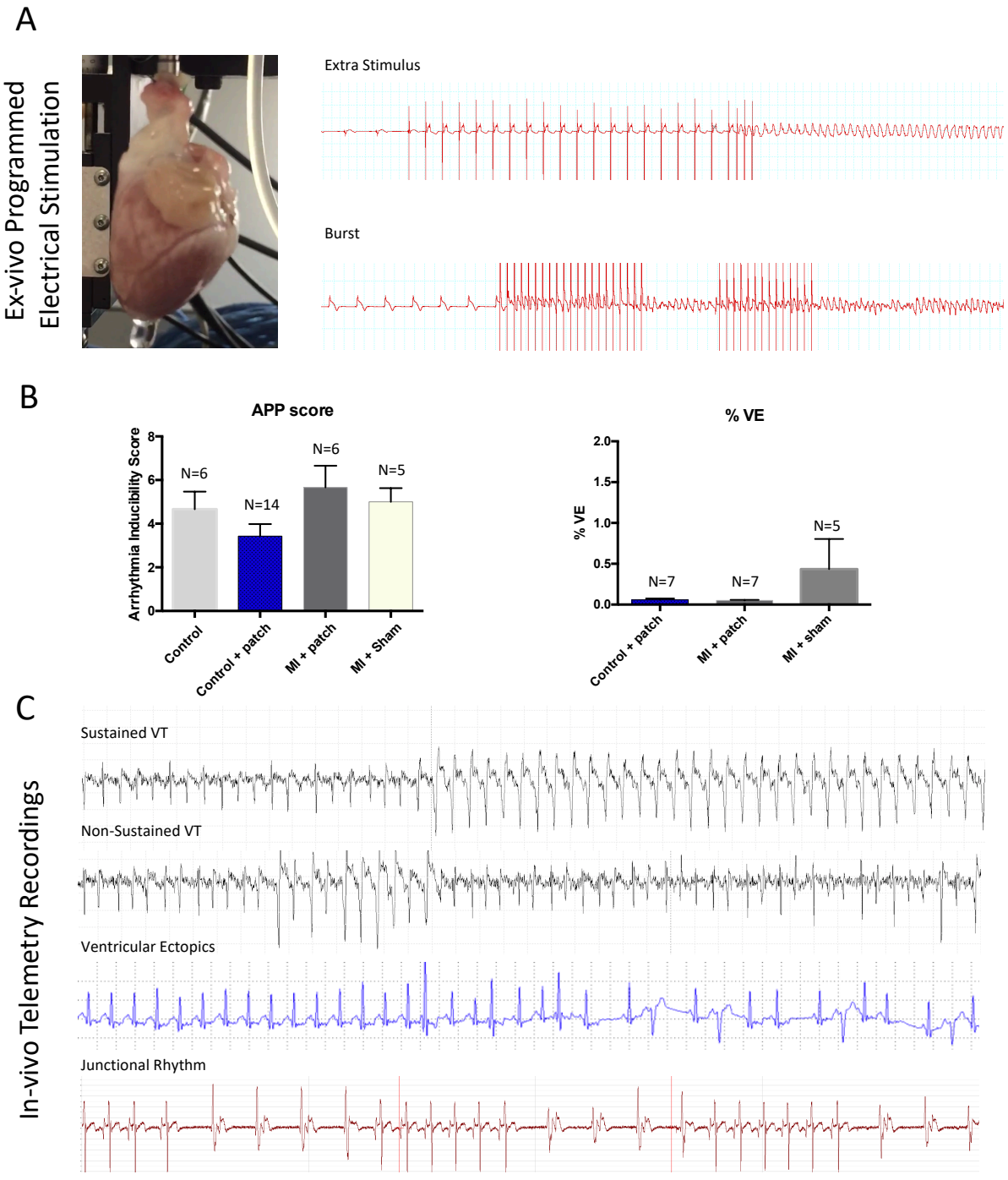
fibrillation) or non-sustained VT. Ventricular ectopic couplets were found in 5/7 animals and ventricular ectopics detected in all animals (Figure 5-9C).

In the EHT/MI group (n=7), in 1 animal multiple runs of non-sustained ventricular tachycardia were found in a single 24 hour period of recording (from a total of 28 days) lasting: 59 beats; 17beats; 50 beats and 17 beats (Figure 5-9C). In a further 3 (from 7) animals non-sustained VT (>3 consecutive beats) was detected. In no animal was sustained VT recorded (VT > 30 seconds in duration). In all 7 animals, ventricular ectopics were detected. In 1 animal, a bradyarrhythmia was detected (junctional rhythm; Figure 5-9C).

In Sham/MI group (n=5), 1 animal suffered from an episode of clinically significant sustained VT (747 beats; 2minutes 29 seconds). No obvious adverse features were noted and the animal survived to explant (1 month). 3 out of 5 non-sustained VT was reported and VE couplets and VEs were detected in all animals.

In all groups, the overall incidence of ventricular ectopics was low (0.06 ± 0.02% [control/EHT] vs 0.05 ± 0.01% [MI/EHT], vs 0.4 ± 0.4% [MI/Sham] p=0.9; p=0.77; Figure 5-9B). In 3 out of 5 animals suffered from non-sustained VT and all 5 VE couplets and VEs were documented.

**Figure 5-9: Arrhythmogenic potential of EHTs**




*A) Macroscopic image of heart attached to Langendorff system; ECG traces of hearts subjected to Extrastimulus (S1S4; upper panel) and Burst protocols (lower panel); B) Bar charts of arrhythmia inducibility scores obtained from ex-vivo programmed electrical stimulation protocols and bar chart of % of ventricular ectopics (VEs) analysed from in-vivo telemetry recordings. C) ECG traces obtained*

*from animals obtained from in-vivo electrocardiographic monitoring.*

## 5.10 Discussion

The main findings of this chapter of this thesis are: 1) EHTs were successfully engrafted onto both control and infarcted hearts; 2) Troponin cell retention progressively decreased over time; 3) The EHTs did not appear to be pro-arrhythmic in nature; 4) EHTs improved function when grafted onto infarcted hearts.

### Optimisation of in-vivo grafting protocol

#### Immunosuppression

Several steps needed to be optimised to develop a protocol that was reliable and robust for use. Regarding immunosuppression, ciclosporin and methylprednisolone were used in this study as this combination has been used in other small animal stem cell grafting studies including guinea pig / rat as well as post human cardiac and renal transplant patients.(Weinberger *et al.*, 2016)(Zimmermann *et al.*, 2006) Regarding rabbit specific immunosuppression protocols, I was not aware of any published papers regarding the use of stem cell grafting in rabbits. However, studies involving ciclosporin have been well tolerated at certain doses (up to 10mg/kg), with reported side effects of gingival hypertrophy, weight loss and nephrotoxicity at higher doses (similar side effects in humans).(Ryffel *et al.*, 1983)(Jean *et al.*, 2009)

Preliminary data suggested that even with a higher dose immunosuppression protocol, there was evidence of immune cell infiltration (Macrophage / Iba-1 positive cells) at 1-2 weeks, indicating that a degree of immune mediated rejection may have been present. This could be due to a number of reasons including: 1) inadequate immunosuppression dose; 2) inadequate type of immunosuppression administered; and 3) the xenograft nature of the grafting protocol (human EHTs on rabbit host).

The dose of the immunosuppression was relatively high and in some cases animals were beginning to show signs of chronic immunosuppression such as weight loss and poor wound healing so increasing the dose further was not a viable option. More recent studies have looked at administering additional pharmacological agents as well as calcineurin inhibitors and steroids.

For example, a study by Zhu et al, explored the use of multiple drug regimen immunosuppression protocols (ciclosporin, methylprednisolone, basiliximab) in infarcted non-human primates. (Zhu et al., 2018) When compared to a strategy of ciclosporin alone, the multiple drug regime resulted in greater cell retention, less immune cell response, and less apoptotic cells. However, long term retention was still not found with no transplanted cells detected at 140 days.(Zhu et al., 2018) Triple immunosuppression regimes have also been used in other large animal studies using human derived embryonic stem cells (ciclosporin, methylprednisolone, Abatacept). (Liu *et al.*, 2018).

Additionally, the use of basiliximab (chimeric (human/murine) monoclonal antibody) has been shown to reduce the incidence of acute rejection when added to dual or triple therapy immunosuppression regimes in human clinical trials of renal transplant patients. (McKeage and McCormack, 2010)

Therefore the addition of another immunosuppressive agent that targets another molecular pathway in addition to our immunosuppression protocol may have improved cellular retention and integration. One of limitations of this study is that blood levels of ciclosporin were not taken, but since the dose was relatively high, it

was felt that taking multiple blood samples from an animal recovering from surgery would cause additional stress to the animal. It is also important to mention that since human cells were used, the degree of rejection would presumably be higher than with an allogenic or autologous source and work is ongoing in the Harding lab to definitively answer this question. Other possible causes of lack of cell retention are discussed on page 235.

**Attachment method**

Initial EHTs were grafted on with surgical Histoacryl glue. This method facilitated the attachment of the EHT to the epicardial surface; however, no definitive evidence of the EHT remained using this method and therefore conventional surgical attachment using Prolene sutures was used. It could be that the glue encapsulated the EHT and therefore starved the cells of oxygen causing the cell to die. Whether or not the issues with gluing were due to the type of glue used remains to be seen. It is possible that using fibrin glue (similar to EHT matrix) may have had a different outcome. This would not happen with surgical attachment. One downside with using the suture method was the inadvertent myocardial injury cause by damaging blood vessels with an intramyocardial course since they were not easily visualised from the epicardial surface. On some occasions, if an intramyocardial vessel was injured, pressure was applied to cause haemostasis. Notably 2 animals died intraoperatively specifically from inadvertent blood vessel injury (out of 53 (3.8%) animals that underwent epicardial suturing; overall mortality rate of surgeries 17.0% (n=9)).

Another important issue to mention regarding the EHT grafting process was that during surgery the pericardium is relatively intact. During surgery, incision is made in

the pericardium along the atrioventricular border, upon which the heart is slipped out of the pericardial sac. After grafting the EHT, the heart is placed back into the pericardial sac and the EHT is sandwiched between the epicardial surface and the pericardium. This is an important point and an added advantage of the rabbit model specifically, since the pericardium could shield the EHT from damage / inflammation by the surrounding structures whilst providing growth factors to support cell survival. Indeed this is a technique that has clinical relevance. In the first in human study involving embryonic progenitor cells, the pericardium was used to surgically attach the patch in a way to act as a shield and provide pericardium associated growth factors and cells to act as a "natural bioreactor".(Menasché *et al.*, 2018)

**Prosurvival cocktail**

In the first grafting experiment, we found that due to the relative area in the centre of the EHT devoid of cells there could have a necrotic core due to inadequate diffusion of nutrients with thicker grafts. This has been a concern as grafts are upscaled in size as research groups move towards clinical translation. This prompted the use of a prosurvival cocktail, which has been proven to inhibit cardiomyocyte death post intramyocardial injection. The prosurvival cocktail was designed to be used in experiments involving intramyocardial injection of stem cells to make the transplanted cells more resistant to hypoxia and shield them from the hostile environment during the early integration phase. The original method included the use of matrigel, and various drugs including ciclosporin (to attenuate cyclophilin D dependent mitochondrial pathways), pinacidil (mimic ischaemic preconditioning), ZVAD-fmk (caspase inhibitor), Bcl-XL (inhibit mitochondrial death pathways). In addition, cells were heat shocked at least 24 hour prior to injection (See methods

section 2.7 for full details).(Laflamme *et al.*, 2007) We used the same protocol as previously published but since the cells were already contained in a hydrogel containing matrigel, we omitted the step of using Matrigel (which was originally used to prevent anoikis). Although, due to cost and time we did not specifically assess the effect of the prosurvival cocktail in this study, we did not however observe any evidence of a necrotic core on any samples after we started using a prosurvival cocktail. Additionally, we did not find any difference between the inner and outer halves in terms of capillary density, indicating that the grafts were fully vascularised throughout the EHT. This is reassuring since it is likely that thicker grafts may be needed for the first in human trials since human ventricles are normally 8-12mm in thickness.

**Cellular retention**

After successful set up of the model, it was important to ascertain long term retention using the EHT method of hiPSC-CM delivery. Retention was assessed at serial time points up to one month in duration and the final percentage of troponin positive cells relative to day 0 was 23.3 ± 6.8%. In a study by Gao et al, for example in a swine study, the engraftment rate was 10.9±1.8% at 4 weeks after the transplantation.(Gao *et al.*, 2018). In contrast, in the paper by Weinberger et al using a cryoinjury model in guinea pigs, the grafts proliferated at one month post grafting. Long term studies involving smaller animals have found evidence of retention up to 7 months (220 days) in duration.(Riegler *et al.*, 2015) Notably, in that study however the grafts were not associated with an improvement in cardiac function.

In our study, the troponin retention significantly decreased after two weeks, H+E

staining showed many nuclei consistent with inflammatory cells and preliminary data on Iba-1 staining revealed strongly positive areas. These preliminary data led us to the hypothesis that this could be consistent with immune mediated rejection as previously mentioned.

Other possible reasons could be cell death / necrosis due to ischaemia or apoptosis due to inadequate blood supply or lack of electromechanical integration. Future work could involve staining for apoptotic markers including caspase. The effect of ischaemia in the perigrafting period was minimised with the use of a pro survival cocktail and the grafts appeared vascularised with the host. Additionally, at 1 week we found that cellular retention was relatively preserved relative to day 0 indicating that possible the cells were resistant to hypoxia in the early integration phase without vessel formation. However, when compared to native myocardium the capillary density in the graft was lower (175 CD31/mm2 vs 2000 CD31/mm2 in native myocardium) and the vessels were morphologically small and capillary like in most instances, which may indicate an insufficient blood supply to the grafts.(Brown and Hudlicka, 1991) However, the percentage of troponin +ve cells in the graft relative to rabbit myocardium was significantly lower (approx. 80% in native versus 20% at 1 week), indicating that perhaps a lower density of blood vessels may have been sufficient. Further blood vessel characterisation is needed to ascertain in detail the type of vessels; for example, staining for alpha smooth muscle actin, vascular cell adhesion molecule, vascular endothelial growth factor and intercellular adhesion molecule type-1.

Long term cellular retention is critical if pursuing a muscle replacement strategy as

opposed to a paracrine based strategy. Notably, in the first in man clinical trial that has been approved in Japan, immunosuppression will only be given for one month in duration, which acts as a kill switch or safety feature since cells are from an allogenic source. Therefore, rather than replacing the lost muscle, an improvement would be paracrine in nature. The paracrine effect is the main mechanism of improvement in intracoronary and intramyocardial studies since it is well known that the vast majority of cells are washed away after 24 hours.(Madonna *et al.*, 2016) Therefore, prolonged paracrine release could be one of the major mechanisms of improvement using EHT technology. In other studies, involving macaques and intramyocardial injection – sustained retention was present up to 3 months. However relative to day 0 it is unknown what the retention would have been since during the index procedure a large number of cells were administered by intramyocardial injection (1 billion cells) and it is unlikely that that this number of cells were present at 3 months.(Chong *et al.*, 2014) Therefore, to overcome the relatively poor retention at one month found in this thesis future work could include using EHTs with a higher absolute cell number.

**EHTs and arrhythmia**

The development of arrhythmias has long been a theoretical concern from the beginning of the cardiac regeneration field. The numerous clinical trials involving SC-CM however have not really reported arrhythmia since the seminal MAGIC trial involving skeletal myoblasts.(Menasché *et al.*, 2008) Arrhythmias have however been reported after programmed electrical provocation studies with bone marrow stem cells with 5/9 patients developing induced monomorphic VT and 1/9 polymorphic VT.(Hendrikx *et al.*, 2006) Most clinical studies do not specifically provoke arrhythmia and therefore the low reported level of pathological arrhythmia

may not be a proper reflection of safety of SC-CM grafting.

Recent preclinical studies in large animal models have however reignited the concern regarding arrhythmia. In a landmark study from the Murry lab, macaques who underwent intramyocardial injection of around 1 billion hESC-CM, a common finding was the development of arrhythmias, in the transient early vulnerable period (0-3 weeks post grafting).(Chong *et al.*, 2014) Notably, the incidence of arrhythmias reduced in frequency over several weeks and this was hypothesised to be due to the better coupling with the host or increased maturation of the hESC-CM graft. The arrhythmias were relatively well tolerated, but obviously give renewed concern for the future use of pluripotent stem cell derivatives and the development of arrhythmias with prolonged cell retention. There are many potential mechanisms of arrhythmia formation including re-entry mechanisms, due to areas of heterogenous myocardium (and hiPSC-CM graft) resulting in abnormal wavefront propagation. Other mechanisms result from aberrant impulse generation and include triggered activity which include early/late after depolarisations (due to abnormalities in intracellular calcium handling / action potential prolongation) or enhanced automaticity (especially as hiPSC-CM have intrinsic pacemaker activity). For example, in swine / guinea pig studies, implantation of a relatively small number of hESC-CM, the intrinsic activity of the cells were able to take over the pacemaker activity of the heart if the SA and AV nodes were suppressed.(Kehat *et al.*, 2004)(Xue *et al.*, 2005) Interestingly, in a recent study macaque transplantation of ~750 million hESC-CMs improved cardiac function with a global left ventricular ejection fraction increase of 10.6 ± 0.9% vs. 2.5 ± 0.8% in controls.(Liu *et al.*, 2018) Grafts electrically coupled with the host heart but a subset of animals experienced

graft-associated ventricular arrhythmias. In this study, further arrhythmia characterisation was performed via catheter based electrophysiological studies using the CARTO III mapping system and subjected to programmed electrical stimulation protocols. Overall, 12 EP studies were performed on 8 animals (3 control versus 5 hESC-CM treated) and 10 studies (from 8 animals) yielded data on arrhythmia inducibility. There was no difference in arrhythmia inducibility score between vehicle and hESC-CM treated groups. Activation maps were obtained from 3 animals (2 treated and 1 control) and in each case the VT originated from a focal region from a region of low voltage scar tissue and was induced by pacing and terminated by overdrive pacing, which indicated a microreentry mechanism. In the cell treated group (n=2), the VT was spontaneous and hearts could be overdrive paced (300 bpm) only temporarily, and the arrhythmia was refractory to electrical cardioversion therefore exhibiting features of abnormal impulse generation. The numbers in this study were too small to draw reliable conclusions; however, this study was the first to characterise arrhythmias in such a detailed way.

In another more recent study, swine were subjected to intramyocardial injections of hESC-CMs ($1 \times 10^9$ hESC-CMs (n = 7) or vehicle alone (n = 7)).(Romagnuolo et al., 2019) hESC-CM recipients developed frequent monomorphic VT starting approximately 3-4 days post grafting, which then peaked at around day 10 and during that window, 4 out of 6 animals were in sustained VT over 80% of each day. In addition, 2 out of 7 animals died during the arrhythmogenic period; 1 animal on day 16 with sustained VT that converted to ventricular fibrillation and another that was euthanized due to severe heart failure and sustained VT (day 13). By contrast, in the vehicle alone group, in 3 out if 7 animals only a low incidence of VT was

detected. In a subset of animals, (cell treated n=3; vehicle n=4) catheter based electroanatomical mapping was performed and a focal mediated mechanism was the determined mechanism in the cell treated animals. Similarly to the macaque study, the incidence of arrhythmia dissipated over time and all animals were in normal sinus rhythm at one month. The focal mechanism would be more consistent with the relative immature phenotype of the cells engrafted (only ~30% MLC2v+ ), and indeed the in-vivo maturation that occurred during this study (up to >90% MLC2v+) may account of the decrease in arrhythmia burden seen after 3 weeks post transplantation. The use of immature cells for grafting is a balance between the development of pathological arrythmia due to heterogeneity, and the hypoxia resistance that is provided by using foetal like cells, as opposed to mature cells which may not survive the early integration phase due to lack of blood supply / adequate supply of nutrients.(Harding, 2014)

It is known from the currently clinically use delivery methods that the majority of cells are washed away or die due to ischaemia within a 24 hour period.(Madonna *et al.*, 2016) Therefore with newer strategies that improve cell retention under preclinical investigation, including engineered heart tissue, the development and issue of arrhythmias may resurface. Therefore, a critical assessment of ventricular arrhythmias was essential in this PhD, to identify any potential mechanisms, especially in the infarcted animals where the environment is hostile and therefore there is a greater substrate an propensity for arrhythmia formation.

In this study, arrhythmias were assessed in both ex-vivo methodologies and in-vivo with telemetry recordings. The overall burden of arrhythmia was low, with no

clinically relevant sustained arrhythmia detected in any animal that underwent EHT grafting. In addition, programmed electrical stimulation did not find any difference in arrhythmia inducibility score between control and graft treated animals. The limitations of our method were the intermittent recordings as opposed to continuous recordings and absence of in-vivo programmed electrical stimulation recordings and electroanatomical mapping.

However, our data is relatively consistent with the literature on the engineered heart tissue modality of grafting. For example in a study by Gao et al, grafting of EHTs onto swine did not induce ventricular arrhythmia over control as determined by continuous ECG monitoring with no significant differences in incidence of VT / VF between controls and grafted animals.(Gao *et al.*, 2018) Additionally, programmed electrical stimulation did not reveal any increase propensity to arrhythmia formation in the grafted animals.(Gao *et al.*, 2018) More recently, a subgroup analysis from the previous Weinberger paper has been published involving the subset of animals who underwent telemetric monitoring.(Pecha *et al.*, 2019) 37 animals underwent telemetry implantation, and surviving animals post cryoinjury (n=10 hEHTs, n=8 controls) were included in the final analysis. Animals in both groups developed non-clinically significant arrhythmia including premature ventricular contractions, couplets, triplets and non-sustained VT, but no animals in either group suffered from sustained ventricular tachycardia or ventricular fibrillation.

Therefore, the lack of arrhythmia seen may be due to the modality of delivery. It has been noted in these studies, that a fibrous layer exists between the EHT and the host which may prevent electromechanical coupling. If no connexins form between

the host and the graft, there is no theoretical substrate for the formation of arrhythmia.

Our data regarding lack of effective coupling is also relatively consistent with the literature. For example, in 4 out of 9 rabbit hearts that underwent optical mapping at 2 different institutions, there was evidence of spontaneous calcium transient activity found in the graft but only possible evidence of coupling in 1 animal, with spontaneous rates significantly lower than the host. Similarly to our data, Jackman et al found no evidence of coupling when grafts were placed onto rat hearts despite effective vascularisation with the host.(Jackman *et al.*, 2018) In addition, Shadrin et al also found no evidence of coupling, and evidence of a fibrous layer between the host and graft.(Shadrin *et al.*, 2017) In contrast, Weinberger et al found evidence of coupling in only a subset of hearts.(Weinberger *et al.*, 2016) Notably the faster heart rates of small animals when compared to human cells may prevent coupling and data in large animals with more human like ventricular rates may increase the likelihood of coupling.

**EHTs and left ventricular function**

The majority of preclinical studies in small and large animals models have shown the beneficial effects of engineered heart tissue regarding improvements in left ventricular function of anywhere between 20-30% from baseline.(Weinberger *et al.*, 2016)(Gao *et al.*, 2018)(Zimmermann *et al.*, 2006) Since a significant number of studies have not shown any reliable and effective evidence of coupling, a paracrine modality may at least be partly responsible.(Jackman *et al.*, 2018)(Shadrin *et al.*, 2017) As well as providing prolonged paracrine release, the EHT may provide wall

support and prevent reverse remodelling.(Weinberger, Mannhardt and Eschenhagen, 2017) Future work should investigate minimising the fibrous layer and trying to improve electromechanical coupling between the graft and the host.

Preliminary work from Prof Terracciano's lab has also shown that hiPSC-CM can couple to myocardial slices almost immediately on point stimulation of slice (1 Hz) prior to any gap junctions forming. This has led the group to believe that mechanotransduction may account for some improvement in function when using EHTs. Mechanotransduction, via stimulation of stretch activated receptors in the hiPSC-CM may enable the cells in the graft to beat in sync with the host and therefore provide contractile support even if not electrically coupled but this is merely hypothesis forming at present.(Martinac, 2004)(Reed, Kohl and Peyronnet, 2014)

The improvement seen in this study was in line with previously published studies; however, the improvement in function was in a myocardial infarction model and not a heart failure model which is more clinically relevant. The current modality of delivery requires an open sternotomy and therefore will never be implanted in an emergent myocardial infarction type scenario that is treated in a minimally invasive way with percutaneous coronary intervention. It must also be stated that although measurements were performed by experienced blinded echocardiographers and there was good correlation between the two values, the study was single blind since the operator performing the animal surgery could tell if the patch was fibrin cell free or contained cells. This is because the two patches are clearly distinguishable. Future work could use irradiated cells that would look identical to normal EHTs. In addition, although randomisation tables were not used, CBS staff chose animals for

surgery without knowledge of whether the surgery to be performed was sham or EHT. Therefore, although the results of this study are encouraging, it is essential to perform a “preclinical blinded randomised trial” in a heart failure model prior to any phase I human clinical trial. Work is ongoing in the Harding lab and our collaborating centre in Glasgow with Prof Godfrey Smith to undertake this.

**Conclusion**

The results of this chapter of this thesis describe the successful EHT in-vivo grafting model that was set up at Imperial College London. Serial time points were assessed up to one month in duration and the engraftment rate was 23.3 ± 6.8% at 4 weeks. If the long term goal is to replace muscle rather than provide prolonged paracrine release it is likely that a greater cell number will need to be transplanted. Consistent with the literature the EHTs do not appear to be excessively pro-arrhythmic in nature, as assessed both by ex-vivo electrical stimulation protocols and in-vivo telemetry recordings. Additionally, EHT grafting improvement left ventricular function but did not effectively electrically couple to the host. Future work should include improving electrical coupling and increasing cellular retention by using improved immunosuppression protocols, increasing cell number and using allogenic / autologous cell sources. If these improvements are successful, a randomised, blinded study confirming benefit will be essential prior to any first in man study. Nevertheless, work in this thesis proves that EHT are an exciting potentially modality for the regenerative medicine field.

# Chapter 6: Ex-vivo testing of a conductive polymer patch

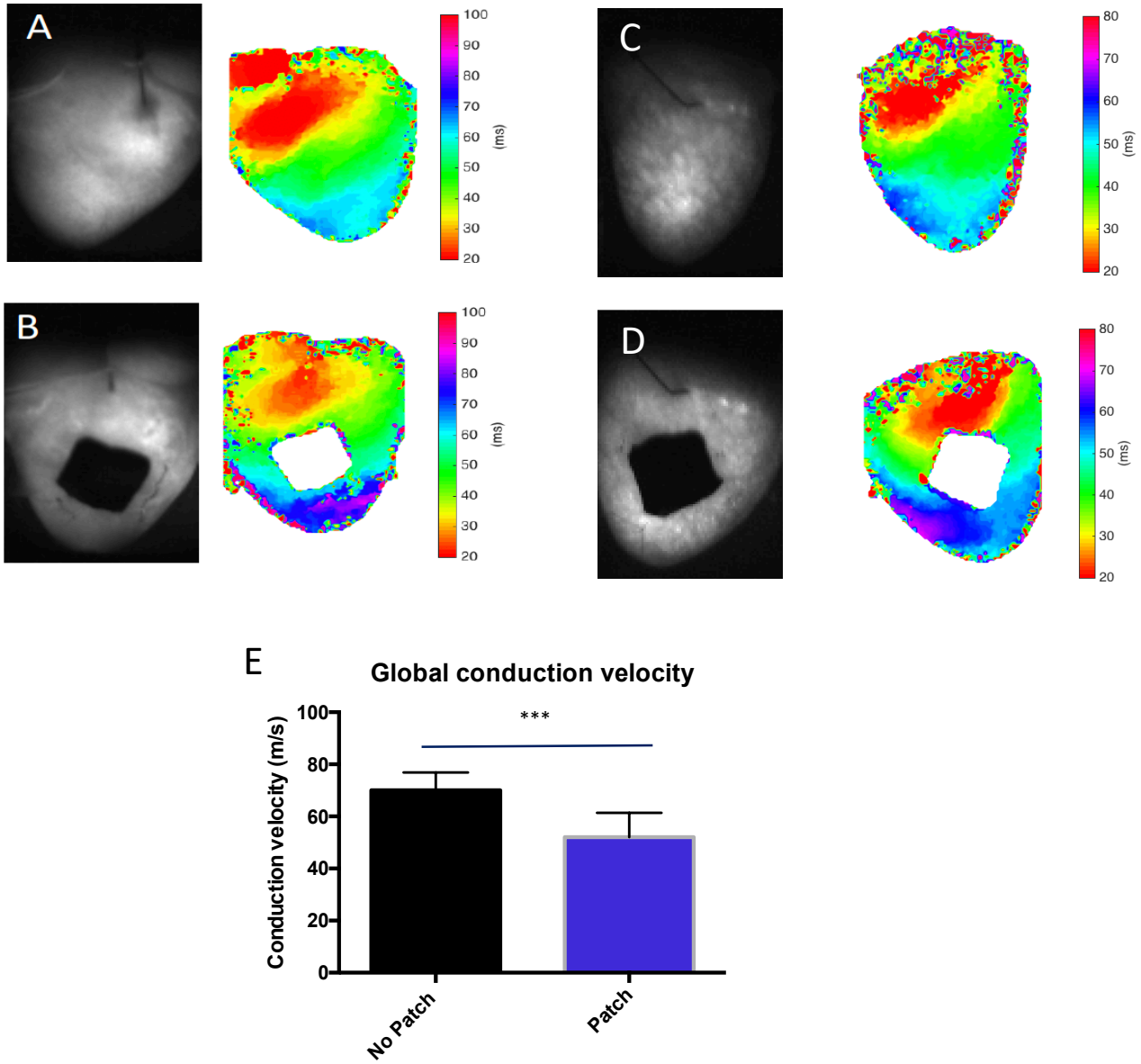
## Introduction

Due to the increased potential for arrhythmia post stem cell grafting into heterogenous infarcted scar tissue, conductive polymers have recently been investigated as a vehicle for pluripotent stem cell delivery.(Cui, Yang and Li, 2016) The paradigm behind the use of conductive polymers is two-fold. Firstly, to act as a bridge to synchronise electrical impulses between zones of surviving tissue and across areas of scar. In addition, the conductive patches could also act as an electrical “sink” or capacitor to modulate aberrant electrical wavefronts arising as a result of heterogenous scarred myocardium and / or immature cells contained within the graft. Data in small animals models have shown that conductive polymers are able to alter the electrophysiology of the heart, promote angiogenesis and cell attachment.(Mawad et al., 2016)(Mihardja, Sievers and Lee, 2008)(Kai et al., 2011). Data from the Harding group have previously shown that conductive polymers were able to affect conduction velocities of rat hearts and the patches were non-arrhythmogenic in nature. However, to date data regarding larger animal models with thicker ventricles is lacking. Therefore, the final results chapter of this thesis aimed to ascertain what effect a conductive polymer patch had on larger rabbit hearts ex-vivo. Experiments were performed on a Langendorff apparatus with both control and infarcted hearts with optical mapping experiments performing using the voltage sensitive rh237 dye. Arrhythmogenicity was tested by subjecting perfused hearts to programmed electrical stimulation protocols.

### 6.1 Conductive Polymers affect conduction delay

To determine whether the PANI conductive polymer patch had an immediate electrophysiological effect on a larger rabbit heart, ex-vivo optical mapping studies were firstly performed on control rabbit hearts. Hearts were explanted as described in Methods section 2.11. After a 15-20min stabilisation period on the Langendorff apparatus, the conductive polymer was surgically attached to the heart (4 x sutures; 8.0 Prolene), placed in a custom-built Perspex chamber and hearts loaded with the transmembrane voltage dye rh237. Full details in Methods section 2.12. Since surgical attachment inevitably causes myocardial injury, histoacryl glue was tried as a fixative (n=2). The glue however interfered optical mapping analyses so patches were sutured with 8.0 Prolene (minimal profile). As can be seen in the representative activation maps shown in Figure 6-1A-D ([A/B 1$^{st}$ animal] / [C/D 2$^{nd}$ animal]), ex-vivo surgical attachment of the conductive polymer patch to the epicardial surface caused an immediate significant reduction in global conduction delay over the epicardial surface of the heart (70.6 $\pm$ 6.8cm/s [without patch] vs 52.0 $\pm$ 9.3cm/s [with patch] p=0.0002; n=8; Figure 6-1E).

**Figure 6-1**: **Conductive polymers affect global conduction delay**




*A/B) Representative macroscopic images (monochrome, left hand side) of control heart with and without patch with representative activation maps on the right side. C/D) An additional heart is shown with macroscopic images on left hand side followed by activation maps on right hand side. E) Bar chart of global conduction delay measurements before and after application of the conductive polymer (n=8). Data presented as mean ± SEM; analysed by paired student t-test;* ***=p<0.001.

### 6.2 - Conduction polymers do not appear to affect action potential duration

Since the conductive polymer patch significantly affected global conduction delay, it was important to understand whether the conduction velocity changes were dependent on changes in action potential morphology / duration since action potential duration is one of the key factors affecting conduction velocity (Representative action potential traces in Figure 6-2A).

This was primarily performed by assessing regions of interest at the base (i.e. away from the patch) and apex of the heart (i.e. near the patch) (Figure 6-2B/C) and whether there were any changes in APD 90 (ms) before and after surgical attachment of the patch. As can be seen in Figure 6-2D, there were no significant differences in APD 90 duration between the apex and the base prior to attachment of the patch (150.3 $\pm$ 12.6 ms [apex] vs 154.3 $\pm$ 10.8 ms [base], p = ns). Furthermore, after attachment of the patch, there were no significant differences found in APD 90 duration at the base of the heart (156.9 $\pm$ 10.5 ms) and the apex of the heart (near the patch; 151.4 $\pm$ 19.5 ms, p = ns).

The results of this figure imply that the conduction velocity changes appear to be independent of alterations in action potential morphology. The next step in was to ascertain whether the conductive polymer patch affected the electrophysiology of infarcted hearts (more clinically relevant scenario).

**Figure 6-2: Conductive polymers do not appear to affect action potential duration**

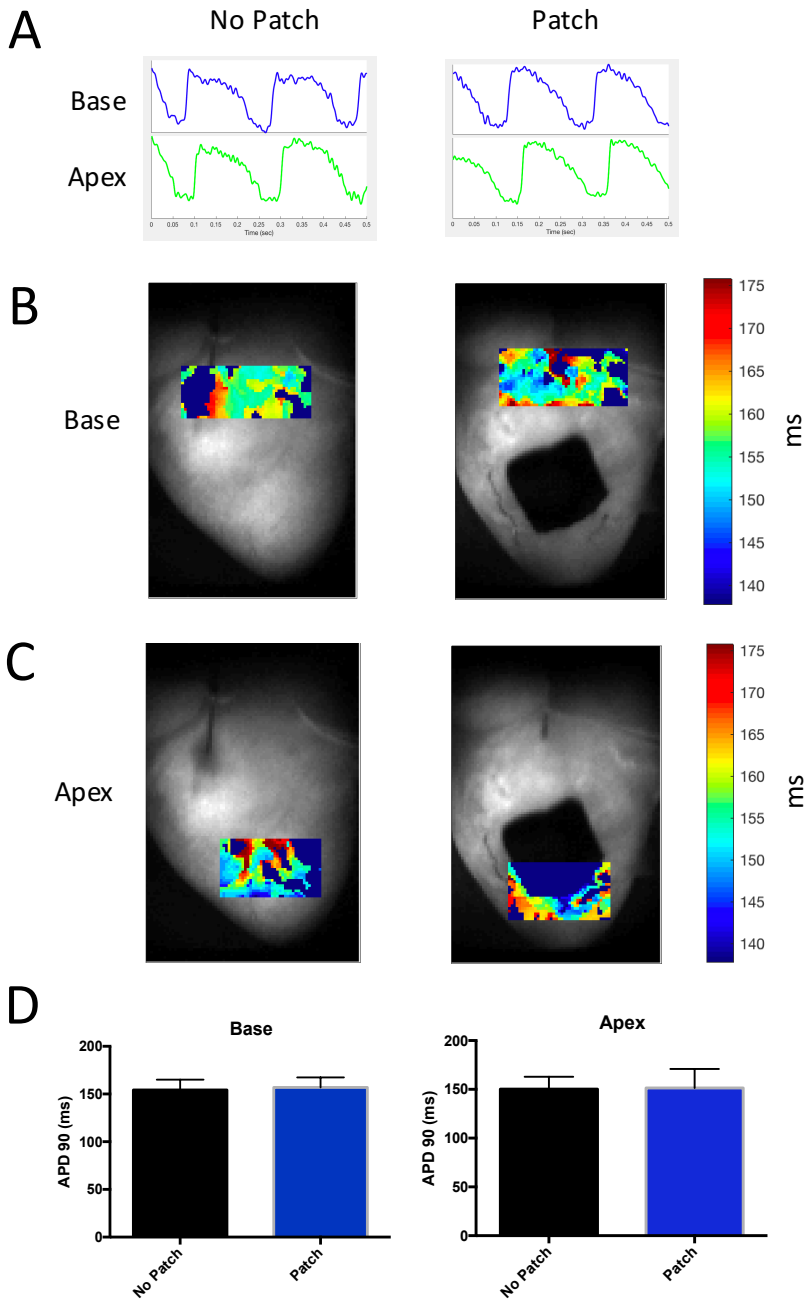



*Figure legend: A) Action potential morphology taken from base and apex with both patch off (left panel) and patch on (right panel). B) Action potential region of interest taken from base with patch off (left panel) and patch on (right panel); C) Action*

*potential region of interest taken from apex with patch off (left panel) and patch on (right panel); D) Bar charts comparing action potential duration 90 (APD 90 [ms]) with patch on and patch off from the base (left panel) and apex (right panel). ms = milliseconds. Data presented as mean ± SEM; analysed by paired student t-test.*

### 6.3 Conduction velocity does not appear to be changed when applying the patch to infarcted hearts

One of the main translational aims of using a conductive polymer patch would be on infarcted hearts, with the idea of restoring homogenous conduction propagation over areas of heterogenous myocardium as a result of scar tissue.(Cui, Yang and Li, 2016) Ex-vivo optical mapping experiments were performed on rabbit hearts (n=5) that had undergone marginal artery ligation 30.6 ± 5.05 days prior to explantation. Myocardial infarction was confirmed by ST elevation, echocardiographic evidence of a regional wall motion abnormality and histological staining as per results section Chapter 4-1/3. Hearts were explanted as per methods section 2.11 and the patch attached ex-vivo over the infarcted area and borderzone. Representative activation maps of an infarcted heart with and without patch attachment are shown in Figure 6-3A/B.

On measuring conduction velocity with and without the patch, there did not appear to be any significant changes in conduction velocities, either globally or away or near the patch (Figure 6-3C). In addition there were no significant changes in APD 90 with and without patch attachment (Figure 6-3D/E)  However, the voltage signal was significantly noisy / weak in areas of infarcted tissue, which was probably due to poor signal from lack of myocardium and scar tissue, making interpretation of both global conduction velocities and action potential measurements difficult and non-reproducible.  Therefore caution must be taken when interpreting results from the infarcted hearts and further detailed mapping studies are required to make any firm conclusions.

**Figure 6-3: Conductive polymers do not appear to affect conduction velocity of infarcted hearts**

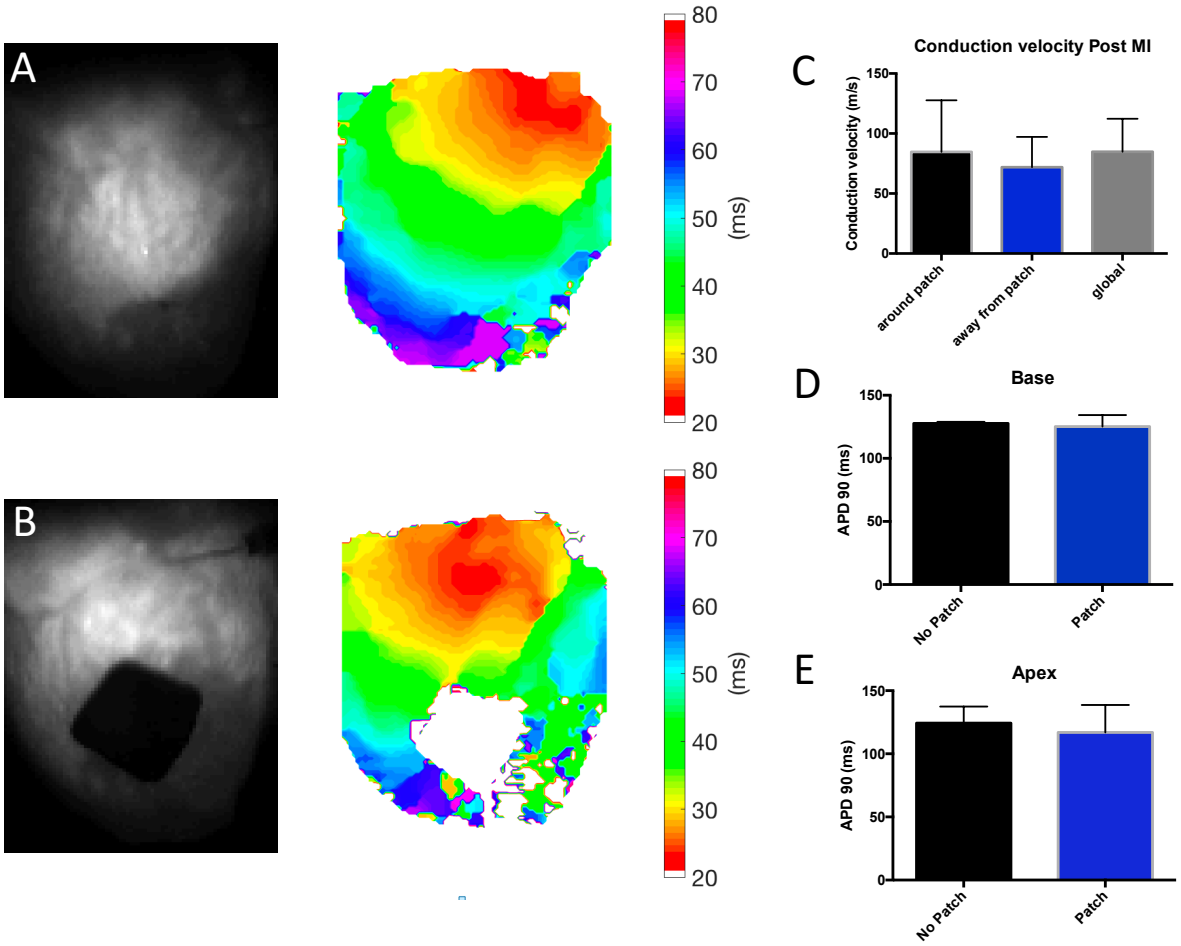



*Figure legend: Representative activation maps of infarct region without (A) and with the patch (B) across the borderzone of the infarct region; C) Bar chart comparing global conduction velocity, conduction velocity around the patch and away from the patch; D) Bar chart comparing the action potential duration 90 (ms) at the base of the left ventricle with patch on and off; E) Bar graph comparing APD 90 (ms) at apex with and without patch (n=5). Data presented as mean ± SEM; analysed by paired student t-test and one-way ANOVA as appropriate.*

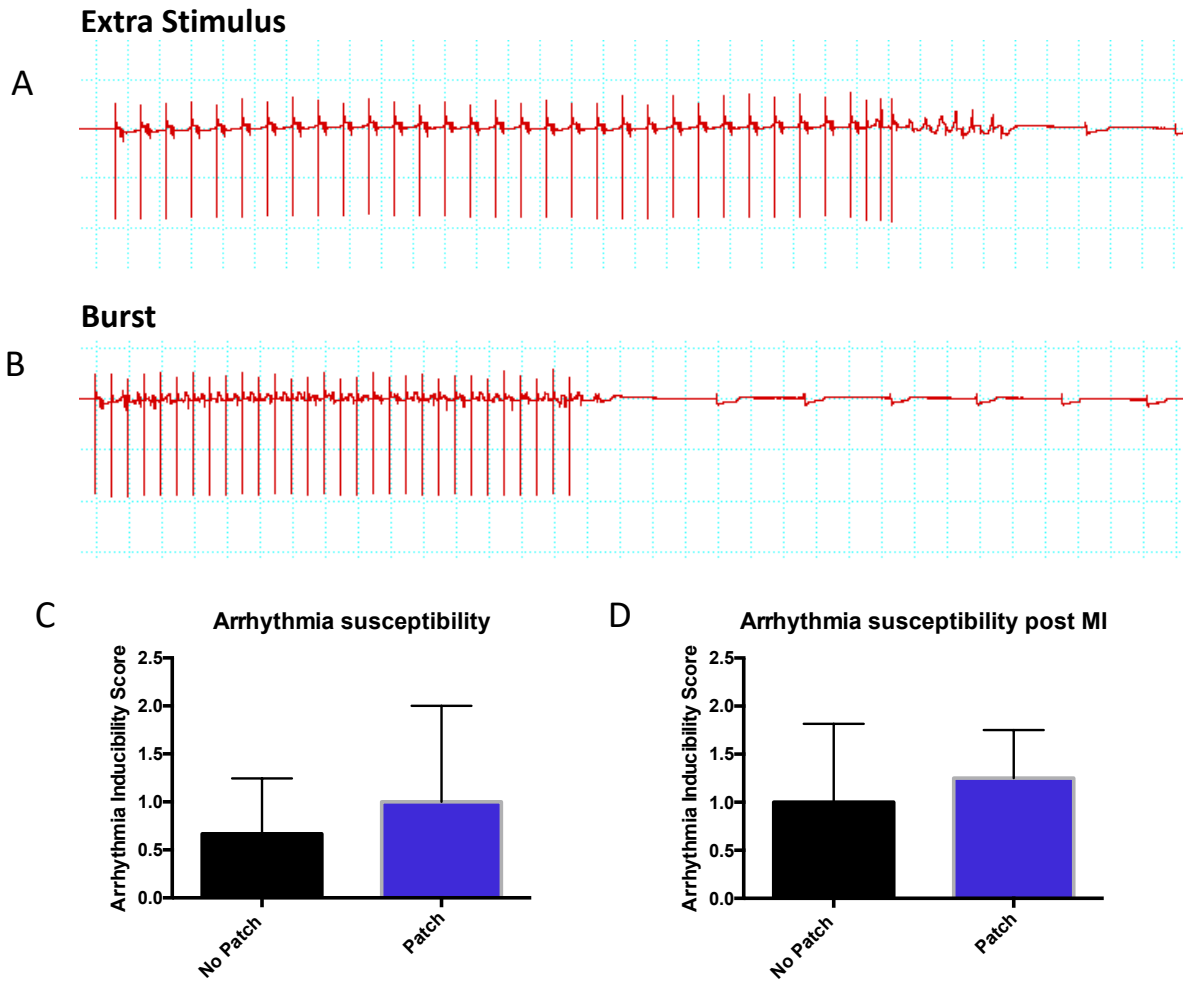
### 6.4 Conductive polymers do not appear to be pro-arrhythmic

Since it was established that the conductive polymer appeared to alter the electrophysiology of the epicardial surface of control rabbit hearts without affecting action potential duration it was important to ascertain whether the conductive polymer was pro-arrhythmic in nature.

The susceptibility to arrhythmia formation was assessed by performing ex-vivo optical mapping studies and programmed electrical stimulation. The susceptibility to arrhythmia was dependent on whether a ventricular pathological arrhythmia (sustained / non-sustained) was invoked by either extra stimulus (Figure 6-4A) or burst pacing (Figure 6-4B) protocols.

The preliminary results of the subset of hearts in which ex-vivo programmed electrical stimulation protocols were carried out indicated that surgical attachment of the patch was not pro-arrhythmic in nature in both control (arrhythmic inducibility score $0.67 \pm 0.3$ (n=3) without patch vs $1 \pm 0.6$ (n=3) with patch; Figure 6-4C) and infarcted hearts (arrhythmia inducibility score $1 \pm 0.4$ (n=4) without patch vs $1.3 \pm 0.3$ (n=4) with patch; Figure 6-4).

**Figure 6-4: The conductive polymer patch does not appear to be pro-arrhythmic in nature**




*Representative traces of extra-stimulus (A) and burst pacing protocols (B) are shown in the ECG traces. Bar chart showing arrhythmia inducibility score of control hearts (n=3 no patch; n=3 patch) (C) and in infarcted hearts (n=4 no patch; n=4 patch) (D). Data presented as mean ± SEM; analysed by paired student t-test.*

## 6.5 Discussion

The main findings of this chapter of this thesis are: 1) the conductive polymer appeared to immediately alter the electrophysiology of the heart when applied to control hearts; 2) The effects were independent of changes in action potential duration; and 3) the patch was not associated with any significant changes in arrhythmogenicity.

### Conductive polymers

Cardiac patches are a promising modality to use in cardiac regeneration. They have been shown to have a beneficial effect on cardiac function in infarcted hearts. This could be via mechanical support by decreasing wall stress to the failing ventricle or if containing hiPSC-CM allowing the continuous release of paracrine factors and by providing extra ventricular contraction.(Fernández-Avilés *et al.*, 2017)(Madonna *et al.*, 2019) Recently, there has been interest in developing patches that can potentially electrically couple (conductive) to native myocardium due to their intrinsic electroactive nature. Various conductive materials have been explored including conjugated polymers, carbon nanotubes, carbon based materials including graphene/graphene oxide and metallic nanoparticles or nanowires consisting of gold.(Meng *et al.*, 2013)(Balint, Cassidy and Cartmell, 2014) (Li *et al.*, 2014)(Saravanan *et al.*, 2018) Promising preclinical data in small animals (rat) have been reported. For example, the enhancement of a cardiac scaffold with conductivity (polypyrrole-chitosan hydrogel) resulted in enhanced electrical coupling in-vitro, and a decreased QRS duration (improved conduction) with an improvement in ventricular function 8 weeks after myocardial infarction / injection.(Mihic *et al.*, 2015) It has also been shown to improve cell retention when compared to patches that were not conductive in nature.(Li *et al.*, 2014)

The patch used to carry out the experiments in this study consisted of PANI doped with phytic acid on the surface of a chitosan film. Data regarding this patch, but on a significantly smaller scale (25mm$^2$ vs 100mm$^2$) have been recently published by Prof Stevens' / Harding's groups tested on an in-vivo rat model and ex-vivo on rat myocardial tissue slices.(Mawad *et al.*, 2016) The manufacturing process of the patches was similar to the smaller patches previously used (Courtesy of Dr Kella Kapnisi).(Mawad *et al.*, 2016) In the Mawad study, the patch was electrically stable in oxidised form for up to two weeks. It was shown using ex-vivo optical mapping experiments in healthy and infarcted hearts that the conduction velocity was affected instantly after attachment of the patch to the epicardial surface. Interestingly, the conduction velocity on control hearts was reduced and the opposite occurred in infarcted hearts. The main focus of the experiments in this chapter were to see if the results could be replicated in a larger animal model with a relatively thicker ventricle (1-1.5mm rat vs 2-3 mm rabbit).

The findings of the Mawad paper were partly replicated since we found that the patch slowed global conduction velocity in control hearts to a similar degree. In the paper by Mawad et al, the conduction velocity in control hearts reduced from 66.3 ± 4.3 cm/s to 47.8 ± 5.1 cm/s ($P < 0.02$, $n = 5$), whilst in our study the conduction velocity reduced from 70.6 ± 6.8cm/s [without patch] vs 52.0 ± 9.3cm/s [with patch] p=0.0002.

In contrast, the similarities in affecting conduction velocity in control hearts were not replicated in infarcted hearts. In the Mawad paper, an improvement in the apical infarcted region from 24.3 ± 4.9 cm/s to 30.1 ± 4.2 cm/s ($P < 0.05$, $n = 5$) was found.

In our paper, there was significant noise to make interpretation of any changes difficult and unreliable. Since rh237 binds to the membrane of cardiomyocytes, it is understandable why the signal was noisy in areas relatively devoid of myocytes. (Efimov, Nikolski and Salama, 2004) Additionally, increasing the dose of rh237 administered did not seem to increase the signal. Interestingly though a reliable signal could be seen in infarcted hearts in the smaller rat model.(Mawad *et al.*, 2016) This may be due to the earlier 2 week time point of explantation, where the scar was not fully formed and therefore a sufficiently higher concentration of cardiomyocytes could have been present rather than a thinned established scar.(Sun and Weber, 2000) Alternatively it could be due to differences in anatomy and collateral circulation between species. Rats have a relatively higher amount of collateral circulation and therefore there could have been a greater concentration of myocytes in the infarcted region.(Maxwell, Hearse and Yellon, 1987) Notably, in both animals models, application of the patch caused minimal effects to the action potential duration / morphology.

Any material that can affect conduction velocity could be pro-arrhythmic especially if a slowing of conduction occurs. Heterogeneous depolarisation through healthy tissue and scar tissue can promote the development of re-entrant mechanisms.(Dumotier, 2015) This is in contrast to early and delayed after depolarisations which specifically are related to intracellular calcium concentrations or pacemaker currents which are related to spontaneous activity.(Dumotier, 2015) Therefore, it was critical to perform arrhythmia provocation protocols and reassuringly the patch did not increase the propensity for arrhythmia formation after ex-vivo assessment. In contrast, the patch did not appear to be antiarrhythmic, which would be beneficial in the proarrhythmic

post infarct environment.

**Future work**

The results of the experiments carried out in this chapter form a basis for future work in this area. Identifying the exact mechanism of how the conductive polymer affected conduction velocity; for example, by performing mathematical modelling experiments is of critical importance. This work is currently ongoing with our collaborating group (Prof Steven Niederer).

Since we were unable to detect a reliable signal in the infarcted region of rabbit hearts, the conductive polymer could be tested on hearts that had undergone ischaemia-reperfusion injuries. This model is likely to be of greater translational importance and clinical relevance due to the widespread adoption of primary percutaneous angioplasty world-wide. With ischaemia reperfusion, as opposed to a permanent ligation model, there will be a relatively higher concentration of myocytes contained in the infarct region and therefore the signal may be less noisy.(Lindsey *et al.*, 2018)

Importantly, there were no significant changes in arrhythmogenicity when the patch was applied ex-vivo. Whilst ex-vivo work can provide some indication as to the arrhythmogenicity of a certain substrate, further in-vivo work is needed with both telemetry monitoring to assess spontaneous arrhythmia and in-vivo arrhythmia provocation protocols before any firm conclusions can be made.

It is possible that suturing may have affected conduction velocity due to ischemic

micro injury; however, the sutures used were 8.0 prolene with minimal profile. In the study by Mawad et al, a laser was used to attach the patch (photoadhesion with green laser), therefore minimising epicardial injury.(Mawad *et al.*, 2016) This laser was not available during the experiments presented in this chapter. Preliminary experiments were performed with gluing the patch; however, the glue interfered with the rh237 signal and caused significant noise making interpretation of the results impossible.

In addition to testing the effect of the conductive polymer, a non-conductive polymer should have been used to act as a control group. This would elucidate whether the observed effect on control heart was due to the electrical activity rather than the mechanical properties of the scaffold. Also it is important to ascertain whether the conduction velocity changes were persistent after immediate removal of the patch to see if the changes were permanent or reversible.

Finally, ex-vivo optical mapping analyses epicardial surface conduction, therefore whether or not the conductive polymer affected transmural conduction remains to be seen and further dedicated transmural optical mapping studies are needed. However, this is a limitation of whole heart optical mapping studies in general.

**Translational outlook**

The paradigm behind the use of conductive polymers is to act as a vehicle for pluripotent stem cell delivery onto infarcted hearts when there is a potential for an increase in arrhythmia. It is hoped that by acting as an electrical sink, the relative disorganised depolarisation that occurs with heterogenous scarred myocardium and

immature cells contained within the graft will not propagate into pathological arrhythmia.(Balint, Cassidy and Cartmell, 2014)(Cui, Yang and Li, 2016) However, it has become apparent that engineered heart tissue does not appear to be proarrhythmic in nature in numerous animal models.(Weinberger *et al.*, 2016)(Gao *et al.*, 2018) These findings are consistent with experiments carried out in this thesis. This could be related to mode of delivery (epicardial patch versus intramyocardial injection) or the higher basal beating rates found in small animal models preventing electrical coupling to human iPSC-CM with lower basal beating rates. If there is lack of electrical coupling, the use of a conductive polymer in conjunction with hiPSC-CM EHTs may be of less importance. However, an infarcted heart has by definition impaired conduction and conductive polymers therefore may be of benefit, even if there is a lack of arrhythmias with EHT grafting. Additionally, if the cells are injected intramyocardially, where it has been reported that there is an increased propensity for arrhythmia, there may be a use for conductive polymers if they can be applied in a minimally invasive way.(Chong *et al.*, 2014)(Liu *et al.*, 2018)

**Conclusion**

In summary, the conductive nature of the patch affected myocardial electrophysiology, by slowing global conduction. The changes did not appear to be arrhythmogenic after programmed electrical stimulation with extra stimulus and burst pacing protocols. These preliminary findings suggest that the conductive polymer may be safe to use as a vehicle to aid hiPSC-CM graft integration. Future work should include the in-vitro assessment of hiPSC-CM coupling to the patch and in-vivo assessment of arrhythmogenicity with and without the addition of hiPSC-CM seeded onto the patch.

# Chapter 7: Final Discussion

## 7.1 Introduction

The final discussion will critically appraise the results presented in this thesis, the use of engineered heart tissue / hiPSC-CM as future treatment modalities for chronic heart failure and the further work needed to move from the preclinical to the clinical stage. Then, an evaluation of the initial aims and hypotheses of this thesis will be discussed.

## 7.2 Are EHTs a suitable modality for the future of regenerative medicine?

Engineered heart tissue was first pioneered by Prof Eschenhagen last century, and the field has steadily evolved over time.(Eschenhagen *et al.*, 1997) The potential advantages with using EHTs as a therapeutic modality for treating heart failure are vast and it has the potential to revolutionise the treatment of heart failure. For example, one of the long term goals of the technology is to replace the lost / damaged muscle that occurs in end stage heart failure and therefore potentially reverse the disease process. Currently, there are no other modalities of treatment that can do this except cardiac transplantation, and there will never be enough donors as required.

Whilst cellular retention appears to be a major advantage of EHTs over existing modalities (intra-myocardial / intracoronary) with long term retention of cells several months reported, more work is needed to improve cell retention further if a muscle replacement strategy is to be pursued (versus paracrine). For example, with the work presented in this thesis it was found that nearly 80% of the cells were lost at one month and some groups have reported only 10% of the cells remaining in large animals models.(Gao *et al.*, 2018) Whether or not this is related to the xenograft

nature of the grafts remains to be elucidated.

If a muscle replacement strategy is to be pursued, electromechanical integration is prerequisite. The lack of electrical coupling observed in most studies and this thesis does suggest that at present prolonged paracrine factor release could be a major mediator of repair.(Jackman *et al.*, 2018)(Shadrin *et al.*, 2017) Further work is needed regarding our hypothesis of mechanotransduction. It has been noted that a fibrous layer exists between the graft / host and more research is required to ascertain the cause, and devise new strategies to minimise it. If there is less physical distance between the graft and the host, gap junctions can form and electrical synchronisation may improve. Intramyocardial delivery of a very large number of cells results in electrical integration and therefore it may be possible that a combined approach is need to improve efficacy further, for example, intramyocardial cell injection and engineered heart tissue grafting in the same setting.

It is important to note that the ventricle of a human heart is significantly thicker than a rabbit heart, and to date EHTs approaching 1cm (normal human ventricle wall diameter) in thickness are lacking which again may be necessary if pursuing a muscle replacement strategy. Recently, one group has stacked together multiple individual EHTs in layers to create fused EHTs up to 1cm in diameter and containing up to 800 x $10^6$ myocytes (Zimmerman presented at ESC 2019, unpublished). Whilst the grafts used in this thesis were approximately 1-1.5mm thick and survived relatively well to one week without the addition of endothelial cells, it is likely that any upscaling in thickness will need a preformed vascular network to promote survival since the diffusion of nutrients / oxygen through a graft of several millimetres will be

insufficient. However, preliminary experiments involving added non-cardiomyocytes in this thesis resulted in extreme thinning and poor force production, but further work is needed to definitively answer this question, for example the effect of adding endothelial cells without fibroblasts.

Finally, a thoracotomy and therefore open heart surgery is needed to place the patch with current technology. Guidelines state that open heart surgery (CABG) is a class I indication for revascularisation in patients with poor ejection fraction, and therefore if the technology remains as it is, these are probably the patients that will undergo treatment first. In contrast, intracoronary and intramyocardial delivery routes can be administered in a minimally invasive way via a catheter delivered either by the wrist or the groin. Work is ongoing in the Stevens' /Harding's labs regarding minimally invasive ways of delivering the technology, using memory EHTs that can be delivered via a needle into the pericardial space, which then expand to a preformed shape; however, these studies are ongoing and not at an advanced stage. Data from another group has shown feasibility of this approach but in a small animal model.(Montgomery *et al.*, 2017)

### 7.3 Are iPSC-CM the correct cell type in regenerative medicine?

The development of induced pluripotent stem cells is undoubtedly one of this century greatest scientific advances and has the potential to revolutionise the treatment of cardiovascular disease.(Takahashi K et al, 2006) IPS derived cardiomyocytes have also expanded the way we understand diseases via disease modelling and are providing a treatment platform for testing new pharmaceuticals / toxicology screening.(Yoshida and Yamanaka, 2017) Pluripotent stem cells, which can be embryological or somatic cell derived (induced) are currently the sole cell type that

can actually produce bona fide cardiomyocytes, with current next generation differentiation protocols able to generate hundreds of millions / up to 1 billion cells in a single differentiation at ever increasing efficiencies along with rapidly decreasing costs.(Oikonomopoulos, Kitani and Wu, 2018) When used as a regenerative medicine tool they have also been shown to electrically couple to the host in large animal models and relatively long term engraftment rates have been shown up to 3 months in duration.(Chong *et al.*, 2014)(Liu *et al.*, 2018)(Shiba *et al.*, 2016)

HiPSC-CM have the potential to cause a paradigm shift in the treatment of heart failure by providing a potentially autologous treatment option to reverse the disease process (if derived from a human somatic cell source). For example, a clinical future potential scenario could be patient X, who is seen in a routine clinic appointment with advanced heart failure refractory to existing treatment methods. He is deemed suitable for EHT therapy and a skin / blood or even urine sample is taken from the patient. The somatic cells are the differentiated ex-vivo into cardiomyocytes, an EHT is created and then implanted back into the patient as a day case procedure. Will this scenario ever become a reality? At the moment, the whole process takes a number of months and is extremely costly. It is also known that that hiPSC-CMs from disease patients do not behave in the same way as healthy donors, and exhibit some characteristics of the underlying disease process.(Smith *et al.*, 2018) Therefore, allogenic cell banks that are HLA matched from healthy donors, and have undergone extensive prior testing may be a more suitable option. Indeed, HLA hiPSC-CMs banks are being created in Japan at present.

Whilst iPSC-CM have several advantages over other cell types, fundamentally

hiPSC-CM are still foetal in phenotype and lack several characteristics that make them mature. These include lack of t-tubules, sarcomere disorganisation and a reliance on glycolysis as opposed to fatty acid oxidation. Various techniques have been employed to make them more adult like but they still remain fundamentally immature.(Yoshida and Yamanaka, 2017) The immature characteristics will introduce heterogeneity into myocardium, which is pro-arrhythmic and has been observed in large animal preclinical studies.(Romagnuolo *et al.*, 2019)(Chong *et al.*, 2014) Indeed, in-vivo maturation of the grafts has coincided with a reduction in the incidence of arrhythmias in preclinical studies.(Romagnuolo *et al.*, 2019) However, this is balanced against an increased susceptibility to hypoxia and reduced proliferative ability.

Other limitations and concerns are regarding the formation of teratomas.(Chen, Matsa and Wu, 2016) Although metabolic selection and improved differentiation and purification protocols have limited the proportion of undifferentiated pluripotent cells, we still do not know what level of purity is considered safe for the first in human studies. Longer follow up periods are needed past 3 months to fully evaluate the risk of teratoma formation, as well as long term analyses of cell survival, arrhythmogenicity and effects on left ventricular function.

### 7.4 Insights from rabbit EHT grafting

The rabbit model was a suitable bridge between small and large animals models and the experiments contained in this thesis revealed insights into retention rates at a stratified time points up to 1 month as well as detailed information of graft vascularisation, safety and efficacy. Importantly, the EHTs did not provoke

arrhythmia when compared to controls with no animal (from 14 that underwent EHT grafting) suffering from a clinically significant arrhythmia (e.g sustained ventricular tachycardia / ventricular fibrillation). These findings are consistent with the literature.(Gao *et al.*, 2018)(Pecha *et al.*, 2019)

The lack of electromechanical coupling and fibrous layer that was observed is an important hurdle that needs to be overcome. This is a consistent finding that could be due to a persistent inflammatory reaction due to the xenograft nature of the graft. This could be overcome by using cells that are HLA matched or using different more enhanced immunosuppressive regimes. Further work is needed however to characterise the patches and compare them to human muscle characteristics (conduction velocities, force production). For example, even with the best available patches reported the conduction velocities and force generated are still below human equivalents.(Ronaldson-Bouchard *et al.*, 2018)

### 7.5 Moving from animal to human experiments

The traditional natural evolution from preclinical to phase I clinical trials involves testing in small animal models including mice and rat with a move to larger animal models including pig and macaque if efficacy is shown. The rabbit was a suitable intermediate and enabled us to test an upscaled patch of a potentially clinically relevant size. It is likely that a larger cell number will be needed for the first in human clinical trials and this would need to include either a larger patch or multiple patches implanted on the same patient. For example, 10-15 upscaled EHTs would contain a clinical relevant cell number of between 700 million - 1 billion cells (theoretical capacity of 68 million in each EHT). Since they are relatively easily attached to the epicardial surface with fine sutures, we do not see any potential issues regarding

using multiple patches, especially when implanting onto a much larger human ventricle (when compared to a rabbit).

Finally, a fully randomised blinded pre-clinical trial would be needed to show efficacy before any attempt at seeking approval for a first-in-human trial, with good laboratory practice and good manufacturing practice guidelines. Therefore, a GMP line would need to be tested first and work is ongoing with our collaborator (Prof Denning lab) regarding EHT consisting of GMP compatible line. Furthermore, whether efficacy needs to be tested in a large model remains to be seen and the Harding group is planning to gather advice from the Medicines & Healthcare products Regulatory Agency (MHRA).

The only 2 active clinical programs using this cell type at the moment use an allogenic approach as opposed to an autologous approach. In addition, it is likely that the majority of the first-in-human trials will follow this approach.(Eschenhagen and Weinberger, 2019) The main reasons for this include: 1) allogenic cells can be from either from an hESC or hiPSC source. The human embryonic source is by some believed to be the less manipulated preferred cell type; 2) estimates and calculations predict that only a limited number of hiPSC lines would be needed to match the majority of any given general population in terms of major histocompatibility complexes or human leukocyte antigens; 3) The regulatory issues associated with the use of a GMP line that has been extensively tested for genomic stability and viral contamination would be significantly less as opposed to lines from each patient produced in a time limited way; 4) Large numbers of cardiomyocytes could be differentiated from extensively tested approved lines, cryopreserved, quality

control tested and then used as an off the shelf product; and 5) this model has the potential to be an immediate and viable business model. (Eschenhagen and Weinberger, 2019)

The quality control testing and off the shelf business model is probably why all planned and ongoing trials are using this allogenic model. The first-in-human clinical study was carried out in France, and involved the transplantation of fibrin based patches containing human embryonic cardiovascular progenitors (hESC- derived SSEA-1+; stage-specific embryonic antigen-1; marker loss of pluripotency).(Menasché *et al.*, 2018) Cells were not HLA matched and from an allogenic source. Immunosuppression was stopped after 4 weeks to act as a safety feature. A recently approved trial is due to start in Japan using cell sheet technology has replicated this type of approach with stopping immunosuppression after 4 weeks. The cell number is around 100million which could generate new myocardium but the discontinuation of immunosuppression will cause allogenic cell death. Any long-term benefit of this type of approach will therefore be paracrine in nature. However, the trial was designed purely to assess safety and it is unlikely that prolonged periods of immunosuppression would have had prior ethical approval (Eschenhagen and Weinberger, 2019)

For an allogenic approach to provide muscle replacement, lifelong immunosuppression would be needed. Chronic immunosuppression is associated with kidney failure, severe infections, skin tumours. For a renal or heart transplant, the benefits of transplantation outweigh the negative effects of lifelong immunosuppression. At the present time with existing technologies, the risk benefit

ratio is unclear regarding cell therapy for end-stage heart failure. Creating a universal cell donor line would circumvent these issues. A study involving CRISPR-Cas has been recently published in mice, showing long term retention without immunosuppression using MHC class I and II inactivated and CD47 over expressed cells (hiPSC derived smooth muscle, endothelial and cardiomyocytes).(Deuse *et al.*, 2019) However, a GMP universal cell donor line would need to undergo extensive testing and gene editing produces additional safety issues because of off target effects. Therefore a commercial / human trial product is a long way from a reality. (Eschenhagen and Weinberger, 2019)

So why is the autologous approach being neglected currently? The first articles reported that undifferentiated iPSCs were rejected in syngeneic recipients which implied that the reprogramming procedures utilised and in-vitro culturing practices caused aberrations that were recognised as foreign by the host recipient.(Garreta *et al.*, 2018) However newer studies do suggest long term integration without immunosuppression. For example, long term retention of cells up to 1 year were found after transplantation of autologous hiPSC-derived retinal epithelial cells to a patient with macular degeneration.(Mandai *et al.*, 2017) The other arguments include the opposite of the beneficial factors of using an allogenic source namely, lack of off the shelf product, cost, lack of business model, time, quality control and rigours of cell line testing. Currently, the process of differentiation and reprogramming to make a viable product takes 4 months but with ever increasing and efficient protocols this may improve.(Eschenhagen and Weinberger, 2019)

Autologous approaches to hiPSC cell therapy are ongoing in other organ systems. For example, autologous limbal stem cells (Holoclar) are being used to hopefully

repair damaged corneas by replacing epithelial cells. If successful, an autologous hiPSC-CM therapy for ischaemic heart disease may be a reality in the future. (Eschenhagen and Weinberger, 2019)

## 7.6 Conclusion

The final part of this thesis discusses the aims and hypotheses, limitations of the current work and future work needed in this area.

## 7.7 Review of Aims

### 7.7.1 Characterisation of upscaled EHT

Upscaling was a collaborative effort with Prof Eschenhagen's group who designed the larger equipment and kindly provided it to us. The creation of the larger EHTs was relatively straightforward and similar to first generation EHTs. The upscaling in size was primarily due to an increase in x and y axis as opposed to the z axis. A challenging part was the optimisation of the cell number and the volume of work required to differentiate larger cell numbers (Courtesy Brian Wang, Oisin King, Thomas Owen).

Another challenging part was to develop a way to assess contraction kinetics as the original "White Box" could not handle the 6-well plate. We used a dedicated high frame camera and analysed EHT contraction / relaxation using open source software (Muscle Motion). Whilst the contraction kinetics provided useful information on in-vitro maturation, actual force production would have been more useful to judge as a benchmark against human tissue and first generation EHTs. Work is ongoing using a force transducer that is used to assess the viability and force measurements of ultra-thin myocardial slices.

Other techniques such as measuring calcium transients and immunostaining were relatively straight-forward since the methods had been established at Imperial

College with the first generation EHTs. The use of gCaMP hiPSC-CMs was a major advantage in the fact that we could analyse calcium transients in-vitro without dye loading (Obtained from Conklin laboratory, USA) during various stages of EHT maturation. Difficulties however occurred when assessing conduction velocities. The MEA array was used to assess conduction velocity; however, on occasion the signal was noisy and inadequate. This may be due to the holes in the EHT or the fact that EHT consists of cells contained within a fibrin based hydrogrel that could act as an insulating layer thereby hindering electrical wavefront detection. Therefore, a more reliable way of assessing conduction velocity in vitro is needed.

### 7.7.2 Development of in-vivo rabbit EHT grafting model

The development of the rabbit model was overall the hardest part of my PhD since there was a lack of expertise involving rabbit surgery at Imperial College London during the set up. However, the extensive help from our collaborators in Glasgow was invaluable in making it a success. Specifically, Mr Michael Dunne (Animal technician) visited Imperial College during the first surgeries to supervise and sign me off as competent to perform the surgery without supervision. In addition, help from the CBS staff (specifically Ms Hannah Jones and Mr Phil Rawson) and Veterinary surgeons (Dr Lindsay Benson and Dr Alasdair Gallie) was also vital. Several steps needed to be optimised (including attachment method and immunosuppression optimisation). Overall, the implementation of the model was however a success and I received an award from Imperial College (Provost's award for excellence in animal research) during the second year of my PhD. This was a team award to represent excellent collaboration between a researcher and CBS staff when performing animal research. Future work to improve the model further will try

and increase cell retention and this will likely involving a multi drug immunosuppression protocol.

### 7.7.3 Development of rabbit in-vivo EHT myocardial infarction model

The myocardial infarction model was implemented based on the SOP from Glasgow University. I trained in Glasgow to learn the skills required and the first procedures at Imperial were performed under direct supervision with the animal technician (Mr Michael Dunne) from Glasgow university. This was invaluable and enabled the successful set up at Imperial College. The infarcts were of mild / moderate category but nevertheless were sufficient to identify a difference between EHTs and fibrin control patches.

### 7.7.4 Development of in-vivo rabbit heart failure model

The development of the in-vivo rabbit heart failure model was technically the most complex of all of the surgeries as it required two thoracotomies which resulted in the development of adhesions. Whilst feasibility was shown, myocardial function did return to baseline on explant without EHT implantation. Therefore the model as it stands will be insufficient to test the efficacy of EHT over sham fibrin control patches. Whether or not this issue will arise with larger infarct sizes remains to be seen. Work is ongoing with our collaborator regarding a minimally invasive way of creating the infarct which will address the adhesion issue and also should cause less stress to the animal having to recover from two open surgeries.

## 7.8 Review of hypotheses

### 7.8.1 Engineered heart tissue will mature in-vitro over time

The upscaled engineered heart tissue matured over time in-vitro as assessed by calcium transients, cellular alignment and contraction kinetics. Dynamic rocking culture coupled with auxotonic load from the posts was used to mature them, which is similar to other groups. Whether or not the addition of electrical stimulation or hormonal treatment would have improved maturation is an area of future research.

### 7.8.2 The encapsulation of hiPSC-CM in the EHT will increase cell retention

In this study, the engraftment rate was approximately 25% at 4 weeks with a steady decline over serial time points. When compared to historical data on intracoronary and intramyocardial injection this modality of delivery has far superior retention rates.

### 7.8.3 EHT will provoke arrhythmia when grafted onto infarcted rabbit hearts

This hypothesis was incorrect and may be related to the modality of delivery since intramyocardial injection is associated with an increase in arrhythmia burden. The fibrous layer that forms between the EHT and the host may prevent electromechanical coupling and therefore arrhythmia formation.

### 7.8.4 EHT will improve function in an intermediate model of myocardial infarction

We found a significant increase in ventricular function in the cell treated group when EHTs were grafted onto infarcted hearts. Whilst the echocardiographic correlation between the two blinded echocardiographers was significant, it was single blind in nature (the animal operator knew which patch was inserted onto which animal).

Therefore efficacy should be tested in a fully blinded manner and work is ongoing to perform this at two centres (Imperial College and Glasgow).

### 7.8.5 A conductive polymer patch will alter myocardial conduction when grafted onto the epicardium

It was discovered during ex-vivo optical mapping experiments that the conductive polymer appeared to slow conduction velocity around the patch. The findings were not replicated in infarcted hearts. These findings are consistent with data previously published by our collaborative research group in a rat model. It was disappointing regarding data from the infarcted hearts due to the noisy signal and future work could consider an ischaemia reperfusion mechanism or different animal model.

## 7.9 Limitations of current work

There were several limitations to this current work which will be summarised below.

### 7.9.1 In-vitro work

**The addition of non-cardiomyocytes to EHTs**

Firstly, regarding optimisation of the large EHTs, we did not fully investigate the addition of non-cardiomyocytes to the patches. The poor force contractions and extensive thinning seen with the addition of fibroblasts / endothelial cells may be due to the ratio of cells used and a lower ratio of non-cardiomyocytes may have been beneficial.

**Cell number**

Although we found that between 15-20 million cells was the optimal cell number, this

number is likely to be below what is required for human clinical translational studies. Based on data from smaller EHTs, the theoretical maximum number of cells that could be contained in one patch is 68million. Additionally, immunostaining of EHTs with troponin T indicated that the cellular density was relatively sparse at 15-20 million, indicating that there is ample room to increase cell number. Therefore, further work is needed to assess feasibility of increasing the cell number in each patch. Using patches with a greater cell number will be resource intensive and therefore the plan is to collaborate with one of the BHF centres in Nottingham (Prof Denning's lab) which has a robotic facility for creating larger numbers of cells.

**Gene analysis / PCR**

Whilst we did assess several maturation markers including contraction kinetics, calcium transients, and troponin T alignment, other parameters would have been beneficial. For example, force measurements ($mN/mm^2$) would have provided a means to compare to human tissue. Although we did attempt to assess conduction velocities, further n-numbers are needed in both groups to draw any reliable conclusions. In addition, the analysis of gene expression markers; for example, by RNA sequencing, especially when compared to conventional 2D cell monolayers would have been interesting. For example, both ventricular and atrial forms of myosin light chain are expressed in both atrial and immature ventricular myocytes but the atrial isoform is downregulated in in mature ventricular myocytes. Other genes that could have been useful to analyse include structural (TNNI3, MYL2, MYOM2), excitation- contraction coupling (CASQ2, S100A1, PLN), and metabolic (COX6A2, CKMT2, CKM) markers of myocyte maturation.(Shadrin *et al.*, 2017) However, since this has been extensively validated in the smaller EHTs it

was not deemed essential.

### 7.9.2 In-vivo work

#### Echocardiography

Echocardiographic measurements are inherent to variability. MRI assessment of left ventricular function and volumes is the gold standard with superior resolution but due to logistics and excessive cost this was not possible.

#### Telemetry

The telemetry system was useful and clinical grade; however, intermitted recordings were taken (average 1 minute every 5 minutes with newer system). A more accurate system would include continuous telemetry monitoring, since clinically significant arrhythmia could have occurred in a time period which was not being recorded by the transmitter.

#### Translational Model

Although we successfully set up the myocardial infarction model at Imperial College to test efficacy of the EHT, this is not a clinically relevant scenario. As mentioned previously EHT efficacy needs to be tested on a heart failure model where the scar is established.

### 7.9.3 Ex-vivo work

#### Conductive polymer

Although we were able to show that the conduction of the surface of the heart was immediately affected by the conductive polymer patch it is clear that more extensive

testing is needed and the data obtained is preliminary. For example, by performing experiments using appropriate controls (non-conductive patch) and laser attachment instead of suturing to cause minimal injury to the epicardial surface. The lack of signal in a permanent MI model may be related to the lack of collateral circulation in the rabbit model when compared to rat and an ischaemia reperfusion model may be more appropriate. The fact that the patch appears to slow epicardial conduction may not be advantageous since it could predispose to re-entry arrhythmia. Future work should include co-application of the patch with hiPSC-CM.

**Optical Mapping**

Some of the optical mapping experiments were performed with experts at Glasgow University which was helpful and the fact that genetically encoded calcium indicator (gCaMP6F) hiPSC-CMs were used (instead of dye loading) meant that there was no doubt that the calcium signal obtained originated from myocytes within the graft. In the subset of hearts in which no signal was found, immunohistochemistry revealed that troponin was still present in grafts. Further detailed mapping studies could administer lipophilic dyes if the gCAMP signal is silenced, as previously reported.(Weinberger *et al.*, 2016) Further dual voltage and calcium imaging studies could also be carried out to analyse the relationship between the voltage signal originating from the myocardium and the calcium signal in the grafts which could help identify electrical coupling. This work is ongoing with our collaborators at Glasgow University.

### 7.10 Concluding remarks

The work carried out in this PhD has set a strong foundation for future preclinical requirements and a move towards first in human studies. We have shown that the upscaled EHT patch matured in-vitro and showed signs of integration and efficacy in-vivo.

Future steps should include improving immunosuppression protocols to improve cell retention and graft integration. If these steps are successful the next step would be to performed a fully blinded randomised preclinical study performed with a GMP cell line and according to GLP protocols. Only after these steps have been proven to be successful should the process begin to move towards a first in human trial.

Towards the end of this PhD, the retraction of over 30 papers of one of the pioneers of stem cell treatment caused a wave of controversy and a sway of public opinion further towards scepticism of the whole field. This was on a background of numerous disappointing phase I/II clinical trials involving cardiac stem cells, bone marrow stem cells and mesenchymal stem cells.

It must be stated however that iPSC and ESC are the only cell types that can make bonafide cardiomyocytes in-vitro. The preclinical work carried out in thesis and by other groups involving EHTs / biomaterials and hiPSC-CM is far advanced when compared to the cell types and methods of administration used in the first clinical studies. Additionally, there is still a great unmet need for novel therapies for heart failure with a relatively static mortality rate over the last 20 years, being worse than several of the most common cancers, with approximately 1 in 2 patients dying from

end stage heart failure at 5 years. The rush for novel therapies however should not underpin the evaluation of adequately designed preclinical randomised trials and reliable science to drive the field forward.

## 8: Bibliography

Abou-Saleh, H., Zouein, F. A., El-Yazbi, A., Sanoudou, D., Raynaud, C., Rao, C., Pintus, G., Dehaini, H. and Eid, A. H. (2018) 'The march of pluripotent stem cells in cardiovascular regenerative medicine.', *Stem cell research & therapy*. England, 9(1), p. 201. doi: 10.1186/s13287-018-0947-5.

Agah, R., Kirshenbaum, L. A., Abdellatif, M., Truong, L. D., Chakraborty, S., Michael, L. H. and Schneider, M. D. (1997) 'Adenoviral delivery of E2F-1 directs cell cycle reentry and p53- independent apoptosis in postmitotic adult myocardium in vivo', *Journal of Clinical Investigation*. doi: 10.1172/JCI119817.

Ahuja, P., Sdek, P. and MacLellan, W. R. (2007) 'Cardiac myocyte cell cycle control in development, disease, and regeneration.', *Physiological reviews*. doi: 10.1152/physrev.00032.2006.

Akerboom, J., Rivera, J. D. V., Rodríguez Guilbe, M. M., Malavé, E. C. A., Hernandez, H. H., Tian, L., Hires, S. A., Marvin, J. S., Looger, L. L. and Schreiter, E. R. (2009) 'Crystal structures of the GCaMP calcium sensor reveal the mechanism of fluorescence signal change and aid rational design', *Journal of Biological Chemistry*. doi: 10.1074/jbc.M807657200.

Balint, R., Cassidy, N. J. and Cartmell, S. H. (2014) 'Conductive polymers: Towards a smart biomaterial for tissue engineering', *Acta Biomaterialia*. doi: 10.1016/j.actbio.2014.02.015.

Bartunek, J., Behfar, A., Dolatabadi, D., Vanderheyden, M., Ostojic, M., Dens, J., El Nakadi, B., Banovic, M., Beleslin, B., Vrolix, M., Legrand, V., Vrints, C., Vanoverschelde, J. L., Crespo-Diaz, R., Homsy, C., Tendera, M., Waldman, S., Wijns, W. and Terzic, A. (2013) 'Cardiopoietic Stem Cell Therapy in Heart Failure', *Journal of the American College of Cardiology*. doi: 10.1016/j.jacc.2013.02.071.

Bartunek, J., Terzic, A., Davison, B. A., Filippatos, G. S., Radovanovic, S., Beleslin, B., Merkely, B., Musialek, P., Wojakowski, W., Andreka, P., Horvath, I. G., Katz, A., Dolatabadi, D., El Nakadi, B., Arandjelovic, A., Edes, I., Seferovic, P. M., Obradovic, S., Vanderheyden, M., *et al.* (2017) 'Cardiopoietic cell therapy for advanced ischaemic heart failure: Results at 39 weeks of the prospective, randomized, double blind, sham-controlled CHART-1 clinical trial', *European Heart Journal*. doi: 10.1093/eurheartj/ehw543.

Bélichard, P., Savard, P., Cardinal, R., Nadeau, R., Gosselin, H., Paradis, P. and Rouleau, J. L. (1994) 'Markedly different effects on ventricular remodelling result in a decrease in inducibility of ventricular arrhythmias', *Journal of the American College of Cardiology*. doi: 10.1016/0735-1097(94)90440-5.

Bloom, M. W., Greenberg, B., Jaarsma, T., Januzzi, J. L., Lam, C. S. P., Maggioni, A. P., Trochu, J. N. and Butler, J. (2017) 'Heart failure with reduced ejection fraction', *Nature Reviews Disease Primers*. doi: 10.1038/nrdp.2017.58.

Boch, J. (2011) 'TALEs of genome targeting', *Nature Biotechnology*. doi: 10.1038/nbt.1767.

Boettcher, M. and McManus, M. T. (2015) 'Choosing the Right Tool for the Job: RNAi, TALEN, or CRISPR', *Molecular Cell*. doi: 10.1016/j.molcel.2015.04.028.

Bolli, R., Chugh, A. R., D'Amario, D., Loughran, J. H., Stoddard, M. F., Ikram, S., Beache, G. M., Wagner, S. G., Leri, A., Hosoda, T., Sanada, F., Elmore, J. B., Goichberg, P., Cappetta, D., Solankhi, N. K., Fahsah, I., Rokosh, D. G., Slaughter, M. S., Kajstura, J., *et al.* (2011) 'Cardiac stem cells in patients with ischaemic cardiomyopathy (SCIPIO): Initial results of a randomised phase 1 trial', *The Lancet*. doi: 10.1016/S0140-6736(11)61590-0.

Borchert, T., Hübscher, D., Guessoum, C. I., Lam, T. D. D., Ghadri, J. R.,

Schellinger, I. N., Tiburcy, M., Liaw, N. Y., Li, Y., Haas, J., Sossalla, S., Huber, M. A., Cyganek, L., Jacobshagen, C., Dressel, R., Raaz, U., Nikolaev, V. O., Guan, K., Thiele, H., *et al.* (2017) 'Catecholamine-Dependent β-Adrenergic Signaling in a Pluripotent Stem Cell Model of Takotsubo Cardiomyopathy', *Journal of the American College of Cardiology*. doi: 10.1016/j.jacc.2017.06.061.

Breckwoldt, K., Letuffe-Brenière, D., Mannhardt, I., Schulze, T., Ulmer, B., Werner, T., Benzin, A., Klampe, B., Reinsch, M. C., Laufer, S., Shibamiya, A., Prondzynski, M., Mearini, G., Schade, D., Fuchs, S., Neuber, C., Krämer, E., Saleem, U., Schulze, M. L., *et al.* (2017) 'Differentiation of cardiomyocytes and generation of human engineered heart tissue', *Nature Protocols*. doi: 10.1038/nprot.2017.033.

Brown, M. D. and Hudlicka, O. (1991) 'Capillary supply and cardiac performance in the rabbit after chronic dobutamine treatment', *Cardiovascular Research*. doi: 10.1093/cvr/25.11.909.

Burridge, P. W., Matsa, E., Shukla, P., Lin, Z. C., Churko, J. M., Ebert, A. D., Lan, F., Diecke, S., Huber, B., Mordwinkin, N. M., Plews, J. R., Abilez, O. J., Cui, B., Gold, J. D. and Wu, J. C. (2014) 'Chemically Defined and Small Molecule-Based Generation of Human Cardiomyocytes', *Nat Methods*. doi: 10.1038/nmeth.2999.

de By, T. M. M. H., Mohacsi, P., Gummert, J., Bushnaq, H., Krabatsch, T., Gustafsson, F., Leprince, P., Martinelli, L., Meyns, B., Morshuis, M., Netuka, I., Potapov, E., Zittermann, A., Delmo walter, E. M. and Hetzer, R. (2015) 'The European Registry for Patients with Mechanical Circulatory Support (EUROMACS): First annual report', *European Journal of Cardio-thoracic Surgery*. doi: 10.1093/ejcts/ezv096.

Caspi, O., Huber, I., Kehat, I., Habib, M., Arbel, G., Gepstein, A., Yankelson, L., Aronson, D., Beyar, R. and Gepstein, L. (2007) 'Transplantation of Human

Embryonic Stem Cell-Derived Cardiomyocytes Improves Myocardial Performance in Infarcted Rat Hearts', *Journal of the American College of Cardiology*. doi: 10.1016/j.jacc.2007.07.054.

Chan, H. H. L., Meher Homji, Z., Gomes, R. S. M., Sweeney, D., Thomas, G. N., Tan, J. J., Zhang, H., Perbellini, F., Stuckey, D. J., Watt, S. M., Taggart, D., Clarke, K., Martin-Rendon, E. and Carr, C. A. (2012) 'Human cardiosphere-derived cells from patients with chronic ischaemic heart disease can be routinely expanded from atrial but not epicardial ventricular biopsies', *Journal of Cardiovascular Translational Research*. doi: 10.1007/s12265-012-9389-0.

Chen, I. Y., Matsa, E. and Wu, J. C. (2016) 'Induced pluripotent stem cells: at the heart of cardiovascular precision medicine.', *Nature reviews. Cardiology*. doi: 10.1038/nrcardio.2016.36.

Chen, J., Huang, Z. P., Seok, H. Y., Ding, J., Kataoka, M., Zhang, Z., Hu, X., Wang, G., Lin, Z., Wang, S., Pu, W. T., Liao, R. and Wang, D. Z. (2013) 'Mir-17-92 cluster is required for and sufficient to induce cardiomyocyte proliferation in postnatal and adult hearts', *Circulation Research*. doi: 10.1161/CIRCRESAHA.112.300658.

Chen, V. C., Ye, J., Shukla, P., Hua, G., Chen, D., Lin, Z., Liu, J. chang, Chai, J., Gold, J., Wu, J., Hsu, D. and Couture, L. A. (2015) 'Development of a scalable suspension culture for cardiac differentiation from human pluripotent stem cells', *Stem Cell Research*. doi: 10.1016/j.scr.2015.08.002.

Chien, K. R., Frisén, J., Fritsche-Danielson, R., Melton, D. A., Murry, C. E. and Weissman, I. L. (2019) 'Regenerating the field of cardiovascular cell therapy', *Nature Biotechnology*. doi: 10.1038/s41587-019-0042-1.

Chong, J. J. H., Yang, X., Don, C. W., Minami, E., Liu, Y. W., Weyers, J. J., Mahoney, W. M., Van Biber, B., Cook, S. M., Palpant, N. J., Gantz, J. A., Fugate, J.

A., Muskheli, V., Gough, G. M., Vogel, K. W., Astley, C. A., Hotchkiss, C. E., Baldessari, A., Pabon, L., *et al.* (2014) 'Human embryonic-stem-cell-derived cardiomyocytes regenerate non-human primate hearts', *Nature*. doi: 10.1038/nature13233.

Chong, J. J. H. and Murry, C. E. (2014) 'Cardiac regeneration using pluripotent stem cells-Progression to large animal models', *Stem Cell Research*. doi: 10.1016/j.scr.2014.06.005.

Chow, A., Stuckey, D. J., Kidher, E., Rocco, M., Jabbour, R. J., Mansfield, C. A., Darzi, A., Harding, S. E., Stevens, M. M. and Athanasiou, T. (2017) 'Human Induced Pluripotent Stem Cell-Derived Cardiomyocyte Encapsulating Bioactive Hydrogels Improve Rat Heart Function Post Myocardial Infarction', *Stem Cell Reports*. doi: 10.1016/j.stemcr.2017.09.003.

Chowdhury, R. A., Tzortzis, K. N., Dupont, E., Selvadurai, S., Perbellini, F., Cantwell, C. D., Ng, F. S., Simon, A. R., Terracciano, C. M. and Peters, N. S. (2018) 'Concurrent micro-to macro-cardiac electrophysiology in myocyte cultures and human heart slices', *Scientific Reports*. doi: 10.1038/s41598-018-25170-9.

Chung, E. S., Miller, L., Patel, A. N., Anderson, R. D., Mendelsohn, F. O., Traverse, J., Silver, K. H., Shin, J., Ewald, G., Farr, M. J., Anwaruddin, S., Plat, F., Fisher, S. J., AuWerter, A. T., Pastore, J. M., Aras, R. and Penn, M. S. (2015) 'Changes in ventricular remodelling and clinical status during the year following a single administration of stromal cell-derived factor-1 non-viral gene therapy in chronic ischaemic heart failure patients: The STOP-HF randomized Phase II trial', *European Heart Journal*. doi: 10.1093/eurheartj/ehv254.

Coats, A. J. S., Pieske, B., Linde, C., Jankowska, E. A., Ruschitzka, F., Rutten, F. H., Rosano, G. M. C., Bueno, H., Riley, J. P., Cleland, J. G. F., Parissis, J. T.,

González-Juanatey, J. R., Ruilope, L. M., Jessup, M., van der Meer, P., Nihoyannopoulos, P., Anker, S. D., Harjola, V.-P., Falk, V., *et al.* (2016) '2016 ESC Guidelines for the diagnosis and treatment of acute and chronic heart failure: The Task Force for the diagnosis and treatment of acute and chronic heart failure of the European Society of Cardiology (ESC)Developed with the special contribution of', *European Heart Journal*, 37(27), pp. 2129–2200. doi: https://doi.org/10.1093/eurheartj/ehw128.

Coker, S. J. (1989) 'Anesthetized rabbit as a model for ischemia- and reperfusion-induced arrhythmias: Effects of quinidine and bretylium', *Journal of Pharmacological Methods*. doi: 10.1016/0160-5402(89)90064-8.

Cook, C., Cole, G., Asaria, P., Jabbour, R. and Francis, D. P. (2014) 'The annual global economic burden of heart failure', *International Journal of Cardiology*, 171(3). doi: 10.1016/j.ijcard.2013.12.028.

Cui, Z., Yang, B. and Li, R. K. (2016) 'Application of Biomaterials in Cardiac Repair and Regeneration', *Engineering*. doi: 10.1016/J.ENG.2016.01.028.

Denning, C., Borgdorff, V., Crutchley, J., Firth, K. S. A., George, V., Kalra, S., Kondrashov, A., Hoang, M. D., Mosqueira, D., Patel, A., Prodanov, L., Rajamohan, D., Skarnes, W. C., Smith, J. G. W. and Young, L. E. (2016) 'Cardiomyocytes from human pluripotent stem cells: From laboratory curiosity to industrial biomedical platform', *Biochimica et Biophysica Acta - Molecular Cell Research*. doi: 10.1016/j.bbamcr.2015.10.014.

Deuse, T., Hu, X., Gravina, A., Wang, D., Tediashvili, G., De, C., Thayer, W. O., Wahl, A., Garcia, J. V., Reichenspurner, H., Davis, M. M., Lanier, L. L. and Schrepfer, S. (2019) 'Hypoimmunogenic derivatives of induced pluripotent stem cells evade immune rejection in fully immunocompetent allogeneic recipients', *Nature*

*Biotechnology*. doi: 10.1038/s41587-019-0016-3.

Don, C. W. and Murry, C. E. (2013) 'Improving survival and efficacy of pluripotent stem cell-derived cardiac grafts', *Journal of Cellular and Molecular Medicine*. doi: 10.1111/jcmm.12147.

Dumotier, B. M. (2015) 'A straightforward guide to the basic science behind arrhythmogenesis', *Postgraduate Medical Journal*. doi: 10.1136/postgradmedj-2014-305647rep.

Eder, A., Hansen, A., Uebeler, J., Schulze, T., Neuber, C., Schaaf, S., Yuan, L., Christ, T., Vos, M. A. and Eschenhagen, T. (2014) 'Effects of proarrhythmic drugs on relaxation time and beating pattern in rat engineered heart tissue', *Basic Research in Cardiology*. doi: 10.1007/s00395-014-0436-7.

Eder, A., Vollert, I., Hansen, A. and Eschenhagen, T. (2016) 'Human engineered heart tissue as a model system for drug testing', *Advanced Drug Delivery Reviews*. doi: 10.1016/j.addr.2015.05.010.

Efimov, I. R., Nikolski, V. P. and Salama, G. (2004) 'Optical imaging of the heart', *Circulation Research*. doi: 10.1161/01.RES.0000130529.18016.35.

Eisner, D. A., Caldwell, J. L., Kistamás, K. and Trafford, A. W. (2017) 'Calcium and Excitation-Contraction Coupling in the Heart', *Circulation Research*. doi: 10.1161/CIRCRESAHA.117.310230.

Engel, F. B., Schebesta, M., Duong, M. T., Lu, G., Ren, S., Madwed, J. B., Jiang, H., Wang, Y. and Keating, M. T. (2005) 'p38 MAP kinase inhibition enables proliferation of adult mammalian cardiomyocytes', *Genes and Development*. doi: 10.1101/gad.1306705.

Eschenhagen, T., Fink, C., Remmers, U., Scholz, H., Wattchow, J., Weil, J., Zimmermann, W., Dohmen, H. H., Schäfer, H., Bishopric, N., Wakatsuki, T. and

Elson, E. L. (1997) ‘Three-dimensional reconstitution of embryonic cardiomyocytes in a collagen matrix: a new heart muscle model system.’, *FASEB journal : official publication of the Federation of American Societies for Experimental Biology*.

Eschenhagen, T. and Weinberger, F. (2019) ‘Heart Repair With Myocytes’, *Circulation research*. doi: 10.1161/CIRCRESAHA.118.314336.

Eulalio, A., Mano, M., Ferro, M. D., Zentilin, L., Sinagra, G., Zacchigna, S. and Giacca, M. (2012) ‘Functional screening identifies miRNAs inducing cardiac regeneration’, *Nature*. doi: 10.1038/nature11739.

‘Expression of concern: The SCIPIO trial’ (2015) *The Lancet*. doi: 10.1016/S0140-6736(14)60608-5.

Ezzaher, A., el Houda Bouanani, N. and Crozatier, B. (2017) ‘Force-frequency relations and response to ryanodine in failing rabbit hearts’, *American Journal of Physiology-Heart and Circulatory Physiology*. doi: 10.1152/ajpheart.1992.263.6.h1710.

Fernández-Avilés, F., Sanz-Ruiz, R., Climent, A. M., Badimon, L., Bolli, R., Charron, D., Fuster, V., Janssens, S., Kastrup, J., Kim, H.-S., Lüscher, T. F., Martin, J. F., Menasché, P., Simari, R. D., Stone, G. W., Terzic, A., Willerson, J. T., Wu, J. C., Fernández-Avilés, F., *et al.* (2017) ‘Global position paper on cardiovascular regenerative medicine’, *European Heart Journal*. doi: 10.1093/eurheartj/ehx248.

Fisher, S. A., Doree, C., Mathur, A. and Martin-Rendon, E. (2015) ‘Meta-analysis of cell therapy trials for patients with heart failure’, *Circulation Research*. doi: 10.1161/CIRCRESAHA.116.304386.

Fukushima, S., Varela-Carver, A., Coppen, S. R., Yamahara, K., Felkin, L. E., Lee, J., Barton, P. J. R., Terracciano, C. M. N., Yacoub, M. H. and Suzuki, K. (2007) ‘Direct intramyocardial but not intracoronary injection of bone marrow cells induces

ventricular arrhythmias in a rat chronic ischemic heart failure model', *Circulation*. doi: 10.1161/CIRCULATIONAHA.106.662577.

Gabisonia, K., Prosdocimo, G., Aquaro, G. D., Carlucci, L., Zentilin, L., Secco, I., Ali, H., Braga, L., Gorgodze, N., Bernini, F., Burchielli, S., Collesi, C., Zandonà, L., Sinagra, G., Piacenti, M., Zacchigna, S., Bussani, R., Recchia, F. A. and Giacca, M. (2019) 'MicroRNA therapy stimulates uncontrolled cardiac repair after myocardial infarction in pigs', *Nature*. doi: 10.1038/s41586-019-1191-6.

Gao, L., Gregorich, Z. R., Zhu, W., Mattapally, S., Oduk, Y., Lou, X., Kannappan, R., Borovjagin, A. V., Walcott, G. P., Pollard, A. E., Fast, V. G., Hu, X., Lloyd, S. G., Ge, Y. and Zhang, J. (2018) 'Large cardiac muscle patches engineered from human induced-pluripotent stem cell-derived cardiac cells improve recovery from myocardial infarction in swine', *Circulation*. doi: 10.1161/CIRCULATIONAHA.117.030785.

Garreta, E., Sanchez, S., Lajara, J., Montserrat, N. and Belmonte, J. C. I. (2018) 'Roadblocks in the Path of iPSC to the Clinic', *Current Transplantation Reports*. doi: 10.1007/s40472-018-0177-x.

Giannini, F., Ruparelia, N., Del Furia, F., Romano, V., Ancona, M., Mangieri, A., Regazzoli, D., Latib, A., Godino, C., Ancona, F., Candilio, L., Jabbour, R., Colombo, A. and Montorfano, M. (2017) 'A Novel Technique for Prosthetic Valve Retrieval After Transcatheter Aortic Valve Embolization', *Canadian Journal of Cardiology*, 33(7). doi: 10.1016/j.cjca.2017.03.027.

Godier-Furnémont, A. F. G., Tiburcy, M., Wagner, E., Dewenter, M., Lämmle, S., El-Armouche, A., Lehnart, S. E., Vunjak-Novakovic, G. and Zimmermann, W. H. (2015) 'Physiologic force-frequency response in engineered heart muscle by electromechanical stimulation', *Biomaterials*. doi: 10.1016/j.biomaterials.2015.03.055.

Hansen, A., Eder, A., Bönstrup, M., Flato, M., Mewe, M., Schaaf, S., Aksehirlioglu, B., Schwörer, A., Uebeler, J. and Eschenhagen, T. (2010) 'Development of a drug screening platform based on engineered heart tissue', *Circulation Research*. doi: 10.1161/CIRCRESAHA.109.211458.

Harding, S. E. (2014) 'Large stem cell-derived cardiomyocyte grafts: Cellular ventricular assist devices?', *Molecular Therapy*. doi: 10.1038/mt.2014.97.

Hare, J. M., Fishman, J. E., Gerstenblith, G., DiFede Velazquez, D. L., Zambrano, J. P., Suncion, V. Y., Tracy, M., Ghersin, E., Johnston, P. V., Brinker, J. A., Breton, E., Davis-Sproul, J., Schulman, I. H., Byrnes, J., Mendizabal, A. M., Lowery, M. H., Rouy, D., Altman, P., Wong Po Foo, C., *et al.* (2012) 'Comparison of allogeneic vs autologous bone marrow-derived mesenchymal stem cells delivered by transendocardial injection in patients with ischemic cardiomyopathy: The POSEIDON randomized trial', *JAMA - Journal of the American Medical Association*. doi: 10.1001/jama.2012.25321.

Hashimoto, H., Olson, E. N. and Bassel-Duby, R. (2018) 'Therapeutic approaches for cardiac regeneration and repair', *Nature Reviews Cardiology*. doi: 10.1038/s41569-018-0036-6.

Hassink, R. J., Pasumarthi, K. B., Nakajima, H., Rubart, M., Soonpaa, M. H., De La Rivière, A. B., Doevendans, P. A. and Field, L. J. (2008) 'Cardiomyocyte cell cycle activation improves cardiac function after myocardial infarction', *Cardiovascular Research*. doi: 10.1093/cvr/cvm101.

Hendrikx, M., Hensen, K., Clijsters, C., Jongen, H., Koninckx, R., Bijnens, E., Ingels, M., Jacobs, A., Geukens, R., Dendale, P., Vijgen, J., Dilling, D., Steels, P., Mees, U. and Rummens, J. L. (2006) 'Recovery of regional but not global contractile function by the direct intramyocardial autologous bone marrow transplantation: Results from

a randomized controlled clinical trial', *Circulation*. doi: 10.1161/CIRCULATIONAHA.105.000505.

Henning, R. J. (2011) 'Stem cells in cardiac repair', *Future Cardiology*. doi: 10.2217/fca.10.109.

Hinson, J. T., Chopra, A., Nafissi, N., Polacheck, W. J., Benson, C. C., Swist, S., Gorham, J., Yang, L., Schafer, S., Sheng, C. C., Haghighi, A., Homsy, J., Hubner, N., Church, G., Cook, S. A., Linke, W. A., Chen, C. S., Seidman, J. G. and Seidman, C. E. (2015) 'Titin mutations in iPS cells define sarcomere insufficiency as a cause of dilated cardiomyopathy', *Science*. doi: 10.1126/science.aaa5458.

Hirt, M. N., Sörensen, N. A., Bartholdt, L. M., Boeddinghaus, J., Schaaf, S., Eder, A., Vollert, I., Stöhr, A., Schulze, T., Witten, A., Stoll, M., Hansen, A. and Eschenhagen, T. (2012) 'Increased afterload induces pathological cardiac hypertrophy: A new in vitro model', *Basic Research in Cardiology*. doi: 10.1007/s00395-012-0307-z.

Hofmann, M., Wollert, K. C., Meyer, G. P., Menke, A., Arseniev, L., Hertenstein, B., Ganser, A., Knapp, W. H. and Drexler, H. (2005) 'Monitoring of bone marrow cell homing into the infarcted human myocardium', *Circulation*. doi: 10.1161/01.CIR.0000163546.27639.AA.

Huang, N. F., Serpooshan, V., Morris, V. B., Sayed, N., Pardon, G., Abilez, O. J., Nakayama, K. H., Pruitt, B. L., Wu, S. M., Yoon, Y., Zhang, J. and Wu, J. C. (2018) 'Big bottlenecks in cardiovascular tissue engineering', *Communications Biology*. doi: 10.1038/s42003-018-0202-8.

Hughes, G. C., Post, M. J., Simons, M. and Annex, B. H. (2015) 'Translational Physiology: Porcine models of human coronary artery disease: implications for preclinical trials of therapeutic angiogenesis', *Journal of Applied Physiology*. doi: 10.1152/japplphysiol.00465.2002.

Ieda, M., Fu, J. D., Delgado-Olguin, P., Vedantham, V., Hayashi, Y., Bruneau, B. G. and Srivastava, D. (2010) 'Direct reprogramming of fibroblasts into functional cardiomyocytes by defined factors', *Cell*. doi: 10.1016/j.cell.2010.07.002.

Iseoka, H., Miyagawa, S., Fukushima, S., Saito, A., Masuda, S., Yajima, S., Ito, E., Sougawa, N., Takeda, M., Harada, A., Lee, J.-K. and Sawa, Y. (2017) 'Pivotal Role of Non-cardiomyocytes in Electromechanical and Therapeutic Potential of Induced Pluripotent Stem Cell-Derived Engineered Cardiac Tissue', *Tissue Engineering Part A*. doi: 10.1089/ten.tea.2016.0535.

Isorni, M.-A., Casanova, A., Piquet, J., Bellamy, V., Pignon, C., Puymirat, E. and Menasche, P. (2015) 'Comparative Analysis of Methods to Induce Myocardial Infarction in a Closed-Chest Rabbit Model', *BioMed Research International*. doi: 10.1155/2015/893051.

Jabbour, A., Hayward, C. S., Keogh, A. M., Kotlyar, E., McCrohon, J. A., England, J. F., Amor, R., Liu, X., Li, X. Y., Zhou, M. D., Graham, R. M. and MacDonald, P. S. (2011) 'Parenteral administration of recombinant human neuregulin-1 to patients with stable chronic heart failure produces favourable acute and chronic haemodynamic responses', *European Journal of Heart Failure*. doi: 10.1093/eurjhf/hfq152.

Jackman, C. P., Ganapathi, A. M., Asfour, H., Qian, Y., Allen, B. W., Li, Y. and Bursac, N. (2018) 'Engineered cardiac tissue patch maintains structural and electrical properties after epicardial implantation', *Biomaterials*. doi: 10.1016/j.biomaterials.2018.01.002.

Jackman, C. P., Carlson, A. L. and Bursac, N. (2016) 'Dynamic culture yields engineered myocardium with near-adult functional output', *Biomaterials*. doi: 10.1016/j.biomaterials.2016.09.024.

Jean, S. M., Sharma, P., Taylor, D. and Mook, D. (2009) 'Cyclosporine-induced

gingival overgrowth in New Zealand white rabbits (Oryctolagus cuniculus)', *Comparative Medicine*.

Ben Jehuda, R., Eisen, B., Shemer, Y., Mekies, L. N., Szantai, A., Reiter, I., Cui, H., Guan, K., Haron-Khun, S., Freimark, D., Sperling, S. R., Gherghiceanu, M., Arad, M. and Binah, O. (2018) 'CRISPR correction of the PRKAG2 gene mutation in the patient's induced pluripotent stem cell-derived cardiomyocytes eliminates electrophysiological and structural abnormalities', *Heart Rhythm*. doi: 10.1016/j.hrthm.2017.09.024.

Kai, D., Prabhakaran, M. P., Jin, G. and Ramakrishna, S. (2011) 'Polypyrrole-contained electrospun conductive nanofibrous membranes for cardiac tissue engineering', *Journal of Biomedical Materials Research - Part A*. doi: 10.1002/jbm.a.33200.

Karantalis, V., Difede, D. L., Gerstenblith, G., Pham, S., Symes, J., Zambrano, J. P., Fishman, J., Pattany, P., McNiece, I., Conte, J., Schulman, S., Wu, K., Shah, A., Breton, E., Davis-Sproul, J., Schwarz, R., Feigenbaum, G., Mushtaq, M., Suncion, V. Y., *et al.* (2014) 'Autologous mesenchymal stem cells produce concordant improvements in regional function, tissue perfusion, and fibrotic burden when administered to patients undergoing coronary artery bypass grafting: The prospective randomized study of mesenchymal stem ce', *Circulation Research*. doi: 10.1161/CIRCRESAHA.114.303180.

Kattman, S. J., Witty, A. D., Gagliardi, M., Dubois, N. C., Niapour, M., Hotta, A., Ellis, J. and Keller, G. (2011) 'Stage-specific optimization of activin/nodal and BMP signaling promotes cardiac differentiation of mouse and human pluripotent stem cell lines', *Cell Stem Cell*. doi: 10.1016/j.stem.2010.12.008.

Kawamura, M., Miyagawa, S., Fukushima, S., Saito, A., Miki, K., Funakoshi, S.,

Yoshida, Y., Yamanaka, S., Shimizu, T., Okano, T., Daimon, T., Toda, K. and Sawa, Y. (2017) 'Enhanced Therapeutic Effects of Human iPS Cell Derived-Cardiomyocyte by Combined Cell-Sheets with Omental Flap Technique in Porcine Ischemic Cardiomyopathy Model', *Scientific Reports*. doi: 10.1038/s41598-017-08869-z.

Kehat, I., Kenyagin-Karsenti, D., Snir, M., Segev, H., Amit, M., Gepstein, A., Livne, E., Binah, O., Itskovitz-Eldor, J. and Gepstein, L. (2001) 'Human embryonic stem cells can differentiate into myocytes with structural and functional properties of cardiomyocytes', *Journal of Clinical Investigation*. doi: 10.1172/JCI200112131.

Kehat, I., Khimovich, L., Caspi, O., Gepstein, A., Shofti, R., Arbel, G., Huber, I., Satin, J., Itskovitz-Eldor, J. and Gepstein, L. (2004) 'Electromechanical integration of cardiomyocytes derived from human embryonic stem cells', *Nature Biotechnology*. doi: 10.1038/nbt1014.

Kensah, G., Lara, A. R., Dahlmann, J., Zweigerdt, R., Schwanke, K., Hegermann, J., Skvorc, D., Gawol, A., Azizian, A., Wagner, S., Maier, L. S., Krause, A., Dräger, G., Ochs, M., Haverich, A., Gruh, I. and Martin, U. (2013) 'Murine and human pluripotent stem cell-derived cardiac bodies form contractile myocardial tissue in vitro', *European Heart Journal*. doi: 10.1093/eurheartj/ehs349.

Kolesky, D. B., Homan, K. A., Skylar-Scott, M. A. and Lewis, J. A. (2016) 'Three-dimensional bioprinting of thick vascularized tissues', *Proceedings of the National Academy of Sciences*. doi: 10.1073/pnas.1521342113.

Konermann, M., Sanner, B. M., Horstmann, E., Grotz, J., Laschewski, F., Josephs, W., Odenthal, H. J. and Sturm, A. (1997) 'Changes of the left ventricle after myocardial infarction--estimation with cine magnetic resonance imaging during the first six months.', *Clinical cardiology*. United States, 20(3), pp. 201–212. doi: 10.1002/clc.4960200305.

van Laake, L. W., Passier, R., Monshouwer-Kloots, J., Verkleij, A. J., Lips, D. J., Freund, C., den Ouden, K., Ward-van Oostwaard, D., Korving, J., Tertoolen, L. G., van Echteld, C. J., Doevendans, P. A. and Mummery, C. L. (2007) 'Human embryonic stem cell-derived cardiomyocytes survive and mature in the mouse heart and transiently improve function after myocardial infarction', *Stem Cell Research*. doi: 10.1016/j.scr.2007.06.001.

Van Laake, L. W., Passier, R., Doevendans, P. A. and Mummery, C. L. (2008) 'Human embryonic stem cell-derived cardiomyocytes and cardiac repair in rodents', *Circulation Research*. doi: 10.1161/CIRCRESAHA.108.175505.

Van Laake, L. W., Van Donselaar, E. G., Monshouwer-Kloots, J., Schreurs, C., Passier, R., Humbel, B. M., Doevendans, P. A., Sonnenberg, A., Verkleij, A. J. and Mummery, C. L. (2010) 'Extracellular matrix formation after transplantation of human embryonic stem cell-derived cardiomyocytes', *Cellular and Molecular Life Sciences*. doi: 10.1007/s00018-009-0179-z.

Laflamme, M. A., Chen, K. Y., Naumova, A. V., Muskheli, V., Fugate, J. A., Dupras, S. K., Reinecke, H., Xu, C., Hassanipour, M., Police, S., O'Sullivan, C., Collins, L., Chen, Y., Minami, E., Gill, E. A., Ueno, S., Yuan, C., Gold, J. and Murry, C. E. (2007) 'Cardiomyocytes derived from human embryonic stem cells in pro-survival factors enhance function of infarcted rat hearts', *Nature Biotechnology*. doi: 10.1038/nbt1327.

Laflamme, M. A. and Murry, C. E. (2005) 'Regenerating the heart', *Nature Biotechnology*. doi: 10.1038/nbt1117.

de Lange, W. J., Grimes, A. C., Hegge, L. F. and Ralphe, J. C. (2012) 'Ablation of cardiac myosin–binding protein-C accelerates contractile kinetics in engineered cardiac tissue', *The Journal of General Physiology*. doi: 10.1085/jgp.201210837.

De Lange, W. J., Grimes, A. C., Hegge, L. F., Spring, A. M., Brost, T. M. and Ralphe, J. C. (2013) 'E258K HCM-causing mutation in cardiac MyBP-C reduces contractile force and accelerates twitch kinetics by disrupting the cMyBP-C and myosin S2 interaction', *The Journal of General Physiology*. doi: 10.1085/jgp.201311018.

Laughner, J. I., Ng, F. S., Sulkin, M. S., Arthur, R. M. and Efimov, I. R. (2012) 'Processing and analysis of cardiac optical mapping data obtained with potentiometric dyes', *American Journal of Physiology-Heart and Circulatory Physiology*. doi: 10.1152/ajpheart.00404.2012.

Lemoine, M. D., Mannhardt, I., Breckwoldt, K., Prondzynski, M., Flenner, F., Ulmer, B., Hirt, M. N., Neuber, C., Horváth, A., Kloth, B., Reichenspurner, H., Willems, S., Hansen, A., Eschenhagen, T. and Christ, T. (2017) 'Human iPSC-derived cardiomyocytes cultured in 3D engineered heart tissue show physiological upstroke velocity and sodium current density', *Scientific Reports*. doi: 10.1038/s41598-017-05600-w.

Lemoine, M. D., Krause, T., Koivumäki, J. T., Prondzynski, M., Schulze, M. L., Girdauskas, E., Willems, S., Hansen, A., Eschenhagen, T. and Christ, T. (2018) 'Human Induced Pluripotent Stem Cell-Derived Engineered Heart Tissue as a Sensitive Test System for QT Prolongation and Arrhythmic Triggers', *Circulation: Arrhythmia and Electrophysiology*. doi: 10.1161/CIRCEP.117.006035.

Leonard, A., Bertero, A., Powers, J. D., Beussman, K. M., Bhandari, S., Regnier, M., Murry, C. E. and Sniadecki, N. J. (2018) 'Afterload promotes maturation of human induced pluripotent stem cell derived cardiomyocytes in engineered heart tissues', *Journal of Molecular and Cellular Cardiology*. doi: 10.1016/j.yjmcc.2018.03.016.

Li, Q., Lin, H., Du, Q., Liu, K., Wang, O., Evans, C., Christian, H., Zhang, C. and Lei, Y. (2018) 'Scalable and physiologically relevant microenvironments for human

pluripotent stem cell expansion and differentiation', *Biofabrication*. doi: 10.1088/1758-5090/aaa6b5.

Li, X., Zhou, J., Liu, Z., Chen, J., Lü, S., Sun, H., Li, J., Lin, Q., Yang, B., Duan, C., Xing, M. M. and Wang, C. (2014) 'A PNIPAAm-based thermosensitive hydrogel containing SWCNTs for stem cell transplantation in myocardial repair', *Biomaterials*. doi: 10.1016/j.biomaterials.2014.03.067.

Li, Y., Asfour, H. and Bursac, N. (2017) 'Age-dependent functional crosstalk between cardiac fibroblasts and cardiomyocytes in a 3D engineered cardiac tissue', *Acta Biomaterialia*. doi: 10.1016/j.actbio.2017.04.027.

Li, Y., He, L., Huang, X., Bhaloo, S. I., Zhao, H., Zhang, S., Pu, W., Tian, X., Li, Yi, Liu, Q., Yu, W., Zhang, L., Liu, X., Liu, K., Tang, J., Zhang, H., Cai, D., Ralf, A. H., Xu, Q., *et al.* (2018) 'Genetic lineage tracing of nonmyocyte population by dual recombinases', *Circulation*. doi: 10.1161/CIRCULATIONAHA.118.034250.

Lian, X., Hsiao, C., Wilson, G., Zhu, K., Hazeltine, L. B., Azarin, S. M., Raval, K. K., Zhang, J., Kamp, T. J. and Palecek, S. P. (2012) 'Robust cardiomyocyte differentiation from human pluripotent stem cells via temporal modulation of canonical Wnt signaling', *Proceedings of the National Academy of Sciences of the United States of America*. doi: 10.1073/pnas.1200250109.

Lin, Z. and Pu, W. T. (2014) 'Strategies for cardiac regeneration and repair', *Science Translational Medicine*. doi: 10.1126/scitranslmed.3006681.

Lindsey, M. L., Bolli, R., Canty, J. M., Du, X.-J., Frangogiannis, N. G., Frantz, S., Gourdie, R. G., Holmes, J. W., Jones, S. P., Kloner, R. A., Lefer, D. J., Liao, R., Murphy, E., Ping, P., Przyklenk, K., Recchia, F. A., Schwartz Longacre, L., Ripplinger, C. M., Van Eyk, J. E., *et al.* (2018) 'Guidelines for experimental models of myocardial ischemia and infarction', *American Journal of Physiology-Heart and*

*Circulatory Physiology*. doi: 10.1152/ajpheart.00335.2017.

Liu, Y.-W., Chen, B., Yang, X., Fugate, J. A., Kalucki, F. A., Futakuchi-Tsuchida, A., Couture, L., Vogel, K. W., Astley, C. A., Baldessari, A., Ogle, J., Don, C. W., Steinberg, Z. L., Seslar, S. P., Tuck, S. A., Tsuchida, H., Naumova, A. V, Dupras, S. K., Lyu, M. S., *et al.* (2018) 'Human embryonic stem cell-derived cardiomyocytes restore function in infarcted hearts of non-human primates.', *Nature biotechnology*. doi: 10.1038/nbt.4162.

Loh, K. M. M., Chen, A., Koh, P. W. W., Deng, T. Z. Z., Sinha, R., Tsai, J. M. M., Barkal, A. A. A., Shen, K. Y. Y., Jain, R., Morganti, R. M. M., Shyh-Chang, N., Fernhoff, N. B. B., George, B. M. M., Wernig, G., Salomon, R. E. E. A., Chen, Z., Vogel, H., Epstein, J. A. A., Kundaje, A., *et al.* (2016) 'Mapping the Pairwise Choices Leading from Pluripotency to Human Bone, Heart, and Other Mesoderm Cell Types', *Cell*. doi: 10.1016/j.cell.2016.06.011.

Lozano, R., Naghavi, M., Foreman, K., Lim, S., Shibuya, K., Aboyans, V., Abraham, J., Adair, T., Aggarwal, R., Ahn, S. Y., AlMazroa, M. A., Alvarado, M., Anderson, H. R., Anderson, L. M., Andrews, K. G., Atkinson, C., Baddour, L. M., Barker-Collo, S., Bartels, D. H., *et al.* (2012) 'Global and regional mortality from 235 causes of death for 20 age groups in 1990 and 2010: A systematic analysis for the Global Burden of Disease Study 2010', *The Lancet*. doi: 10.1016/S0140-6736(12)61728-0.

Lund, L. H., Edwards, L. B., Dipchand, A. I., Goldfarb, S., Kucheryavaya, A. Y., Levvey, B. J., Meiser, B., Rossano, J. W., Yusen, R. D. and Stehlik, J. (2016) 'The Registry of the International Society for Heart and Lung Transplantation: Thirty-third Adult Heart Transplantation Report—2016; Focus Theme: Primary Diagnostic Indications for Transplant', *Journal of Heart and Lung Transplantation*. doi: 10.1016/j.healun.2016.08.017.

Madonna, R., Van Laake, L. W., Davidson, S. M., Engel, F. B., Hausenloy, D. J., Lecour, S., Leor, J., Perrino, C., Schulz, R., Ytrehus, K., Landmesser, U., Mummery, C. L., Janssens, S., Willerson, J., Eschenhagen, T., Ferdinandy, P. and Sluijter, J. P. G. (2016) 'Position Paper of the European Society of Cardiology Working Group Cellular Biology of the Heart: Cell-based therapies for myocardial repair and regeneration in ischemic heart disease and heart failure', *European Heart Journal*. doi: 10.1093/eurheartj/ehw113.

Madonna, R., Van Laake, L. W., Botker, H. E., Davidson, S. M., De Caterina, R., Engel, F. B., Eschenhagen, T., Fernandez-Aviles, F., Hausenloy, D. J., Hulot, J.-S., Lecour, S., Leor, J., Menasché, P., Pesce, M., Perrino, C., Prunier, F., Van Linthout, S., Ytrehus, K., Zimmermann, W.-H., *et al.* (2019) 'ESC Working Group on Cellular Biology of the Heart - Tissue Engineering and Cell-Based Therapies for Cardiac Repair in Ischemic Heart Disease and Heart Failure', *Cardiovascular Research*. doi: 10.1093/cvr/cvz010.

Makkar, R. R., Smith, R. R., Cheng, K., Malliaras, K., Thomson, L. E. J., Berman, D., Czer, L. S. C., Marbán, L., Mendizabal, A., Johnston, P. V., Russell, S. D., Schuleri, K. H., Lardo, A. C., Gerstenblith, G. and Marbán, E. (2012) 'Intracoronary cardiosphere-derived cells for heart regeneration after myocardial infarction (CADUCEUS): A prospective, randomised phase 1 trial', *The Lancet*. doi: 10.1016/S0140-6736(12)60195-0.

Maliken, B. D. and Molkentin, J. D. (2018) 'Undeniable Evidence That the Adult Mammalian Heart Lacks an Endogenous Regenerative Stem Cell', *Circulation*. doi: 10.1161/CIRCULATIONAHA.118.035186.

Mamas, M. A., Sperrin, M., Watson, M. C., Coutts, A., Wilde, K., Burton, C., Kadam, U. T., Kwok, C. S., Clark, A. B., Murchie, P., Buchan, I., Hannaford, P. C. and Myint,

P. K. (2017) ‘Do patients have worse outcomes in heart failure than in cancer? A primary care-based cohort study with 10-year follow-up in Scotland’, *European Journal of Heart Failure*. doi: 10.1002/ejhf.822.

Mandai, M., Watanabe, A., Kurimoto, Y., Hirami, Y., Morinaga, C., Daimon, T., Fujihara, M., Akimaru, H., Sakai, N., Shibata, Y., Terada, M., Nomiya, Y., Tanishima, S., Nakamura, M., Kamao, H., Sugita, S., Onishi, A., Ito, T., Fujita, K., *et al.* (2017) ‘Autologous induced stem-cell-derived retinal cells for macular degeneration’, *New England Journal of Medicine*. doi: 10.1056/NEJMoa1608368.

Mandegar, M. A., Huebsch, N., Frolov, E. B., Shin, E., Truong, A., Olvera, M. P., Chan, A. H., Miyaoka, Y., Holmes, K., Spencer, C. I., Judge, L. M., Gordon, D. E., Eskildsen, T. V., Villalta, J. E., Horlbeck, M. A., Gilbert, L. A., Krogan, N. J., Sheikh, S. P., Weissman, J. S., *et al.* (2016) ‘CRISPR Interference Efficiently Induces Specific and Reversible Gene Silencing in Human iPSCs’, *Cell Stem Cell*. doi: 10.1016/j.stem.2016.01.022.

Mannhardt, I., Breckwoldt, K., Letuffe-Brenière, D., Schaaf, S., Schulz, H., Neuber, C., Benzin, A., Werner, T., Eder, A., Schulze, T., Klampe, B., Christ, T., Hirt, M. N., Huebner, N., Moretti, A., Eschenhagen, T. and Hansen, A. (2016) ‘Human Engineered Heart Tissue: Analysis of Contractile Force.’, *Stem cell reports*. doi: 10.1016/j.stemcr.2016.04.011.

Mannhardt, I., Eder, A., Dumotier, B., Prondzynski, M., Kr-amer, E., Traebert, M., Flenner, F., Stathopoulou, K., Lemoine, M. D., Carrier, L., Christ, T., Eschenhagen, T. and Hansen, A. (2017) ‘Blinded contractility analysis in hipsc-cardiomyocytes in engineered heart tissue format: Comparison with human atrial trabeculae’, *Toxicological Sciences*. doi: 10.1093/toxsci/kfx081.

Martinac, B. (2004) ‘Mechanosensitive ion channels: Molecules of

mechanotransduction', *Journal of Cell Science*. doi: 10.1242/jcs.01232.

Mauritz, C., Martens, A., Rojas, S. V., Schnick, T., Rathert, C., Schecker, N., Menke, S., Glage, S., Zweigerdt, R., Haverich, A., Martin, U. and Kutschka, I. (2011) 'Induced pluripotent stem cell (iPSC)-derived Flk-1 progenitor cells engraft, differentiate, and improve heart function in a mouse model of acute myocardial infarction', *European Heart Journal*. doi: 10.1093/eurheartj/ehr166.

Mawad, D., Mansfield, C., Lauto, A., Perbellini, F., Nelson, G. W., Tonkin, J., Bello, S. O., Carrad, D. J., Micolich, A. P., Mahat, M. M., Furman, J., Payne, D., Lyon, A. R., Gooding, J. J., Harding, S. E., Terracciano, C. M. and Stevens, M. M. (2016) 'A conducting polymer with enhanced electronic stability applied in cardiac models', *Science Advances*. doi: 10.1126/sciadv.1601007.

Maxwell, M. P., Hearse, D. J. and Yellon, D. M. (1987) 'Species variation in the coronary collateral circulation during regional myocardial ischaemia: A critical determinant of the rate of evolution and extent of myocardial infarction', *Cardiovascular Research*. doi: 10.1093/cvr/21.10.737.

McKeage, K. and McCormack, P. L. (2010) 'Basiliximab: A review of its use as induction therapy in renal transplantation', *BioDrugs*. doi: 10.2165/11203990-000000000-00000.

Menasché, P., Alfieri, O., Janssens, S., McKenna, W., Reichenspurner, H., Trinquart, L., Vilquin, J.-T., Marolleau, J.-P., Seymour, B., Larghero, J., Lake, S., Chatellier, G., Solomon, S., Desnos, M. and Hagège, A. A. (2008) 'The Myoblast Autologous Grafting in Ischemic Cardiomyopathy (MAGIC) trial: first randomized placebo-controlled study of myoblast transplantation.', *Circulation*. doi: 10.1161/CIRCULATIONAHA.107.734103.

Menasché, P., Vanneaux, V., Hagège, A., Bel, A., Cholley, B., Parouchev, A.,

Cacciapuoti, I., Al-Daccak, R., Benhamouda, N., Blons, H., Agbulut, O., Tosca, L., Trouvin, J. H., Fabreguettes, J. R., Bellamy, V., Charron, D., Tartour, E., Tachdjian, G., Desnos, M., *et al.* (2018) 'Transplantation of Human Embryonic Stem Cell–Derived Cardiovascular Progenitors for Severe Ischemic Left Ventricular Dysfunction', *Journal of the American College of Cardiology*. doi: 10.1016/j.jacc.2017.11.047.

Meng, X., Stout, D. A., Sun, L., Beingessner, R. L., Fenniri, H. and Webster, T. J. (2013) 'Novel injectable biomimetic hydrogels with carbon nanofibers and self assembled rosette nanotubes for myocardial applications', *Journal of Biomedical Materials Research - Part A*. doi: 10.1002/jbm.a.34400.

Metra, M. and Teerlink, J. R. (2017) 'Seminar Heart failure', *Lancet*. doi: 10.1016/S0140-6736(17)31071-1.

Mihardja, S. S., Sievers, R. E. and Lee, R. J. (2008) 'The effect of polypyrrole on arteriogenesis in an acute rat infarct model', *Biomaterials*. doi: 10.1016/j.biomaterials.2008.07.021.

Mihic, A., Cui, Z., Wu, J., Vlacic, G., Miyagi, Y., Li, S. H., Lu, S., Sung, H. W., Weisel, R. D. and Li, R. K. (2015) 'A conductive polymer hydrogel supports cell electrical signaling and improves cardiac function after implantation into myocardial infarct', *Circulation*. doi: 10.1161/CIRCULATIONAHA.114.014937.

Minami, E. and Murry, C. E. (2007) 'Response to "Comment on 'Transplantation of undifferentiated murine embryonic stem cells in the heart: teratoma formation and immune response'"', *The FASEB Journal*. doi: 10.1096/fj.07-0503ufm.

Miyamoto, K., Akiyama, M., Tamura, F., Isomi, M., Yamakawa, H., Sadahiro, T., Muraoka, N., Kojima, H., Haginiwa, S., Kurotsu, S., Tani, H., Wang, L., Qian, L., Inoue, M., Ide, Y., Kurokawa, J., Yamamoto, T., Seki, T., Aeba, R., *et al.* (2018)

‘Direct In Vivo Reprogramming with Sendai Virus Vectors Improves Cardiac Function after Myocardial Infarction’, *Cell Stem Cell*. doi: 10.1016/j.stem.2017.11.010.

Montgomery, M., Ahadian, S., Davenport Huyer, L., Lo Rito, M., Civitarese, R. A., Vanderlaan, R. D., Wu, J., Reis, L. A., Momen, A., Akbari, S., Pahnke, A., Li, R. K., Caldarone, C. A. and Radisic, M. (2017) ‘Flexible shape-memory scaffold for minimally invasive delivery of functional tissues’, *Nature Materials*. doi: 10.1038/nmat4956.

Mosqueira, D., Mannhardt, I., Bhagwan, J., Lis-Slimak, K., Katili, P., Scott, E., Hassan, M., Prondzynski, M., Harmer, S. C., Tinker, A., Smith, J. G. W., Carrier, L., Williams, P. M., Gaffney, D., Eschenhagen, T., Hansen, A. and Denning, C. (2018) ‘CRISPR/Cas9 editing in hPSC-cardiomyocytes highlights arrhythmias, hypo-contractility and energy depletion as potential therapeutic targets for HCM’, *European Heart Journal*. doi: 10.1093/eurheartj/ehy249.

Mummery, C. L., Zhang, J., Ng, E. S., Elliott, D. A., Elefanty, A. G. and Kamp, T. J. (2012) ‘Differentiation of human embryonic stem cells and induced pluripotent stem cells to cardiomyocytes: A methods overview’, *Circulation Research*. doi: 10.1161/CIRCRESAHA.110.227512.

Myles, R. C., Burton, F. L., Cobbe, S. M. and Smith, G. L. (2011) ‘Alternans of action potential duration and amplitude in rabbits with left ventricular dysfunction following myocardial infarction’, *Journal of Molecular and Cellular Cardiology*. doi: 10.1016/j.yjmcc.2010.11.019.

N., G., N., E. H. B., A., C. and B., C. (1990) ‘Left ventricular function and beta-adrenoceptors in rabbit failing heart’, *American Journal of Physiology - Heart and Circulatory Physiology*.

Naito, H., Melnychenko, I., Didié, M., Schneiderbanger, K., Schubert, P.,

Rosenkranz, S., Eschenhagen, T. and Zimmermann, W. H. (2006) 'Optimizing engineered heart tissue for therapeutic applications as surrogate heart muscle', *Circulation*. doi: 10.1161/CIRCULATIONAHA.105.001560.

Nakai, J., Ohkura, M. and Imoto, K. (2001) 'A high signal-to-noise ca2+ probe composed of a single green fluorescent protein', *Nature Biotechnology*. doi: 10.1038/84397.

Nakane, T., Masumoto, H., Tinney, J. P., Yuan, F., Kowalski, W. J., Ye, F., Leblanc, A. J., Sakata, R., Yamashita, J. K. and Keller, B. B. (2017) 'Impact of Cell Composition and Geometry on Human Induced Pluripotent Stem Cells-Derived Engineered Cardiac Tissue', *Scientific Reports*. doi: 10.1038/srep45641.

Nam, Y.-J., Song, K., Luo, X., Daniel, E., Lambeth, K., West, K., Hill, J. A., DiMaio, J. M., Baker, L. A., Bassel-Duby, R. and Olson, E. N. (2013) 'Reprogramming of human fibroblasts toward a cardiac fate', *Proceedings of the National Academy of Sciences*. doi: 10.1073/pnas.1301019110.

Neidig, L. E., Weinberger, F., Palpant, N. J., Mignone, J., Martinson, A. M., Sorensen, D. W., Bender, I., Nemoto, N., Reinecke, H., Pabon, L., Molkentin, J. D., Murry, C. E. and van Berlo, J. H. (2018) 'Evidence for Minimal Cardiogenic Potential of Stem Cell Antigen 1–Positive Cells in the Adult Mouse Heart', *Circulation*. doi: 10.1161/circulationaha.118.035273.

Nelson, T. J., Martinez-Fernandez, A., Yamada, S., Perez-Terzic, C., Ikeda, Y. and Terzic, A. (2009) 'Repair of acute myocardial infarction with induced pluripotent stem cells induced by human stemness factors', *Circulation*. doi: 10.1161/CIRCULATIONAHA.109.865154.

Odiete, O., Hill, M. F. and Sawyer, D. B. (2012) 'Neuregulin in cardiovascular development and disease.', *Circulation research*. doi:

10.1161/CIRCRESAHA.112.267286.

Oikonomopoulos, A., Kitani, T. and Wu, J. C. (2018) 'Pluripotent Stem Cell-Derived Cardiomyocytes as a Platform for Cell Therapy Applications: Progress and Hurdles for Clinical Translation', *Molecular Therapy*. doi: 10.1016/j.ymthe.2018.02.026.

Olson, E. N. (2014) 'MicroRNAs as therapeutic targets and biomarkers of cardiovascular disease', *Science Translational Medicine*. doi: 10.1126/scitranslmed.3009008.

Patel, A. N., Henry, T. D., Quyyumi, A. A., Schaer, G. L., Anderson, R. D., Toma, C., East, C., Remmers, A. E., Goodrich, J., Desai, A. S., Recker, D. and DeMaria, A. (2016) 'Ixmyelocel-T for patients with ischaemic heart failure: a prospective randomised double-blind trial', *The Lancet*. doi: 10.1016/S0140-6736(16)30137-4.

Pecha, S., Yorgan, K., Röhl, M., Geertz, B., Hansen, A., Weinberger, F., Sehner, S., Ehmke, H., Reichenspurner, H., Eschenhagen, T. and Schwoerer, A. P. (2019) 'Human iPS cell-derived engineered heart tissue does not affect ventricular arrhythmias in a guinea pig cryo-injury model', *Scientific Reports*. doi: 10.1038/s41598-019-46409-z.

Perin, E. C., Willerson, J. T., Pepine, C. J., Henry, T. D., Ellis, S. G., Zhao, D. X. M., Silva, G. V., Lai, D., Thomas, J. D., Kronenberg, M. W., Martin, A. D., Anderson, R. D., Traverse, J. H., Penn, M. S., Anwaruddin, S., Hatzopoulos, A. K., Gee, A. P., Taylor, D. A., Cogle, C. R., *et al.* (2012) 'Effect of transendocardial delivery of autologous bone marrow mononuclear cells on functional capacity, left ventricular function, and perfusion in chronic heart failure: The FOCUS-CCTRN trial', *JAMA - Journal of the American Medical Association*. doi: 10.1001/jama.2012.418.

Pfannkuche, K., Neuss, S., Pillekamp, F., Frenzel, L. P., Attia, W., Hannes, T., Salber, J., Hoss, M., Zenke, M., Fleischmann, B. K., Hescheler, J. and Šarić, T.

(2010) ‘Fibroblasts Facilitate the Engraftment of Embryonic Stem Cell-Derived Cardiomyocytes on Three-Dimensional Collagen Matrices and Aggregation in Hanging Drops’, *Stem Cells and Development*. doi: 10.1089/scd.2009.0255.

Podesser, B., Wollenek, G., Seitelberger, R., Siegel, H., Wolner, E., Firbas, W. and Tschabitscher, M. (1997) ‘Epicardial branches of the coronary arteries and their distribution in the rabbit heart: The rabbit heart as a model of regional ischemia’, *Anatomical Record*. doi: 10.1002/(SICI)1097-0185(199704)247:4<521::AID-AR11>3.0.CO;2-R.

Pogwizd, S. M. and Bers, D. M. (2008) ‘Rabbit models of heart disease’, *Drug Discovery Today: Disease Models*. doi: 10.1016/j.ddmod.2009.02.001.

Porrello, E. R., Mahmoud, A. I., Simpson, E., Johnson, B. A., Grinsfelder, D., Canseco, D., Mammen, P. P., Rothermel, B. A., Olson, E. N. and Sadek, H. A. (2013) ‘Regulation of neonatal and adult mammalian heart regeneration by the miR-15 family.’, *Proceedings of the National Academy of Sciences of the United States of America*. doi: 10.1073/pnas.1208863110.

Qian, K., Huang, C. L., Chen, H., Blackbourn, L. W., Chen, Y., Cao, J., Yao, L., Sauvey, C., Du, Z. and Zhang, S. C. (2014) ‘A simple and efficient system for regulating gene expression in human pluripotent stem cells and derivatives’, *Stem Cells*. doi: 10.1002/stem.1653.

Qian, L., Huang, Y., Spencer, C. I., Foley, A., Vedantham, V., Liu, L., Conway, S. J., Fu, J. D. and Srivastava, D. (2012) ‘In vivo reprogramming of murine cardiac fibroblasts into induced cardiomyocytes’, *Nature*. doi: 10.1038/nature11044.

Rao, C., Prodromakis, T., Kolker, L., Chaudhry, U. A. R., Trantidou, T., Sridhar, A., Weekes, C., Camelliti, P., Harding, S. E., Darzi, A., Yacoub, M. H., Athanasiou, T. and Terracciano, C. M. (2013) ‘The effect of microgrooved culture substrates on

calcium cycling of cardiac myocytes derived from human induced pluripotent stem cells', *Biomaterials*. doi: 10.1016/j.biomaterials.2012.11.055.

Redd, M. A., Zeinstra, N., Qin, W., Wei, W., Martinson, A., Wang, Y., Wang, R. K., Murry, C. E. and Zheng, Y. (2019) 'Patterned human microvascular grafts enable rapid vascularization and increase perfusion in infarcted rat hearts', *Nature Communications*. doi: 10.1038/s41467-019-08388-7.

Reed, A., Kohl, P. and Peyronnet, R. (2014) 'Molecular candidates for cardiac stretch-activated ion channels', *Global Cardiology Science and Practice*. doi: 10.5339/gcsp.2014.19.

Ren, Y., Lee, M. Y., Schliffke, S., Paavola, J., Amos, P. J., Ge, X., Ye, M., Zhu, S., Senyei, G., Lum, L., Ehrlich, B. E. and Qyang, Y. (2011) 'Small molecule Wnt inhibitors enhance the efficiency of BMP-4-directed cardiac differentiation of human pluripotent stem cells', *Journal of Molecular and Cellular Cardiology*. doi: 10.1016/j.yjmcc.2011.04.012.

Riegler, J., Tiburcy, M., Ebert, A., Tzatzalos, E., Raaz, U., Abilez, O. J., Shen, Q., Kooreman, N. G., Neofytou, E., Chen, V. C., Wang, M., Meyer, T., Tsao, P. S., Connolly, A. J., Couture, L. A., Gold, J. D., Zimmermann, W. H. and Wu, J. C. (2015) 'Human engineered heart muscles engraft and survive long term in a rodent myocardial infarction model', *Circulation Research*. doi: 10.1161/CIRCRESAHA.115.306985.

Riolobos, L., Hirata, R. K., Turtle, C. J., Wang, P. R., Gornalusse, G. G., Zavajlevski, M., Riddell, S. R. and Russell, D. W. (2013) 'HLA engineering of human pluripotent stem cells', *Molecular Therapy*. doi: 10.1038/mt.2013.59.

Romagnuolo, R., Masoudpour, H., Porta-Sánchez, A., Qiang, B., Barry, J., Laskary, A., Qi, X., Massé, S., Magtibay, K., Kawajiri, H., Wu, J., Valdman Sadikov, T.,

Rothberg, J., Panchalingam, K. M., Titus, E., Li, R. K., Zandstra, P. W., Wright, G. A., Nanthakumar, K., *et al.* (2019) 'Human Embryonic Stem Cell-Derived Cardiomyocytes Regenerate the Infarcted Pig Heart but Induce Ventricular Tachyarrhythmias', *Stem Cell Reports*. doi: 10.1016/j.stemcr.2019.04.005.

Ronaldson-Bouchard, K., Ma, S. P., Yeager, K., Chen, T., Song, L. J., Sirabella, D., Morikawa, K., Teles, D., Yazawa, M. and Vunjak-Novakovic, G. (2018) 'Advanced maturation of human cardiac tissue grown from pluripotent stem cells', *Nature*. doi: 10.1038/s41586-018-0016-3.

Ryffel, B., Donatsch, P., Madörin, M., Matter, B. E., Rüttimann, G., Schön, H., Stoll, R. and Wilson, J. (1983) 'Toxicological evaluation of cyclosporin A', *Archives of Toxicology*. doi: 10.1007/BF00302721.

Sadahiro, T. (2019) 'Cardiac regeneration with pluripotent stem cell-derived cardiomyocytes and direct cardiac reprogramming.', *Regenerative therapy*. Netherlands, 11, pp. 95–100. doi: 10.1016/j.reth.2019.06.004.

Sala, L., van Meer, B. J., Tertoolen, L. G. J., Bakkers, J., Bellin, M., Davis, R. P., Denning, C., Dieben, M. A. E., Eschenhagen, T., Giacomelli, E., Grandela, C., Hansen, A., Holman, E. R., Jongbloed, M. R. M., Kamel, S. M., Koopman, C. D., Lachaud, Q., Mannhardt, I., Mol, M. P. H., *et al.* (2017) 'MUSCLEMOTION', *Circulation Research*. doi: 10.1161/circresaha.117.312067.

Sala, L., Van Meer, B. J., Tertoolen, L. G. J., Bakkers, J., Bellin, M., Davis, R. P., Denning, C., Dieben, M. A. E., Eschenhagen, T., Giacomelli, E., Grandela, C., Hansen, A., Holman, E. R., Jongbloed, M. R. M., Kamel, S. M., Koopman, C. D., Lachaud, Q., Mannhardt, I., Mol, M. P. H., *et al.* (2018) 'Musclemotion: A versatile open software tool to quantify cardiomyocyte and cardiac muscle contraction in vitro and in vivo', *Circulation Research*. doi: 10.1161/CIRCRESAHA.117.312067.

Sanganalmath, S. K. and Bolli, R. (2013) ‘Cell therapy for heart failure: A comprehensive overview of experimental and clinical studies, current challenges, and future directions’, *Circulation Research*. doi: 10.1161/CIRCRESAHA.113.300219.

Saravanan, S., Sareen, N., Abu-El-Rub, E., Ashour, H., Sequiera, G. L., Ammar, H. I., Gopinath, V., Shamaa, A. A., Sayed, S. S. E., Moudgil, M., Vadivelu, J. and Dhingra, S. (2018) ‘Graphene Oxide-Gold Nanosheets Containing Chitosan Scaffold Improves Ventricular Contractility and Function After Implantation into Infarcted Heart’, *Scientific reports*. doi: 10.1038/s41598-018-33144-0.

Schwartz, P. J., Gnecchi, M., Dagradi, F., Castelletti, S., Parati, G., Spazzolini, C., Sala, L. and Crotti, L. (2019) ‘From patient-specific induced pluripotent stem cells to clinical translation in long QT syndrome Type 2’, *European Heart Journal*. doi: 10.1093/eurheartj/ehz023.

Schwarzer, M. (2015) ‘Models to Investigate Cardiac Metabolism’, in *The Scientist’s Guide to Cardiac Metabolism*. doi: 10.1016/b978-0-12-802394-5.00008-x.

Sekine, H., Shimizu, THobo, K., Sekiya, S., Yang, J., Yamato, M., Kurosawa, H., Kobayashi, E. and Okano, T. (2008) ‘Endothelial cell coculture within tissue-engineered cardiomyocyte sheets enhances neovascularization and improves cardiac function of ischemic hearts.’, *Circulation*. doi: 10.1161/CIRCULATIONAHA.107.757286.

Shadrin, I. Y., Allen, B. W., Qian, Y., Jackman, C. P., Carlson, A. L., Juhas, M. E. and Bursac, N. (2017) ‘Cardiopatch platform enables maturation and scale-up of human pluripotent stem cell-derived engineered heart tissues’, *Nature Communications*. doi: 10.1038/s41467-017-01946-x.

Shiba, Y., Gomibuchi, T., Seto, T., Wada, Y., Ichimura, H., Tanaka, Y., Ogasawara,

T., Okada, K., Shiba, N., Sakamoto, K., Ido, D., Shiina, T., Ohkura, M., Nakai, J., Uno, N., Kazuki, Y., Oshimura, M., Minami, I. and Ikeda, U. (2016) 'Allogeneic transplantation of iPS cell-derived cardiomyocytes regenerates primate hearts', *Nature*. doi: 10.1038/nature19815.

Smith, J. G. W., Owen, T., Bhagwan, J. R., Mosqueira, D., Scott, E., Mannhardt, I., Patel, A., Barriales-Villa, R., Monserrat, L., Hansen, A., Eschenhagen, T., Harding, S. E., Marston, S. and Denning, C. (2018) 'Isogenic Pairs of hiPSC-CMs with Hypertrophic Cardiomyopathy/LVNC-Associated ACTC1 E99K Mutation Unveil Differential Functional Deficits', *Stem Cell Reports*. doi: 10.1016/j.stemcr.2018.10.006.

Smith, J. R., Maguire, S., Davis, L. A., Alexander, M., Yang, F., Chandran, S., ffrench-Constant, C. and Pedersen, R. A. (2008) 'Robust, Persistent Transgene Expression in Human Embryonic Stem Cells Is Achieved with AAVS1-Targeted Integration', *Stem Cells*. doi: 10.1634/stemcells.2007-0039.

Stöhr, A., Friedrich, F. W., Flenner, F., Geertz, B., Eder, A., Schaaf, S., Hirt, M. N., Uebeler, J., Schlossarek, S., Carrier, L., Hansen, A. and Eschenhagen, T. (2013) 'Contractile abnormalities and altered drug response in engineered heart tissue from Mybpc3-targeted knock-in mice', *Journal of Molecular and Cellular Cardiology*. doi: 10.1016/j.yjmcc.2013.07.011.

Sun, Y. and Weber, K. T. (2000) 'Infarct scar: A dynamic tissue', *Cardiovascular Research*. doi: 10.1016/S0008-6363(00)00032-8.

Takahashi K, Tanabe K, Ohnuki M, Narita M, Ichisaka T, Tomoda K, Y. S. (2006) 'Induction of pluripotent stem cells from mouse embryonic and adult fibroblast cultures by defined factors.', *Cell*. doi: 10.1016/j.cell.2006.07.024.

Tan, M.-Y., Xia, B., Xiao, Z., Fan, Z.-W., Zhou, H., Guo, X. and Huang, Y.-C. (2017)

‘Development of a new model for acute myocardial infarction in rabbits.’, *The Journal of veterinary medical science*. Japan, 79(3), pp. 467–473. doi: 10.1292/jvms.16-0114.

Taylor, C. J., Ordóñez-Mena, J. M., Roalfe, A. K., Lay-Flurrie, S., Jones, N. R., Marshall, T. and Hobbs, F. D. R. (2019) ‘Trends in survival after a diagnosis of heart failure in the United Kingdom 2000-2017: population based cohort study’, *BMJ (Online)*. doi: 10.1136/bmj.l223.

Tiburcy, M., Hudson, J. E., Balfanz, P., Schlick, S., Meyer, T., Liao, M. L. C., Levent, E., Raad, F., Zeidler, S., Wingender, E., Riegler, J., Wang, M., Gold, J. D., Kehat, I., Wettwer, E., Ravens, U., Dierickx, P., Van Laake, L. W., Goumans, M. J., *et al.* (2017) ‘Defined engineered human myocardium with advanced maturation for applications in heart failure modeling and repair’, *Circulation*. doi: 10.1161/CIRCULATIONAHA.116.024145.

Tirziu, D., Giordano, F. J. and Simons, M. (2010) ‘Cell Communications in the Heart’, *Circulation*. doi: 10.1161/circulationaha.108.847731.

Tohyama, S., Tanosaki, S., Someya, S., Fujita, J. and Fukuda, K. (2017) ‘Manipulation of Pluripotent Stem Cell Metabolism for Clinical Application’, *Current Stem Cell Reports*. doi: 10.1007/s40778-017-0073-9.

Tulloch, N. L., Muskheli, V., Razumova, M. V., Korte, F. S., Regnier, M., Hauch, K. D., Pabon, L., Reinecke, H. and Murry, C. E. (2011) ‘Growth of engineered human myocardium with mechanical loading and vascular coculture’, *Circulation Research*. doi: 10.1161/CIRCRESAHA.110.237206.

Uzun, A. U., Mannhardt, I., Breckwoldt, K., Horváth, A., Johannsen, S. S., Hansen, A., Eschenhagen, T. and Christ, T. (2016) ‘Ca2+-currents in human induced pluripotent stem cell-derived cardiomyocytes effects of two different culture

conditions', *Frontiers in Pharmacology*. doi: 10.3389/fphar.2016.00300.

Wada, R., Muraoka, N., Inagawa, K., Yamakawa, H., Miyamoto, K., Sadahiro, T., Umei, T., Kaneda, R., Suzuki, T., Kamiya, K., Tohyama, S., Yuasa, S., Kokaji, K., Aeba, R., Yozu, R., Yamagishi, H., Kitamura, T., Fukuda, K. and Ieda, M. (2013) 'Induction of human cardiomyocyte-like cells from fibroblasts by defined factors', *Proceedings of the National Academy of Sciences*. doi: 10.1073/pnas.1304053110.

WALKER, N. L., BURTON, F. L., KETTLEWELL, S., SMITH, G. L. and COBBE, S. M. (2007) 'Mapping of Epicardial Activation in a Rabbit Model of Chronic Myocardial Infarction:.', *Journal of Cardiovascular Electrophysiology*. doi: 10.1111/j.1540-8167.2007.00858.x.

Wang, Q., Shui, B., Kotlikoff, M. I. and Sondermann, H. (2008) 'Structural Basis for Calcium Sensing by GCaMP2', *Structure*. doi: 10.1016/j.str.2008.10.008.

Watson, S. A., Duff, J., Bardi, I., Zabielska, M., Atanur, S. S., Jabbour, R. J., Simon, A., Tomas, A., Smolenski, R. T., Harding, S. E., Perbellini, F. and Terracciano, C. M. (2019) 'Biomimetic electromechanical stimulation to maintain adult myocardial slices in vitro', *Nature Communications*. doi: 10.1038/s41467-019-10175-3.

Weinberger, F., Breckwoldt, K., Pecha, S., Kelly, A., Geertz, B., Starbatty, J., Yorgan, T., Cheng, K. H., Lessmann, K., Stolen, T., Marielle, S. C., Smith, G., Reichenspurner, H., Hansen, A. and Eschenhagen, T. (2016) 'Cardiac repair in Guinea pigs with human engineered heart tissue from induced pluripotent stem cells', *Science Translational Medicine*. doi: 10.1126/scitranslmed.aaf8781.

Weinberger, F., Mannhardt, I. and Eschenhagen, T. (2017) 'Engineering Cardiac Muscle Tissue: A Maturating Field of Research', *Circulation Research*. doi: 10.1161/CIRCRESAHA.117.310738.

Welch, S., Plank, D., Witt, S., Glascock, B., Schaefer, E., Chimenti, S., Andreoli, A.

M., Limana, F., Leri, A., Kajstura, J., Anversa, P. and Sussman, M. A. (2002) 'Cardiac-specific IGF-1 expression attenuates dilated cardiomyopathy in tropomodulin-overexpressing transgenic mice', *Circulation Research*. doi: 10.1161/01.RES.0000013780.77774.75.

Xue, T., Cho, H. C., Akar, F. G., Tsang, S. Y., Jones, S. P., Marbán, E., Tomaselli, G. F. and Li, R. A. (2005) 'Functional integration of electrically active cardiac derivatives from genetically engineered human embryonic stem cells with quiescent recipient ventricular cardiomyocytes: Insights into the development of cell-based pacemakers', *Circulation*. doi: 10.1161/01.CIR.0000151313.18547.A2.

Yoshida, Y. and Yamanaka, S. (2017) 'Induced Pluripotent Stem Cells 10 Years Later', *Circulation Research*. doi: 10.1161/CIRCRESAHA.117.311080.

Yusen, R. D., Edwards, L. B., Kucheryavaya, A. Y., Benden, C., Dipchand, A. I., Dobbels, F., Goldfarb, S. B., Levvey, B. J., Lund, L. H., Meiser, B. and Stehlik, J. (2014) 'The registry of the international society for heart and lung transplantation: Thirty-first adult lung and heart-lung transplant report - 2014; Focus theme: Retransplantation', in *Journal of Heart and Lung Transplantation*. doi: 10.1016/j.healun.2014.08.004.

Zhang, L., Sultana, N., Yan, J., Yang, F., Chen, F., Chepurko, E., Yang, F. C., Du, Q., Zangi, L., Xu, M., Bu, L. and Cai, C. L. (2018) 'Cardiac Sca-1 + cells are not intrinsic stem cells for myocardial development, renewal, and repair', *Circulation*. doi: 10.1161/CIRCULATIONAHA.118.035200.

Zhu, K., Wu, Q., Ni, C., Zhang, P., Zhong, Z., Wu, Y., Wang, Y., Xu, Y., Kong, M., Cheng, H., Tao, Z., Yang, Q., Liang, H., Jiang, Y., Li, Q., Zhao, J., Huang, J., Zhang, F., Chen, Q., *et al.* (2018) 'Lack of Remuscularization Following Transplantation of Human Embryonic Stem Cell-Derived Cardiovascular Progenitor Cells in Infarcted

Nonhuman Primates', *Circulation Research*. doi: 10.1161/CIRCRESAHA.117.311578.

Zimmermann, W. H., Schneiderbanger, K., Schubert, P., Didié, M., Münzel, F., Heubach, J. F., Kostin, S., Neuhuber, W. L. and Eschenhagen, T. (2002) 'Tissue engineering of a differentiated cardiac muscle construct', *Circulation Research*. doi: 10.1161/hh0202.103644.

Zimmermann, W. H., Melnychenko, I., Wasmeier, G., Didié, M., Naito, H., Nixdorff, U., Hess, A., Budinsky, L., Brune, K., Michaelis, B., Dhein, S., Schwoerer, A., Ehmke, H. and Eschenhagen, T. (2006) 'Engineered heart tissue grafts improve systolic and diastolic function in infarcted rat hearts', *Nature Medicine*. doi: 10.1038/nm1394.

## 9: Supplementary Appendix

### 9.1 Tyrode's Solution SOP (Rabbit Heart)

| | mM | MW | g/L | 10x Stock / L |
|---|---|---|---|---|
| NaCL | 128.2 | 58.44 | 7.49 | 74.92 |
| CaCL2 (2H20) | 1.3 | 147.02 | 0.191 | |
| KCl | 4.7 | 74.55 | 0.35 | 3.5 |
| MgCL2 (6H20) | 1.05 | 203.31 | 0.213 | 2.13 |
| NaH2PO4 | 1.19 | 119.98 | 0.14 | 1.418 |
| NaHCO3 | 20 | 84.01 | 1.68 | 16.8 |
| Glucose | 11.1 | 180.16 | 2 | 20 |

| | |
|---|---|
| O2 | 95% |
| CO2 | 5% |
| T | 36.5 |
| pH | 7.25 - 7.35 |

1) The first step is to place 1 litre of distilled water into a suitable container and place on a stirrer

2) Then sequentially place all components of the Tyrode's solution (except calcium chloride) into the beaker containing 1 litre of distilled water to make a 10x stock

3) Once dissolved place into a fresh beaker – the 10x stock can be stored in 4 $^{o}$C for up to 2 weeks. If stored stock solution is cloudy discared and make a fresh solution

4) If performing Langendorff experiments – place 200ml of the 10x stock into a 2 litre

beaker and fill the beaker with 1.8ml of distilled water to make 2 litres.

5) Place the 2 litres of stock solution (200ml 10x and 1.8 litre Tyrode's) into the Radoti Langendorff container and bubble 02 (95%) / C02 (5%)

6) Then add CaCL2 to the 2 litre solution

7) Wait until solution is heated to required temperature and pH before performing any experiments

## 9.2 EHT stock solutions (Quick Reference)

1) EHT media (to make up 50ml):

Typically made and stored in 50ml Falcon tubes at 4 $^{o}$C:

- **5ml** Horse serum (10%),
- Insulin **50µl** (0.1%, 10µg/ml),
- Aprotinin **50µl** (0.1% of 33µg/ml),
- **500µl** (1% penicillin/streptomycin).
- **45ml** DMEM + / +.

2) NKM media (to make up 50ml)

- 10% inactive fetal calf serum **(5ml)**
- 1% glutamine; 200mM **(500µl)**
- 1% penicillin/streptomycin **(500µl)**
- DMEM **(44ml)**

3) Aprotinin:

- Add 33mg per 1ml of sterile cell culture grade water. Aliquoted into 50µl PCR tubes and then stored in freezer at -20 $^{o}$C.

4) Fibrinogen:

- 200mg/ml (sterile) in pre-warmed 0.9% Sodium Chloride solution
- Add 72.1µl aprotinin (33mg/ml stock) to 25ml fibrinogen solution
- Mix, aliquot into 100µl and store at -20 $^{o}$C.

5) Thrombin:

- 100U/ml made up in 60% sterile PBS and 40% sterile water.
- Aliquot and store -20 $^{o}$C

6) 10x DMEM solution:

- dissolve 670mg DMEM powder in 5ml cell culture grade water,
- sterile filter and store at +4 $^{o}$C

7) 2x DMEM:

- 2ml 10x DMEM solution
- 2ml Horse serum 2ml,
- 0.2ml of penicillin / streptomycin
- 5.8ml cell culture grade water
- sterile filter and store at +4 $^{o}$C.

## 9.3 List of antibodies used with concentrations

| | | | |
|---|---|---|---|
| **Primary Antibodies** | | | |
| Troponin T | Abcam | AB45932 | 1 in 200 |
| Alpha Actinin | Sigma | A7811 | 1 in 500 |
| ki67 | Abcam | AB9260 | 1 in 250 |
| ku80 | Abcam | ab119935 | 1 in 250 |
| Vimentin | Thermo Fisher | PAI-10003 | 1 in 2000 |
| CD31 | Novus biologicals | NB600-562 | 1 in 25 |
| Troponin T | Abcam | AB10214 | 1 in 500 |
| | | | |
| **Secondary Antibodies** | | | |
| Phalloidin 488 | Sigma | 49409 | 1 in 50 |
| Alexa donkey anti rabbit 488 | Invitrogen | A32790 | 1 in 400 |
| Alexa donkey anti mouse 546 | Invitrogen | A10036 | 1 in 400 |
| Alexa goat anti mouse 647 | Invitrogen | A-21235 | 1 in 400 |
| Hoechst | Thermofisher | 33342 | 1 in 1000 |
| Goat anti mouse (Biotin) | Jackson immunoresearch | 115-067-003 | 1 in 500 |
| Goat anti Rabbit IgG (Biotin) | antibodies online | ABIN2039429 | 1 in 500 |

## 9.4 Wax staining protocol (Courtesy of Lorraine Lawrence)

### Ku 80 / trop / CD31 wax sections

***Always use a positive control slide (Tonsil)***

1. Dewax. 2X15 minutes in **Neo clear**

2. Rinse 30 seconds X2 absolute alcohol.

While dewaxing make up other solutions – citrate buffer

3. Block endogenous peroxidases by incubating sections in Methanolic Hydrogen Peroxide for 10 mins (100ml methanol, 1ml 30 volume peroxide e.g. 450ml methanol and 4.5ml peroxide for one white container).

4. Antigen retrieve by boiling in Citrate buffer pH 6 for 10 minutes. (2.94g Tri sodium Citrate dihydrate/litre distilled water [on histology shelf] **DM water tap**) put some citrate buffer in extra beaker to keep warm – not to cool down. 4 lots of 2.5mins.

5. Rinse in tap water *Sections can be left here safely if emergency happens!*

5. Rinse in PBS. Apply PAP pen ring round section.DO NOT ALLOW SECTION TO DRY OUT or will get high background staining.

6. Block in 5 to 10% serum in PBS (species that secondary antibody raised in e.g. secondary was raised in Goat use NGS) for 1 hour room temperature.

7. Apply Anti Ku80 antibody (1:200 to 1:1000 diluted in the blocking serum as above) Abcam –ab119935.Also apply IgG2b controls to negative slides and leave the PBS control in the blocking serum. Incubate 4C O/N.

8. Wash 3X5 mins wash buffer (0.1% Triton –X-100 in PBS pH7.4).

9. Incubate 1 hour in Goat anti mouse biotinylated secondary antibody at 1:500(Jackson immunoresearch 115-067-003).DO NOT USE SERUM CONTAINING diluents owing to high background. **While incubating make up ABC reagent.**

10. Wash 3X5 mins wash buffer.

11. Incubate in ABC (*just use PBS at pH 7.4*) reagent 30 minutes – **no longer –or get high background.**

12. Wash 3X5 mins wash buffer. Make up DAB kit during last buffer wash

13. Apply DAB kit for 2 to 10 minutes (5ml distilled water – DM – do not use nickel enhancer [blue]). Check development using microscope.

14. Wash in running water for 10 minutes to neutralise DAB.

15. Counterstain with Haematoxylin

the slides were washed in running tap water for 10minutes to neutralise the DAB. The slides were then immersed in 200µl of Vector® Haematoxylin counterstain (Vector Labs) per sample for 5-10 minutes. The sections were then dipped 10x with deionized / distilled water and then the sections were left in running tap water for 5 minutes.

16. dehydrate, clear and mount (DCM).

- 70% IMS 30 seconds with agitation(dehydration)
- 90% IMS 30 seconds with agitation(dehydration)
- 100% IMS 30 seconds with agitation(dehydration)
- 100% IMS 30 seconds with agitation(dehydration)
- 100% IMS 30 seconds with agitation(dehydration)
- Histoclear or Aqua clear or Xylene (Clearing steps)5 minutes
- Histoclear or Aqua clear or Xylene (Clearing steps)5 minutes
- Histoclear or Aqua clear or Xylene (Clearing steps)5 minutes
- Mounting with DPX mountant and coverslip.

17. At press lift on machine and leave for 1 hour on flat surface to dry.

# Permissions for Reuse of Figures

Thank you for your order.

This Agreement between Richard Jabbour ("You") and Springer Nature ("Springer Nature") consists of your license details and the terms and conditions provided by Springer Nature and Copyright Clearance Center.

Your confirmation email will contain your order number for future reference.

| | |
|---|---|
| **License Number** | 4781310208638 |
| **License date** | Mar 03, 2020 |

Printable Details

## Licensed Content

| | |
|---|---|
| **Licensed Content Publisher** | Springer Nature |
| **Licensed Content Publication** | Nature |
| **Licensed Content Title** | Human embryonic-stem-cell-derived cardiomyocytes regenerate non-human primate hearts |
| **Licensed Content Author** | James J. H. Chong et al |
| **Licensed Content Date** | Apr 30, 2014 |

## Order Details

| | |
|---|---|
| **Type of Use** | Thesis/Dissertation |
| **Requestor type** | academic/university or research institute |
| **Format** | print and electronic |
| **Portion** | figures/tables/illustrations |
| **Number of figures/tables/illustrations** | 1 |
| **High-res required** | no |
| **Will you be translating?** | no |
| **Circulation/distribution** | 1 - 29 |
| **Author of this Springer Nature content** | no |

## About Your Work

| | |
|---|---|
| **Title** | Preclinical Testing of an Upscaled Tissue Engineered Stem Cell Patch Towards Use in Translational Studies |
| **Institution name** | Imperial College London |
| **Expected presentation date** | Jan 2022 |

## Additional Data

| | |
|---|---|
| **Portions** | Figure 1 |

## Requestor Location

| | |
|---|---|
| **Requestor Location** | Richard Jabbour<br>3 Allsworth Close<br>Newington<br><br>Sittingbourne, ME9 7NW<br>United Kingdom<br>Attn: Richard Jabbour |

## Tax Details

## Price

| | |
|---|---|
| **Total** | 0.00 USD |

| | |
|---|---|
| **License Number** | 4781300511350 |
| **License date** | Mar 03, 2020 |

Printable Details

## Licensed Content

| | |
|---|---|
| **Licensed Content Publisher** | Wolters Kluwer Health, Inc. |
| **Licensed Content Publication** | Circulation Research |
| **Licensed Content Title** | Calcium and Excitation-Contraction Coupling in the Heart |
| **Licensed Content Author** | David A. Eisner, Jessica L. Caldwell, Kornél Kistamás, et al |
| **Licensed Content Date** | Jul 7, 2017 |
| **Licensed Content Volume** | 121 |
| **Licensed Content Issue** | 2 |

## Order Details

| | |
|---|---|
| **Type of Use** | Dissertation/Thesis |
| **Requestor type** | University/College |
| **Sponsorship** | No Sponsorship |
| **Format** | Print and electronic |
| **Will this be posted on a password protected website?** | Yes |
| **Portion** | Figures/tables/illustrations |
| **Number of figures/tables/illustrations** | 1 |
| **Author of this Wolters Kluwer article** | No |
| **Will you be translating?** | No |
| **Intend to modify/adapt the content** | No |

## About Your Work

| | |
|---|---|
| **Title** | Preclinical Testing of an Upscaled Tissue Engineered Stem Cell Patch Towards Use in Translational Studies |
| **Institution name** | Imperial College London |
| **Expected presentation date** | Jan 2022 |

## Additional Data

| | |
|---|---|
| **Portions** | 1 |

## Requestor Location

| | |
|---|---|
| **Requestor Location** | Richard Jabbour<br>3 Allsworth Close<br>Newington<br><br>Sittingbourne, ME9 7NW<br>United Kingdom<br>Attn: Richard Jabbour |

## Tax Details

| | |
|---|---|
| **Publisher Tax ID** | EU826013006 |

## Price

| | |
|---|---|
| **Total** | 0.00 USD |

## Order Completed

Thank you for your order.

This Agreement between Richard Jabbour ("You") and Wolters Kluwer Health, Inc. ("Wolters Kluwer Health, Inc.") consists of your license details and the terms and conditions provided by Wolters Kluwer Health, Inc. and Copyright Clearance Center.

Your confirmation email will contain your order number for future reference.

| | |
|---|---|
| **License Number** | 4781301415677 |
| **License date** | Mar 03, 2020 |

Printable Details

### Licensed Content

| | |
|---|---|
| **Licensed Content Publisher** | Wolters Kluwer Health, Inc. |
| **Licensed Content Publication** | Circulation Research |
| **Licensed Content Title** | Development of a Drug Screening Platform Based on Engineered Heart Tissue |
| **Licensed Content Author** | Arne Hansen, Alexandra Eder, Marlene Bönstrup, et al |
| **Licensed Content Date** | May 6, 2010 |
| **Licensed Content Volume** | 107 |
| **Licensed Content Issue** | 1 |

### Order Details

| | |
|---|---|
| **Type of Use** | Dissertation/Thesis |
| **Requestor type** | University/College |
| **Sponsorship** | No Sponsorship |
| **Format** | Print and electronic |
| **Will this be posted on a password protected website?** | Yes |
| **Portion** | Figures/tables/illustrations |
| **Number of figures/tables/illustrations** | 1 |
| **Author of this Wolters Kluwer article** | No |
| **Will you be translating?** | No |
| **Intend to modify/adapt the content** | No |

### About Your Work

| | |
|---|---|
| **Title** | Preclinical Testing of an Upscaled Tissue Engineered Stem Cell Patch Towards Use in Translational Studies |
| **Institution name** | Imperial College London |
| **Expected presentation date** | Jan 2022 |

### Additional Data

| | |
|---|---|
| **Portions** | 2 |

### Requestor Location

| | |
|---|---|
| **Requestor Location** | Richard Jabbour<br>3 Allsworth Close<br>Newington<br><br>Sittingbourne, ME9 7NW<br>United Kingdom<br>Attn: Richard Jabbour |

### Tax Details

| | |
|---|---|
| **Publisher Tax ID** | EU826013006 |

### Price

| | |
|---|---|
| **Total** | 0.00 USD |

Thank you for your order.

This Agreement between Richard Jabbour ("You") and Wolters Kluwer Health, Inc. ("Wolters Kluwer Health, Inc.") consists of your license details and the terms and conditions provided by Wolters Kluwer Health, Inc. and Copyright Clearance Center.

Your confirmation email will contain your order number for future reference.

| | |
|---|---|
| **License Number** | 4781311507329 |
| **License date** | Mar 03, 2020 |

Printable Details

### Licensed Content

| | |
|---|---|
| **Licensed Content Publisher** | Wolters Kluwer Health, Inc. |
| **Licensed Content Publication** | Circulation Research |
| **Licensed Content Title** | Engineering Cardiac Muscle Tissue |
| **Licensed Content Author** | Florian Weinberger, Ingra Mannhardt, Thomas Eschenhagen |
| **Licensed Content Date** | Apr 28, 2017 |
| **Licensed Content Volume** | 120 |
| **Licensed Content Issue** | 9 |

### Order Details

| | |
|---|---|
| **Type of Use** | Dissertation/Thesis |
| **Requestor type** | University/College |
| **Sponsorship** | No Sponsorship |
| **Format** | Print and electronic |
| **Will this be posted on a password protected website?** | Yes |
| **Portion** | Figures/tables/illustrations |
| **Number of figures/tables/illustrations** | 2 |
| **Author of this Wolters Kluwer article** | No |
| **Will you be translating?** | No |
| **Intend to modify/adapt the content** | No |

### About Your Work

| | |
|---|---|
| **Title** | Preclinical Testing of an Upscaled Tissue Engineered Stem Cell Patch Towards Use in Translational Studies |
| **Institution name** | Imperial College London |
| **Expected presentation date** | Jan 2022 |

### Additional Data

| | |
|---|---|
| **Portions** | figure 1 and figure 5 |

### Requestor Location

| | |
|---|---|
| **Requestor Location** | Richard Jabbour<br>3 Allsworth Close<br>Newington<br><br>Sittingbourne, ME9 7NW<br>United Kingdom<br>Attn: Richard Jabbour |

### Tax Details

| | |
|---|---|
| **Publisher Tax ID** | EU826013006 |

### Price

| | |
|---|---|
| **Total** | 0.00 USD |

## Order Completed

Thank you for your order.

This Agreement between Richard Jabbour ("You") and Oxford University Press ("Oxford University Press") consists of your license details and the terms and conditions provided by Oxford University Press and Copyright Clearance Center.

Your confirmation email will contain your order number for future reference.

| | |
|---|---|
| **License Number** | 4781320319135 |
| **License date** | Mar 03, 2020 |

Printable Details

### Licensed Content

| | |
|---|---|
| **Licensed Content Publisher** | Oxford University Press |
| **Licensed Content Publication** | European Heart Journal |
| **Licensed Content Title** | Global position paper on cardiovascular regenerative medicine |
| **Licensed Content Author** | Fernández-Avilés, Francisco; Sanz-Ruiz, Ricardo |
| **Licensed Content Date** | May 30, 2017 |
| **Licensed Content Volume** | 38 |
| **Licensed Content Issue** | 33 |

### Order Details

| | |
|---|---|
| **Type of Use** | Thesis/Dissertation |
| **Requestor type** | Educational Institution/Non-commercial/ Not for-profit |
| **Format** | Print and electronic |
| **Portion** | Figure/table |
| **Number of figures/tables** | 1 |
| **Will you be translating?** | No |

### About Your Work

| | |
|---|---|
| **Title** | Preclinical Testing of an Upscaled Tissue Engineered Stem Cell Patch Towards Use in Translational Studies |
| **Institution name** | Imperial College London |
| **Expected presentation date** | Jan 2022 |

### Additional Data

| | |
|---|---|
| **Portions** | 1 |

### Requestor Location

| | |
|---|---|
| **Requestor Location** | Richard Jabbour<br>3 Allsworth Close<br>Newington<br><br>Sittingbourne, ME9 7NW<br>United Kingdom<br>Attn: Richard Jabbour |

### Tax Details

| | |
|---|---|
| **Publisher Tax ID** | GB125506730 |

### Price

| | |
|---|---|
| **Total** | 0.00 USD |

Thank you for your order.

This Agreement between Richard Jabbour ("You") and Wolters Kluwer Health, Inc. ("Wolters Kluwer Health, Inc.") consists of your license details and the terms and conditions provided by Wolters Kluwer Health, Inc. and Copyright Clearance Center.

Your confirmation email will contain your order number for future reference.

| | |
|---|---|
| **License Number** | 4781321003839 |
| **License date** | Mar 03, 2020 |

Printable Details

### Licensed Content

| | |
|---|---|
| **Licensed Content Publisher** | Wolters Kluwer Health, Inc. |
| **Licensed Content Publication** | Circulation Research |
| **Licensed Content Title** | Meta-Analysis of Cell Therapy Trials for Patients With Heart Failure |
| **Licensed Content Author** | Sheila A Fisher, Carolyn Doree, Anthony Mathur, et al |
| **Licensed Content Date** | Jan 28, 2015 |
| **Licensed Content Volume** | 116 |
| **Licensed Content Issue** | 8 |

### Order Details

| | |
|---|---|
| **Type of Use** | Dissertation/Thesis |
| **Requestor type** | University/College |
| **Sponsorship** | No Sponsorship |
| **Format** | Print and electronic |
| **Will this be posted on a password protected website?** | Yes |
| **Portion** | Figures/tables/illustrations |
| **Number of figures/tables/illustrations** | 1 |
| **Author of this Wolters Kluwer article** | No |
| **Will you be translating?** | No |
| **Intend to modify/adapt the content** | No |

### About Your Work

| | |
|---|---|
| **Title** | Preclinical Testing of an Upscaled Tissue Engineered Stem Cell Patch Towards Use in Translational Studies |
| **Institution name** | Imperial College London |
| **Expected presentation date** | Jan 2022 |

### Additional Data

| | |
|---|---|
| **Portions** | 3 |

### Requestor Location

| | |
|---|---|
| **Requestor Location** | Richard Jabbour<br>3 Allsworth Close<br>Newington<br><br>Sittingbourne, ME9 7NW<br>United Kingdom<br>Attn: Richard Jabbour |

### Tax Details

| | |
|---|---|
| **Publisher Tax ID** | EU826013006 |

### Price

| | |
|---|---|
| **Total** | 0.00 USD |

Thank you for your order.

This Agreement between Richard Jabbour ("You") and Wolters Kluwer Health, Inc. ("Wolters Kluwer Health, Inc.") consists of your license details and the terms and conditions provided by Wolters Kluwer Health, Inc. and Copyright Clearance Center.

Your confirmation email will contain your order number for future reference.

Printable Details

| | |
|---|---|
| **License Number** | 4781330479705 |
| **License date** | Mar 03, 2020 |

### Licensed Content

| | |
|---|---|
| **Licensed Content Publisher** | Wolters Kluwer Health, Inc. |
| **Licensed Content Publication** | Circulation |
| **Licensed Content Title** | Monitoring of Bone Marrow Cell Homing Into the Infarcted Human Myocardium |
| **Licensed Content Author** | Michael Hofmann, Kai C. Wollert, Gerd P. Meyer, et al |
| **Licensed Content Date** | Apr 25, 2005 |
| **Licensed Content Volume** | 111 |
| **Licensed Content Issue** | 17 |

### Order Details

| | |
|---|---|
| **Type of Use** | Dissertation/Thesis |
| **Requestor type** | University/College |
| **Sponsorship** | No Sponsorship |
| **Format** | Print and electronic |
| **Will this be posted on a password protected website?** | Yes |
| **Portion** | Figures/tables/illustrations |
| **Number of figures/tables/illustrations** | 1 |
| **Author of this Wolters Kluwer article** | No |
| **Will you be translating?** | No |
| **Intend to modify/adapt the content** | No |

### About Your Work

| | |
|---|---|
| **Title** | Preclinical Testing of an Upscaled Tissue Engineered Stem Cell Patch Towards Use in Translational Studies |
| **Institution name** | Imperial College London |
| **Expected presentation date** | Jan 2022 |

### Additional Data

| | |
|---|---|
| **Portions** | 1 |

### Requestor Location

| | |
|---|---|
| **Requestor Location** | Richard Jabbour<br>3 Allsworth Close<br>Newington<br><br>Sittingbourne, ME9 7NW<br>United Kingdom<br>Attn: Richard Jabbour |

### Tax Details

| | |
|---|---|
| **Publisher Tax ID** | EU826013006 |

### Price

| | |
|---|---|
| **Total** | 0.00 USD |

Printable Details

| | |
|---|---|
| **License Number** | 4781300132082 |
| **License date** | Mar 03, 2020 |

### Licensed Content

| | |
|---|---|
| **Licensed Content Publisher** | Springer Nature |
| **Licensed Content Publication** | Nature Reviews Disease Primers |
| **Licensed Content Title** | Heart failure with reduced ejection fraction |
| **Licensed Content Author** | Michelle W. Bloom et al |
| **Licensed Content Date** | Aug 24, 2017 |

### Order Details

| | |
|---|---|
| **Type of Use** | Thesis/Dissertation |
| **Requestor type** | academic/university or research institute |
| **Format** | print and electronic |
| **Portion** | figures/tables/illustrations |
| **Number of figures/tables/illustrations** | 4 |
| **High-res required** | no |
| **Will you be translating?** | no |
| **Circulation/distribution** | 1 - 29 |
| **Author of this Springer Nature content** | no |

### About Your Work

| | |
|---|---|
| **Title** | Preclinical Testing of an Upscaled Tissue Engineered Stem Cell Patch Towards Use in Translational Studies |
| **Institution name** | Imperial College London |
| **Expected presentation date** | Jan 2022 |

### Additional Data

| | |
|---|---|
| **Portions** | Figure 1-3,8 |

### Requestor Location

| | |
|---|---|
| **Requestor Location** | Richard Jabbour<br>3 Allsworth Close<br>Newington<br><br>Sittingbourne, ME9 7NW<br>United Kingdom<br>Attn: Richard Jabbour |

### Tax Details

### Price

| | |
|---|---|
| **Total** | 0.00 USD |

## Order Completed

Thank you for your order.

This Agreement between Richard Jabbour ("You") and Wolters Kluwer Health, Inc. ("Wolters Kluwer Health, Inc.") consists of your license details and the terms and conditions provided by Wolters Kluwer Health, Inc. and Copyright Clearance Center.

Your confirmation email will contain your order number for future reference.

| | |
|---|---|
| **License Number** | 4781331471253 |
| **License date** | Mar 03, 2020 |

Printable Details

### Licensed Content

| | |
|---|---|
| **Licensed Content Publisher** | Wolters Kluwer Health, Inc. |
| **Licensed Content Publication** | Circulation Research |
| **Licensed Content Title** | Induced Pluripotent Stem Cells 10 Years Later |
| **Licensed Content Author** | Yoshinori Yoshida, Shinya Yamanaka |
| **Licensed Content Date** | Jun 9, 2017 |
| **Licensed Content Volume** | 120 |
| **Licensed Content Issue** | 12 |

### Order Details

| | |
|---|---|
| **Type of Use** | Dissertation/Thesis |
| **Requestor type** | University/College |
| **Sponsorship** | No Sponsorship |
| **Format** | Print and electronic |
| **Will this be posted on a password protected website?** | Yes |
| **Portion** | Figures/tables/illustrations |
| **Number of figures/tables/illustrations** | 1 |
| **Author of this Wolters Kluwer article** | No |
| **Will you be translating?** | No |
| **Intend to modify/adapt the content** | No |

### About Your Work

| | |
|---|---|
| **Title** | Preclinical Testing of an Upscaled Tissue Engineered Stem Cell Patch Towards Use in Translational Studies |
| **Institution name** | Imperial College London |
| **Expected presentation date** | Jan 2022 |

### Additional Data

| | |
|---|---|
| **Portions** | 2 |

### Requestor Location

| | |
|---|---|
| **Requestor Location** | Richard Jabbour<br>3 Allsworth Close<br>Newington<br><br>Sittingbourne, ME9 7NW<br>United Kingdom<br>Attn: Richard Jabbour |

### Tax Details

| | |
|---|---|
| **Publisher Tax ID** | EU826013006 |

### Price

| | |
|---|---|
| **Total** | 0.00 USD |

## Order Completed

Thank you for your order.

This Agreement between Richard Jabbour ("You") and Springer Nature ("Springer Nature") consists of your license details and the terms and conditions provided by Springer Nature and Copyright Clearance Center.

Your confirmation email will contain your order number for future reference.

| | |
|---|---|
| **License Number** | 4781331100649 |
| **License date** | Mar 03, 2020 |

Printable Details

### Licensed Content

| | |
|---|---|
| **Licensed Content Publisher** | Springer Nature |
| **Licensed Content Publication** | Nature Reviews Cardiology |
| **Licensed Content Title** | Induced pluripotent stem cells: at the heart of cardiovascular precision medicine |
| **Licensed Content Author** | Ian Y. Chen et al |
| **Licensed Content Date** | Mar 24, 2016 |

### Order Details

| | |
|---|---|
| **Type of Use** | Thesis/Dissertation |
| **Requestor type** | academic/university or research institute |
| **Format** | print and electronic |
| **Portion** | figures/tables/illustrations |
| **Number of figures/tables/illustrations** | 1 |
| **High-res required** | no |
| **Will you be translating?** | no |
| **Circulation/distribution** | 1 - 29 |
| **Author of this Springer Nature content** | no |

### About Your Work

| | |
|---|---|
| **Title** | Preclinical Testing of an Upscaled Tissue Engineered Stem Cell Patch Towards Use in Translational Studies |
| **Institution name** | Imperial College London |
| **Expected presentation date** | Jan 2022 |

### Additional Data

| | |
|---|---|
| **Portions** | 2 |

### Requestor Location

| | |
|---|---|
| **Requestor Location** | Richard Jabbour<br>3 Allsworth Close<br>Newington<br><br>Sittingbourne, ME9 7NW<br>United Kingdom<br>Attn: Richard Jabbour |

### Tax Details

### Price

| | |
|---|---|
| **Total** | 0.00 USD |

## Order Completed

Thank you for your order.

This Agreement between Richard Jabbour ("You") and Oxford University Press ("Oxford University Press") consists of your order details and the terms and conditions provided by Oxford University Press and Copyright Clearance Center.

| | |
|---|---|
| **License number** | Reference confirmation email for license number |
| **License date** | Mar, 11 2020 |

### Licensed Content

| | |
|---|---|
| **Licensed Content Publisher** | Oxford University Press |
| **Licensed Content Publication** | European Heart Journal |
| **Licensed Content Title** | 2016 ESC Guidelines for the diagnosis and treatment of acute and chronic heart failure: The Task Force for the diagnosis and treatment of acute and chronic heart failure of the European Society of Cardiology (ESC)Developed with the special contribution of the Heart Failure Association (HFA) of the ESC |
| **Licensed Content Author** | Ponikowski, Piotr; Voors, Adriaan A |
| **Licensed Content Date** | 2016-05-20 |
| **Licensed Content Volume** | 37 |
| **Licensed Content Issue** | 27 |

### Order Details

| | |
|---|---|
| **Type of Use** | Thesis/Dissertation |
| **Requestor type** | Educational Institution/Non-commercial/ Not for-profit |
| **Format** | Print and electronic |
| **Portion** | Figure/table |
| **Number of figures/tables** | 1 |
| **Will you be translating?** | No |

### About Your Work

| | |
|---|---|
| **Title** | Preclinical Testing of an Upscaled Tissue Engineered Stem Cell Patch Towards Use in Translational Studies |
| **Institution name** | Imperial College London |
| **Expected presentation date** | Jan 2022 |

### Additional Data

| | |
|---|---|
| **Portions** | Figure 7.1 |

## Order Completed

Thank you for your order.

This Agreement between Richard Jabbour ("You") and Elsevier ("Elsevier") consists of your license details and the terms and conditions provided by Elsevier and Copyright Clearance Center.

Your confirmation email will contain your order number for future reference.

| | |
|---|---|
| **License Number** | 4781340287545 |
| **License date** | Mar 03, 2020 |

Printable Details

### Licensed Content

| | |
|---|---|
| **Licensed Content Publisher** | Elsevier |
| **Licensed Content Publication** | Journal of the American College of Cardiology |
| **Licensed Content Title** | Transplantation of Human Embryonic Stem Cell–Derived Cardiovascular Progenitors for Severe Ischemic Left Ventricular Dysfunction |
| **Licensed Content Author** | Philippe Menasché,Valérie Vanneaux,Albert Hagège,Alain Bel,Bernard Cholley,Alexandre Parouchev,Isabelle Cacciapuoti,Reem Al-Daccak,Nadine Benhamouda,Hélène Blons,Onnik Agbulut,Lucie Tosca,Jean-Hugues Trouvin,Jean-Roch Fabreguettes,Valérie Bellamy et al. |
| **Licensed Content Date** | Jan 30, 2018 |
| **Licensed Content Volume** | 71 |
| **Licensed Content Issue** | 4 |
| **Licensed Content Pages** | 10 |
| **Journal Type** | HS |

### Order Details

| | |
|---|---|
| **Type of Use** | reuse in a thesis/dissertation |
| **Portion** | figures/tables/illustrations |
| **Number of figures/tables/illustrations** | 1 |
| **Format** | both print and electronic |
| **Are you the author of this Elsevier article?** | No |
| **Will you be translating?** | No |

### About Your Work

| | |
|---|---|
| **Title** | Preclinical Testing of an Upscaled Tissue Engineered Stem Cell Patch Towards Use in Translational Studies |
| **Institution name** | Imperial College London |
| **Expected presentation date** | Jan 2022 |

### Additional Data

| | |
|---|---|
| **Portions** | 1 |

## Order Completed

Thank you for your order.

This Agreement between Richard Jabbour ("You") and Wolters Kluwer Health, Inc. ("Wolters Kluwer Health, Inc.") consists of your license details and the terms and conditions provided by Wolters Kluwer Health, Inc. and Copyright Clearance Center.

Your confirmation email will contain your order number for future reference.

| | |
|---|---|
| **License Number** | 4781350485216 |
| **License date** | Mar 03, 2020 |

Printable Details

### Licensed Content

| | |
|---|---|
| **Licensed Content Publisher** | Wolters Kluwer Health, Inc. |
| **Licensed Content Publication** | Circulation Research |
| **Licensed Content Title** | MUSCLEMOTION |
| **Licensed Content Author** | Luca Sala, Berend J. van Meer, Leon G.J. Tertoolen, et al |
| **Licensed Content Date** | Dec 27, 2017 |
| **Licensed Content Volume** | 122 |
| **Licensed Content Issue** | 3 |

### Order Details

| | |
|---|---|
| **Type of Use** | Dissertation/Thesis |
| **Requestor type** | University/College |
| **Sponsorship** | No Sponsorship |
| **Format** | Print and electronic |
| **Will this be posted on a password protected website?** | Yes |
| **Portion** | Figures/tables/illustrations |
| **Number of figures/tables/illustrations** | 1 |
| **Author of this Wolters Kluwer article** | No |
| **Will you be translating?** | No |
| **Intend to modify/adapt the content** | No |

### About Your Work

| | |
|---|---|
| **Title** | Preclinical Testing of an Upscaled Tissue Engineered Stem Cell Patch Towards Use in Translational Studies |
| **Institution name** | Imperial College London |
| **Expected presentation date** | Jan 2022 |

### Additional Data

| | |
|---|---|
| **Portions** | 1 |

### Requestor Location

### Tax Details